EFFECT OF QUIESCENCE ON DEVELOPMENT AND EPIGENETIC STATUS OF CLONED EMBRYOS

Benedetta Alessandra Pallante

Ph.D

University of Edinburgh

2002

DECLARATION

I declare that this thesis has been composed by myself and has not been submitted for any previous degree. The work described herein is my own and all work of other authors is duly acknowledged. I also acknowledge all assistance given to me during the course of these studies.

ABSTRACT

Quiescence affects development to term of cloned embryos. There are suggestions that developmental potential of cloned embryos and changes in their epigenetic status may be correlated. This project aimed at finding a well-characterised model of cell quiescence and use it to investigate effects of quiescence on epigenetic status of cloned embryos.

Different synchronization methods were used to synchronize Mouse Foetal fibroblasts in G0 and G1. Specific positive (p130, p27) and negative markers of quiescence (FITC) were used to characterise cells. Serum starvation was the best method to synchronize cells in G0, whereas incubation for 24h with 4mM hydroxyurea or 800uM mimosine, was used to synchronize cells in G1. However, Mouse Foetal Fibroblasts did not represent a good model of quiescence. Serum starvation and synchronization with mimosine and hydroxyurea produced mixed populations of diploid (2N) and tetraploid cells (4N). Furthermore, serum starvation produced a mixed population of quiescent and non-quiescent cells.

T-lymphocytes were used as an alternative model of cell quiescence and Interleukin-2 receptor α or CD25 was used as a negative marker of quiescence. Synchronization in G1 was obtained by activation for 24h with 8ug/ml phythoemagglutinin and 4nM IL-2 in the presence of 1mM hydroxyurea, and subsequent selection of $CD25^+$ cells by magnetic cell sorting. In the G1 population >90% cells were diploid and non-quiescent ($CD25^+$). Freshly isolated T-lymphocytes were synchronized in G0, with >90% of the cells being diploid and quiescent ($CD25^-$).

Comparison of well-characterised quiescent and non-quiescent T-cell populations showed that quiescence has great effects on sub-nuclear localisation of non-histone proteins and post-translational histone modifications. Proteins of the Heterochromatin 1 (HP1) family are non-histone proteins that colocalise with pericentromeric heterochromatin and non-constitutive chromatin so changes in their distribution associate with changes in chromatin organisation. Immunolocalisation studies of HP1 proteins showed that all three isoforms, M31/hHP1β, mHP1α/hHP1α, M32/hHP1γ, had a condensed distribution in quiescent nuclei and became dispersed in non-quiescent cells. Changes in M31 distribution were the most consistent and were

correlated with expression of the activation markers CD25 and PCNA, confirming the association between quiescence and chromatin status. In $CD25^-/PCNA^-$ cells, M31 had a more condensed sub-nuclear distribution than in $CD25^+/PCNA^+$ cells.

Quiescence also altered the acetylation status of histone H4 on lysines 2-4, 5 and 12. Immunolocalisation studies showed that, under conditions that induce expression of CD25 and PCNA, histone H4 became hyperacetylated.

Finally, G0 and G1 lymphocytes were used in nuclear transfer experiments. Quiescence affected timing of premature chromosome condensation in cloned embryos. Time of metaphase plate formation and chromosome condensation were delayed in G0-derived embryos, compared to G1 embryos. Rates of development to blastocyst were very low (<5%), regardless of cell cycle stage of donor cells, and similar abnormalities were observed in developmentally arrested G0 and G1-derived embryos. No post-implantation development was observed from 2-cell embryo transfers, regardless of cell cycle. The effects of quiescence might have been masked by the overall low efficiency of T-cells for nuclear transfer.

Quiescence affected epigenetic status of cloned embryos. M31 distribution patterns were similar in control and cloned embryos at the 2-cell stage. However at the 4-cell stage none of the G1-derived embryos and 33% of G0 embryos had M31 distribution patterns similar to controls. Differences observed between G0 and G1-derived embryos showed that G0 chromatin might be more favourable to remodelling. Changes in the acetylation levels of histone H4, on lysines 5 and 12, observed in the first 3h after reconstruction and at the 2 and 4-cell stages, were similar in control and nuclear transfer embryos, derived from both G0 and G1 T-cells. However, significant differences were observed in acetylation patterns at the 2 and 4-cell stage, associated with transcriptional activation. A low proportion of cloned embryos (0-33%) had acetylation patterns similar to those of control embryos, at the 2 and 4-cell stages. Differences were also observed in G0 and G1-derived nuclear transfer embryos G1-derived embryos were similar to controls at the 2-cell stage, but failed to retain the typical peripheral, acetylation pattern at the 4-cell stage. In G0-derived embryos, appearance of acetylation patterns similar to controls was delayed till the 4-cell stage. The pattern of H4 acetylation is dependent on DNA replication and transcriptional activation. A possible explanation is that abnormal acetylation patterns may reflect

abnormalities in the spatial and temporal regulation of DNA replication and/or transcriptional activation of the donor cell genome.

Although quiescence did not affect *in vitro* developmental potential of cloned embryos it induced changes in non-histone and histone proteins that might affect post-implantation development.

PUBLICATIONS AND AWARDS

Publications arising from thesis

Pallante BA, Samuel K, Telfer EE, Ansell J, Wilmut I (2001). Mouse T-lymphocytes are an ideal model to compare the nuclear transfer efficiency of G0 and G1 cells. Theriogenology, 55 (1): 282.

Pallante BA, Gao S, McGarry M, Telfer EE, Ansell J, Samuel K, Wilmut I (2002). Comparison of *in vitro* developmental potential of G0 and G1 cells after nuclear transfer. Theriogenology, 57 (1): 366.

Pallante B, Ainslie A, McGarry M, Ferrier P, Gao S, Wilmut I (2003). Chromatin structure in cloned mouse embryos. Theriogenology, 59 (1). In Press.

Other Publications

Pizzi F, Pallante B, Gandini G (2001). Chapter 4.1-Cryopreservation techniques for pig genetic resources conservation: a review. In: Characterisation and cryopreservation of pig genetic resources in Europe. Eds.: Ollivier L, Glodek P, Gandini G, Delgado JV. EAAP publication n°. 104.

Gao S, McGarry M, Ferrier P, Pallante B, Gasparrini B, Fletcher J, Harkness L, De Sousa P, McWhir J and Wilmut I (2002). Effect of confluence and heterozygosity on production of cloned mice from embryonic stem cells. Biology of Reproduction. In Press.

Awards

First Prize, PhD Student Competition, Roslin Institute, 13 October 2001.

Third Prize, Research Student Competition, I.E.T.S. Meeting, Foz Do Iguacu, 12-15 Jnauary 2002.

AKNOWLEDGEMENTS

Many thanks to Prof. Ian Wilmut for giving me the chance of joining his group and providing me with the financial support, equipment and materials required to carry out this PhD project. I thank him for supervising the experimental work and the writing up of this thesis. I am also grateful because, no matter how busy, he always took time to discuss ideas or problems with me. I will really miss those discussions. I would also like to thank him for providing the financial support required for this PhD.

I am very grateful to Dr. Evelyn Telfer, for the guidance and help she has given me during this PhD and the writing up of this thesis. Above all, I would like to thank her for being there for me every time I needed support and encouragement. She certainly takes very good care of her students.

I would like to thank Prof. Fulvio Gandolfi, from the University of Milan for suggesting me to do a PhD at the Roslin Institute, in the first place.

Many thanks to Prof. John Ansell, for giving me the chance of conducting T lymphocyte experiments in his laboratories, at the Western General Hospital. It was a very useful experience that gave me the chance of developing an essential part of this project.

A special thank you to Kay Samuel and Dr. Martin Waterfall, for receiving me in their research group and patiently teaching me the basic immunology techniques and FACS analysis. During the months we worked together I had the chance of appreciating them not only as terrific professionals but also as wonderful people.

Dr. Ron Gao and Michelle McGarry for carrying out the nuclear transfer experiments with T-lymphocytes. Mouse nuclear transfer requires extraordinary technical skills, that very few people in the world possess. These two professionals are certainly among those few. I would also like to thank Ron for his contagious optimism and enthusiasm, two qualities essential for scientific progress.

I would like to thank Dr. Prim Singh, for all the constructive discussions we had about chromatin remodelling and non-histone proteins. He helped me putting my project into a new, more innovative perspective.

I would also like to thank Tricia Ferrier, because, far more than teaching me tissue culture techniques, she taught me how to appreciate and enjoy working with somatic cells.

I would like to thank Judy Fletcher for sharing with me some of her huge knowledge about immunocytochemistry. I would also like to thank her for bringing so much joy in everyday laboratory work, helping to create a very pleasant work environment.

I would like to thank Dr. Jie Zhue, for the constructive discussions we had about cell cycle and activation and, above all, for his friendship and constant encouragement that supported me throughout this PhD.

This project was funded by the Faculty of Veterinary Medicine of the *Universitá degli Studi di Milano* and by Prof. Ian Wilmut.

To my dear dad

and to my grandparents,

my best reasons to work in science

CONTENTS

LIST OF FIGURES

LIST OF TABLES

ABBREVIATIONS

~	Similar to
CAK	Cdk-activating kinase
Cdk(s)	Cyclin-dependent kinase
Cki(s)	Cdk-inhibitors
DAPI	4', 6-diamino-2-phenylindole
f.c.	final concentration
FACS	Fluorescence Activated Cell Sorter
FCS	Foetal Calf Serum
FITC	Fluorescein isothyocyanate
HP1	Heterochromatin Protein 1
HU	Hydroxyurea
IL-2	Interleukin-2
IL-2Rα	Interleukin-2 receptor α or CD25
MACS	Magnetic Cell Sorting
MFF	Mouse Foetal Fibroblasts
MPF	Meiosis/Mitosis Promoting Factor
NT	Nuclear Transfer
PCC	Premature Chromosome Condensation
PCNA	Proliferating Cell Nuclear Antigen
PF	Paraformaldehyde
PHA	Phytohemagglutinin
PI	Propidium iodide
RNAse	Ribonuclease
R-PE	Phycoerythrin
TcR	T cell Receptor
TXR	Texas Red
vs	Compared to
2-mercaptoethanol	2-ME
Nuclear Envelop Breakdown	NEBD
hours post-activation	hpa

CHAPTER 1

INTRODUCTION

1.1 NUCLEAR TRANSFER EFFICIENCY

Although cloning has been used to produce healthy and fertile offspring, it is still a very inefficient technique (Table 1.1). Pre-implantation development (blastocyst rate) does not seem to be a problem in most mammals (40% mice, 20% sheep and cattle) with the only exception of pigs (1%-5%). The main losses occur during post-implantation development and after birth. Foetal survival rates (7.5%-8%sheep; 1.1%-6.7% mice; 9%-14 % cattle) are significantly lower than those obtained after natural mating (92%, sheep; Walker *et al.,* 1992) and IVF (39% cattle Wells *et al.,* 1998a). Foetal losses as a consequence of NT procedures are usually associated, in most species (sheep, cattle, mouse), with the Large Offspring Syndrome (LOS; Young *et al.*, 1998) characterised by oversized foetuses and placentas. This abnormal foetal phenotype is a common feature of IVF and NT derived foetuses and has been partially correlated with *in vitro* embryo culture conditions (Walker *et al.*, 1996; Garry *et al.,* 1996). However recent reports in mouse (Eggan *et al.,* 2001) have shown that, although the birth and placental weights of IVF derived foetuses are significantly higher than control, *in vivo* derived foetuses, these are still significantly lower than those of nuclear transfer derived foetuses. The same observation was made in sheep where weights of cloned lambs were found to be higher than the average expected with *in vitro* produced sheep embryos (Thomson *et al.*, 1995; Holm *et al.*, 1996).

Nuclear transfer efficiency is further reduced by the poor rates of survival to adulthood of cloned animals ranging from 62%-65% in cattle and sheep to 45% in mice (Tab 1.1). These perinatal survival rates are lower than the ones obtained from natural mating (92%, sheep; Nash *et al.,* 1996). Most deaths are associated with respiratory failure, with the appearance of froth in the airways (sheep, Wells *et al.*, 1998b; Wilmut *et al.*, 1997; cattle, Wells *et al.*, 1998a; Cibelli *et al.*, 1998; mouse,

Table 1.1 Somatic Cell Nuclear Transfer

Species	Cell type	Stage of development	Cell cycle stage	Recipient cytoplast	Activation time	Fused or injected\ reconstructed (%)	Blastocyst\fused or injected (%)	Live births\ n° transferred (%)	Surviving offspring\ Live births	Reference
Mice	ES	E	Cycling	MII	FBA	?	110\?	15\110 (13.6)	7\15 (46.7)	Rideout *et al.* (2000)
Mice	ES	E	G0\G1	MII	FBA	1300\?	181\1300 (13.9)	4\179 (2.2)	4\4 (100)	Wakayama *et al.* (1999)
Mice	ES	E	G2\M	MII	FBA	465\?	142\465 (30.5)	4\135 (0.7)	1\4 (25)	Wakayama *et al.*(1999)
Mice	ES	E	M	MII+2-cell[1]	FBA	162\275 (59.0)	90\162 (55.5)	1\81 (1.2)	0\1 (0)	Amano *et al.* (2001a)
Mice	ES	E	M	MII	FBA	393\885 (44.4)	142\393 (36.1)	1\73 (1.3)	0\1 (0)	Amano *et al.* (2001a)
Mice	ES	E	M	MII	FBA	3620\4852 (74.6)	2007\3620 (55.4)	19\1903 (1.0)	3\19 (15.8)	Amano *et al.* (2001b)
Mice	Sertoli	A	G0\G1	MII	FBA	1189\ (70-80%)	297\1189 (24.9)	7\215 (3.3)	7\7 (100)	Ogura *et al.* (2000)
Mice	Sertoli	A	Cycling	MII	FBA	501\ (70-80%)	119\501 (23.7)	2\126 (1.6)	2\2 (100)	Ogura *et al.* (2000)
Mice	Sertoli	A	G0\G1	MII	FBA	156\(70-80%)	20\156 (50)	7\105 (6.7)	7\7 (100)	Ogura *et al.* (2000)
Mice	Cumulus	A	G0\G1	MII	FBA	2468\? (79-95)	1385\2468	31\1385 (2.2)	22\31 (71.0)	Wakayama *et al.* (1998)
Mice	Tail tip cells	A	G0\G1 Cycling	MII	FBA	633\717(88.3)	241\633 (38.0)	3\274 (1.1)	1\3 (33.3)	Wakayama and Yanagimachi (1999)
Mice	B-lymphocyte [4]	A	G0\G1	MII	FBA	630\?	21\630 (3.3)	16\159 (10.1)	13\16 (81.2)	Hochedlinger and Jaenisch (2002)
Mice	T-lymphocyte [4]	A	G0\G1	MII	FBA	350\?	20\350 (5.7)	1\101 (0.9	0\1 (0.0)	Hochedlinger and Jaenisch (2002)
Sheep	Epithelial-like	E	G0\G1	TII or MII	A\F, ABF, FBA	244\?	34\244 (13.9)	5\34 (14.7)	3\5 (60.0)	Campbell *et al.* (1996a)
Sheep	Epithelial-like	E	G0\G1	MII	A\F	385\465 (82.8)	126\385 (32.7)	4\87 (4.6)	4\4 (100)	Wilmut *et al.* (1997)
Sheep	Epithelial-like	E	G0\G1	MII	A\F	386\665 (58)	75\386 (19.4)	3\75 (4)	2\3 (66.7)	Wells *et al.* (1998b)
Sheep	Fibroblast-like	E	G0\G1	MII	A\F	345\589 (58.6)	90\345 (26.1)	10\81 (12.3)	3\10 (30.0)	Wells *et al.* (1998b)
Sheep	Fibroblast	F	G0\G1	MII	A\F	507\	69\507 (13.6)	7\67 (10.4)	5\7 (71.4)	Schnieke *et al.* (1997)
Sheep	Fibroblast	F	G0\G1	MII	A\F	417\	80\417 (19.2)	14\80 (17.5)	3\14 (21.4)	McCreath *et al.* (2000)
Sheep	Fibroblast	F	G0\G1	MII	A\F	172\203 (84.7)	47\172 (27.3)	3\40 (7.5)	2\3 (66.7)	Wilmut *et al.* (1997)
Sheep	Mammary gland	A	G0\G1	MII	A\F	277\ 434 (63.8)	29\277 (10.5)	1\29 (3.4)	1\1 (100)	Wilmut *et al.* (1997)
Muflon	Granulosa	A	G0\G1	MII	A\F	23\	7\23 (30.3)	1\7 (14.3)	1\1 (100)	Loi *et al.*, 2001
Goat	Fibroblast	F	G0\G1	MII or TII	A\F	157\285 (55)	112\157 (71.3)	3\112 (2.7)	3\3 (100)	Baguisi *et al.* (1999)
Cow	Fibroblast	F	Cycling	MII	FBA	174\242 (71.9)	35\174 (20.1)	2\7 (28%)	1\2 (50.0)	Zakhartchenko *et al.*. (1999a)
Cow	Fibroblast	F	Cycling	MII	FBA	276\?	33\276 (12)	4\28 (14.3)	3\4 (75.0)	Cibelli *et al.* (1998)
Cow	Mammary gland	A	G0\G1	MII	FBA	140\223 (63)	36\140 (26)	1\4 (25)	1\1 (100)	Zakhartchenko *et al.* (1999b)
Cow	Ear skin	A	G0\G1	MII	FBA	82\92 (89)	49\82 (59.7)	1\16 (6)	0\1 (0.0)	Zakhartchenko *et al.*. (1999b)
Cow	Ear skin	A	G0\G1	MII	A\F	338\821 (41.1)	103\338(30.4)	6\39(15.4)	4\6 (66.7)	Kubota *et al.* (2000)
Cow	Muscle	A	G0\G1 Cycling	MII TII	A\F or ABF	346\515 (67.1)	73\346 (21)	4\26 (15.4,)	4\4 (100)	Shiga *et al.* (1999)
Cow	Oviduct	A	G0\G1	MII	A\F	94\150 (63)	20\94 (21.2)	3\4 (75)	2\3 (66.7)	Kato *et al.* (1998)
Cow	Cumulus	A	G0\G1	MII	A\F	47\99 (47)	18\47 (38.3)	5\6 (83.3)	2\5 (40.0)	Kato *et al.* (1998)
Cow	Granulosa	A	G0\G1	MII	FBA	412\434 (95)	164\412 (39)	2\74 (9)	1\2 (50.0)	Wells *et al.* (1998a)
Cow	Granulosa	A	G0\G1	MII	FBA	552\713 (77.4)	282\552 (51)	10\100 (10)	10\10 (100)	Wells *et al.* (1999)
Cow	Lymphocyte	A	G0\G1	MII+TII[1]	FBA	316\353 (90)	60\316 (19)	1\19 (5.2)	1\1 (100)	Galli *et al.* (1999)
Pig	Granulosa	A	Cycling	MII+ Zygote[2]	A\F	401\1368 (29.3)	-	5\401 (1.2)	5\5 (100)	Polejaeva *et al.*, 2000

Donor cells in the table are differentiated, somatic cells. Stem cells (ES-cells) were included for completeness. Donor cells were of embryonic (E), foetal (F) or adult (A) origin. Recipient cytoplasts were either metaphase II (MII, non-activated) or telophase II (TII, activated) oocytes. In some experiments[1,2,3] nuclei were transferred to a MII oocyte and then blastomeres were transferred either to a TII oocyte, a zygote or a 2-cell embryo (re-cloning). Activation occurred at the time of fusion (A\F), before fusion (ABF) or after fusion (FBA). In one experiment[4] development to term was obtained by combining the Nuclear Transfer and tetraploid aggregation (Nagy *et al.*, 1993) techniques.

Eggan *et al.*, 2001) and with abnormalities of the system immune (Renard *et al.*, 1999). These features have not been described before as a result of *in vitro* embryo culture and they are likely to result entirely from incomplete and abnormal reprogramming of the donor nucleus. There are two main elements that may affect reprogramming and nuclear transfer efficiency:

1) Embryonic ploidy (cytogenetic effect);

2) Reprogramming of donor nucleus (epigenetic effect);

Maintenance of correct ploidy has an immediate effect on pre-implantation development (blastocyst rate), whereas correct and complete reprogramming is essential for post-implantation development and perinatal survival, though it may also affect pre-implantation development. Both LOS and cloned offspring syndromes have been associated with presence of abnormal embryo epigenetic status and, in particular, with abnormal methylation of imprinted genes and genomic DNA (Young *et al.*, 1998).

Many factors may affect nuclear transfer efficiency by influencing the ploidy and/or the reprogramming process in the cloned embryos (for review see Sun and Moor, 1995; Colman, 2000): developmental stage of donor cells (reprogramming); cell type (reprogramming); cell cycle stage of recipient oocyte (ploidy and reprogramming); cell cycle stage of the donor cell (ploidy and reprogramming); genetic background (Eggan *et al.*, 2001).

1.2 EFFECT OF CELL CYCLE COORDINATION ON NUCLEAR TRANSFER EFFICIENCY

1.2.1 Cell cycle stage of recipient cytoplast

Nuclear changes taking place during oocyte maturation/meiosis and after fertilisation or activation are associated with changes of the cytoplasmic environment. Particularly important for nuclear transfer are changes occurring in the state of activation of the maturation/meiosis/mitosis promoting factor (MPF; Masui and Markert, 1971; Nurse, 1990) that is a potential reprogramming factor. MPF is a protein kinase complex formed by a Cyclin-Dependent Kinase (CDK),

$p34^{cdc2}$/CDK1, and by its regulatory subunit, cyclin B1. Activation of this complex leads to cell cycle resumption and progression through the G2/M-phase. MPF kinase activity (Campbell *et al.,* 1996b) and localisation (Hagtin *et al.,* 1998) vary according to cell cycle stage of the oocyte. In mature oocytes (MII), MPF is activated (high kinase activity) and is localised in the oocyte nucleus. Upon fertilisation or activation, after the nuclear envelope breaks down, MPF is released into the cytoplasm where it remains active for a short period, reaching a basal level of activity upon pronuclear formation. Once in the cytoplasm, MPF becomes associated with the microtubules and centrosomes and then, in the zygote, it is sequestered by the pronuclei. The levels of MPF will then increase transiently during M-phase of each embryonic cell cycle.

MPF activity declines over a 6h period, after Sr^{2+} activation, in mouse; a 5h period, after electrical activation (Liu *et al.*, 1997), in sheep; a 12 h period, after electrical activation (Lai *et al.*, 2001), in pigs; a 10h period, after electrical activation, in cattle (Barnes *et al.*, 1993). MPF levels also decline as a result of oocyte aging (Kikuchi *et al.,* 2000). This explains why the decline in MPF levels induced by activation is quicker in aged oocytes (Tian *et al.,* 2002) and suggests that assessment of the right combination of oocyte age and activation stimuli is required to achieve optimal activation (e.g. pig, Ikeda and Takahashi, 2001).

Nuclear transfer experiments involve the fusion or injection of a single cell or nucleus (karyoplast) into a recipient cytoplast obtained by enucleation of a MII oocyte, with high levels of MPF activity, or a pre-activated, oocyte or zygote with low levels of MPF activity. According to the different states of activation of the oocyte and the different levels of MPF activity three different NT systems can be identified:

1) **Short exposure (minutes) to high MPF activity**, that occurs when non-activated (MII) oocytes are used as recipients and fusion and activation are simultaneous (e.g. electrofusion) or occur at very short distance (AF system; review by Prather and First, 1990). This method is the most commonly used in agricultural animals (Campbell *et al.,* 1995; 1996a; Wilmut *et al*, 1997; Collas and Robl, 1991; Prather *et al.*, 1990; Kanka *et al.*, 1991).

2) **Prolonged exposure (>1h) to high MPF activity**, that occurs when non-activating fusion methods are used and fusion and activation are carried out hours (1-6h) apart (fusion before activation or FBA system). This method has been mainly used in mouse (Wakayama *et al.*, 1998), where non-activating fusion methods are more commonly used although it has been used with good results also in cattle (Stice *et al.*, 1996; Cibelli *et al.*, 1998; Wells *et al.*, 1998a; 1998b).

3) **Exposure to low MPF activity,** that occurs when pre-activated oocytes or zygotes are used as recipients (activation before fusion or ABF system).

The levels of MPF found in the different systems are associated with morphological events with important implications for the ploidy and the reprogramming of reconstructed embryos. The morphological changes observed in the AF and the FBA system, where there are high levels of MPF, are very similar. As described in mouse (Czolowska *et al.*, 1984; Tsunoda *et al.*, 1989), rabbit (Stice and Robl 1988; Collas and Robl, 1991), pig (Prather *et al.*, 1990), cattle (Prather *et al.*, 1987; Kanka *et al.*, 1991) and sheep (Willasden, 1986; Smith and Wilmut, 1989) these morphological events are: 1) induction of NEBD, followed by 2) premature chromosome condensation (PCC); 3) spindle formation; 4) pseudo-polar body exclusion; 5) pseudo-pronuclear formation and nuclear swelling; 6) DNA replication and cytokinesis. Among the morphological events taking place after transfer to a MII oocyte (AF and FBA system) NEBD, PCC and, in mouse, extrusion of pseudo-polar body, have very important effects on ploidy and chromosomal integrity depending on the cell-cycle stage of the donor cell (Campbell *et al.*, 1996b). NEBD, PCC and nuclear swelling are also thought to be essential for reprogramming of gene expression (Collas *et al.*, 1992a).

In the absence of MPF activity (ABF system), none of the morphological events, previously described, take place.

1.2.2 Cell cycle stage of donor cells

The first cell cycle experiments were carried out in the early 90's using embryonic donor cells from early cleavage embryos (blastomeres; for review see

Heynman and Renard, 1996) or blastocyst stage embryos (ICM, ES-cells; Keefer *et al.,* 1994; Illmensee and Hoppe, 1981; Smith and Wilmut, 1989; Wakayama *et al.*, 1999). About 79%-100% of the blastomeres from early cleavage embryos (Barnes *et al.,* 1993; Campbell *et al.*, 1993; 1995; Collas *et al.*, 1992b) and 26-64% of inner cell mass (ICM) cells or embryonic stem cells (ES-cells), isolated from blastocyst stage embryos, are in S-phase (Tsunoda and Kato, 1997; Wakayama *et al.*, 1999; Zhou *et al.*, 2001). Embryonic nuclear transfer experiments were carried out with asynchronous blastomeres, in S-phase. Alternatively, donor blastomeres were synchronized in G1/S, using DNA synthesis inhibitors (e.g. aphidicholine, cycloheximide, hydroxyurea), and in G2/M, using inhibitors of tubulin polymerisation (e.g. nocodazole or colcemid; Cheong *et al.*, 1993; Kwon and Kono, 1996; Campbell *et al.*, 1995; Liu *et al.*, 1997).

Somatic cell nuclear transfer offered new opportunities to investigate the effect of cell cycle stage of donor cells on nuclear transfer efficiency. The cell cycle of somatic cells differs from the embryonic cell cycle because it is longer (20-24h vs 9-16h) and has well defined gap-phases. The cell cycle profile of somatic cells is characterised by 60-65% G0/G1 cells, 10-15% G2/M cells, and 20-25% S-phase cells. The percentages of cells in S-phase further decline to 0-1% in quiescent (G0) cells, such as terminally differentiated, post-mitotic cells (permanent G0), or mitotic cells that are confluent or have been serum-starved (temporary G0). Somatic cells are more easily synchronized in a G0/G1 and G2/M-phase than blastomeres. Furthermore, somatic cells, unlike blastomeres, can be synchronized either in a quiescent (G0) as well as a non-quiescent (G1), diploid state.

1.2.3 Cell cycle coordination: effects on ploidy and chromosomal integrity

The first cell cycle coordination experiments (reviews by Campbell *et al.*, 1996b; Kono, 1997) were carried out using mouse (Kono *et al.*, 1991, 1992; Kato and Tsunoda, 1992; Cheong *et al.*, 1993; Kwon and Kono, 1996; Tsunoda and Kato, 1997; Otaegui *et al.*, 1994) and rabbit (Collas and Robl, 1990; 1991; Collas *et al.*, 1992a, 1992b) donor blastomeres that could be easily synchronized in G1/early S,

G2/late S and M. The results of these experiments demonstrated that transfer of G1/S donor cells to recipient MII oocytes resulted in higher blastocyst rates (Cheong *et al.*, 1993; Tsunoda and Kato, 1997; Otaegui *et al.*, 1994), better blastocyst quality (i.e. higher cell numbers; Cheong *et al.*, 1993) and higher rates of post-implantation development (Tsunoda and Kato, 1997). These data were also confirmed in cattle (Campbell *et al.*, 1993) and pig (Verma *et al.*, 1998).

An explanation for this is that after transfer to an MII cytoplast, with high MPF activity, nuclei re-enter the cell cycle in S-phase, regardless of their stage, in response to the NEBD signal. NEBD, induced by MPF nuclear lamin kinase activity, acts as a positive signal for DNA replication, regardless of cell cycle stage of donor nucleus. Cell fusion experiments showed that heterokaryons produced by fusion of vertebrate cells in M-phase and interphase (G1, S, G2-phase) display NEBD and PCC (Johnson and Rao, 1970b) and induce S- and G2-nuclei to re-replicate their DNA (Johnson and Rao, 1970a). Experiments with *Xenopus* egg cell-free system proved that NEBD acts as a signal for DNA replication regardless of the cell cycle stage of the nucleus. In this system G2 nuclei exposed to S-phase extracts would not replicate in the presence of an intact nuclear envelope, but would undergo re-replication after permeabilisation with detergent treatment (Blow and Laskey, 1988; Leno *et al.*, 1992) or induction of NEBD and PCC (Hutchinson *et al.*, 1993). These data were also confirmed by nuclear transfer experiments in cattle (Campbell *et al.*, 1993; Barnes *et al.*, 1993) which proved the strict correlation between high MPF levels, NEBD and DNA replication and demonstrated that, because of this correlation, any nucleus transferred to a MII oocyte will resume its cycle from S-phase regardless of its cell cycle stage. In this experiment NEBD occurred in 100% of nuclei transferred to MII oocytes 0hpa, in 50% of nuclei transferred to MII oocytes 5-8 hpa, in 0% of nuclei transferred to S-phase cytoplasts (pre-activated oocytes) 9-10hpa. In the same experiment it was demonstrated, using BrdU incorporation, that 100% of nuclei, regardless of their cell cycle stage (G1, S, G2/M), replicated their DNA after transfer to MII oocytes. However, in the absence of NEBD, after transfer to pre-activated oocytes, 94-100% of G1 and S-phase nuclei initiated or completed DNA replication, and 0% of G2/M nuclei duplicated their DNA (Campbell *et al.*, 1993). It was concluded that, at least in cattle and rabbit, after

transfer to MII oocytes, only 2N nuclei (G1, early S-phase) will retain diploidy whereas transfer of 4N (G2/M) and 2-4N (late S-phase) will result in tetraploidisation and aneuploidy (Collas *et al.*, 1992a: 1992b; Campbell *et al.*, 1993; Campbell *et al.*, 1996b).

However, in mouse (Kono *et al.*, 1992), sheep (Liu *et al.*, 1997) and pig (Lai *et al.*, 2001) transfer of G2/M nuclei to MII oocytes is also possible. This occurs because, in the absence of cytochalasin B, oocytes from these species extrude a pseudo-polar body and, with it, half of their DNA becoming diploid. Pseudo-polar body extrusion takes place 3-4hpa, before pseudo-pronuclear formation and DNA replication. In mouse it was shown (Kono *et al.*, 1992) that when 2-cell blastomeres synchronized in G2/M (4N) were transferred to MII oocytes and activated in the absence of CB, about 78-85% formed a PB (2N) and a PN (2N). Under these conditions 81% of the embryos had normal ploidy, 25-26% developed to the blastocyst stage and 12.2 % developed to term. However, in the presence of cytochalasin B, G2/M nuclei (4N) were unable to extrude half of their genome into a polar body, and formed two diploid nuclei (2x2N), that became tetraploid nuclei after DNA re-replication, just like observed in cattle and rabbit. The only way transfer of G2/M nuclei into MII oocytes can result in development in mouse, in the presence of cytochalasin B, or in cattle and rabbit regardless of the presence of cytochalasin B, is by serial nuclear transfer or re-cloning. In this case each of the diploid pronuclei resulting from the G2/M donor nucleus are transferred to a recipient zygote for a second round of cloning (Kwon and Kono, 1996). Under these conditions the transfer of a G2/M (1x 4N) nucleus is transformed into the transfer of two diploid nuclei (2x2N) into two recipient cytoplasts. This is technically very demanding and the limited results obtained so far do not justify its application.

In pigs and sheep (Lai *et al.*, 2001; Liu *et al.*, 1997) pseudo polar body extrusion occurs spontaneously only after transfer of G2/M nuclei, whereas in mouse it occurs spontaneously also after transfer of G1/S nuclei to MII oocytes (Kono *et al.*, 1992). Therefore, addition of cytochalasin B, in mouse, is essential to prevent haploidisation of G1/S nuclei after transfer to MII oocytes (Cheong *et al.*, 1993; Wakayama *et al.*, 1998), whereas it can be omitted in pigs and sheep.

Transfer of donor cells in S-phase to MII oocytes results in abnormal ploidy and reduced NT efficiency in all species. Efficiency of transfer of S-phase donor cells to MII oocytes is also reduced by loss of chromosomal integrity, resulting from premature chromosome condensation (PCC). Descriptive studies in mouse have shown that, during PCC, G1/S (2N) nuclei condense into one or two clumps of chromatin that later form one (Cheong *et al.*, 1993) or two (Wakayama *et al.*, 1998) pseudo-pronuclei, with an overall diploid DNA content (2N). Donor nuclei in G2/M condense into two clumps of chromatin, containing each a diploid content of DNA (2x2N; Cheong *et al.*, 1993; Wakayama *et al.*, 1998). As a result of PCC, S-phase nuclei condense into a variety of complex structures, usually organised into three or more clumps, containing a diploid/tetraploid content of DNA (2-4N, Cheong *et al.*, 1993; Wakayama *et al.*, 1998). Finally, chromatin of G1/S and G2/M nuclei condenses into individualised, elongated chromosomes respectively with single (2N nuclei; Kono *et al.*, 1993; Wakayama *et al.*, 1998) or double-stranded (4N nuclei; Kono *et al.*, 1992; Kwon and Kono, 1996) chromatids. Double chromatid chromosomes, which can correctly bind to the mitotic spindle, align in a metaphase plate (Kwon and Kono, 1996), whereas single chromatid chromosomes fail to form a metaphase plate and maintain a random distribution (Wakayama *et al.*, 1998). The S-phase chromatin does not form chromosomes and acquires, instead, a pulverised appearance (Schwartz *et al.*, 1971) associated with a high incidence of abnormalities (Johnson and Rao, 1970b; Collas *et al.*, 1992ab; Campbell *et al.*, 1993).

When nuclei are transferred to pre-activated oocytes (universal recipient), with low MPF activity, all nuclei, regardless of their cell cycle stage, retain normal ploidy and chromosomal integrity. The explanation for this is that, in the absence of MPF activity, NEBD and PCC donor nuclei resume the cell cycle where they had left it. In sheep, cattle and mouse higher rates of pre and post-implantation development were obtained when S-phase donor blastomeres were transferred to pre-activated oocytes rather than MII oocytes. (Campbell *et al.* 1995; Barnes *et al.*, 1993; Tsunoda and Kato, 1997).

In conclusion, normal development, after nuclear transfer, can be obtained under two experimental conditions:

1) Transfer to a pre-activated oocyte of all nuclei, regardless of their cell cycle stage;

2) Transfer to a MII oocyte of G1/S nuclei, in all species, and G2/M nuclei, in mouse, sheep, pigs and cows.

Although normal development can be obtained with G2/M nuclei, the higher efficiency rates obtained with G1/S nuclei make them a better option. Studies using 2-cell blastomeres (Cheong *et al.*, 1993) showed that G1/S nuclei, activated in the presence of cytochalasin B (97% without polar body, 97% diploid), gave significantly higher cleavage rates (97% vs 78%), higher blastocyst rates (78% vs 21%) and higher blastocyst cell numbers (62 vs 37) than G2/M nuclei, activated in the absence of cytochalasin B (67% with PB, 67% diploid). A similar result was obtained when mouse foetal fibroblasts, synchronized in M-phase with nocodazole where transferred to MII oocytes and then activated in the absence of cytochalasin B (87-91% with PB, 87-91% diploid; Ono *et al.*, 2001a). Under these conditions 37% developed to blastocyst but no embryo developed to term. When using serial nuclear transfer, that is thought to enhance nuclear reprogramming, about 30% developed to blastocyst and 1.8% developed to term, with 60% surviving to adulthood. These results are worse than the results obtained using more differentiated, diploid cells after transfer to a recipient MII oocyte, in the presence of CB (Wakayama *et al*, 1998; Ogura *et al.*, 2000). In these experiments freshly isolated cumulus cells and Sertoli cells or contact-inhibited tail tip cells, were used as nuclear donors and 34-60% of cloned embryos developed to blastocyst, 2.2-5.7% developed to term and 68-71% of pups survived to adulthood. In these experiments a single round of nuclear transfer was carried out.

1.2.4 Cell cycle coordination: effects on reprogramming

There are many reports that support the idea that recipient MII oocytes have a higher reprogramming potential than pre-activated oocytes. In mouse, blastomeres from 8-cell embryos failed to develop (McGrath and Solter, 1984) beyond the 4-cell stage, after transfer to zygotes, but were able to support development to term after transfer to MII oocytes (Tsunoda *et al.*, 1987). Transfer of cumulus cells to MII

oocytes around the time of activation (AF system) gave higher blastocyst rates than cells transferred to oocytes that had been activated 1h before fusion or zygotes (ABF system; Wakayama *et al.,* 2000b). Similar results were obtained in cattle where transfer of embryonic nuclei to zygotes resulted in limited embryo development (Robl *et al.*, 1986), while transfer of 8 to 16-cell blastomeres to MII oocytes resulted in development to term (Prather *et al.*, 1987).

Extended exposure of donor nuclei to MII oocytes, achieved by delaying the time of activation after fusion (FBA system) is also beneficial for reprogramming and increases nuclear transfer efficiency. A delay of 1-3h in mouse (Wakayama *et al.*, 1998; Wakayama *et al.*, 2000b) and of 4-5h in cattle (Wells *et al.*, 1998b) increased blastocyst rates and rates of foetal development compared to simultaneous fusion and activation (Stice *et al.*, 1996; Wells *et al.*, 1998a).

Re-cloning, that extends exposure of the donor nucleus to conditioning factors in the recipient ooplasm by serial rounds of cloning also improved development of cloned embryos. Previous experiments in amphibians showed that embryos reached later stages of development after re-cloning (Orr *et al*, 1986). Studies in cattle (Zakhartchenko *et al.*, 1999a) demonstrated that blastocyst rates significantly increased between the first and second round of cloning (20-39% vs 52-55%), though this evidence remains controversial (Peura and Trounson, 1998).

The higher reprogramming potential of MII oocytes is attributed to the fact that their cytoplasm contains reprogramming factors that are present or available only for a limited time around the time of activation. The maturation/mitosis/meiosis promoting factor (MPF) has been indicated as one of these factors. MPF induces morphological events such as nuclear envelope breakdown (NEBD), PCC and nuclear swelling thought to enhance the remodelling of donor nucleus.

NEBD enhances reprogramming by enabling immediate and direct exposure of chromatin to epigenetic factors like MPF or lamins, which are present or available in the recipient ooplasm for a very short time (2-3h) around activation. Changes in chromatin structure are also though to be directly involved in the remodelling process (Croston and Kadonaga, 1993; Koide *et al.*, 1994). In mouse (Cheong *et al.*, 1994), the reprogramming potential of nuclei that underwent PCC (PCC) was compared with that of nuclei that did not undergo PCC (NPCC). The conclusion was

that only PCC nuclei retained normal ploidy and were able to support development to term, whereas NPCC nuclei had all a tetraploid chromosome constitution, and were not able to support development to term (Cheong *et al.*, 1994). Nuclear swelling is also considered a characteristic of nuclear reprogramming (Gurdon, 1986; Kono *et al.*, 1992) and it is likely to arise due to the exchange of cytoplasmic factors between the nucleus and the cytoplasm (Prather and First, 1990; Kikyo and Wolffe, 2000). Nuclear swelling decreases greatly as fusion and activation become separated temporally (Czlowska *et al.*, 1984) and is no longer observed at the pronuclear stage (Barnes *et al.*, 1987). In mouse, remodelling of donor thymocytes only took place when they were transferred to an oocyte within 3 hours after activation (Szöllösi *et al.*, 1988).

These data suggest that the cytoplasm of MII oocytes contains "epigenetic factors" required for nuclear remodelling (Gurdon, 1986) that are no longer available or present in the zygote. One explanation is that some reprogramming factors, available in limited supply, are released to the cytoplasm following Germinal Vescicle Breakdown (GVBD) and become associated again with the pronuclei during their formation (Prather and First, 1990; Aronson and Solter, 1987). Lamins might belong to this category of reprogramming factors, since they are usually present in the cytoplasm but they move to the nucleus when the nuclear membrane is reassembled after mitosis (Gerace and Blobel, 1980).

Another explanation might be that reprogramming factors have short lives (Prather and First, 1990) and are present only around the time of activation (up to 3h after activation in mouse; Szöllösi *et al.*, 1988). MPF has been indicated as one of the main reprogramming factors present in MII oocytes that disappear after activation.

In conclusion MII oocytes, with high MPF levels, have a significantly higher reprogramming and developmental potential than pre-activated oocytes (activated more than 1h before fusion) or zygotes. This is due to the fact that when nuclei are fused around the time of activation (AF), as a consequence of NEBD, they are immediately exposed to reprogramming factors (lamins, MPF). However when nuclei are fused more than an hour after activation, the nuclear envelope remains intact and the donor chromatin is not exposed to reprogramming factors, which are anyway low (MPF) or not available (lamins), in this system. Finally, a delay in

activation of 1-3 h (FBA) significantly increases the developmental potential of cloned embryos compared to the AF system, because donor chromatin is exposed to reprogramming factors for a longer period (Wakayama *et al.*, 1998; Wakayama *et al.*, 2000b).

These observations, together with previous information acquired about cell cycle coordination, indicate that maintenance of correct ploidy and chromosomal integrity and maximal reprogramming efficiency can be achieved by transferring diploid (G0/G1) cells to MII oocytes .

1.3 EFFECT OF QUIESCENCE (G0) OF DONOR CELLS ON NUCLEAR TRANSFER EFFICIENCY

Synchronization of blastomeres in a diploid state (G1) was difficult and transient due to the short length of this phase in the embryonic cell cycle. Nuclear transfer (NT) with somatic cells, with a longer cell cycle and longer gap-phases, meant that donor cells could be synchronized more efficiently in a diploid state. Furthermore, experiments with somatic cells showed that synchronization of donor cells in a diploid, quiescent state (G0) might increase nuclear plasticity and enhance reprogramming efficiency. In the first experiments using cells isolated from the inner cell mass (ICM) or embryonic disk (ED) of blastocyst stage or late stage embryos, development to term was obtained in cattle (Keefer *et al.*, 1994; Collas and Barnes, 1994) and sheep (Smith and Wilmut, 1989; Campbell *et al.*, 1995), but only when freshly isolated cells (passage 0) or cells from very early passages (passage<3) were used as donors. No development to term was obtained when sheep cells, cultured for more than six passages, were used as donors (Campbell *et al.*, 1996a). The decrease in nuclear transfer efficiency correlated with the appearance of morphological and molecular markers of differentiation (Campbell *et al.*, 1996a). It had been reported that ICM and ED cells, isolated from mammals other than mouse, remained undifferentiated and totipotent up to passage 3, but after 2-3 passages in culture, unlike mouse ES-cells, they acquired an epithelial or fibroblast-like morphology and after passage 6, they expressed the differentiation markers cytokeratin and lamin A/C

(Galli *et al.*, 1994). A major breakthrough came when five lambs were successfully cloned by fusing differentiating cells isolated from the ED of a late sheep embryo (day 9) that had been cultured for 6-13 passages, to MII oocytes (Campbell *et al.*, 1996a). Once more the cell cycle proved to play a pivotal role in nuclear transfer since the only difference between this experiment and the previous, unsuccessful ones was that donor cells had been synchronized in a diploid, quiescent state (G0) by serum deprivation (Campbell *et al.*, 1996a). Previous NT studies, using blastomeres as nuclear donors, proved that synchronization of donor cells in a diploid, non-quiescent state (G1) before transfer to a MII oocyte was highly beneficial for nuclear transfer. Serum deprivation represented an efficient way to synchronize somatic cells in a diploid state. However, serum deprivation also induced nuclear quiescence, associated with changes in chromatin conformation (Whitfield *et al.*, 1985) that might extend the plasticity of the donor nucleus, making it more amenable to reprogramming and more capable to support development of cloned embryos.

The question whether quiescence of donor nuclei is mandatory for development to term of reconstructed embryos has still to be answered.

Most successful cloning experiments, carried out after this groundbreaking experiment, have been done using quiescent, donor cells (Table 1.1). The result obtained by Campbell *et al.* (1996a) was confirmed by the birth of more lambs cloned using quiescent, epithelial-like (Wells *et al.*, 1997) or fibroblast-like (Wells *et al.*, 1998b), embryonic cell lines, isolated from the ICM of late blastocysts (day 8), and cultured for 8-16 passages. Most importantly, the same technique, used to reprogram differentiating, embryonic cell lines, was used to produce Dolly, the first mammal cloned from adult cells, isolated from the mammary gland of a 6 year old ewe, that had been serum-starved before transfer to a recipient MII oocyte (Wilmut *et al.*, 1997). After Dolly's birth, most successful NT experiments, using somatic cells of adult or foetal origin, have been done, in a variety of species, using quiescent cells (Table 1.1). In some experiments post-mitotic, terminally differentiated cells, like cumulus cells or Sertoli cells that are naturally in a quiescent state, were used as donors. In other experiments, mitotic somatic cells, that had been cultured and induced into quiescence either by serum deprivation or contact inhibition, were used as donors and transferred to recipient MII oocytes.

There are many reports suggesting a positive effect of quiescence on nuclear transfer. Earlier, nuclear transfer experiments in Amphibian showed that quiescence of donor cells improved nuclear transfer efficiency compared to cycling cells. Nucleated, frog erythrocytes, that are terminally differentiated and quiescent, were able to support development to a later stage (feeding tadpole) than cells which still retained replicative potential, such as embryonic myotomes (Gurdon *et al.*, 1984) and spleenocytes (Wabl *et al.*, 1975), used in previous experiments (DiBerardino *et al.*, 1986). Later experiments carried out in cattle (Hill *et al.*, 1998; Zakhartchenko *et al.*, 1999a) showed that serum-starved quiescent cells gave significantly higher blastocyst rates (39% vs 20%) and pregnancy rates at day 30 (78% vs 33%) and day 90 (63% vs 33%) compared to cycling cells. These observations were confirmed in rabbit where quiescence of donor cells (i.e. foetal fibroblasts) significantly improved development of cloned embryos (Galat *et al.*, 1998). Recent experiments in cattle (Wells, 2002) showed that quiescence of donor nuclei significantly increased efficiency of development to term of cloned embryos.

However, there are also a few reports challenging the theory that quiescence might be beneficial for nuclear reprogramming. In some cases, terminally differentiated, quiescent cells, such as neurons, have failed to support development to term, suggesting that the G0 state in itself may not be sufficient to enable complete and correct reprogramming of donor nucleus. There have been reports, in cattle, of non-quiescent foetal fibroblasts supporting development to term (Cibelli *et al.*, 1998; Vignon *et al.*, 1998). However, there are indications that donor cells used in one of these experiments (Cibelli *et al.*, 1998) may have not been cycling but, at least partially, quiescent: the proportion of cells in S-phase had been overestimated, due to fixation artifacts (Campbell, 1998); quiescent cells are also present in populations of mitotically active cells, especially in the small-cell population, that is usually selected for nuclear transfer (Boquest *et al.*, 1999); the foetal fibroblasts used in this experiment, had almost reached confluence, a state which is known to induce quiescence in cultured cells.

Most experiments carried out to assess the effect of quiescence on NT efficiency have compared quiescent donor cells with cycling cells (Hill *et al.*, 1998; Zakhartchenko *et al.*, 1999a). A more correct approach would be to compare the NT

potential of quiescent, diploid cells (G0) with that of non-quiescent, diploid cells (G1), rather than cycling cells. Only with this experimental design it would be possible to discriminate between the positive effects exerted on the ploidy and chromosomal integrity of cloned embryos by the diploid state, from those produced on reprogramming by the quiescence of the donor nucleus. Comparison of the developmental potential of G0 and G1 cells is made difficult by the lack of specific markers of cell quiescence, necessary to obtain well-characterised populations of donor cells in G0 or G1. To date only "putative" G0 and G1 cells have been compared (Kasinatham *et al.*, 2001; Wells, 2002), with contradicting results. An American study, carried out in cattle, showed no significant difference in the blastocyst rate of putative G1 fibroblasts, obtained by mitotic shake-off and replating, and putative G0 fibroblasts, synchronized by contact inhibition (Kasinatham *et al.*, 2001). However, the same study also showed that putative G1 cells were able to support development to term more efficiently than putative G0 cells. These results are in contrast with more recent data, in cattle, where putative G0 cells, synchronized by serum starvation, gave significantly higher rates of development to term than putative G1 cells, obtained by shake off and replating (Wells, 2002). Other data (Wrenzicky *et al.*, 2001), from the same laboratory in New Zealand, showed that embryos derived from putative G1 cells had significantly higher levels of expression of genes correlated with poor embryo quality, like the interferon-tau gene (IFτ), than embryos derived from putative G0 cells.

There is also some indirect evidence suggesting that quiescence might be beneficial for development of cloned embryos, by creating an epigenetic status more amenable to reprogramming. Embryonic cells are totipotent, because they have unrestricted genomic potential or unrestricted potential for gene expression. During development, as they differentiate into the different somatic tissues, their genomic potential becomes restricted through the imposition of epigenetic controls that establish tissue specific patterns of gene expression. These repressive chromatin structures are difficult to disassemble. There are three main layers of epigenetic repression of gene expression, that prevent transcriptional activation in a tissue-specific manner: 1) methylation of CpG dinucleotides; 2) acetylation/deacetylation of

histone H4; 3) changes in chromatin conformation controlled by composition and modification status of histone- (H1, H1°, H2A, H2B, H4, H5) and non-histone proteins (Polycomb proteins HMG_1, HP1). The stable nature of these epigenetic changes is the result of the fact that, apart from establishing states of gene repression during development, they also have to maintain them in the adult, through cycles of DNA replication, chromosome condensation and segregation. During remodelling, after transfer of a differentiated nucleus to a recipient oocyte, these chromatin repressive structures have to be removed to re-establish totipotency. However, their stable nature might impose a formidable obstacle to the development of cloned embryos, as suggested by reports showing persistence of epigenetic structures typical of differentiated cells in cloned embryos (Kang *et al.*, 2001). There is also evidence suggesting that quiescence might help the removal of these repressive structures, making quiescent chromatin more amenable to reprogramming. Three issues are discussed in this paragraph: how epigenetic patterns are established during embryo development and differentiation; how they are successfully or unsuccessfully removed during reprogramming; how quiescence might help the remodelling process.

Methylation of CpGs is the main covalent modification found in vertebrate embryos (Antequera *et al.*, 1989; Keshet *et al.*, 1986). During pre-implantation development, up to the blastocyst stage, genomic DNA is demethylated with percentages of methylated genomic DNA ranging from 9% in *in vitro* derived blastocyst, 5% in *in vivo* derived blastocysts and 3% in parthenogenetic blastocysts (Kang *et al.*, 2001). At the time of gastrulation and organogenesis, as embryonic cells differentiate into different somatic tissues, *de novo* methylation takes place mainly directed by DNA methyltransferase 3a (Dnmt3a) and Dnmt3b, which recognise both demethylated and hemimethylated DNA. Through the activity of these enzymes tissue-specific patterns of methylation, monoallelic expression of imprinted genes and X chromosome inactivation are established. In adult somatic tissues about 50-80% of genomic CpGs are methylated and this level is maintained stable through cycles of DNA replication by Dnmt1, which has a great affinity for hemimethylated DNA (Newel-Price *et al.*, 2000).

After transfer to a recipient oocyte somatic chromatin has to be heavily demethylated to reach methylation levels as low as those observed in *in vivo* or *in vitro* derived embryos (5-9%). Failure to erase tissue specific methylation patterns during pre-implantation development may result in establishment of aberrant methylation patterns, during post-implantation development. Analysis of the methylation status of cloned embryos and foetuses has shown that: cloned blastocyst are aberrantly and ectopically hypermethylated compared to control embryos (cattle; Kang *et al.*, 2001; Bourc'his *et al.*, 2001); placentas and tissues of cloned foetuses have altered levels of expression and levels of methylation of imprinted and non-imprinted genes (mouse; Humpherys *et al.*, 2001; Ohgane *et al.*, 2001; Inoue *et al.* 2002); placentas of cloned foetuses have abnormal methylation patterns of imprinted genes (mouse; Humpherys *et al.*, 2001).

For cloning experiments with mouse ES-cells it has been suggested that epigenetic instability of ES-cell lines might have contributed to the problem (Humpherys *et al.*, 2001). However placentas from mouse clones derived from more stable, somatic cells (e.g. cumulus cells, Sertoli cells) also had significantly lower mRNA levels of non-imprinted (Igfbp2, Igfbp6, Vegfr2/Flk1 and Esx1) and imprinted genes (Peg1/Mest, Meg1/Grb10, Meg3/Gtl2; Inoue *et al.*, 2002).

As previously suggested for the Large Offspring Syndrome, (Young *et al.*, 1998), abnormalities in methylation levels and patterns described in cloned embryos and foetuses might also account for some also the foetal and perinatal losses observed in nuclear transfer experiments as a result of the "cloned" offspring syndrome (Thomson *et al.*, 1995; Holm *et al.*, 1996; Eggan *et al.*, 2001).

Quiescence of the donor nucleus might help the reprogramming process by enhancing the demethylation process. This suggestion is supported by a report (Baqir and Smith, 2000) showing that contact inhibition or serum starvation, known to induce quiescence in somatic cells, significantly reduced methylation levels and expression of the imprinted genes Igf2 and H19. There are no reports to date comparing methylation levels and patterns in foetuses cloned from quiescent and non-quiescent cells.

Another important layer of epigenetic control of gene repression is deacetylation/acetylation of histone H4 (for review see Newell-Price *et al.*, 2000). Acetylated chromatin localises with RNA polymerase II, which suggests that acetylation of histone H4 associates with transcriptional activation, whereas histone H4 deacetylation is associated with transcriptional repression. Chromatin acetylation status results from the balance in the activity of two groups of enzymes: histone acetyl-transferases (HATs) and histone deacetylases (HDACs). These enzymes are associated with chromatin remodelling complexes, which act in an ATPase-dependent manner, since structural modification requires energy. HATs usually associate with chromatin remodelling complexes (SWI/SNF, NURF, ACF, CHRAC, RSC) containing: TATA binding proteins (TBP; e.g. Ada, Spt), that recruit HATs to the chromatin template; an ATPase, supplying the energy for the remodelling machine (Snf2 for SWI/SNF, ISWI for all the others); a transcriptional co-activator that might (Gnc5 for SWI/SNF) or may not (Gal4.VP16, for all complexes) possess intrinsic acetyltransferase activity. As the chromatin template is hyperacetylated (triacetylated, tetracetyalted or more) by HATs, it is also remodelled into a decondensed conformation (euchromatin), hypersensitive to DNA-se I digestion and accessible to transcriptional activation. On the contrary, HDACs (HDAC1, HDAC2) usually bind to an histone binding protein (Rbac46/48) and associate with chromatin remodelling complexes containing: repressor proteins (MeCP2, MBD2a, MBD3), with a methylated CpG binding domain (MBD), used to recruit HDACs to sites of methylated chromatin, and a transcriptional repressor domain (TRD); an ATPase (e.g. Mi2β); a co-repressor (MTA-2) which might (Rpd3) or may not (MTA-2, Sin3A, SAP30, SAP18) have intrinsic deacetylase activity. As the chromatin template, that had previously been methylated, becomes deacetylated (deacetylated, monoacetylated, diacetylated), the chromatin is remodelled in a condensed, nuclease resistant form (heterochromatin), inaccessible to transcription factors.

Studies in *Xenopus* have shown that until the time of ZGA embryonic nuclei are transcriptionally inactive, and virtually deacetylated. *Xenopus* oocytes store large quantities of diacetylated histone H4 which, after fertilisation, is incorporated into the chromatin of early embryos, and further deacetylated into the mono or deacetylated (Dimitrov *et al.*, 1993; Ryan *et al.*, 1999). At this stage active

acetylation does not take place and HDACs activity is prevalent. However around the time of ZGA, when the embryo becomes transcriptionally active, hyperacetylated H4 (tri or tetra-acetylated) form becomes predominant and the chromatin is decondensed by the SWI/SNF machine (Gelius *et al.*, 1999; Kikyo and Wolffe, 2000). In mouse ZGA takes place at the 2-cell stage and it is marked by hyperacetylation of histone H4 (Worrad *et al.*, 1995) and H3 (Stein *et al.*, 1997) that takes place at the periphery of the pronuclei. This peripheral acetylation pattern is temporally restricted to ZGA and disappears after the 4-cell stage, although a diffuse nuclear acetylation pattern is present in later stages of development (Worrad *et al.*, 1995; Stein *et al.*, 1997). During embryo development acetylation/deacetylation patterns will be established in a tissue specific manner. Recent studies showed that parental mono-allelic deacetylation of imprinted genes takes place (Feil *et al.*, 1997) and that selective deacetylation on imprinted genes and their methylation are linked (Gregory *et al.*, 2001; 2002). Contribution of acetylation in parental imprinting was confirmed by a report showing how trichostatin-A (TSA), an inhibitor of deacetylase activity, resulted in hyperacetylation, increased DNase-sensitivity and over expression of the maternally imprinted gene U2af1-rs2 in mouse (Gregory *et al.*, 2001; 2002). Deacetylation also contributes to X chromosome inactivation (Heard *et al.*, 1997).

Considering the complementarity of the methylation and deacetylation process in gene silencing of somatic cells, it is possible to speculate that, not only methylation patterns, but also acetylation patterns, associated with changes in chromatin structure, will have to be "reprogrammed", after nuclear transfer, by the maternal histone acetylase, accumulated in mature oocytes (Ryan *et al.*, 1999). Female gametes accumulate large quantities of remodelling complexes involved in chromatin decondensation and acetylation, such as the SWI/SNF remodelling complex in *Drosophila*, and BRG1, a SWI/SNF like complex, in *Xenopus* (Gelius *et al.*, 1999). The role of these complexes in normal embryos development is to make sure that homeotic genes can be activated at the correct time, when ZGA takes place.

Nuclear transfer experiments in *Xenopus* showed that (Kikyo *et al.*, 2000) SWI/SNF-like complexes, also play a major role in the in the decondensation of the donor chromatin, at the time of nuclear swelling, suggesting that changes in chromatin conformation and creation of new patterns of acetylation are an important

part of the reprogramming process. Just like observed for methylation, incomplete or incorrect erasure of somatic acetylation/deacetylation patterns in donor cells might led to incorrect patterns of gene expression.

Quiescence might facilitate erasure of pre-existing acetylation patterns easier, increasing reprogramming efficiency. Terminally differentiated cells, such as erythrocytes (Dimitrov *et al.*, 1993) and T-lymphocytes (Pogo *et al.*, 1966), are quiescent (0-1% cycling), therefore they are transcriptionally inactive, with more than 90% of their histone H4 in an hypoacetylated form. However, to date there are no data in the literature comparing acetylation patterns of cloned embryos with those of control embryos, and assessing the possible influence of the donor cell cycle on these acetylation patterns.

Chromatin conformation is also determined by composition of histone and non-histone, chromatin proteins. Chromatin protein composition changes dramatically during development and differentiation, so that chromatin of differentiated cells differs greatly from that of embryonic cells. For this reason it not surprising that remodelling of the donor chromatin structure is an important element of nuclear reprogramming (Kikyo *et al.*, 2000). In the first hours after nuclear transfer, after Premature Chromosome Condensation (PCC), the donor nucleus doubles in size as the chromatin decondenses. This event, known as nuclear swelling, is considered the morphological expression of nuclear reprogramming and is thought to be essential for successful cloning (Kikyo and Wolffe, 2000; Kikyo *et al.*, 2000). Nuclear swelling results from the exchange of proteins between the nucleus and the cytoplasm. During nuclear swelling about 75-80% of proteins, associated with the donor chromatin, are removed by molecular chaperons (e.g. nucleoplasmin, N1/N2) and are replaced by other proteins contained in the oocyte cytoplasm. These changes in the donor chromatin make it, in a way, more similar to the sperm chromatin (Dimitrov and Wolffe, 1996; Kikyo and Wolffe, 2000). Sperm contains arginine-rich protamines, instead of somatic linker histones (H1), high levels of core histones H3 and H4 and low levels of H2A and H2B. During development, N1/N2 and nucleoplasmin remove protamines and add H2A and H2B core histones. At later stages of development somatic linker-histone H1 is also added.

In nuclear transfer experiments, after transfer of erythrocytes to *Xenopus* eggs, the somatic linker histones H1 and H1° are exchanged for the linker histone B4 and the chromatin structural protein HMG1, usually abundant in early embryos. No changes occur in the composition of somatic core histones, possibly because they are tightly bound to the chromatin (H3, H4, H2A, H2B). Removal of histone H1 has been described also in morula-stage nuclei after transfer to MII oocytes (Bordignon *et al.*, 1999).

Quiescence affects chromatin structure by modifying histone composition (Khochbin and Wolffe, 1994, Dimitrov and Wolffe, 1996). Terminally differentiated G0 cells, such as erythrocytes, contain the linker histone variant H1° (Khochbin and Wolffe, 1994), which is arginine-rich, just like sperm protamines, and for this reason has a greater affinity for nucleoplasmine and is removed from the chromatin more efficiently than histone H1 itself (Dimitrov and Wolffe, 1996). As a result of this, during reprogramming, G0 cells (e.g. erythrocytes) loose all their histone H1° and only part of their H1 variant.

The reprogramming process might target other proteins involved in heterochromatin-mediated gene silencing. Changes in chromatin structural proteins such as Polycomb group (PcG1) and the heterochromatin protein 1 (HP1), may also be required for reprogramming. Studies in *Xenopus* have shown that these proteins are absent in early embryos and appear only after gastrulation, inducing heterochromatin-mediated gene silencing in a tissue-specific manner (Strouboulis *et al.*, 1999).

Experiments in mouse have shown persistence of repressive chromatin structures in cloned embryos (Moreira *et al.*, 2002). In terminally differentiated cumulus cells, the nuclear protein AKAP95 associates with chromatin resistant to DNAse-I and NaCl treatment, suggesting a role in differentiation and heterochromatin gene silencing (Moreira *et al.*, 2002). In NT embryos AKAP95 colocalises with patches of heterochromatin and it is not extracted by nuclease treatment and NaCl treatment, whereas in ICSI and IVF embryos AKAP95 associates with euchromatin, therefore it is almost completely extracted by DNAse-I and NaCl treatment (Moreira *et al.*, 2002). This suggests that in reconstructed embryos proteins such as AKA95 may represent an obstacle to reprogramming by

maintaining the donor chromatin template in a more repressive state compared to normal IVF or ICSI embryos. Other structural proteins like HMG1 are exchanged for histone H1 by nucleoplasmine, at the time of nuclear reprogramming (Dimitrov and Wolffe, 1996).

Quiescence has a great effect on chromatin conformation and on the localisation of sub-nuclear distribution of chromatin structural proteins, and this may also affect the reprogramming process (Bridger *et al.*, 2000; Juan and Darzynkiewicz, 1998).

1.4 CHARACTERISATION OF DONOR CELLS USING G0 AND G1 MARKERS

For NT experiments it would very important to distinguish G0 from G1, in order to compare the efficiency of these two cell cycle stages for NT. However, there is a lack of specific markers of cell quiescence, which makes it difficult to obtain well-characterised populations of cells, either in a G0 or a G1 stage. For this reason donor cells used in most nuclear transfer experiments are defined as being in a G0/G1 stage, rather than at a G0 or G1 stage. Conventional methods of cell cycle analysis are not sufficient to discriminate between G0 and G1 cells. Univariate analysis of cellular DNA content using DNA specific dyes (Propidium Iodide, DAPI, Hoechst, etc) and flow cytometry, can be used to grossly identify cell position in the major phases of the cell cycle (G0/G1, S, G2/M). Nevertheless bivariate or multivariate analysis, where two or more parameters are measured simultaneously, becomes necessary when a more precise discrimination between cell cycle phases is required (G0 vs G1 or G2 vs M). Quiescent cells are either post-mitotic terminally differentiated cells (amphibian nucleated erythrocytes, Sertoli cells, neurons, cumulus cells), or mitotic cells made quiescent by serum deprivation or contact inhibition. Cells in G0 are characterised by a repressive chromatin conformation (heterochromatin; Bridger *et al.*, 2000; Juan and Darzynkiewicz, 1998), hypoacetylated histones (Pogo *et al.*, 1966) and reduced rates of transcription and protein synthesis (Boquest *et al.*, 1998). On the contrary, cells in G1 are characterised by an open chromatin template, more accessible to transcription

factors, prevalence of hyperacetylated histones and higher rates of transcription and protein synthesis than G0 cells. Besides G0 cells express specific cell cycle regulators and other quiescence markers that are not present in more activated G1 cells. In conclusion, although G0 and G1 have the same DNA content (2N), they can be distinguished by considering other discriminating features:

1) Transcriptional activity (histone acetylation, chromatin conformation): low in G0 cell, high in G1 and cycling cells;
2) Protein synthesis levels (reran content, protein content, cytoplasmic diameter): low in G0 cells, high in G1 and cycling cells;
3) Expression of cell cycle specific regulators: G0 cells lack G1 specific regulators (cyclin D1, cyclin E, p21) and express quiescent specific markers (p27, p130);
4) Cell type specific surface markers (Gas3, CD25, transferrin).

1.4.1 Cell cycle specific markers

Cell cycle progression is orchestrated by regulators and each cell cycle stage is regulated and characterised by a specific set of regulative molecules. Specific regulators of progression through G0 and G1 can be used to discriminate between these cell cycle stages.

The regulation of G0 and G1, like that of other stages, occurs at different levels. The first level is represented by proteins of the retinoblastoma family (pRb proteins), which act as negative regulators of cell cycle progression (review by Dyson, 1998). This family includes: the retinoblastoma tumour suppressor protein 1 (pRb1), involved in G1 progression (early/late G1 transition, G1/S transition); p130 or pRb2, involved in G0/G1 progression, and p107, involved in S-phase and G2/M progression. These proteins act as negative cell cycle regulators by repressing the expression of genes essential for cell cycle progression. Retinoblastoma proteins induce an E2F-mediated repression, as demonstrated by the fact that all the genes under their control have an E2F consensus-binding site in their promoter (Dyson, 1998). While pRb1 can bind all five E2F factors (E2F1-E2F5), p130 only binds E2F4, E2F5 and p107 only binds E2F5. Transcriptional repression can occur in two different ways: when E2F act as transcription repressors, retinoblastoma proteins act

as co-repressors, forming E2F/pRb repression complexes which block the promoter; when E2F act as transactivators, they are active when free and inactive when bound by retinoblastoma proteins. E2F4 and E2F5, which form complexes with p130, and, to a lesser extent, with pRb, repress the transcription of genes important for G0/G1 transition (E2F1, E2F2, HsOrc1, B-Myb) and are responsible for G0 maintenance. The important role played by p130 in the maintenance of the quiescent state had already been pointed out by Smith *et al.*, (1996) who also understood its potential as distinguishing marker between G0 and G1. Immunoprecipitation experiments have shown that E2F4 also forms complexes with p107, which inhibits S phase and G2 phase progression. E2F1, E2F2, E2F3, on the contrary, are transactivators of genes important for transition from early to late G1 (cyclin E) and G1/S transition (cyclin A). These factors are inactivated by pRb binding and activated by pRb phosphorylation, that leads to their release.

All the retinoblastoma proteins can be inactivated, and the blocks they represent removed, by phosphorylation. The phosphorylation of these proteins is carried out by cyclin-dependent kinases (Cdk), which therefore act as positive regulators of cell cycle progression. Cdk activity is periodical and is regulated in a cell cycle specific manner (Roberts *et al.,* 1994). Cdk activation requires two things: their association with regulatory subunits called cyclins, the levels of which fluctuate throughout the cell cycle; phosphorylation of Cdks by the Cdk-activating kinase (CAK; Morgan, 1995). Progression through early G1 is mitogen-dependent and pRb dependent, since it depends on the presence of growth factors and inactivating phosphorylation of pRb. The association between mitogenic signals and early G1 progression is achieved by the cyclin D1/Cdk4 and cyclin D1/Cdk6 complexes (Sherr, 1993). As a matter of fact cyclin D1 is short lived ($t_{1/2}$ 25 min) and for its synthesis it relies on growth signals rather than on intracellular stimuli (E2F factors for cyclin E and A). Furthermore, the D1/Cdk4 and D1/Cdk6 complexes are mainly responsible for pRb phosphorylation. Progression through late G1 is mitogen independent and partially pRb-dependent. During this stage the cyclin E/Cdk2 complex (Resnitzky and Reed, 1995; Ohtsubo *et al.*, 1995) completes pRb phosphorylation. The kinase activity of the cyclin A/Cdk2 complex is thought to mediate G1/S transition possibly by inactivating the p107/E2F4 complex and by de-

repressing the transcription of genes important for S-phase progression. The last level of regulation is represented by Cdk inhibitors (CKIs; Sherr and Roberts, 1995) that, by inhibiting Cdk activity, act as negative regulators of cell cycle progression. CKIs bind to cyclin-Cdk complexes and inhibit their catalytic activity either by preventing Cdk from binding cyclins or by inhibiting the activating phosphorylation of Cdks by CAK. Through Cdk levels remain constant throughout the cell cycle, their activity is periodical because of the fluctuations in the levels of cyclins and of CKIs occurring during the cell cycle.

CKIs are negative cell cycle regulators (review by Sherr and Roberts, 1995) and have been extensively studied by cancer researchers because they can act as tumour suppressor genes and their deregulation is implicated in a variety of malignancies (Nobori *et al.*, 1994; Guo *et al.*, 1997; Nakazumi *et al.*, 1998). CKIs are classified into two families, based on their protein sequence similarities and their putative Cdk targets: the INK4 and the CIP/KIP family. CKIs from the INK4 family ($p15^{INK4b}$, $p16^{INK4a}$, $p18^{INK4c}$, $p19^{ARF/INK4d}$) specifically bind Cdk6 complexes. CKIs from the CIP/KIP family ($p21^{CIP1/WARF1}$, $p27^{KIP1}$, $p57^{KIP2}$) are more promiscuous and are able to potently inhibit cyclin D1/Cdk4 and cyclin E/Cdk2 complexes, and, to a lesser extent, other complexes containing Cdk2 or Cdc2/Cdk1. CKIs up regulation can be induced by a variety of stimuli and leads to cell cycle arrest. Particularly important to distinguish between G0 and G1 are p21 and p27. The protein p27 plays a pivotal role in the induction and maintenance of the G0 state, as suggested by many observations. First of all p27 expression is induced by a variety of antimitogenic signals that induce quiescence, such as mitogen (e.g. IL-2, serum) starvation (Nourse *et al.*, 1994; Coats *et al.*, 1996; Coats *et al.*, 1999), cell-cell contact (St. Croix *et al.*, 1998), loss of cell anchorage, TGF-β (Polyak *et al.*, 1994a) and exposure to staurosporine (Kwon *et al.*, 1996). The levels of p27 are high in quiescent cells and decrease as cells re-enter the cell cycle in G1. In serum-starved Balb c/3T3 cells, p27 levels are undetectable in cycling cells but start increasing 4 hours after serum depletion, reaching 60% of the maximum concentration after 12 hours and peaking after 24 hours of serum starvation (Coats *et al.*, 1996). Similarly p27 is highly expressed in serum-starved human diploid fibroblasts (Nourse *et al.*, 1994) and mouse embryo fibroblasts (Coats *et al.*, 1999) but is completely degraded within 24

hours of serum re-stimulation. Other observations suggest that p27 function may be to associate antimitogenic signals with G0 arrest. Researchers have demonstrated that p27 depleted cells loose their ability to exit the cell cycle and continue to grow for several generations in serum free medium (Rivard *et al.*, 1996). Furthermore, p27 antisense cDNA suppresses quiescence in G0 cells (Rivard *et al.*, 1996). The mechanism through which p27 induces G0 arrest is probably by preventing the activation of G1 cyclin/Cdk complexes. It has been demonstrated that p27 binds tightly to cyclin D1/Cdk4 and to cyclin E/Cdk2 complexes and inhibits their activity in a stoichiometric manner (Polyak *et al.*, 1994b), either by preventing cyclin D1 and cyclin E binding or by preventing them from being phosphorylated and activated by CAK. The regulation of p27 expression in response to mitogenic/antimitogenic signals occurs on a translational and a post-translational level rather than on a transcriptional level. When cells enter quiescence p27 levels increase, as a consequence of an increased protein synthesis rate and a decreased proteolysis rate, while mRNA levels remain constant. When cells exit quiescence p27 protein levels decrease as a result of rate of decreased rate of translation and increased rate of degradation. Inactivation and degradation of p27 may involve a different process. Sequestering by cyclin D1/Cdk4, Cdk6, during early G1, and inactivating phosphorylation of p27 on Threonine 187 by the cyclin E/Cdk2 complex, during late G1, are thought to be two of them. It has been demonstrated that although p27 is primarily an inhibitor of cyclin E/Cdk2 kinase activity, in the presence of low concentrations of ATP (<50uM), when ATP concentrations approach physiological levels (>1mM) it becomes also a substrate for cyclin E/Cdk2 phosphorylating activity, resulting in its inactivation (Sheaff *et al.*, 1997). Degradation of p27 also occurs through the ubiquitin-proteasome pathway, which takes place in to steps: 1) transfer of ubiquitin to the p27, mediated by the ubiquitin–conjugating enzyme Cdc34 and a still unknown ubiquitin ligase; 2) proteasome-dependent degradation of ubiquitin tagged p27 (Pagano, 1997). The other member of the CIP/KIP family is the protein p21. Though it shares a great homology with p27, it has very different regulation and function. Unlikely p27 this protein is down regulated in G0 cells and is up regulated as cells re-enter the cell cycle in G1 (Nourse *et al.*, 1994). This suggests that while p27 regulates Cdk activity during quiescence, p21 regulates Cdk

activity in G1 proliferating cells, without contributing or contributing very little to the G0 arrest (Coats *et al.*, 1999). Just like p27, also p21 up regulation leads to G1 arrest, but under different conditions. This protein is in fact the primary mediator of the p53-dependent G1 arrest that occurs following DNA damage (El Deiry *et al.*, 1993) and of growth arrest of senescent cells (Noda *et al.*, 1994). Nevertheless p21 induces growth arrest with the same mechanism as p27, by inhibition of Cdk2/cyclin E and Cdk4/cyclin D1 complexes kinase activity. Unlikely p27, p21 regulation occurs at a transcriptional level.

Regulation of the G0 arrest by antimitogenic signals is cell type specific. In T-lymphocytes p27 is the only mediator of G0 arrest (Coats *et al.*, 1999). However, in mouse embryo fibroblasts (MEFs) p27 is still the primary regulator of G0 arrest but it is not the only one. Previous reports have demonstrated that in p27 null MEFs p21 is able to induce G0 arrest, though to a lesser extent than p27, and that in p27-p21 null MEFs p130, a member of the retinoblastoma family, is able to compensate, inducing complete arrest in G0 after serum starvation (Coats *et al.*, 1999). The important role played by p130 in the maintenance of the quiescent state had already been pointed out by other researchers who also understood its potential as a distinguishing marker between G0 and G1 (Smith *et al.*, 1996).

All these markers can be used to distinguish between cell cycle stages using either immunocytochemistry or flow cytometry techniques

1.4.2 Differences in chromatin conformation and acetylation

Quiescent cells are transcriptionally inactive whereas G1 cells have high levels of transcription. Since transcription is affected by chromatin conformation and acetylation G0 cells will have different acetylation patterns and a different chromatin conformation than G1 cells.

Quiescent cells are characterised by very low levels of histone acetylation. Terminally differentiated, G0 cells like erythrocytes, have such low levels of histone acetylation that they are commonly used as a negative control for acetylation since 90% of their histone H4 is in a mono or deacetylated form, and about 10% is in a diacetylated form (Dimitrov *et al.*, 1993). Other terminally differentiated cells, such

as T-lymphocytes have very low levels of acetylation, which rise dramatically after activation (Pogo *et al.*, 1966).

Nuclear chromatin conformation is also affected by the cell cycle. Chromatin is very condensed during mitosis (M) whereas it is maximally decondensed at the time of entrance in S-phase. Chromatin of G0 cells presents a high level of condensation, even if not as high as cells in M-phase. Changes in chromatin condensation are correlated with changes in DNA *in situ* sensitivity to denaturation. These changes can be detected using flow cytometry and staining with Acridine Orange (AO), a metachromatic fluorochrome, which differentially stains in green non-denatured (double-stranded) DNA and in red denatured (single stranded) DNA. Red fluorescence is associated with decondensed chromatin, whereas green fluorescence is associated with condensed chromatin (Juan and Darzynkiewicz, 1998). With this method cells must be treated with RNAse, which would otherwise be mistaken as single-stranded (denatured) DNA, and fixed before staining. This method has been successfully used to characterise and discriminate quiescent G0 T-lymphocytes from G1 and cycling T-lymphocytes (Juan and Darzynkiewicz, 1998).

1.4.3 Differences in RNA content, protein levels, cell size

Under different experimental conditions AO can be used to distinguish G0 and G1 cells based on their RNA content. As a matter of fact total RNA content is largely composed by ribosomal RNA, and is therefore an estimate of ribosome synthesis and ultimately of protein synthesis. At appropriate concentrations and stringent ionic conditions, AO intercalation into double stranded DNA results in green fluorescence, whereas its binding to single stranded RNA results in red fluorescence (Juan and Darzynkiewicz, 1998). With this system neither RNAse digestion nor fixation is required, but cells must be permeabilised in order for the dye to penetrate the cell membrane and reach the intracellular compartment. The problem with both these methods are that they require very stringent conditions (e.g. dye concentration) that are difficult to obtain because AO is a very unstable dye that tends to attach to plastic ware and then to go back into suspension (Juan and Darzynkiewicz, 1998). However, this method has been used successfully in human T-lymphocytes to compare DNA and RNA content of: freshly isolated, G0 T-

lymphocytes; mitogenically stimulated, cycling T-lymphocytes; T-lymphocytes synchronized in G1 by mitogenic stimulation in the presence of G/S blocking agents. T-cells in G1 had the same DNA content of G0 cells but a content of RNA (mean=60) intermediate between quiescent (mean=50) and activated T-cells (mean=95).

Simultaneous assessment of cell size and nuclear size can also be used to discriminate G0 and G1 cells (Firpo *et al.*, 1994). Nuclear size is correlated with DNA content, whereas cell size is correlated with cytoplasmic protein synthesis. Mean nuclear and cytoplasmic diameters can be measured by flow cytometry and AO staining for DNA/RNA. For this purpose the fluorescent width (FL-W) will have to be considered instead of the fluorescence intensity (FL-H) and green nuclear DNA staining (FL1-W), will be used as a measure of the nuclear size, and the red cytoplasmic RNA staining, will be used as a measure of cytoplasmic size (FLW-3). This method was used to discriminate human T-lymphocytes (Firpo *et al.*, 1994) in G1 and G0. T-cells in G1 and G0, both diploid had the same mean nuclear size (96 vs97), but G1 T-cells had a significantly larger cell size (mean=78), intermediate between that of G0 T-cells (mean=61) and activated T-cells (mean=100).

Another way of distinguishing G0 and G1 cells on the basis of their different protein synthesis rates is by measuring simultaneously DNA content and total protein content. Using this method, researchers showed that serum-starved pig foetal fibroblasts had 87.5% diploid cells (G0/G1), and 48.3% of cells in G0, while contact-inhibited cells had 85.1% diploid cells (G0/G1) 6% G0 cells (Boquest *et al.*, 1999). The main criticism of this method is that protein content in itself is not only correlated with protein synthesis rates but also it is also correlated with cell size. This is also suggested by the fact that the percentages of G0 cells, with low protein content, increased significantly as cell size decreased (Boquest *et al.*, 1999). This could have meant that small cells simply had lower amount of proteins than larger cells, without any difference in protein synthesis.

1.4.4 Surface markers

There are very few surface markers of quiescence and they tend to be cell type specific. In T-lymphocytes quiescent cells do not express the high affinity

interleukin-2 receptor (IL-2α or CD25) and the transferrin receptor (Tf-R; Firpo *et al.*, 1994). These receptors, however, are up regulated after activation, so that a significantly higher number of G1 cells and cycling cells will express CD25 and Tf-R compared to G0 cells (Firpo *et al.*, 1994). So CD25 and Tf-R can be used as negative markers of T-cell quiescence. To date there is only surface, positive marker of cell quiescence. It is a transmembrane protein encoded by the growth arrest-specific gene 3 (Gas3). The Gas genes were first identified in G0 growth arrested mouse NIH3T3 cells (Schneider *et al.*, 1988). Among the Gas genes, Gas3 is the only gene to encode a transmembrane protein (D'Urso and Muller, 1997). The Gas3 gene is up regulated in serum-starved or contacted inhibited G0 fibroblasts on both a transcriptional and translational level (Karlsson *et al.*, 1999). At the moment there are no antibodies commercially available against the protein encoded by the Gas3 gene. However specific antibodies recognising this protein could be produced since this protein has two hydrophilic extracellular domains.

1.5 GENERAL AIMS OF THE PROJECT

1) Find a suitable mouse cell model which can be used to produce well-characterised donor cell populations in G0 and G1 (Chapter 3-5).
2) Transfer G0 and G1 cells to MII oocytes, and produce nuclear transfer mouse embryos (Chapter 6).
3) Compare effect of G0 and G1 on epigenetic changes occurring in the donor nuclei before and after nuclear transfer, focussing on events occurring around the time of reprogramming (1-4-cell stage: Chapter 6).
4) Compare developmental potential of G0 and G1 cells after nuclear transfer (Chapter 6).

CHAPTER 2

GENERAL MATERIALS AND METHODS

2.1 MOUSE FOETAL FIBROBLAST ISOLATION AND SUB-CULTURE

Mouse Foetal Fibroblasts (MFF) were generated from 14-day post-coitus mouse foetuses, of the 129 inbred strain. A total of 15 foetuses were isolated from two female mice. Foetuses were collected in 25ml tubes containing 10ml Phosphate Buffered Saline (PBS; A.1.2), supplemented with 0.2% (v/v) gentamicin 50mg/ml. Foetuses were processed individually. The heads and internal organs of the foetuses were removed and the carcasses rinsed in PBS supplemented with 0.1mg/ml gentamicin. The carcasses were then minced with scissors in a 60mm tissue culture dish (Nunclon) containing 0.25% trypsin/0.04% EGTA (w/v) solution (A.1.3), and incubated at 37°C for 3-5 min. After digestion the cells were resuspended in fresh medium and centrifuged at 200g for 5 min. The pellet was then resuspended in 6ml of culture medium, containing Dulbecco's Modified Eagle's Medium (DMEM) with 10% foetal calf serum (FCS; Globepharm), 2mM L-glutamine, 1mM Sodium pyruvate, 1% (v/v) Mem-amino acids, 0.05mg/ml gentamicin (A.1.1), and plated into 25cm^2 (IWAKI) tissue culture flasks (passage 0). All chemicals used were purchased from Gibco, unless otherwise specified. After 24 hours at 37°C with 5% CO^2, the medium was changed with fresh, culture medium without gentamicin. Cells reached confluence in 24h-72h (maximum time observed 6 days). When 85% confluent, cells were trypsinized and either frozen at passage 0 (total 3-4x10^6 cells/flask, 4-5 vials/flask), or split 1:3 into 75cm^2 tissue culture flasks (IWAKI) and frozen at passage 1 (total 9-10x10^6 cells/flask, 16-18 vials/flask). For freezing cells were trypsinized, washed once with medium and resuspended in 10% FCS medium at a concentration of 1x10^6/ml. The cell suspension was diluted 1:1 with freezing mix, containing 1 part FCS, 1 part DMSO (Hybri-max; Sigma D 2650), 2 parts culture

medium and dispensed into vials (0.5ml/vial). Vials were stored at –80°C overnight, and then at–196°C.

Freezing reduced cell viability. Viability was checked by diluting 100ul of cell suspension 1:2 in 0.5% (w/v) Trypan blue in 0.85% saline solution (Flow Laboratories), and live cells were counted (Trypan blue negative cells) using a haemocytometer. Average viability in frozen/thawed cells was 83.3±8.7%, ranging from 95% to 70%. These values were lower than those found in cultured cells with an average viability of 98.3±0.7% and a minimum observed viability of 97%. However, cells managed to recover in culture, but their ability to recover appeared to be negatively correlated with the time spent in liquid nitrogen.

Each vial contained enough cells ($0.58\pm0.18x10^6$/vial) to plate in a $25cm^2$ flask at a concentration of $23\pm7x10^3/cm^2$, reaching confluence in about 2 days. At confluence cells reached concentrations of $60\text{-}80x10^3/cm^2$ ($1.5\text{-}2x10^6$cells/$25cm^2$ flask, $5\text{-}6.5x10^6$cells/$75cm^2$flask). Cells were usually seeded at a concentration of $14\text{-}15x10^3/cm^2$ (split 1:4; $0.35x10^6$cells/$25cm^2$ flask; $1.05x10^6$cells/$75cm^2$ flask), reaching confluence in 48 hours (passage 0-2) and 72h (passage 3-5). In some experiments cells were also seeded at a concentration $20\text{-}2510^3/cm^2$ (split 1:3) and reached confluence in 48h or at a concentration of $10^4/cm^2$ (1:6) and reached confluence in 96 hours.

2.2 SELECTION OF MOUSE FOETAL FIBROBLAST CELL LINES

Cell line normality was assessed on the basis of karyotyping results (Paragraph 2.3) morphological assessment and life history in culture. Only cell lines that had retained a normal chromosome number (n=40) for at least 4-5 passages in culture were selected. Mouse embryonic stem cells (ES-cells) are karyotipically very stable. The karyotype of a mouse embryonic stem cell line, isolated from the 129 inbred strain (129 ES-cell), that had reached a population doubling level (PDL) of 27 (9 passages, split 1:6), was used as a control. Two out of nine MFF cell lines (MFF1, MFF2) were excluded from further analysis because at passage 2 they had a percentage of normal spreads (46%, 56%) significantly lower than controls (78%,

Table 2.1 Karyotype of Mouse Foetal Fibroblast cell lines

Cell line	Early passage	PDL	% Normal	Late passage	PDL	% Normal	% Loss/PD
129 ES	p9	27	78.0[a]	-	-	-	-
MFF1	p2	3	46.0[b]	-	-	-	-
MFF2	p2	3	56.0[b]	-	-	-	-
MFF3	p2	3	62.5[a]	p4	6.0	58[b]	0.8
MFF4	p2	3	70.0[a]	p4	6.0	54[b]	2.6
MFF5	p2	3	64.0[a]	p6	9.0	53[b]	1.2
MFF6	p2	3	64.0[a]	p4	6.0	50[b]	2.3
MFF7	p2	3	66.0[a]	p5	7.5	50[b]	2.1
MFF8	p2	3	74.0[a]	p5	7.5	68[a]	0.8
MFF9	p2	3	78.0[a]	p4	6.0	71[a]	1.2
Mean±SD	-	-	**64.5±9.5**	-	-	-	**1.6±0.8**

The karyotype of Mouse Foetal Fibroblast (MFF) was checked by counting 50-100 spreads/8 slides for each cell line and calculating the proportion of spreads with a normal chromosome number (n=40; % normal). Es-cell lines are karyotipically very stable. A 129 ES-cell line, karyotyped at 27 population doubling level (27 PDL; passage 9, split 1:6) was used here as a control. MFF cell lines were karyotyped at an early passage and, if found normal, were also karyotyped at a later passage. PDL indicates the population doubling levels or cumulative population doublings, corresponding to each passage. Cell lines that retained normal karyotype (MFF8, MFF9), at least up to passage 4, were selected for the following experiments. The percentage of cells that became karyotipically abnormal after each population doubling (%loss/PD) was also calculated using the formula: (% Normal at an early passage-% Normal at a late passage)/(PDL at a late passage - PDL at an early passage). Cells with different superscripts have significantly different percentages of karyotipically normal cells (two-tailed, Chi-square test, α=0.05).

$p \leq 0.001$; Table 2.1). Two of the remaining seven cell lines, MFF 8 and MFF9, retained a normal karyotype respectively till passage 5 (68%, p=0.26) and 4 (71%, p=0.36), corresponding to a population doubling level of 7.5 and 6 (Table 2.1). The average loss of cells with normal karyotypes at each population doubling was 1.6±0.8% (mean±SD; Table 2.1).

Life history of the two selected cell lines, MFF8 and MFF9, was assessed by thawing a vial from each cell line at passage 1. At each passage cells were split 1:3, and two $25cm^2$ were kept in the incubator, to reduce contamination risks. At each passage cells were counted and viability assessed using the Trypan blue exclusion method. It was possible to calculate:

1) Percentage of live cells, corresponding to percentage of Trypan blue negative cells;
2) Population Doublings (PDs), calculated using the formula: PDs=3.32x(Log10Nc-Log10Ns), where Ns and Nc correspond respectively to cell counts obtained at the time of seeding and confluence (Doyle *et al.*, 1998);
3) Doubling Time (DT), calculated using the formula: DT=days/PDs, where days indicate days taken to reach confluence and PDs population doublings occurred before confluence (Doyle *et al.*, 1998).

Changes in cell morphology were also noted.

The cell line MFF8 (Fig.2.1) was sub-cultured for 45 days, up to passage 7 (split 1:3, PDL 10.2). The cell line MFF9 (Fig.2.1) was sub-cultured for 130 days, up to passage 30 (split 1:3, PDL 56). Three phases were identified in the life history of these cell lines (Fig.2.1), accordingly to previous reports (Doyle *et al.*, 1998; Todaro and Green, 1963):

1) **Normal**, up to passage 3 (PDL≤7.2) and with an average doubling time of 1.96±0.32 days (±SD) for MFF8; up to passage 4 (PDL≤8.4), with a doubling time of 1.4±0.2 days for MFF9 ;
2) **Senescence**, between passage 4 and 5 (PDL 7.1-8.6), with a doubling time of 3.52±0.78 days (±SD) for MFF8; between passage 5 and 10 (PDL 10.2-16.8), with a doubling time of 4.7±2.9 days for MFF9;

Figure 2.1 Life history of selected Mouse Foetal Fibroblast cell lines

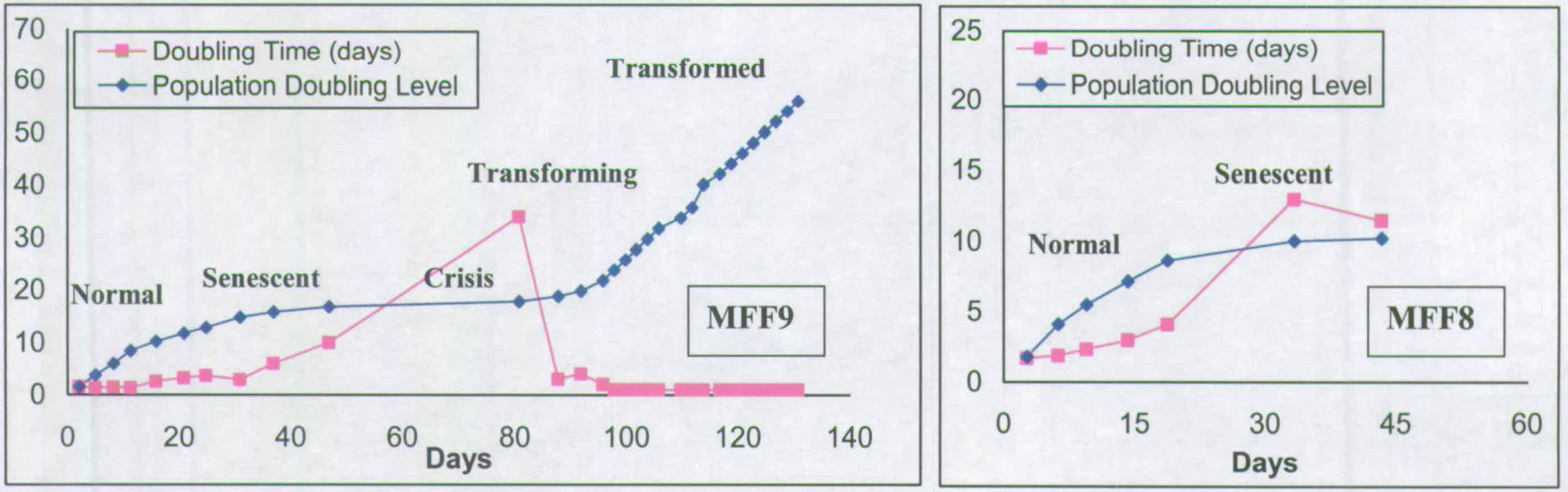

Figure 2.2 Morphological changes in cultured Mouse Foetal Fibroblasts

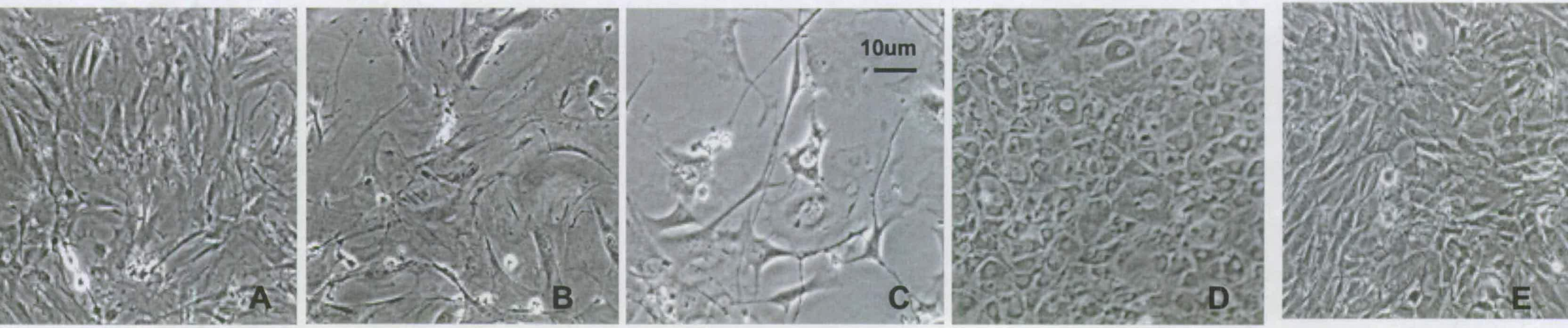

Figure 2.1 Cell lines MFF9 and MFF8 were sub-cultured respectively for 130 days (30 passages) and 43 days (7 passages). Each pink dot corresponds to a passage. At each passage cells were counted and their doubling time (pink line), and cumulative population doubling or population doubling level (PDL; blue line) were calculated. Based on PDL and doubling time, five cell categories were identified in MFF9: normal cells, up to passage 4 (PDL 8.4), with a doubling time of 1.4±0.2 days; senescent cells, between passage 5 (10.2 PDL) and 10 (16.8 PDL), with doubling time of 4.7±2.9 days; crisis at passage 11 (17.8 PDL), with a doubling time of 34 days; transforming cells between passage 12 (19.8 PDL) and passage 14 (23.8 PDL), with a doubling time of 3.0±1.0 days; transformed cells, beyond passage 15 (25.8 PDL), with a doubling time of 1±0. In the MFF8, kept in culture for a shorter period of time, only a normal and a senescent-phase were identified.

Figure 2.2 Brightfield images showing morphological changes in cultured Mouse Foetal Fibroblasts. Compared to normal fibroblasts (A), senescent fibroblasts (B) and cells at crisis point (C) appeared to be elongated and enlarged. During transformation fibroblasts acquired a transient polygonal shape (D) and, finally, a shape resembling that of young fibroblasts, small and elongated (E).

3) **Crisis**, between passage 6 and 7 (PDL 10.0-10.2), with a doubling time of 12.2±1.1 days (mean±SD) for MFF8; at passage 11 (PDL 17.8), with a doubling time of 34 days for MFF9.

In the case of the cell line MFF9, that was sub-cultured for 130 days, the emergence of a transformed cell population was also observed (Fig.2.1). The appearance of two cell populations followed the crisis phase:

4) **Transforming cells**, between passage 12 and 14 (PDL 19.8-23.8), with a doubling time of 3.0±1.0 days (±SD), shorter than that of senescent cells but still longer than that of normal cells;

5) **Transformed cells**, beyond passage 15 (PDL≥25.8), with a doubling time of 1±0.

Changes observed in doubling time were associated with changes in cell morphology (Fig.2.2). Compared to normal fibroblasts (Fig.2.2A), senescent fibroblasts and fibroblasts at crisis point appeared flattened out and enlarged (Fig.2.2B-C). During transformation, clusters of fibroblasts acquired a transient polygonal shape (Fig.2.2D) and, after transformation, a shape resembling that of young fibroblasts, small and elongated (Fig.2.2E).

The β-galactosidase (β-Gal) staining (Paragraph 2.4) was used as a biomarker of senescence, to confirm the senescent state of MFF8 and MFF9. Senescent sheep foetal fibroblasts, isolated from Black Welsh foetuses at passage 45 (split 1:4, PDL=90), were used as a positive control. Senescent MFF, unlike sheep foetal fibroblasts, appeared to be β-Gal negative. This might be due to species differences. The β-galactosidase staining has been effectively used in sheep and human foetal fibroblasts, that senesce after 100-50 PDs and then die off, without the emergence of immortalized cells. Mouse foetal fibroblasts, however, age very early and then transform. This difference associated with the fact that transformed cells are β-Gal negative, might explain this discrepancy.

Based on all these considerations the cell lines MFF8 and MFF9 were selected for synchronization experiments and used up to passage 4, beyond which they tend to senesce and transform.

Features observed in the selected MFF cell lines were similar to those described in the literature (Todaro and Green, 1963; Doyle *et al.*, 1998): normal

features up to 8-10 generations, with a doubling time of 30-60h; senescence and crisis at 10-15 PDs, with a doubling time of 100h or more; transformation at 15-30 PDs, marked by shortening of the doubling time to 14-24h and emergence of a tetraploid population.

2.3 KARYOTYPING

Karyotype of mouse foetal fibroblast primary cell lines was assessed at passage 2 and passage 4 (Fig.2.3). In contact inhibition experiments karyotype of cells that had been kept under contact inhibition for different length of time, at passage 3, were passaged and karyotyped at passage 4.

Cells were plated in $25cm^2$ tissue culture flasks and, when 40-50% confluent, they were trypsinized, washed once with 10% FCS culture medium, gently resuspended in 0.75% (w/v) Na_3citrate $2H_2O$ (BDH) hypotonic solution and incubated at room temperature for 10min. After centrifuging 5min at 200g, cells were fixed for 5min with ice cold, methanol: acetic acid (3:1) solution. After centrifuging at 200g, for 5min, and fixing other two times, cells were smeared onto ice cold 76x26mm glass microscope slides (Blue Star, UK) and, once dry, stained with 3% (w/v) Giemsa (BDH) for 11min. Slides were read using a 100x Fluor oil objective (Nikon), on a Nikon Microphot-SA microscope, and reading 50-100 metaphase plates for each cell line (Fig.2.3).

2.4 β-GALACTOSIDASE STAINING

The β-galactosidase (β-gal) staining was performed as previously described (Dimri *et al.*, 1995). Cells were washed once with PBS and fixed for 3-4min at room temperature with 2% (w/v) formaldehyde and 0.2% (w/v) glutaraldehyde (A.1.4). Cells were washed twice with PBS and stained with 1mg/ml X-gal (Promega) solution in 40mM Na_2HPO_4/citric acid, 5mM Potassium ferrocyanide (Sigma), 5mM Potassium ferricyanide (Sigma), 150mM NaCl, 2mM $MgCl_2$ (A.1.4). Staining was carried out at 37°C, for a minimum of 2-4h and a maximum of 12h-16h. β-gal positive cells had blue nuclei and blue cytoplasm in the perinuclear region.

Figure 2.3 Karyotyping of Mouse Foetal Fibroblasts

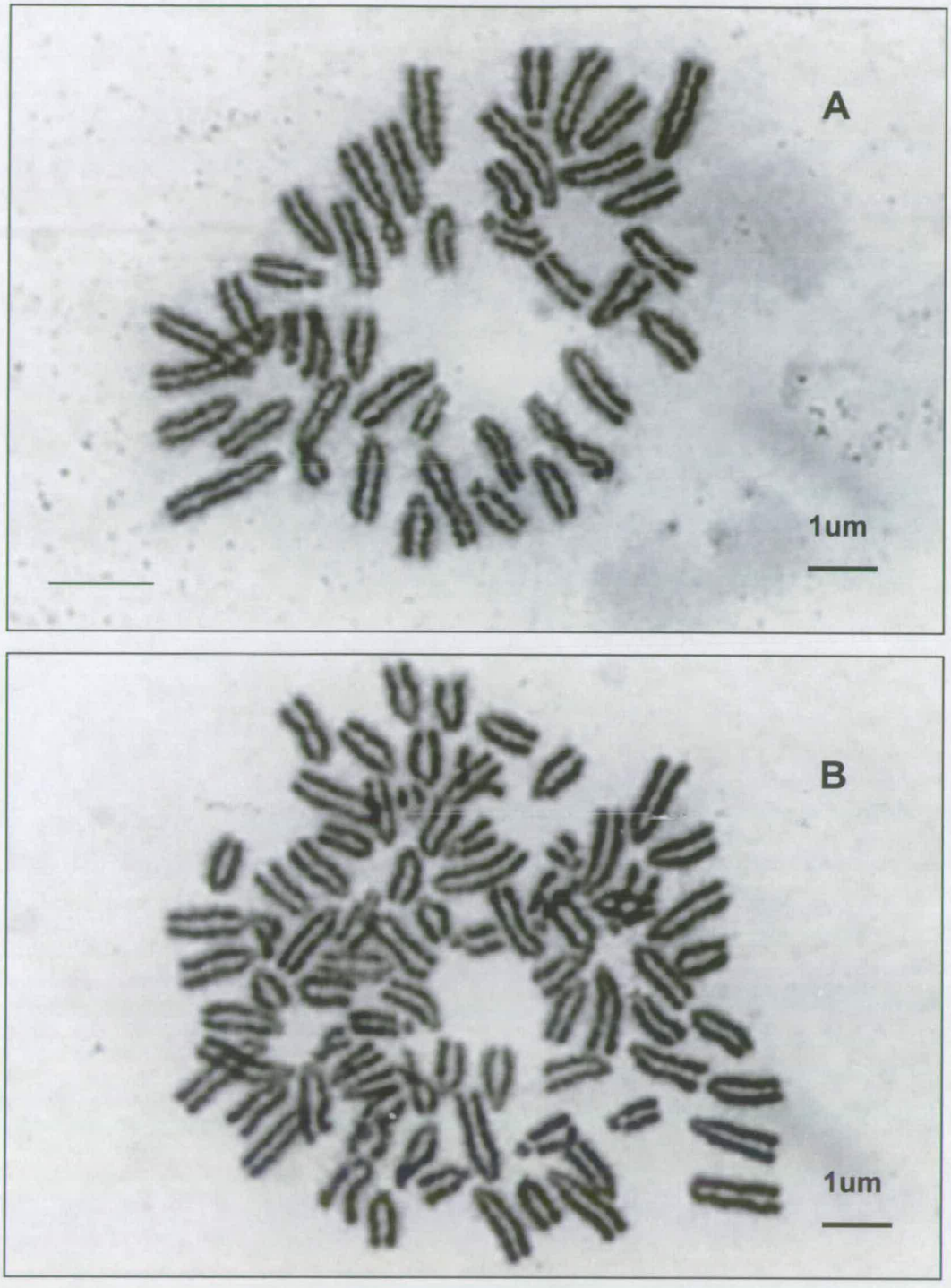

Black and white images of Mouse Foetal Fibroblasts with normal (A; n° chromosomes = 40) and abnormal (B; n° chromosomes = 80) karyotype. Cells were processed as described in paragraph 2.3 and stained with 3% (w/v) Giemsa. Visual examination was carried out with a Nikon Microphot-SA microscope equipped with a 100x oil objective.

2.5 SYNCHRONIZATION OF MOUSE FOETAL FIBROBLASTS IN G0 AND G1

In serum starvation groups, cells were seeded at a low concentration of 10-11x0^3/cm^2, corresponding to 43x10^3cells/2ml/well, in 12 well plates (3.8cm^2/well; IWAKI), for immunocytochemistry, or 0.75x10^6/75cm^2 flasks (IWAKI), in flow cytometry experiments. Cells were cultured with 10% FCS culture medium, for 48h-72h, until they were 50-60% confluent, and then serum-starved. For serum starvation cells were washed two times with PBS and three times with serum starvation medium, and then left incubating in serum starvation medium prepared like culture medium, but with 0.5% FCS or 0.1% FCS. Cells in the control groups (cycling), were sub-confluent cells that had been cultured in 10% FCS medium for 48h-72h, before being fixed and processed.

In contact inhibition experiments cells were seeded a high density of 22.5x10^3/cm^2, corresponding to 45x10^3cells/1ml/well in 24 well plates (1.9cm^2/well), with 1 coverslip/well in PCNA experiments, and 0.55x10^6 cells/25cm^2 flasks, in flow cytometry experiments. Cells were cultured in 10% FCS medium that was changed every 48h. Cells in the control groups (cycling), were sub-confluent cells that had been cultured in 10% FCS medium for 24h, before being fixed and processed.

In G1 synchronization experiments, cells were seeded at an average density of 14x10^3/cm^2, corresponding to 14x10^4cells/0.5ml/slide, placing each slide in a 55cm^2 dish. Slides were incubated for two hours, to allow cells to adhere, before adding, to each dish, 12ml of 10% FCS medium supplemented with the following blocking agents (A.1.5): 400uM-800uM mimosine (Sigma); 1mM, 2mM, 4mM hydroxyurea (Sigma); 0.1uM, 1uM, 2uM methotrexate (Sigma); 5uM, 15uM, 30uM lovastatin (Calbiochem). For flow cytometry, in experiments where hydroxyurea was used as synchronizing agent, cells were seeded in 25cm^2 flasks, in 10% FCS culture medium and 4mM hydroxyurea was added after 2h. Control, cycling cells, were cultured in 10% FCS culture medium, without chemicals, for 24h and 48h. Lovastatin stock was diluted in absolute ethanol, so appropriate lovastatin controls (A.1.5), with the same ethanol concentrations but no lovastatin, were also included:

0.04ul ethanol/ml (control for 5uM lovastatin); 0.12ul ethanol/ml (control for 15uM lovastatin); 0.24ul ethanol/ml (control for 30uM lovastatin).

2.6 FLOW CYTOMETRY OF MOUSE FOETAL FIBROBLASTS

Each sample for flow cytometry contained 0.5-1x10^6/0.5ml. Treatment greatly affected the cell yield. A sample for flow cytometry was obtained from half of a 25cm^2 flask of contact-inhibited cells (2.5x10^6/flask), one 25cm^2 flask of cycling cells (0.6-1.2x10^6/flask) and a 75cm^2 flask of serum-starved cells (0.45-0.89x10^6/flask, average 0.7x10^6). The limited number of passages available for expansion, the high number of cells required for each sample, and the need to include appropriate isotype controls, made these experiments difficult to carry out.

Double staining with **Propidium Iodide** (PI) and **Fluorescein isothyocyanate** (FITC) was performed using a modified method by Boquest *et al.* (1999). About 0.5-1x10^6 cells were resuspended in 100ul of cold, "Saline GM", (6.1mM D^+-glucose, 137mM NaCl, 5.4mM KCl, 1.5mM Na_2HPO_4 $7H_2O$,0.9mM KH_2PO_4, 0.5mM EDTA, in dH_2O; A.3.1) and fixed by adding, dropwise, while vortexing, 4ml 100% methanol (-20°C). After an overnight fixation at –20°C, samples were centrifuged at 300g, for 6min, and washed with 5ml 5mM EDTA in Dulbecco's Phosphate Saline (D-PBS; A.3.1). Cells were stained 1h, at room temperature, with 400ul in staining solution with 20ug/ml PI (Sigma), 100ug/ml RNAse (Sigma) 0.02ug/ml FITC (Sigma) and 0.1% (w/v) NaN_3 in D-PBS (A.3.4). For double staining with **PI** and **p130** cells were fixed in 100% methanol (-20°C), as previously described. For double staining with **PI** and **$p27^{KIP1}$**, samples were fixed in 75% ethanol, by resuspending cells in 1ml cold, "Saline GM" and adding 3ml 100% ethanol, dropwise, while vortexing. After an overnight fixation at –20°C, samples were centrifuged at 300g for 6min, and washed with 5ml D-PBS. Samples were gently resuspended in 0.5ml of 0.25% (v/v) TritonX-100 (Sigma) and 0.1% (w/v) Sodium azide (NaN_3; Sigma) in D-PBS (permeabilising buffer) and incubated 10min, on ice. Samples were washed once with 5ml D-PBS, and incubated 20min, at room temperature in 5ml, D-PBS with 0.1% (w/v) NaN_3 (pH7.3) and 5% goat serum or 2%

FCS, for PI/p27 or PI/p130 staining respectively (blocking buffers). After centrifuging at 300g for 6min, cells were incubated 30min, at 4°C with 3ug/10^6 cells FITC-conjugated mouse anti-p27 (Neomarkers; A.4.1). Alternatively samples were incubated 60min, at room temperature, with 2ug/10^6 cells rabbit anti-human p130 (IgG; Santa Cruz; A.4.1), washed once with D-PBS, and incubated for 60min, at room temperature with 2ug/10^6 FITC-conjugated goat anti-rabbit IgG (Santa Cruz; A.4.2). Controls included: unstained samples and samples incubated with the isotype controls, 3ug/10^6 FITC-conjugated mouse IgG1 (Caltag; A.4.3), and 2ug/10^6 rabbit IgG (Santa Cruz; A.4.3). All antibodies were diluted in blocking buffer. All samples were washed once with 5mM EDTA and incubated 1h, at room temperature, in the dark, with 0.4ml PI solution, with 20ug/ml PI, 100ug/ml RNAse and 0.1% (w/v) NaN_3 in D-PBS (A.3.15). Data were acquired using a FASCan (Becton Dickinson), equipped with an Argon laser line (excitation wavelength 488nm,) and FL3 (emission wavelength 640nm) and FL1 (emission wavelength 520nm) filter sets, respectively for PI (red, peak emission 617nm) and FITC (green, peak emission 520nm). For each sample 10000 events were acquired. Analysis was performed using the CellQuest program (version 3.01, Becton Dickinson). Doublets Discrimination Module was used to exclude cell aggregates from the analysis. Propidium Iodide was used to analyse the following parameters: percentages of apoptotic cells and polyploid cells; percentages of G0/G1, S and G2/M-phase cells. The percentages of $FITC^+$, $p130^+$ and $p27^+$ cells, as well as mean fluorescence and peak fluorescence values were analysed. Expression of markers was evaluated in the whole cell population as well as in sub-population of cells, at a specific cell cycle stage.

2.7 ISOLATION, ACTIVATION AND SYNCHRONIZATION OF T-LYMPHOCYTES

Lymphocytes were isolated from the spleen, thymus and lymph nodes, of 6 week old, CBA/Ca female mice (Chapter 4 and 5), killed by cervical dislocation or CO_2 inhalation, using a modified method previously described (Mishell *et al.*, 1980; Fig.2.4). In some experiments lymphocytes were also isolated from the lymph nodes of C57BL/6 (Chapter 5 and 6), and (C57BL/6xCBA/Ca)F1 (Chapter 6). Animals

Figure 2.4 Murine lymphoid tissues

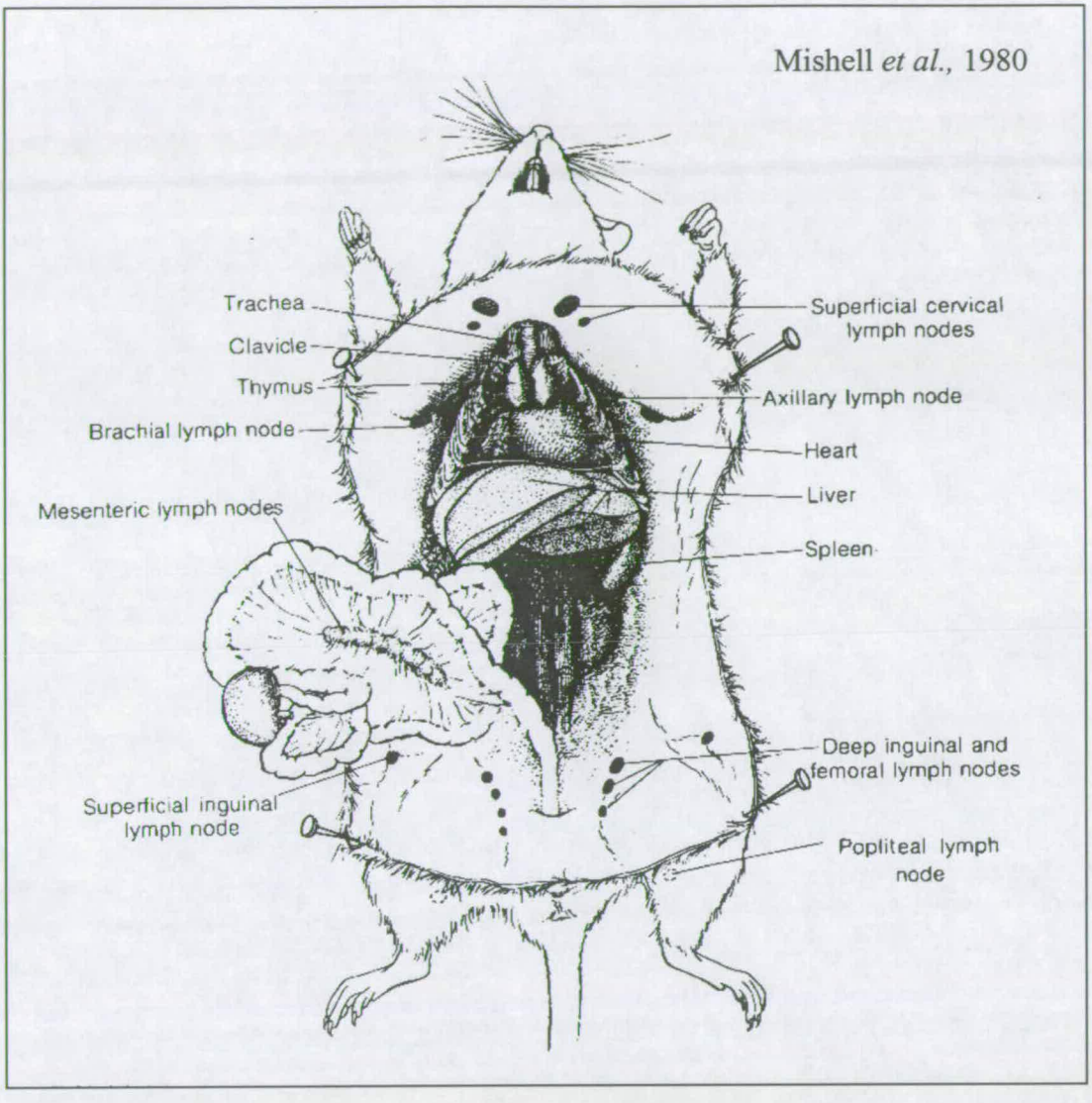

Sites of collection of murine lymphoid tissues. In the experiments described in this project, the following lymphoid tissues were used as a source of T-lymphocytes: thymus; spleen; axillary, brachial and superficial inguinal lymph nodes.

Table 2.2 Proportion of T-lymphocytes in different lymphoid tissues

	Cells/animal ($x10^6$)	T-cells (%)	T-cells/animal ($x10^6$)
Lymph nodes	10.7 ± 3.4^a	90.4 ± 3.1^a	9.7 ± 3.3^a
Spleen	78.5 ± 13.4^b	42.3 ± 7.6^b	32.7 ± 4.0^b
Thymus	187.5 ± 65.0^c	63.6 ± 19.0^c	122.1 ± 65.0^c

Data from three replicates (Chapter 4) are expressed as mean values ± SD. Values within columns with different superscripts differ significantly (1-way ANOVA; Statistica, Windows, 1995; $p<0.05$).

were placed on their back, the skin was sterilised with 75% ethanol. After making a small cut in the pelvic region, the body was stripped of the skin by pulling the two flaps of skin in opposite directions. Axillary, brachial and superficial inguinal lymph nodes (Fig.2.4), appearing like firm translucent bumps, were exposed, by tearing the muscle and fat tissue around them and placed in 20ml tube containing Dulbecco's Phosphate Buffered Saline (D-PBS), without Ca^{2+} and Mg^{2+} and without preservatives (A.2.2). After opening the peritoneal cavity, the spleen (Fig.2.4) was lifted with forceps, freed of the vessels and connective tissue around it with curved scissors, and placed in a 20ml tube with D-PBS. To access the thymus (Fig.2.4), the diaphragm was removed and the ribcage was opened and folded it black, towards the head. The thymus, placed just behind the heart, was lifted with forceps, removed, using curved scissors, and placed in a 20ml tube with D-PBS. Lymphoid tissues could be stored at room temperature for a few hours. The tissue samples were homogenized, in fresh D-PBS, under laminar flow, using a 5ml homogeniser (Jencon). After allowing clumps to settle for a few minutes, the supernatant was transferred to a 15ml tube, and washed once with D-PBS, at 400g, for 10min, and once with culture medium (A.2.1), containing 10% heat inactivated FCS (Globepharm), RPMI-1640, 2mM L-glutamine, 1mM Na-pyruvate, Non-essential amino acids, 100units/ml penicillin and 0.01mg/ml streptomycin. In most experiments culture medium was also supplemented with $5x10^{-5}M$ 2-mercaptoethanol. All reagents for T-cell culture were purchased from Sigma, unless otherwise indicated. White blood cell counts were performed by diluting 100ul of cell suspension 1:2 with Turk's solution (A.2.5), incubating a few seconds, to remove red blood cells, and counting with a haemocytometer or a coulter counter. Freshly isolated cells were also stained for CD3, Gr1 and B220, to assess, respectively, the proportion of T-lymphocytes, B-lymphocytes and myeloid cells (granulocytes and monocytes) in the different lymphoid tissues. The lymph nodes were the lymphoid tissue with the lowest cells yield and the highest percentage of $CD3^+$ cells (T-lymphocytes; Table 2.2). The different lymphoid tissues also contained: 18.2±8.6 % B-lymphocytes and 10.8±8.4% myeloid cells, in the lymph nodes; 48.8±5.5% B-lymphocytes and 18.0±5.3% myeloid cells, in the spleen; 2.0±1.5% B-lymphocytes and 2.4±0.9% myeloid cells, in the thymus.

Differences among mouse strains were only observed in the total cell yield that was higher from lymph nodes of F1 mice (12.1±0.6x10^6/animal) compared to CBA/Ca (5.2±2. 6x10^6/animal) and C57BL/6 (6.6±0.6) inbred strains. The percentages of $CD3^+$ cells were equally high in lymph nodes from different mice strains (>83%).

Cell concentration was adjusted to 10^7/ml. Cells were seeded in 24 well plates at a concentration of 2x10^6/ml/well. Concentrations of 10^6/ml or 5x10^6/ml appeared to be sub-optimal. In activation and PHA titration experiments cells were cultured with phytohemagglutinin (PHA; Sigma) at concentrations between 0.8ug/ml and 16ug/ml (A.2.3), with or without 4nM interleukin-2 (IL-2, Sigma; A.2.4). In synchronization experiments with hydroxyurea (HU), 0.5mM or 1mM HU were added to the wells 5 hours after onset of activation with 8ug/ml PHA and 4nM IL-2, and cells were harvested 24 or 48h after seeding. Proliferation rates in cultured T-cells were assessed by tritiated thymidine ([^{3}H]thymidine) incorporation essay. Briefly, cells were cultured in 96 well plates, at a concentration of 0.2x10^6/100ul/well. Three wells were assigned to each treatment group. Cells were incubated for 18-24h with 1uCi/well (0.037MBq) [^{3}H]thymidine (A.2.5). Plates were then stored at –20°C until analysis by liquid scintillation (Merrill, 1998a).

2.8 SELECTION OF $CD25^+$ CELLS

Positive selection was performed on cells that had been cultured 24h with 8ug/ml PHA and 1mM HU, in 24 well plates. Cells were harvested and washed twice with 0.1% BSA and 1% NaN_3 in D-PBS (FACS buffer; A.3.1). About 10-15x10^6 cells were processed each time. Cells were resuspended at a concentration of 2x10^7/ml in FACS buffer, and labelled with 1ug/10^6 cells of R-Phycoerythrin (R-PE)-conjugated anti-CD25 (Caltag; A.4.1). After incubation for 30min at 4°C, in the dark, cells were washed with 20x labelling volume of 0.5% BSA, 1% NaN_3, 2mM EDTA in D-PBS (MACS buffer; A.3.1). Samples were resuspended at a concentration of 10^7/80ul MACS buffer and labelled for 15min, at 4°C, with 20ul of anti-R-PE or goat anti-rat IgG paramagnetic MicroBeads (Miltenyi Biotec; A.4.3). After washing once and resuspending in 500ul MACS buffer, labelled cells ($CD25^+$)

were enriched on a positive separation column MS^+ (Miltenyi Biotec; A.4.3). In some experiments (Chapter 4) $CD25^-$ cells were enriched on a second MS^+ column, to improve recovery rates. After separation, cells were labelled with $2ug/10^6$ cells FITC-conjugated anti-CD3 antibody (Caltag; A.4.1) and processed for FACS analysis. All steps were performed at 4°C and all centrifugations were carried out at 400g, for 7min.

2.9 FLOW CYTOMETRY OF T-LYMPHOCYTES

Samples, containing $0.5\text{-}1x10^6$, were washed once with cold D-PBS with 0.1% BSA (w/v) and 0.1% NaN_3 (FACS buffer; A.3.1) and resuspended at a concentration of 10^7/ml. Cells were labelled with $1ug/10^6$ cells FITC-conjugated hamster anti-mouse CD3 (Caltag; A.4.1) and $2ug/10^6$ R-Phycoerythrin (R-PE)-conjugated rat anti-mouse interleukin-2 receptor α (IL-2Rα) or CD25 (Caltag; A.4.1) and incubated for 30min at 4°C, in the dark. After two washes, cells were resuspended in 0.4ml FACS buffer and analysed. Alternatively cells were labelled with FITC-conjugated hamster anti-mouse CD3, washed once with FACS buffer and fixed in 300ul of 50% FCS/FACS buffer and 900ul of cold 70% ethanol, added dropwise. After an overnight fixation at 4°C, samples were washed twice with FACS buffer, stained for 1h, at room temperature, with 0.4ml PI staining solution (A.3.3) with 20ug/ml Propidium Iodide (PI) and 100ug/ml ribonuclease A (RNAse A; Sigma) in FACS buffer, and analysed. All centrifuging was performed at 400g for 7min. For assessment of sub-populations in cells isolated from different lymphoid tissues, T-lymphocytes were labelled with FITC-conjugated anti-mouse CD3, as before, B-lymphocytes were labelled with $2ug/10^6$ FITC-conjugated anti-B220 antibody (Caltag; A.4.1) and myeloid cells, with $1ug/10^6$ cells R-PE-conjugated anti-mouse Ly-6G (Gr-1) antibody (Caltag; A.4.1). In some experiments T-cells were also stained with PI/$p27^{KIP1}$. Staining and analysis were performed as described for Mouse Foetal Fibroblasts.

Flow cytometry analysis was performed using a FACSCan (Becton Dickinson), equipped with an Argon laser line (excitation wavelength 488nm) and FL2 and FL1 filter sets, respectively for R-PE (orange, peak emission 575nm) and

FITC (green, peak emission 520nm). For each sample 10000 events were acquired. Analysis was performed using the CellQuest program (version 3.01, Becton Dickinson). Negative controls included unstained samples, for the CD3/CD25 staining, and samples stained only with PI, for the CD3/PIstaining. For analysis of CD25, the percentages of $CD25^+$ cells, as well as mean fluorescence and peak channel, used as measures of CD25 level of expression, were evaluated. PI was used to analyse the following parameters: percentages of apoptotic cells and polyploid cells; percentages of G0/G1, S and G2/M-phase cells. All parameters were evaluated on the whole cell population and in the $CD3^+$ sub-population that included only T-lymphocytes.

2.10 FACS ANALYSIS

2.10.1 FACS analysis of Mouse Foetal Fibroblasts

PI staining was used to perform cell cycle analysis and to set gates on specific sub-populations of cells:

1) No gate, all cells included in the analysis (Fig.2.5). Parameters acquired:
   a) Percentage of hypodiploid cells (<2N; apoptotic cells), considered as apoptotic cells;
   b) Percentage of normoploid cells ($2 \leq N \leq 4$);
   c) Percentage of polyploid cells (>4N), including abnormal cells and cell aggregates.
2) Live gate, using the Doublets Discrimination Module (DDM) to exclude cell aggregates, polyploid (DNA content>4N) and apoptotic (DNA content<2N) cells from the analysis (Fig.2.5). Parameters acquired within the live cell population were:
   a) Percentage of cells with diploid content of DNA (2N), considered as G0/G1-phase cells;
   b) Percentage of cells with di/tetraploid content of DNA (2<N<4), considered as S-phase cells;
   c) Percentage of cells with tetraploid content of DNA (4N), considered as G2/M-phase cells.

Figure 2.5 FACS analysis for CD3/PI staining

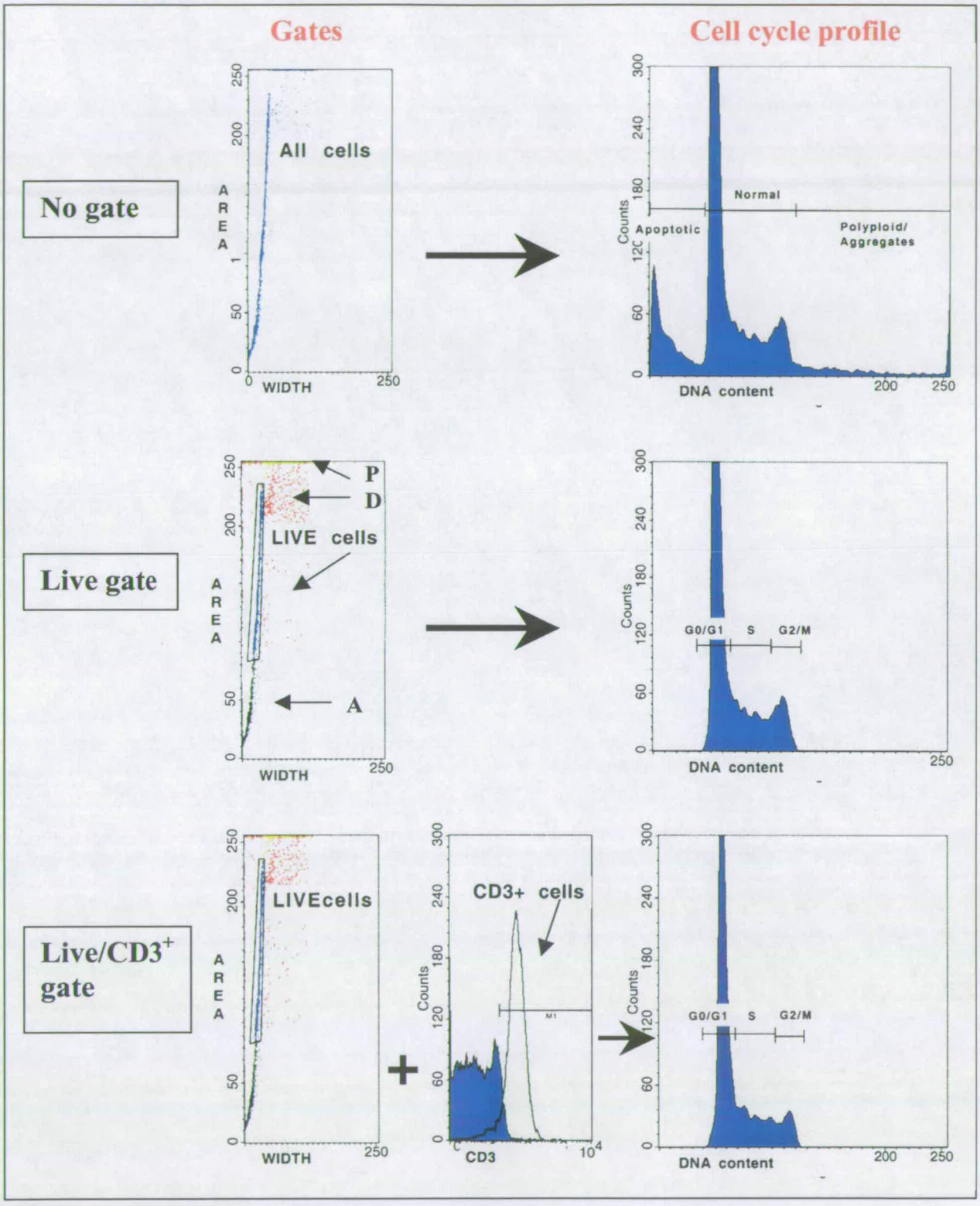

T-cells were stained with anti-CD3-FITC and Propidium Iodide. The following parameters were calculated on the whole cell population: percentages of apoptotic cells (hypodiploid or sub-G0/G1 cells with N<2); normoploid cells (2≤N≤4); polyploid cells (N≥4). Doublets Discrimination Module (Live gate) was used to exclude doublets and aggregates (D), polyploid cells (P) and apoptotic cells (A). Live and $CD3^+$ cells gate were used in conjunction to analyse live, T cells only. Cell cycle profile of live and live/T-cells was assessed by gating G0/G1, S and G2/M cells according to their DNA content. Accuracy of gating was confirmed by calculating DNA indexes: 2N=1.0±0; 4N=1.95±0.05; >4N=4.5±1.5; <2N=0.02±0.02 (Mean±SD; from 50 experiments with MFF and T cells).

Figure 2.6 FACS analysis for CD3/CD25 staining

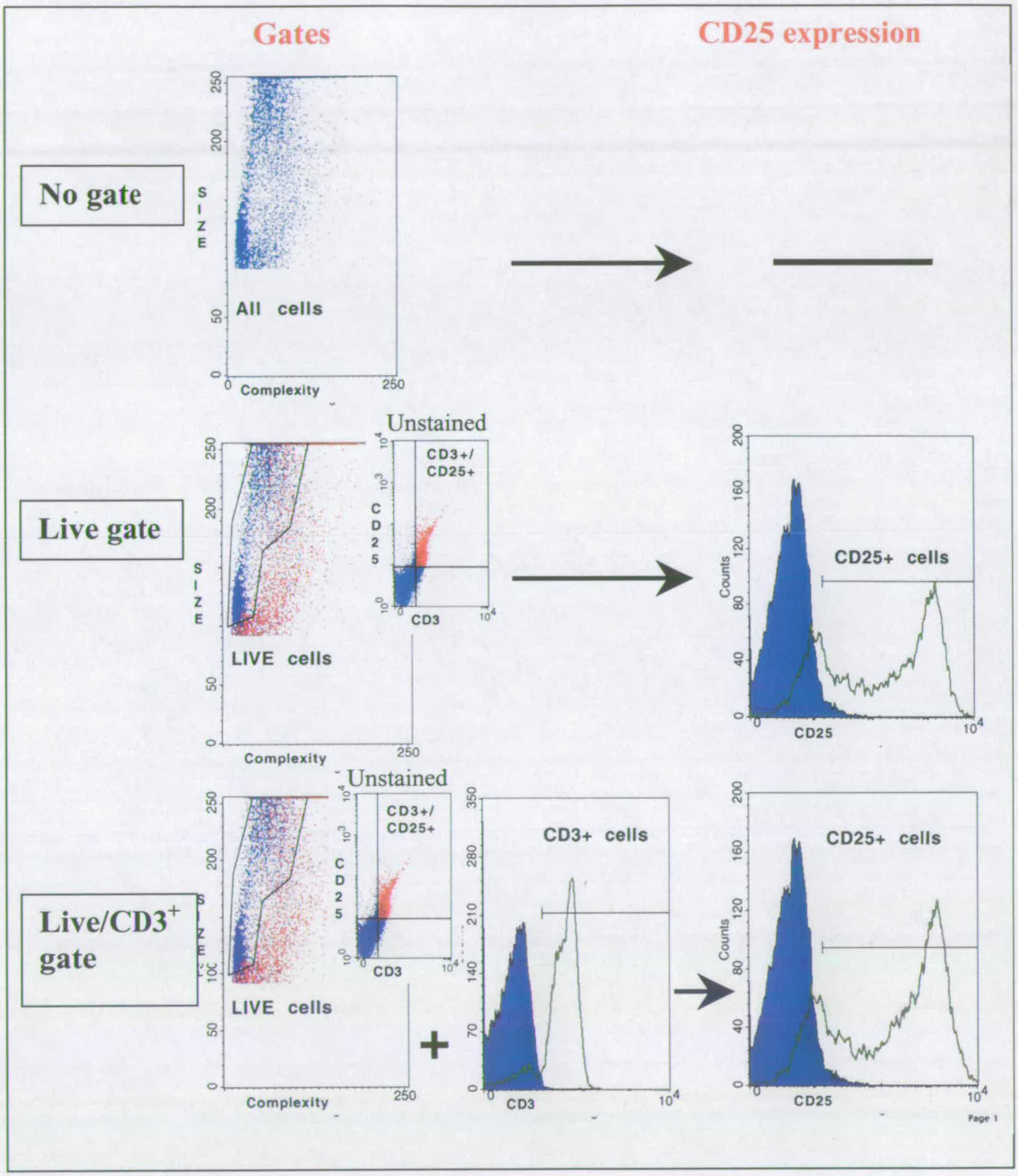

Dead cells, represented in this figure as red dots, were smaller (size=Forward Scatter or FSC) and more complex (complexity=Side Scatter or SSC) than live cells. Dead cells also stained $CD3^+/CD25^+$ in unstained samples. CD25 expression was calculated on live cells (live gate), and Live/T cells (Live/$CD3^+$ gate).

3) PI staining was also used to gate sub-population of cells at specific cell cycle stages: G0/G1, S and G2/M-phase cells.

In MFF double stained with PI and a specific intracellular marker, expression of the specific intracellular marker ($p27^{KIP1}$, p130, FITC) was evaluated using the following gates and parameters:

1) Live gate (=DDM): expression of a marker in all normoploid, singlets (Fig.2.5). Parameters calculated within the gated population:
   a) Percentage positive cells, relatively to a negative control (unstained samples, isotype controls);
   b) Mean fluorescence: levels of expression of the marker in the cell population;
   c) Peak channel: mode.
2) Gating on G0/G1 cells, S cells, G2/M cells: expression of a marker only in cells at a specific cell cycle stage. Parameters analysed, within the gated population:
   a) Percentage of positive cells;
   b) Mean fluorescence;
   c) Peak channel.

2.10.2 FACS analysis of T-lymphocytes

Gates used for FACS analysis, for CD3/CD25 and CD3/PI staining were:

1) Live cells gate. Dead cells and debris were excluded by using a FSC and SSC dot plot, in the CD3/CD25 staining (Fig.2.6), and the DDM module, for the CD3/PI staining (Fig.2.5).
2) $CD3^+$/live cells gate. CD3 receptor was used to gate T-lymphocytes, in the live cell population (Fig.2.5-2.6).

For each of the gated populations, the following parameters of CD25 expression were acquired:

   a) Percentage of $CD25^+$ cells;
   b) Mean fluorescence, used to measure of CD25 level of expression/cell;
   c) Peak Fluorescence, corresponding to CD25 level of expression/cell reached in the majority of the cell population (mode).

For each of the two gated populations the same parameters for the PI staining previously described for Mouse Foetal Fibroblasts (Paragraph 2.10.1), were acquired. For the PI staining no gate was used when assessing the percentages of apoptotic cells (Paragraph 2.10.1).

2.11 IMMUNOCYTOCHEMISTRY OF MOUSE FOETAL FIBROBLAST AND T-LYMPHOCYTES

Mouse Foetal Fibroblasts (MFF) were grown on round glass coverslips (1.3cm^2, BDH, 406/0189/10), placed in 12 or 24 well/plates (1 or 2ml/well), or on 76x26mm microscope glass slides (10cm^2; Blue Star), placed in 55cm^2 dishes (12ml/dish). In G1 synchronization experiments cells were resuspended in 0.5ml of culture medium, seeded on 10cm^2 and incubated for 2h, before adding 12ml medium containing the blocking agents. T-lymphocytes, resuspended at a concentration of 0.5x10^6/ml in culture medium, were centrifuged on cytospin slides (Thermo Shandon; 599 1059), 0.5ml/slide, at 130g, for 5min, and allowed to dry for a few minutes, before processing.

When staining for **Proliferating Cell Nuclear Antigen (PCNA**; modified method by Kill, 1991) cells were washed twice with PBS, fixed and permeabilised for 4 min, with methanol:acetone (1:1) at –20°C. For **cyclin D1** staining, cells were fixed and permeabilised for 5min, with 100% methanol, at –20°C. Cells were then washed three times with ice cold PBS, and incubated overnight, at 4°C, in a humidified atmosphere, with human anti-serum to PCNA (Immuno Concepts; A.4.1), diluted 1:10 in 1% FCS-PBS. Alternatively cells were incubated at 25°C, for 60min with mouse anti-cyclin D1 (Novocastra; A.4.1), diluted at a concentration of 5ug/ml in 1% FCS-PBS. After incubation with primary antibodies, slides were washed five times with 1% FCS-PBS, and incubated for 60min, at room temperature, in the dark, in a humidified atmosphere, with Texas Red (TXR)–conjugated goat anti-human IgG (VectorLaboratories; A.4.2) or fluorescein isothyocyanate (FITC)-conjugated sheep anti-mouse IgG (Diagnostic Scotland; A.4.2), diluted 1:100 in 1% FCS-PBS. Finally, cells were washed three times with 1% FCS-PBS and mounted.

When staining for nuclear antigens, such as PCNA and cyclin D1, it is important to remember that fixation is the most critical step. The use of organic solvents (ethanol, methanol, acetone), as opposed to cross-linking reagents (paraformaldehyde, glutaraldehyde), is highly recommended for fixing for these nuclear antigens because they preserve better antigenicity as opposed to cell structure (Harlow and Lane, 1988). Furthermore, the use of 2% paraformaldehyde followed by acid treatment, for PCNA staining, can produce artefacts (Campbell, 1998). PCNA is expressed in two forms: an insoluble form, which is expressed at low levels in quiescent and senescent cells and highly expressed in cycling cells, where it acts as a processivity factor for DNA polymerase δ (Celis and Bravo, 1984; Bravo and Bravo, 1987); a soluble, nucleoplasmic form, which is constitutively expressed during the cell cycle. Organic solvents only fix the insoluble form, whereas cross-linking reagents destroy the insoluble form and fix the soluble one.

Staining of T-cells was performed with a modified method by Wreggett *et al.* (1994). Slides were washed twice with PBS, and fixed for 10min, with 4% (w/v) paraformaldehyde (PF). Cells were permeabilised for 12min, in Tris Buffer Solution (TBS; A.3.1) with 0.2% Triton X-100 (permeabilising solution) and blocked for 20min with 10% (w/v) non-fat milk (Marvel) in permeabilising buffer (blocking buffer). For **HP1** staining, cells were incubated 60min with 1ug/ml rat monoclonal anti-M31 (AFRC MAC 353; A.4.1), 5ug/ml rat monoclonal anti-M32 (MAC 385; A.4.1) or 1ug/ml purified rabbit anti-serum to mHP1α (M235; A.4.1), all diluted in blocking buffer. The following primary antibodies recognizing histone **H4 acetylation** (H4.Ac; A.4.1) on different lysines were also used: sheep anti-serum to H4.Ac.2-4, diluted 1:800; rabbit anti-sera to: H4.Ac5 (R40), diluted 1:800; to H4.Ac8 (R232), diluted 1:1500; to H4.Ac12 (R101), diluted 1:400; to H4.Ac16 (R251), diluted 1:1500. The antibodies recognizing mouse HP1 proteins were a gift from Dr. Prim Singh; the rabbit anti-sera recognizing acetylated histone H4, except the anti-H4.Ac2-4 antibody (a gift from Dr. Prim Singh), were a gift from Prof. Bryan Turner. For **cyclin D3** staining, cells were stained with mouse anti-human cyclin D3 (Novocastra; A.4.1), diluted 1.20. After three washes with permeabilising buffer, cells were incubated with the correspondent secondary antibody (see A.4.2): FITC-conjugated rabbit anti-rat serum (a gift from Dr. Prim Singh), diluted 1:50;

FITC-conjugated donkey anti-rabbit IgG (Diagnostic Scotland), diluted 1:100; FITC-conjugated anti-sheep IgG (a gift from Dr. Prim Singh), diluted 1:400; FITC-conjugated anti-mouse IgG, diluted 1:50 (Diagnostic Scotland). Cells were finally washed three times with permeabilising buffer and mounted. All antibodies were diluted in blocking buffer. All steps were carried out at room temperature.

T-cells were also double stained for **M31/CD25** or **M31/PCNA**. For M31/CD25, cells were stained with 1ug/0.5-1x10^6cells R-Phycoerythrin (R-PE) conjugated anti-CD25, diluted in FACS buffer, and incubated for 30min, at 4°C, in the dark. After one wash with FACS buffer, the cell suspension was used to prepare cytospin slides that were fixed and processed for M31 staining as for MFF. For M31/PCNA staining, cytospin slides were fixed in PF4%, permeabilised with 0.2% Triton X-100 in TBS (permeabilising buffer) for 12min and blocked in 10% non-fat milk in permeabilising buffer (blocking buffer) for 20min. Slides were stained overnight, at 4°C with anti-PCNA antibody, diluted 1:10 in 1% FCS in D-PBS. After three washes with permeabilising buffer, cells were stained for 60min, at room temperature with 1ug/ml AFRC MAC353 antibody. After three washes with permeabilising buffer, slides were incubated 60min, at room temperature, with the secondary antibody solution containing both FITC-conjugated rabbit anti-rat serum (a gift from Dr. Prim Singh) and TXR-conjugated goat anti-human IgG (VectorLaboratories), diluted respectively 1:50 and 1:100 in blocking buffer. Finally, slides were washed three times with permeabilising buffer and mounted.

Isotype controls for cyclin D1 staining were preincubated with 5ug/ml mouse IgG2a (Sigma; A.4.3) before incubating them with the secondary antibody. Controls for PCNA and HP1 staining were preincubated with blocking buffer, instead of the primary antibody, before incubating them with the secondary antibody.

All slides were mounted with Vectashield Mounting Medium containing 1.5ug/ml 4', 6-diamidino-2-phenylindole (DAPI; VectorLaboratories; A.4.3), and were sealed with PANG (Pangus, Hungary). Slides were stored at 4°C, in the dark, until visual examination.

In experiments with MFF, slides were examined with a 100x Fluor oil objective (Nikon), on a Nikon Microphot-SA microscope equipped for epifluorescence, and supplied with a mercury lamp (100W, Nikon HB 10101AF) and

FITC (Nikon UV-2B; excitation 330-380 nm), TXR (Nikon G-1A; excitation 546-556 nm) and DAPI (Nikon B-2A; excitation 450-490 nm) selective filter sets. Photographs were taken using a photomicrographic attachment (Nikon FX-35DX camera and Microflex UFX-DX).

In T-cell experiments slides were viewed using a Zeiss Axiovert S 100 photomicroscope equipped with FITC (Zeiss 487709), Texas Red (Zeiss 487714) and DAPI (Zeiss 487702) selective filter sets and a 50W mercury arc lamp, using a 40x and 63x Plan Neofluar, oil objectives (Nikon). R-PE fluorescence was detectable with the FITC filter set. This set-up was also equipped with a Hamamatsu Digital camera (C4742-95) and the AQM program (Kinetic Imaging Ltd), for digitalized image acquisition and analysis.

2.12 ANALYSIS OF IMMUNOCYTOCHEMISTRY DATA

A total of 40 cells were acquired, at fixed settings, with a 63x objective, form three images obtained from 1-3 slides, preparing 1 slide/experiment for each staining (1 slide for cyclin D3 and H4.Ac staining; 2 slides for mHP1α, M32, PCNA/M31, CD25/M31; 3 slides for M31). A power 40x objective was used only for acquisition and analysis of H4.Ac5 and H4.Ac12 staining (Chapter 5). Acquired images were then analysed using the AQM program.

Analysis of chromatin markers (mHP1α, M31, M32) and histone H4 acetylation markers (H4.Ac2-4/5/12) was performed in a similar way. The DAPI staining was used to gate the nuclear area in each cell and the brightfield image (Fig.2.7A) was used to gate the cell area. Three groups of parameters were acquired:

1) Morphological features:
   a) Cell area;
   b) Nuclear area;
   c) Cell/nuclear ratio;
   d) Percentage of nuclear area, calculated as: (nuclear area/cell area)x100.
2) Nuclear fluorescence features (Fig.2.7 B):

Figure 2.7 Analysis of intracellular proteins by immunofluorescence

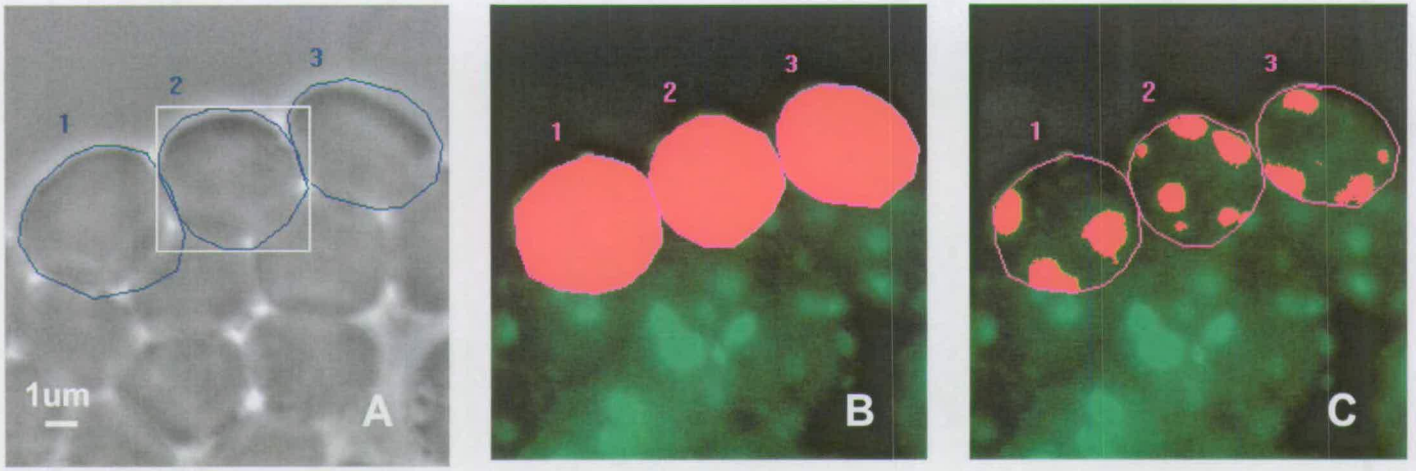

Method used to analyse fluorescence features of intracellular proteins: HP1 proteins, cyclin D3, and, in some experiments, PCNA (Chapter 5). Brightfield images (A) were used to calculate cell area (pixels). DAPI staining was used to calculate nuclear area (image not shown). Overall FITC or TXR fluorescence was calculated by doing a background correction using extracellular fluorescence as background. In the case of M31, that tends to organise into clusters, clusters of fluorescence were analysed by considering only areas of fluorescence with values higher than those found in diffused fluorescence areas. Features of fluorescence acquired using the AQM program (Kinetic Imaging Ltd.) were: integral intensity (pixels of fluorescence), area of fluorescence (pixels), mean fluorescence (0-255 on a greyscale), SD of mean fluorescence (0-255 on a greyscale).

a) Percentage of nuclear area with fluorescence, calculated as: (area of fluorescence/surface area)x100;

b) Integral intensity;

c) Mean intensity, calculated as (integral intensity/area of fluorescence);

d) Peak intensity;

e) SD of mean fluorescence.

3) For M31 staining, clusters of fluorescence features were also acquired (Fig.2.7 C):

a) Percentage of nuclear area with fluorescent clusters, calculated as (area of clusters/surface area) x100;

b) Integral intensity of fluorescent clusters;

c) Mean intensity of clusters, calculated as: (intensity of clusters/area of clusters);

d) Peak intensity of clusters;

e) SD of clusters mean fluorescence;

f) Number of clusters/cell.

Total cell fluorescence features were analysed after subtracting extracellular background fluorescence from intracellular fluorescence using the background correction module. In cells stained with FITC-anti-M31, clusters were analysed by gating only fluorescent areas with FITC fluorescence intensity higher (heterochromatin) than that observed in areas with decondensed chromatin (euchromatin).

For PCNA and cyclin D3 staining, one slide was processed for each experiment (n=3, for PCNA; n=1, for cyclin D3) and 200 cells were counted from three fields/slide. The results were expressed as percentage of $PCNA^+$ or cyclin $D3^+$ cells. However also morphological features and nuclear fluorescence features were also acquired in some experiments (Chapter 5). For cyclin D3 staining, fluorescence could have cytoplasmic or nuclear localisation, corresponding to an inactive or active form of cyclin D3. The cytoplasmic area could not be gated but cytoplasmic parameters could be calculated in the following way:

1) Cytoplasmic area, calculated as: (cell area-nuclear area);

2) Integral cytoplasmic intensity, corresponding to: (integral cell intensity-integral nuclear intensity);

3) Percentage of cytoplasmic area with fluorescence, calculated as: (cell fluorescent area/nuclear fluorescent area) x100;

4) Mean cytoplasmic intensity, corresponding to: (integral cytoplasmic intensity/cytoplasmic fluorescent area).

In the absence of a cytoplasmic gate, the cytoplasmic peak could not be calculated.

For M31-FITC/PCNA-TXR/DAPI triple staining the following parameters were acquired: morphological features; PCNA fluorescence features (mean fluorescence; integral intensity; peak intensity) and the percentages of $PCNA^+$ cells; M31 fluorescence features (mean fluorescence; integral intensity; peak intensity; cluster n°). It was also possible to gate $PCNA^+$ and $PCNA^-$ cells and to assess their chromatin features using the M31 staining.

For M31/CD25-R-PE/DAPI triple staining the following parameters were acquired: morphological features; percentage of $CD25^+$ cells, confirmed by FACS analysis; M31 fluorescence features (mean fluorescence; integral intensity; peak intensity; cluster n°). It was also possible to gate $CD25^+$ and $CD25^-$ cells and to assess their chromatin features using the M31 staining.

Areas and integrative fluorescence were measured in pixels. Mean fluorescence, Peak fluorescence and SD of mean fluorescence were calculated on a 0-255 greyscale.

2.13 T-CELL NUCLEAR TRANSFER

2.13.1 Preparation of G0- and G1- lymphocytes

For each Nuclear Transfer experiment an average of $7.1\pm3.1x10^6$ lymphocytes/animal (mean±SD) with 85.8±6.6% $CD3^+$ cells (6.1 ± 2.8 $x10^6$/animal) were isolated from the lymph nodes of four to eight, six week old females from the following strains: CBA/Ca (5 replicates), C57BL/6 (4 replicates), (C57BL/6xCBA/Ca)F1 (2 replicates). Freshly isolated lymphocytes were used

directly for Nuclear Transfer, as G0 donor cells. For synchronization in G1 about 22-48x10^6 cells/experiment were cultured for 24h in 5% CO_2, at 37.5°C, in medium supplemented with 1mM hydroxyurea (HU), 8ug/ml phytohemagglutinin (PHA) and 4nM interleukin-2 (IL-2). At the end of the incubation, G1 cells were harvested and $CD25^+$ cells were positively selected using magnetic cell sorting (G1/$CD25^+$; see Paragraph 2.8). Donor cells in G0 or G1/$CD25^+$ were washed once with D-PBS and resuspended at a concentration of 1-2x10^6/ml in 10% FCS in RPMI-1640 (A.2.1). Cells were used immediately for Nuclear Transfer. Just prior to manipulation, G0 and G1/$CD25^+$ donor cells were washed once in D-PBS (Sigma) and resuspended Hepes-CZB (Chatot *et al.*, 1989; A.5.10) with 10% (w/v) polyvinylpyrrolidone (PVP, MW 360000; Sigma). The cell cycle profile and the quiescent state of donor cells were assessed by FACS analysis and staining for CD3 and CD25, and CD3 and Propidium Iodide, as previously described. Quality controls included: cultured quiescent cells (G0, cultured), that had been incubated for 24h in medium alone, used as a culture control; cycling cells, that had been activated for 24h with 8 ug/ml PHA and 4 nM IL-2, used as an activation control; G1 cells, that had been activated for 24h with 8 ug/ml PHA, 4 nM IL-2 and 1 mM HU, used as a synchronization control.

2.13.2 Enucleation and lymphocyte nucleus injection

MII oocytes were collected 14 hours after hCG injection of eCG-primed B6D2F1 (C57BL/6 x DBA/2) mice. An average of 23.8±5.3 (mean±SD) and a range of 16.7-33.3 oocytes per mouse were collected in 10 nuclear transfer experiments. Cumulus cell/Oocyte Complexes (COCs) were collected in Hepes-CZB (A.5.10) medium and cumulus cells were removed by incubating the complexes for 4-5min, at room temperature, with 300IU/ml hyaluronidase (Sigma; A.5.6) in Hepes-CZB. Denuded oocytes were rinsed once in Hepes-CZB and placed in CZB medium (Chatot *et al.*, 1989; A.5.5), under 5% (v/v) CO_2 in air and at 37.5°C until enucleation. Micromanipulations were performed using a Nikon inverted microscope (TE300) equipped with an Eppendorf Transfer Man. Groups of 15 oocytes were transferred into a microdrop of Hepes-CZB medium, supplemented with 5ug/ml cytochalasin B (Sigma; A.5.12) placed in the operation dish, on the microscope

stage. Oocytes were firmly held at the end of the holding pipette while the zona pellucida was cored and the oolemma punctured by applying several piezo-pulses to an enucleation pipette. The metaphase II oocyte chromosome-spindle complex, appearing as a translucent region, was aspirated into the enucleation pipette, trying to remove as little volume of ooplasm as possible. The batch of enucleated oocytes was then placed into CZB medium, without cytochalasin B, and held there for up to two hours under 5% (v/v) CO_2 in air and at 37.5°C. The overall enucleation rate was approximately 100 oocytes in 1-2 hours and the survival rates after enucleation were 90.8±9.9% (mean±SD), comparable to those reported in the literature for the same technique (97.9-98.7%; Wakayama *et al.*, 1998). Enucleated oocytes were returned to the operating dish immediately before injection. Just before injection lymphocytes, resuspended in 10% polyvinylpyrrolidone (PVP, 360 KD, ICN), were stripped of their cytoplasm by gently aspirating them in and out of an injection pipette with an inner diameter slightly smaller (5um) than the cell diameter (6-8 um). This procedure was particularly difficult considering the smaller diameter of T-lymphocytes compared to other somatic cell types, such as cumulus cells (cell diameter=10-12um; injection pipette inner diameter=5-7 um), previously used in NT experiments (Wakayama *et al.*, 1998). After isolation, 4-6 nuclei at a time were aspirated into the enucleation/injection pipette and injected, one at a time, into previously enucleated recipient oocytes. In this way each nucleus was immediately injected into an enucleated oocyte only minutes of its isolation. The overall reconstruction rate was of 50-80 NT embryos/2 hours (100 NT embryos/2 hours for ES cells). The survival rate after injection were in the range of 92.9%-94.3%, comparable if not higher than those reported in the literature (Wakayama *et al.*, 1998) for similar somatic cell types such as cumulus cells (79.1-95.3%). After reconstruction NT embryos were kept in CZB medium under 5% (v/v) CO_2 in air, at 37.5°C, for 1-3h before activation.

2.13.3 Oocyte activation

Following a 1-3 hour delay after nuclear transfer (NT) cloned embryos were activated simultaneously by incubating them for 6 hours under 5% (v/v) CO_2 in air, at 37.5°C, in Ca^{2+}-free CZB medium (A.5.5) supplemented with 10mM Strontium

(Sr^{2+}; Sigma; A.5.8) and 5ug/ml cytochalasin B, to prevent polar body extrusion, as previously reported (Wakayama *et al.,* 1998). To assess activation efficiency 10 oocytes/replicate were parthenogenetically activated. Overall activation rates in T-cell nuclear transfer experiments (Paragraph 6.3, 8 replicates) were high, with 100% (86/86) of control oocytes forming pronuclei, 97.7% (84/86) cleaving, 94.2% (81/86) and 86.0% (74/86) reaching respectively the morula and the blastocyst stages. In the experiments carried out to assess occurrence of PCC in the first 3 hours after reconstruction, embryos were incubated in CZB medium under 5% (v/v) CO_2 in air, at 37.5°C, for 3 hours after reconstruction, without being activated.

2.13.4 Embryo culture or embryo transfer

For *in vitro* studies reconstructed or fertilised embryos were cultured in M16 medium (A.5.4; Whittingham, 1971), under 5% (v/v) CO_2 in air, at 37.5°C. CZB culture media had also been tested for embryo culture, but M16 gave better blastocyst quality (higher cell numbers).

In *in vivo* development studies, embryo transfer was performed resuspending five to ten embryos, at the 2-cell or morulae/blastocyst stage, in M2 medium (A.5.3; Fulton and Whittingham, 1978) and by transferring them respectively into the oviducts or uteri of Swiss Webster foster mothers, that had been mated 0.5 or 2.5 days earlier with vasectomized Swiss Webster males. Caesarian section of recipient females was carried out at 19.5 days post coitus (d.p.c), to check for signs of implantation and development.

2.13.5 Control fertilised embryos

Fertilised embryos were collected from female B6D2F1 (C57BL/6 x DBA/2) mice that had been primed with eCG and mated with B6D2F1 males at the time of hCG injection. Fertilisation occurred approximately 10-13 hours after mating (5.30-8.30, day 0) and pronuclear formation about 4-5 hours after fertilisation (13.30, day 0). Animals were killed by cervical dislocation and embryos (25-30/animal) were collected around the time of pronuclear formation, only from females that had a vaginal plug. Embryos were collected in Hepes-CZB medium. Cumulus cells and

sperm attached to the surface were removed by a 4-5min incubation, at room temperature, with 300IU/ml hyaluronidase (Sigma; A.5.6) in Hepes-CZB. Denuded oocytes were rinsed once in M2, placed in 30ul drops (15 embryos/drop) of M16 medium and cultured under 5% (v/v) CO_2 in air, at 37.5°C.

2.13.6 Control Nuclear Transfer embryos from embryonic stem cells

The HRT-deficiency ES cell line HM-1 was derived from an inbred mouse strain 129/Ola and was kindly provided by Dr. Ed Gallagher at passage 19. The yield of chimeric animals and germ-line transmission had been highly proved by injection of HM-1 ES cells into mouse blastocysts. Cells were cultured in GMEM media (GIBCO) supplemented with 15% heat-inactivated FCS, 100 units of leukemia inhibitory factor/ml, 2mM L-glutamine, 1% MEM non-essential amino acid solution (GIBCO) and 1% 2-mercaptoethanol (2-ME). The night before the experiment, the serum concentration was reduced to 5%. Nuclear Transfer experiments were performed using the same protocol used for T-lymphocytes (Paragraphs 2.13.1-2.13.3). Only small ES cells, with a diameter of 7-10um were used for NT. Transfer of ES-cell derived embryos were only performed at the morula/blastocyst stage into the uteri of Swiss Webster foster mothers that had been mated 2.5 days before with vasectomized Swiss Webster male mice.

2.14 IMMUNOCYTOCHEMISTRY OF EMBRYO WHOLE MOUNTS

For double staining, carried out to visualise **chromatin** and **microtubules**, oocytes and embryos were fixed in paraformaldehyde (4%)/picric acid (0.05%) fixative, for 1h at 37°C (A.3.2). Specimens were rinsed twice with D-PBS, and incubated for 30min, at 37°C in D-PBS with 0.1% (v/v) Triton X-100 and 0.3% (w/v) BSA (permeabilising buffer). Specimens were incubated for 30min, at 37°C, in D-PBS with 0.1M glycine and 0.3%(w/v) BSA (blocking buffer) and washed twice in D-PBS with 0.01% (v/v) Triton X-100 and 0.3% (w/v) BSA (washing buffer).

Embryos were incubated for 40min, at 37°C with mouse monoclonal anti-β tubulin (Sigma; A.4.1), diluted 1:300 in blocking buffer, washed three times with washing buffer, and incubated for 40min, at 37°C with FITC-conjugated anti-mouse IgG (Sigma; A.4.2), diluted 1:50 in blocking buffer. After washing three times with washing buffer, cells were mounted with Vectashield antifade (Vector Laboratories; A.4.3) and 10ug/ml PI (Sigma) in D-PBS.

For triple staining for **chromatin**, **microtubules** and **microfilaments**, embryos were fixed at 37°C, for 30min in Complex Fix (modified from Messinger and Albertini, 1991) containing 2% formaldehyde and 0.1% Triton X-100 in Microtubule Stabilization Buffer (20mM Pipes, 1mM $MgCl_2$, 0.5mM EGTA, 1mM DTT, Deuterium Oxide; A.3.2). The fixative was removed by washing twice, for 10min, with 10% goat serum, 0.02% (w/v) NaN_3, 0.001% (v/v) Triton X-100 in D-PBS (10% NGS). Specimens were stained for 1h, at 37°C, in the dark, with Rhodamine-conjugated anti-phalloidin (Molecular Probes; A.4.1), diluted 1:4000, and FITC-conjugated anti-α tubulin (Sigma; A.4.1), diluted 1.500, in D-PBS with 5% goat serum, 0.02% (w/v) NaN_3, and 0.001% (v/v) Triton X-100 (5%NGS). After three washes with 10% NGS, embryos were mounted using Vectashield (Vector Laboratories) with 1.5ug/ml DAPI.

Triple staining for **chromatin, M31** and **PCNA** was carried out on whole mounts of MII oocytes, control and NT embryos (modified method by Wregget *et al.*, 1994). Specimens, collected at selected time points, were washed twice in PBS and fixed in paraformaldehyde (PF) 2% (w/v) overnight at 4°C (A.3.2). After three 10min washes, with cold (4°C) 0.05% (v/v) Tween 20 (Sigma; P1379) in D-PBS, specimens were permeabilised in 0.2% (v/v) Triton X-100 D-PBS for 15 min. After three 10min washes, with 0.05% (v/v) Tween 20 in D-PBS, the specimens were incubated for 1h in 10% FCS (v/v) in PBS (PCNA blocking buffer). Embryos or oocytes were placed in a 30ul drop (15 embryos/drop), with anti-PCNA (Immuno Concepts) antibody diluted 1:10 in PCNA blocking buffer, and incubated overnight, at 4°C, in a humid chamber. After four 15min washes in 0.05% Tween 20 in D-PBS, the specimen were permeabilised again by incubation for 15min, at RT, in 0.2% (v/v) Triton X-100, followed by three, 10min washes in 0.05% Tween 20 in D-PBS and a 1h incubation in 2% BSA (w/v) in D-PBS (M31 blocking buffer). Embryos and

oocytes were then incubated 1h at RT with rat monoclonal anti-M31 (MAC 353) diluted 1:50 in 2% (w/v) BSA in D-PBS. After four, 15 min washes in 0.05% (v/v) Tween20 in D-PBS, indirect immunolabelling was performed by incubating specimens for 1h, at room temperature, in the dark, with Texas red-conjugated anti-human IgG (Vector Laboratories) and FITC conjugated anti-rat serum (a gift from Dr. Prim Singh), diluted, respectively 1:200 and 1:50 in 2% BSA (w/v) in D-PBS. Finally embryos and oocytes were mounted using Vectashield with 1.5ug/ml DAPI.

For double staining for **chromatin** and **acetylated histone H4** (modified method by Worrad *et al.,* 1994) embryos were fixed with 2% PF, overnight, at 4°C. After two 15min washes with 0.05% (v/v) Tween 20 in D-PBS, specimens were permeabilised with 0.2% (v/v) Triton X-100 in D-PBS. After two 15min washes with 0.05% (v/v) Tween 20 in D-PBS, embryos were incubated for 1h with 2% BSA in D-PBS. Embryos were then incubated for 1h with the same panel of primary antibodies, recognizing different acetylated lysines on histone H4, at the following concentrations: anti-histone H4 acetylated on lysine 2-4 (anti-H4.Ac2-4, 1:800); 5 (anti-H4.Ac5, 1:800), 8 (anti-H4.Ac8, 1:1000), 12 (anti-H4.Ac12, 1:400), 16 (anti-H4.Ac16, 1:1000). Specimens were rinsed three times, for 15min, with 0.05% Tween 20 in D-PBS, and then incubated for 1h with the same secondary antibodies, at the same dilutions used for somatic cells, except for the donkey anti-rabbit-IgG (Diagnostic Scotland), diluted 1:150. After washing three times with 0.05% Tween20 in D-PBS, embryos were mounted with Vectashield mounting medium with 1.5ug/ml DAPI.

Triple staining for **chromatin**, **acetylated histone H4** and **PCNA** was performed using the protocol previously described in this paragraph for PCNA, followed by the protocol described for immunolabelling of acetylated histone H4. Embryos were finally mounted with Vectashield mounting Medium with 1.5ug/ml DAPI.

All steps were performed in 30ul drops, containing a maximum of 15-20 embryos, placed on a parafilm layer inside a 60mm (IWAKI) or 90mm petri dish (Bibby Sterilin). Incubations with primary and secondary antibodies were performed in a humid chamber.

Visual examination of embryos and oocytes stained for chromatin and microtubules, was performed using a confocal microscope (Nikon EFD3), equipped with a 100W Mercury lamp, an Argon laser line (Biorad Microscience Division, Model 5400) and a 20x Plan Apo objective (Nikon). FITC (green) and PI (red) signals were detected using a 488/515nm and a 546/590 nm excitation/barrier filter combination respectively. Images were captured using a digital camera and the Confocal Assistant™ program (Version 4.02; Todd Clark Brelje) and were edited with the Adobe-Photoshop program (Windows 2000).

All the other slides were examined under an inverted Zeiss Axiovert S 100 photomicroscope, using the DAPI (Zeiss 487702; emission barrier 400nm), FITC (Zeiss 487709; emission barrier 515nm) and Rhodamine/TXR (Zeiss 487714; emission barrier 573-590nm) selective filter sets and the 40x and 63x oil objectives. Images were captured with the Hamamatsu Digital camera, analysed with the AQM program (Kinetic Imaging Ltd) and edited with the Adobe-Photoshop program, as previously described (Paragraph 2.11). 2-mercaptoethanol

CHAPTER 3

MOUSE FOETAL FIBROBLASTS AS A SOURCE OF G0 AND G1 KARYOPLASTS

3.1 INTRODUCTION

Cells synchronized in G0 or G1 are mainly diploid, with significantly lower percentages of cells in S-phase, compared to cycling cells. Rates of growth-arrest in G0 and G1 populations can be assessed by immunostaining for specific proliferation-associated antigens that include the Proliferating Cell Nuclear Antigen (PCNA), Ki67 and bromodeoxyuridine (Iatropoulos and Williams, 1996, Leonhardt *et al.*, 2000). Alternatively, Propidium Iodide staining and flow cytometry can be used to quantify DNA content in cells and assess percentages of cells in S-phase, characterised by a DNA content (2N/4N) intermediate between that of diploid (2N) and tetraploid cells (4N). Since low percentages of cells in S-phase are a common feature of G0 and G1 cells, a dual parameter analysis, based on DNA content assessment and presence of quiescence markers (for review see Chapter 1), is necessary to discriminate G0 and G1 cells. There are positive and negative markers of cell quiescence, depending whether their levels are up regulated or down regulated upon exit from the cell cycle. Markers of quiescence include:

- **$p27^{KIP1}$**, a cyclin-dependent kinase inhibitor (CKI), highly expressed in G0 cells (positive G0 marker), where it prevents Cdk4 and, to a lesser extent, Cdk2 from binding to, and activating cyclin D1 and cyclin E, necessary for G0/G1 transition (for review see Sherr and Roberts, 1995);
- **p130** or retinoblastoma 2 (pRb2), a nuclear protein, member of the retinoblastoma family of proteins, highly expressed in G0 cells (positive marker), where it binds to, and activates, E2F4 and E2F5, repressors of early G1 gene expression (Smith *et al.*, 1996);

- **total RNA content** (Acridine Orange staining; Juan and Darzynkiewick, 1998) and total protein content (FITC staining; Boquest *et al.*, 1999), that are very low in G0 cells (negative G0 markers), since quiescent cells have low levels of transcription and translation.

There are also qualitative markers of cell quiescence. Quiescence induces changes in chromatin structure. As shown by a modified Acridine Orange staining (Juan and Darzynkiewick, 1998), chromatin is condensed in G0 cells, but it decondenses as cells re-enter the cells cycle. Changes in chromatin status are in line with changes in transcription and translation previously described. Changes in chromatin status are usually mediated by post-translational modifications of histone proteins and changes in sub-nuclear localisation of non-histone proteins (for review see Gregory and Hörz, 1998). Proteins of the Heterochromatin Protein 1 (HP1) family (for review see Jones *et al.*, 2000) are non-histone proteins that colocalise with constitutive, pericentromeric heterochromatin (mouse M31/human hHP1β; mouse mHP1α/human hHP1α) and non-constitutive heterochromatin (mouse M32/human hHP1γ). Changes in sub-nuclear localisation of HP1 proteins associate with changes in chromatin structure induced by cell quiescence. Furthermore, quiescence affects centromere arrangements. Immunostaining of centromeric chromatin with anti-centromere antibodies (ACA) showed that centromeric chromatin is organised into clusters, localised at the periphery of the nucleus (Weimer *et al.*, 1992). Exit from G0 is characterised by dissolution of peripheral clusters. Through its association with pericentromeric chromatin, mouse M31, homologue of human hHP1β, can be used to monitor these specific chromatin changes occurring in quiescent cells and to discriminate between quiescent and non-quiescent cells.

Fibroblasts are a good cell model to compare the developmental potential of G0 and G1 karyoplasts. Adult and foetal fibroblasts have been able to support development to term in all the species cloned up to date. Furthermore, Mouse Foetal Fibroblasts (MFF), together with T-lymphocytes, have been the cell type most commonly used to study the effects of quiescence on cultured cells. All the markers, previously described, have been used to define the quiescent state in mouse foetal

fibroblasts. Several methods to synchronize cultured fibroblasts in G0 and G1 have also been defined.

Fibroblasts can be synchronized in G0 by using one of the following antimitogenic signals: serum starvation (Nourse *et al.*, 1994; Coats *et al.*, 1996; Coats *et al.*, 1999), cell-cell contact (St. Croix *et al.*, 1998), loss of cell anchorage, TGF-β (Polyak *et al.*, 1994ab), staurosporine (Kwon *et al.*, 1996).

Synchronization of cultured fibroblasts in G1 can be achieved by using one of the following methods (for review and protocols see Pagano, 1996):

1) Synchronization in G1/S, by incubation with the blocking agents hydroxyurea and methotrexate;
2) Synchronization in early G1 by:
   a) Incubation with the blocking agent mimosine (Pagano, 1996; Gilbert *et al.*, 1995);
   b) Incubation with the blocking agent lovastatin, that induces G1 arrest by increasing the levels of the CDK inhibitors $p21^{CIP1/WARF1}$ and/or $p27^{KIP1}$.

The experiments described in this chapter were aimed at establishing synchronization protocols, in G0 and G1, for mouse foetal fibroblasts, by using markers previously described, to assess growth-arrest and quiescent state of synchronized cells.

3.2 SYNCHRONIZATION IN G0

3.2.1 Growth-arrest by contact inhibition and serum starvation

3.2.1.1 Aims

Use contact inhibition and serum starvation to synchronize mouse foetal fibroblasts (MFF) in G0 and compare their status with that of sub-confluent MFF, that had been cultured for 24h with 10% FCS (cycling cells), used as a negative control for quiescence.

Consider different experimental conditions:

1) Effect of time (0, 3, 6 days), in contact-inhibited cells;

2) Effect of different serum concentrations (0.5% FCS, 0.1% FCS) and time (0-4 days), for serum-starved cells.

Select experimental conditions that give:

1) Maximal proliferative arrest, assessed using PCNA staining and immunocytochemistry;
2) Minimal collateral effects:
   a) Death (Trypan blue staining) or inability to re-enter the cell cycle (PCNA staining after serum re-stimulation, morphology) of serum-starved cells.
   b) Death (Trypan blue staining) or transformation of contact-inhibited cells (morphology, karyotyping, doubling time after sub-culture);

3.2.1.2 Experimental design

Serum starvation experiments were set up at passage 4, using the mouse foetal fibroblasts (MFF) cell line MFF9 (for selection criteria see Paragraph 2.2).

PCNA staining was used to assess the effects of serum starvation conditions on proliferative arrest and on the ability of cells to re-enter the cell cycle and to start replicating their DNA again.

In a first set of experiments cells, seeded at al low density, were cultured 72h with 10% FCS till 50% confluent (72h), and then serum-starved, with 0.5% or 0.1% FCS, from 1 to 4 days. Two coverslips were fixed and stained for PCNA (for staining protocol see Paragraph 2.11) 48 h after seeding (cycling cells) and every 24h after serum starvation. At each time point a total of 100 cells were counted from the two coverslips. Experiments were carried out in triplicates. Cells were also assessed for morphological changes associated with proliferative arrest such as cell enlargement and flattening out.

In a separate set of experiments, cells that had been serum-starved for 3 days, with medium containing 0.1% or 0.5% FCS, were stimulated to re-enter the cell cycle by adding medium with 20% FCS. Two coverslips were fixed and processed for PCNA at 0h, 4h, 8h, 12h and 24h, 36h, 48h, 72h after serum re-stimulation. Experiments were carried out in three replicates and, for each replicate, the proportion of PCNA positive cells was calculated on 100 cells obtained from the

two coverslips in each treatment group. The percentages of $PCNA^+$ cells found in cycling cells cultured for 48h in 10 % FCS were used as a control of the proliferative state.

Effect of serum starvation on cell viability was assessed by Trypan blue staining. Morphological changes occurring in serum-starved and serum re-stimulated cells were also evaluated.

Contact inhibition experiments were set up using the selected mouse foetal fibroblast (MFF) cell line MFF8, at passage 3 (for selection criteria see Paragraph 2.2).

To assess growth arrest by contact inhibition, using the PCNA staining, cells, seeded at an average density, were cultured until confluent (72h). Confluent cells were kept under contact inhibition conditions for an additional 7 days. Two coverslips were fixed and stained for PCNA, 24 h after seeding (cycling cells); 72h after seeding, when they had reached 90-95% confluence (contact inhibition day 0 or ci0), and every 24h after they had reached confluence (ci1-ci7). Data were collected in three separate experiments, and, in each experiment, the proportion of PCNA positive cells was calculated on 100 cells, counted from the two coverslips in each treatment group.

The effects of time spent under contact inhibition on replication rates, expressed as population doublings/day, on karyotype and on cell morphology were also evaluated.

Three $25cm^2$ flasks of MFF8 at passage 3, sub-cultured from the same passage 1 vial, to avoid variability between one vial and another, were kept under contact inhibition for 0 (ci0), 3 (ci3) and 6 days (ci6). Cells from each group were then sub-cultured for 3 passages, assessing, at each passage, the population doublings/day (for Methods see Paragraph 2.2). For each treatment group, at each passage, three $25cm^2$ flasks were seeded so that calculations were carried out in triplicates. Replication rate can be used as an indication of cell normality, since increased growth rates are a feature of transformed cells.

Viability was also evaluated at each passage using Trypan blue exclusion method (for Methods see Paragraph 2.1).

At passage 4, a forth 25cm^2 flask from each contact-inhibited group (ci3, ci6) was karyotyped (for Methods see Paragraph 2.1), and the proportion of normal spreads was compared with that sub-confluent cells, of the same cell line, at passage 4 and at passage 2.

Cells morphology was also evaluated to detect any signs of transformation. In our experience transformation is usually associated with appearance of clusters of polygonal cells, from which a population of cells, resembling young-fibroblasts, small and elongated, would arise (Paragraph 2.2; Fig.2.1).

3.2.1.3 Statistical Analysis

In serum starvation and serum re-stimulation experiments, data were analysed using a two-way ANOVA. Variables included:

- Proportion of PCNA$^+$ cells (dependent variable);
- Serum concentrations during starvation: 0.5% or 0.1% FCS (1st independent variable);
- Time, after serum starvation and re-stimulation (2nd independent variable);

In contact inhibition experiments, data were analysed using a two-way ANOVA. Variables included:

- Proportion of PCNA$^+$ cells or population doublings/day (dependent variable);
- Time, spent under contact inhibition at passage 3 (1st independent variable);
- Passages, after release from contact inhibition (2nd independent variable).

Viability results from serum starvation experiments were analysed with a one-way ANOVA:

- Percentage of viable cells (dependent variable);
- Treatment group (cycling, serum-starved for 3 days, contact-inhibited for 3 days; independent variable).

Viability results from contact inhibition experiments were analysed with a two-way ANOVA:

- Percentage of viable cells (dependent variable);
- Time, spent under contact inhibition at passage 3 and passages after release from contact inhibition (independent-variables).

Karyotyping results were analysed with a Chi-square contingency test.

All the ANOVA tests were carried out with the program Statistica 4.5 (Windows 1995). Chi-square tests were carried out with GenStat 4.21 (Windows 2000).

3.2.1.4 Results

PCNA staining showed that reduction of replicating cells ($PCNA^+$) observed in serum-starved cells is dependent on time elapsed after serum deprivation (time effect, $p<0.0001$). Shifts in the percentages of cycling cells observed during serum starvation (serum x time interaction, $p=0.71$) were similar in cells serum-starved with 0.1% FCS and 0.5% FCS. The percentages of $PCNA^+$ cells observed in groups serum-starved 24h with 0.5% or 0.1% FCS were significantly lower ($p<0.0001$) than those observed in cycling cells, cultured 24h with 10% FCS (Fig.3.1). At this time morphological changes associated with cell quiescence were also observed (Fig.3.3B). The percentages of $PCNA^+$ cells decreased significantly in the 0.1% FCS ($p<0.02$) and the 0.5% FCS (<0.001) groups till 48h after serum deprivation and then remained constantly low ($p>0.05$% for 0.1% FCS; $p>0.5$% for 0.5% FCS). Overall percentages of $PCNA^+$ cells observed in cells serum-starved with 0.1% FCS (3.7±0.9) were lower than those serum-starved with 0.5% FCS (5.7±1.0, $p<0.03$). The lowest percentages of $PCNA^+$ cells were observed after 72h after serum deprivation, with 0.1% FCS (0.6±0.5%).

Serum re-stimulation experiments showed that average percentages of $PCNA^+$ cells gradually increased after serum re-addition (time effect, $p<0.0001$; Fig.3.2). Overall percentages of $PCNA^+$ cells, including both data from 0.1% and 0.5% groups, progressively increased for the first 12h after serum re-stimulation (1.2±0.6% at 4h; 0.8±0.5% at 8h; 6.0±2.0% at 12h). At 24h, the percentages of $PCNA^+$ cells reached a peak (25.8±2.9%) that was even higher ($p<0.001$) than those observed in cycling cells that had been cultured for 24h with 10% FCS (19.0±2.3%). Cell morphology also changed at this stage (Fig.3.3C). After serum re-stimulation for 24h, the percentages of $PCNA^+$ cells started decreasing reaching, at 48h, a level (9.3±1.8%) similar to that observed at 12h ($p=0.13$) and, at 72h, a level (5.6±0.6%), similar to that observed in serum-starved cells (2.5±0.7%; $p=0.16$).

Figure 3.1 Growth arrest by serum starvation

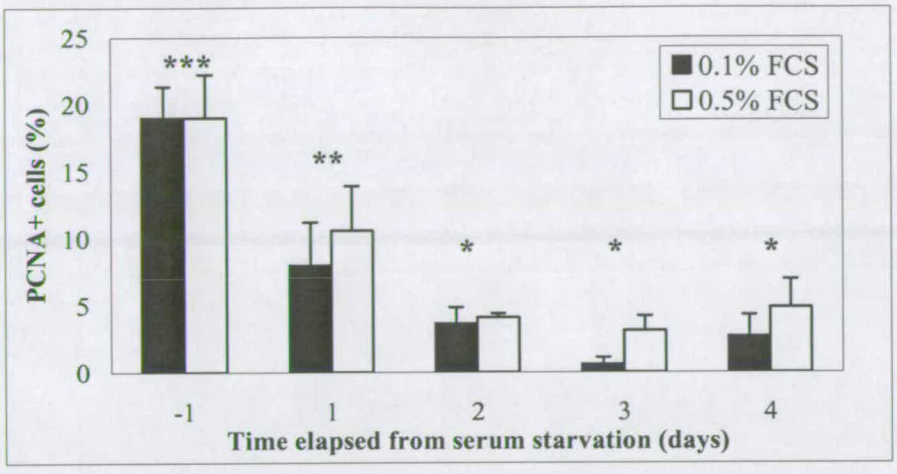

Figure 3.2 Cell cycle re-entry after serum re-stimulation

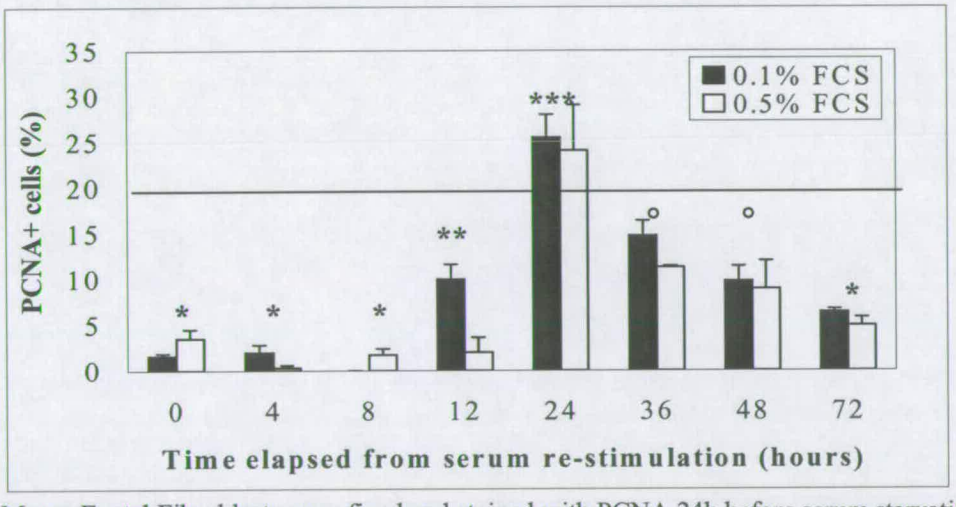

Figure 3.1 Mouse Foetal Fibroblasts were fixed and stained with PCNA 24h before serum starvation (-1) and at a 24h interval after serum starvation (1-4), with 0.1% or 0.5% FCS. Cells fixed 24h before serum starvation had been cultured for 24h in 10% FCS and were considered a control population of cycling cells. In **Figure 3.2** Mouse Foetal Fibroblasts were serum-starved with 0.5% or 0.1% FCS, and then re-stimulated with 20% FCS. Cells were fixed and stained with PCNA at different time points after serum re-stimulation to assess cell cycle re-entry. The horizontal line represents levels of $PCNA^{+}$ cells in groups cultured with 10% FCS (cycling). Only cells at 36h were not significantly different form cycling cells. In Fig.3.1-3.2 data from 3 experiments are summarised as Mean±SEM (two-way ANOVA, α=0.05, Statistica 4.5, Windows 1995).

Figure 3.3 Morphological changes in serum-starved foetal fibroblasts

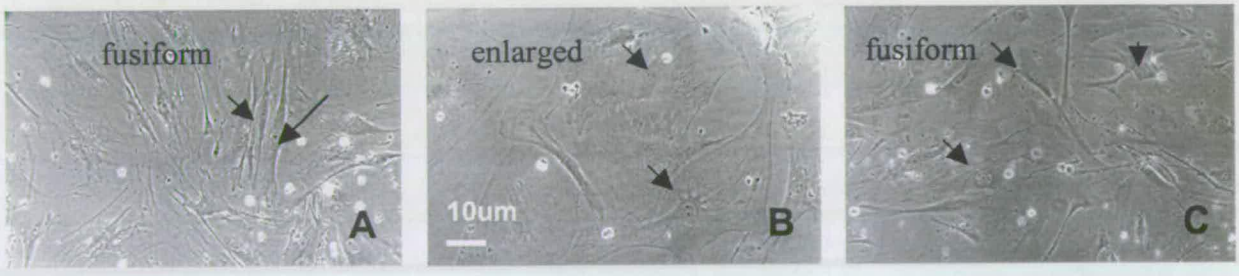

Brightfield photographs of cells cultured with for 24h with 10% FCS (A), serum-starved for 3 days (B), with 0.1% FCS and then re-stimulated for 24h with 20% FCS (C). Cells were enlarged during serum starvation but acquired again a fusiform, fibroblast-like shape after serum re-stimulation. Arrows point at cell nuclei.

The average percentages of cycling cells found in 0.1% FCS groups after serum re-stimulation (9.0±1.8%) were similar (serum effect, $p>0.09$) t0 those observed in 0.5% FCS groups (7.1±1.7%). Shifts in the percentages of $PCNA^+$ cells were also similar in the two groups (treatment x time interaction, $p=0.46$, Fig.3.2).

Trypan blue staining showed that serum-starved cells had high percentages of viable cells (≥94%), similar to those found in cycling cells (≥95%, $p=0.35$).

Contact inhibition induced a time-dependent (time effect, $p<0.0001$) reduction of percentages of cells in S-phase (Fig.3.4). The percentages of $PCNA^+$ cells, observed on the day of confluence, were significantly lower than those observed in sub-confluent cells ($p<0.001$). A further decrease in the percentages of cells in S-phase was observed after 3 days of contact inhibition ($p<0.001$). Beyond this time point the levels of $PCNA^+$ cells remained constantly low ($p>0.1$).

Viability of confluent cells kept under contact inhibition for 0, 3 and 6 days, was high, regardless of time spent under contact inhibition (98.0±0.5%; 99.0±0.8%; 98.3±0.3%; $p>0.4$). Low percentages of apoptotic cells, similar to those found in sub-confluent cells (95.0±1.1%) were found in samples kept under contact inhibition for 3 days, and then stained with Propidium Iodide (97±0.9%, $p=0.56$). However, after sub-culture, depending on time spent under contact inhibition (treatment effect, $p=0.0002$) and on passage number (passage x treatment interaction, $p<0.04$), viability was significantly affected. Overall viability of cells kept under contact inhibitions for 3 days (94.0±1.1%) was significantly lower than viability of cells kept under contact inhibition for 0 (98.6±0.2%) and 6 days (97.9±0.5%). The lowest survival rates were observed at passage 4 and 5 (93%), after which viability increased to levels comparable to those observed in other groups ($p>0.8$).

Contact inhibition also affected number of population doublings/day, used here as a measure of cell growth rates (Fig.3.5). Cells kept under contact inhibition at passage 3, for 3 (ci3p3) and 6 (ci6p3) days, had almost zero population doublings/day, whereas cells, that had just reached confluence, had significantly higher growth rates (doublings/day, $p<0.0001$). In control cells, growth rates remained unchanged at passage 4 and then decreased significantly at passage 5 and 6 ($p<0.0001$), reaching values close to zero. After a temporary decrease in cell

Figure 3.4 Growth arrest by contact inhibition

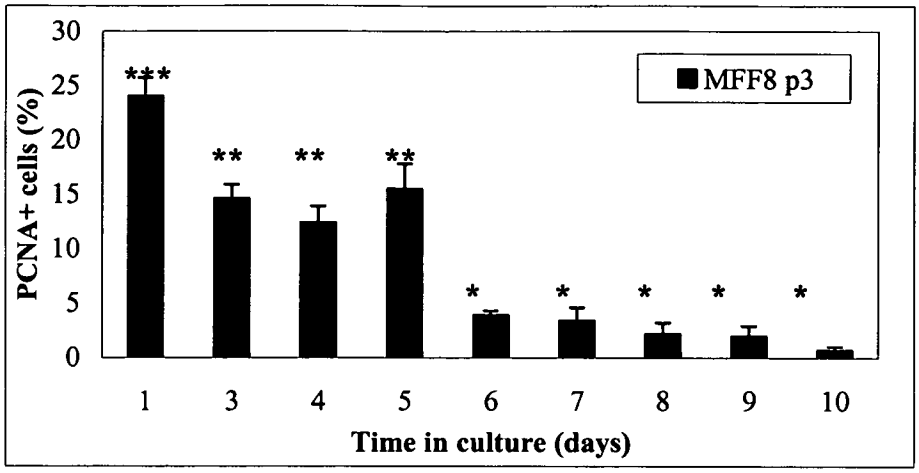

Figure 3.5 Effect of contact inhibition on replication time

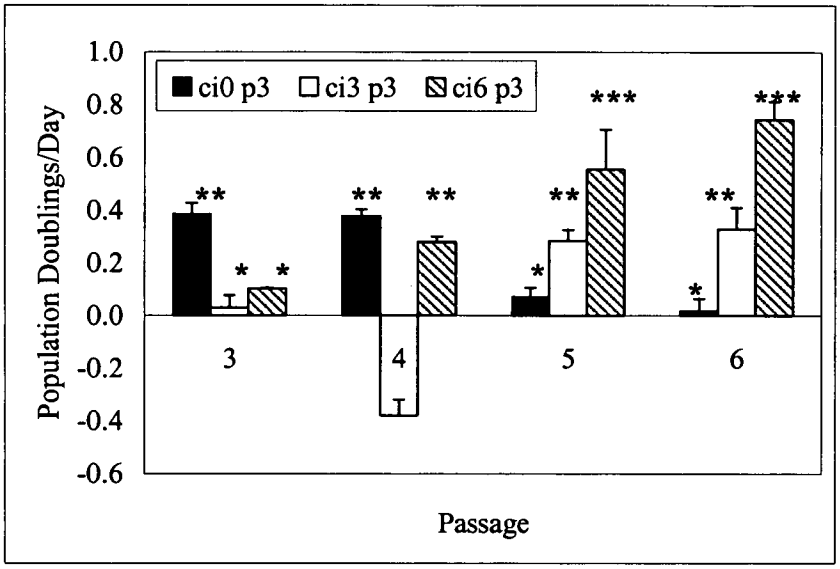

Figure 3.6 Effect of contact inhibition on karyotype

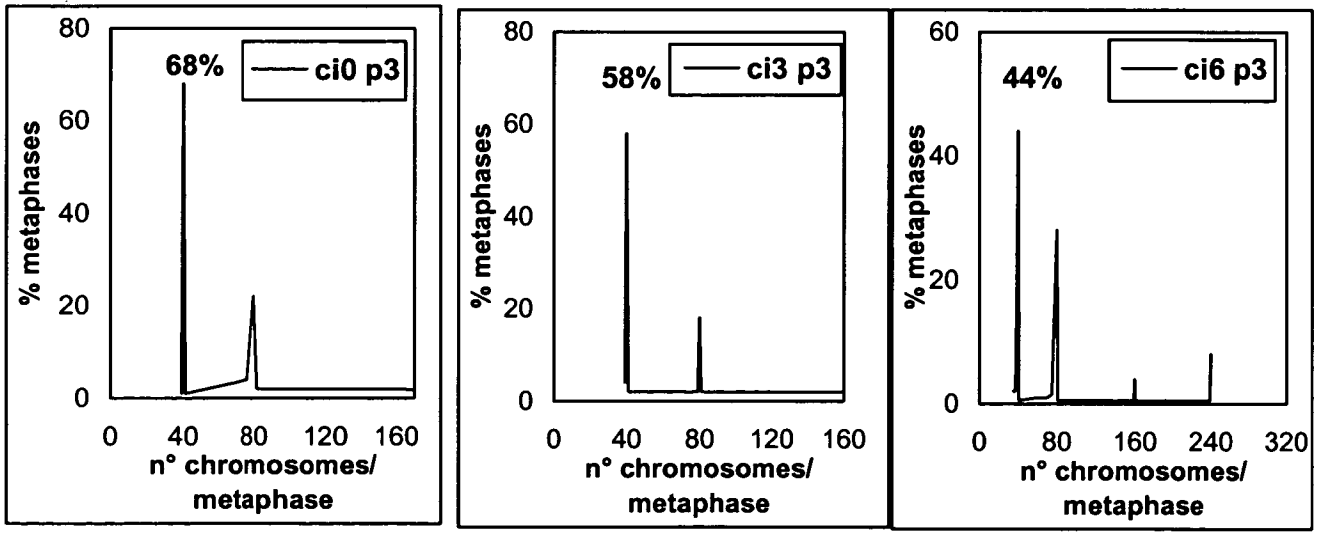

Figure 3.4 Mouse Foetal Fibroblasts (MFF) at passage 3 were cultured in 10% FCS medium for 10 days. Cells were confluent at day 3 (ci0). Percentages of cells in S-phase ($PCNA^+$) were calculated in sub-confluent cells (day 1), and cells that had been under contact inhibition for a maximum of 7 days (day 10 of culture). Significant reductions in percentages of $PCNA^+$ cells were observed at day 3 (ci0) and day 6 (ci3), after 3 days under contact inhibition. Data are expressed as mean±SEM of three experiments (α=0.05; one-way ANOVA; Statistica 4.5, Windows 1995).

Figure 3.5 Mouse Foetal Fibroblasts (MFF) that had been kept under contact inhibition, at passage 3 (p3), for 0 (ci0), 3 (ci3) and 6 days (ci6), were sub-cultured for further 4 passages. At each passage, population doublings/day were calculated, and used as a measure of cell growth rate. Data are expressed as mean±SEM of results of three counts carried out on three flasks/group, at each passage (α=0.05; 2-way ANOVA; Statistica 4.5, Windows 1995).

Figure 3.6 Mouse Foetal Fibroblasts that had been kept under contact inhibition, at passage 3, for 0 (ci0p3), 3 (ci3p3) and 6 (ci6p3) days, were sub-cultured and karyotyped at passage 4. Multiple populations of polyploid cells (>4N) were visible after 6 days of contact inhibition.

numbers, observed at passage 4, growth rates of cells, that had been kept under contact inhibition for 3 days (ci3p3), started to increase steadily. Growth rates of cells, that had been under contact inhibition for 6 days (ci6p3), increased steadily at each passage (Fig.3.5). By passage 5, number of population doublings/day in contact-inhibited cells was higher than that observed in control cells ($p>0.0003$; Fig.3.5).

The percentages of cells with normal karyotype found at passage 4 in populations that had been under contact inhibition for 3 days (29/50, 58%) were comparable to those found in control, sub-confluent cells (34/50, 68%; $p=0.30$; Fig.3.6). Cells that had been under contact inhibition for 6 days, at passage 4 had significantly lower percentages (22/50, 44%) of cells with normal karyotype than controls ($p=0.016$; Fig.3.6).

Morphological analysis showed clusters of transforming cells (Fig.2.2D) at passage 5 and transformed cells (Fig.2.2E) at passage 6, for cells that had been kept under contact inhibition for 3 days at passage 3. Transformed cells were already visible at passage 4 in populations that had been kept under contact inhibition for 6 days, at passage 3.

3.2.1.5 Discussion

To induce growth-arrest MFF had to be serum-starved for at least 2 days. Serum starvation with 0.1% FCS was more efficient in reducing percentages of cells in S-phase than 0.5% FCS. Most efficient growth-arrest was achieved after 3 days of serum starvation with 0.1% FCS.

The gradual increase in $PCNA^+$ cells observed after serum re-stimulation demonstrated that serum starvation did not impair ability of cells to re-enter the cell cycle. At 24h, the percentages of $PCNA^+$ cells were even higher than those found in control, cycling cells that had been cultured for 24h with 10% FCS. This effect may have resulted from the fact that cells, that had been previously serum-starved, had a better level of synchronization in S-phase than asynchronous, control cells. The gradual reduction in $PCNA^+$ cells observed after 24h of serum re-stimulation leading, after 72h, to levels comparable to those found in serum-starved cells, indicated that cells were reaching confluence.

Cells, that had been serum-starved with 0.1% FCS, had the same ability to re-enter the cell cycle as cells treated with 0.5% FCS, as suggested by the similar overall levels of cycling cells found in the two groups. The lag time (24h) before the highest DNA replication rate was achieved, was also not affected by the serum concentration used to induce proliferative arrest. Trypan blue staining showed that serum starvation had no detrimental effect on cell viability.

Although contact inhibition for three days significantly reduced the percentages of cells in S-phase, maximal growth-arrest was achieved after 3 days of contact inhibition. Growth-arrest was also confirmed by the low number of doublings/day observed in cells that had bee under contact inhibition for 3 or 6 days.

Contact inhibition did not affect immediately cell viability, but it reduced survival rates after sub-culture, at least in cells that had been under contact inhibition for 3 days. High death rates were observed in cells kept under contact inhibition for 3 days, at passage 4 and 5. The high death rates observed at passage 4 might explain the drop in population doublings/day observed at this stage. Contact inhibition at passage 3, for 6 days (ci6p3) did not affect viability after sub-culture, possibly because transformed cells had already replaced suffering cells. The fastest growth rates (population doublings/day) observed in this treatment group, compared to cells that had been under contact inhibition for 3 days, regardless of the passage considered, supports this explanation. The abnormal karyotype found in this treatment group, at passage 4, and the appearance of transformed like-cells, at that time, also support this idea.

Control cells, that were passaged immediately after reaching confluence, were senescing by passage 5 and 6, as suggested by their growth rates close to zero and as previously observed for this cells line (Paragraph 2.2). The lower population doublings/day observed at passage 4, in cells that had been kept under contact inhibition for 3 and 6 days, suggests the presence of a lag phase following growth-arrest. The increase in population doublings/day, at passage 5 and 6, at a time when control cells are senescing, could be interpreted as a sign of transformation. Other two observations support this explanation: appearance of transformed cells at passage 4 and 6, respectively in cells that had been kept under contact inhibition for 6 or 3 days; abnormal karyotype, at passage 4, that had been observed in cells that

had been contact-inhibited for 6 days. These observations, together with the persistence of a normal karyotype at passage 4, also suggests that transformation of cells contact-inhibited for a shorter time (3 days) might occur at a later passage.

3.2.1.6 Conclusions

On the basis of these observations, two protocols were selected because of their ability to induce growth-arrest, with the least risks of inducing cell death or transformation:

a) Serum starvation for 72h, with medium containing 0.1% FCS
b) Contact inhibition for 72h, in medium containing 10% FCS

3.2.2 Quiescence by contact inhibition and serum starvation

3.2.2.1 Aims

Assess if, under the selected experimental conditions, serum starvation and contact inhibition can be used to produce quiescent MFF, characterised by:

1) High levels of positive quiescence markers ($p27^{KIP}1$, p130);
2) Low levels of negative quiescence markers (FITC staining);
3) Changes in chromatin structure (HP1 proteins).

3.2.2.2 Experimental Design

Three treatment groups were considered:

1) Cycling cells, sub-confluent and cultured in 10% FCS for 24h;
2) Serum-starved cells, cultured in 0.1% FCS for 3 days;
3) Contact-inhibited cells, cultured in 10% FCS till confluent and kept under contact inhibition for three days.

Bivariate analysis was carried out, with three staining:

1) Propidium Iodide and $p27^{KIP1}$ staining (PI/$p27^{KIP1}$);
2) Propidium Iodide (PI) and p130 staining (PI/p130);
3) Propidium Iodide (PI) and FITC staining (PI/FITC);

Propidium Iodide staining (for Methods see Paragraph 2.6-2.10.1) gave information about cells cycle profile of growth-arrested cells, based on their DNA

content (2N=G0/G1; 2/4N=S-phase; 4N=G2/M). It also gave information about apoptotic rates (<2N) and the percentages of polyploid cells (>4N). It was also used to gate diploid cells (2N=G0/G1) and assess the percentages of diploid cells, as opposed to the percentages of total cells, expressing (G0), or not expressing (G1), quiescence markers.

The cell line MFF9 was used in all FACS experiments, within passage 4, before the onset of senescence or transformation (see Paragraph 2.2 for selection criteria).

Three replicate experiments were carried out for each group and staining.

Descriptive studies of HP1 proteins sub-nuclear localisation were carried out in serum-starved cells, using indirect immunofluorescence and epifluorescent microscopy (for Methods see Paragraph 2.11).

3.2.2.3 Statistical analysis

All data were analysed with a one-way ANOVA (Statistica 4.5, Windows 2000). Variables included:

1) Percentages of cells expressing a marker ($p27^+$, $p130^+$, $FITC^+$) or with a certain DNA content (2N, 2/4N, 4N, >2N, >4N; dependent variable);
2) Treatment group, cycling, serum-starved or contact-inhibited (independent variable).

3.2.2.4 Results

Cell cycle analysis (Fig.3.7A) showed a significant decrease in S-phase cells in contact-inhibited and serum-starved cells, compared to cycling cells ($p<0.0001$). The reduction of the percentages of replicating cells observed in synchronized cells, was associated with an increase in the percentages of G0/G1 ($p>0.05$ for serum-starved cells; $p<0.001$, for contact-inhibited) and G2/M cells ($p<0.0001$ for serum-starved cells; $p=0.04$ for contact-inhibited).

Figure 3.7 Cell cycle profile and expression of quiescence markers in serum-starved and contact-inhibited cells

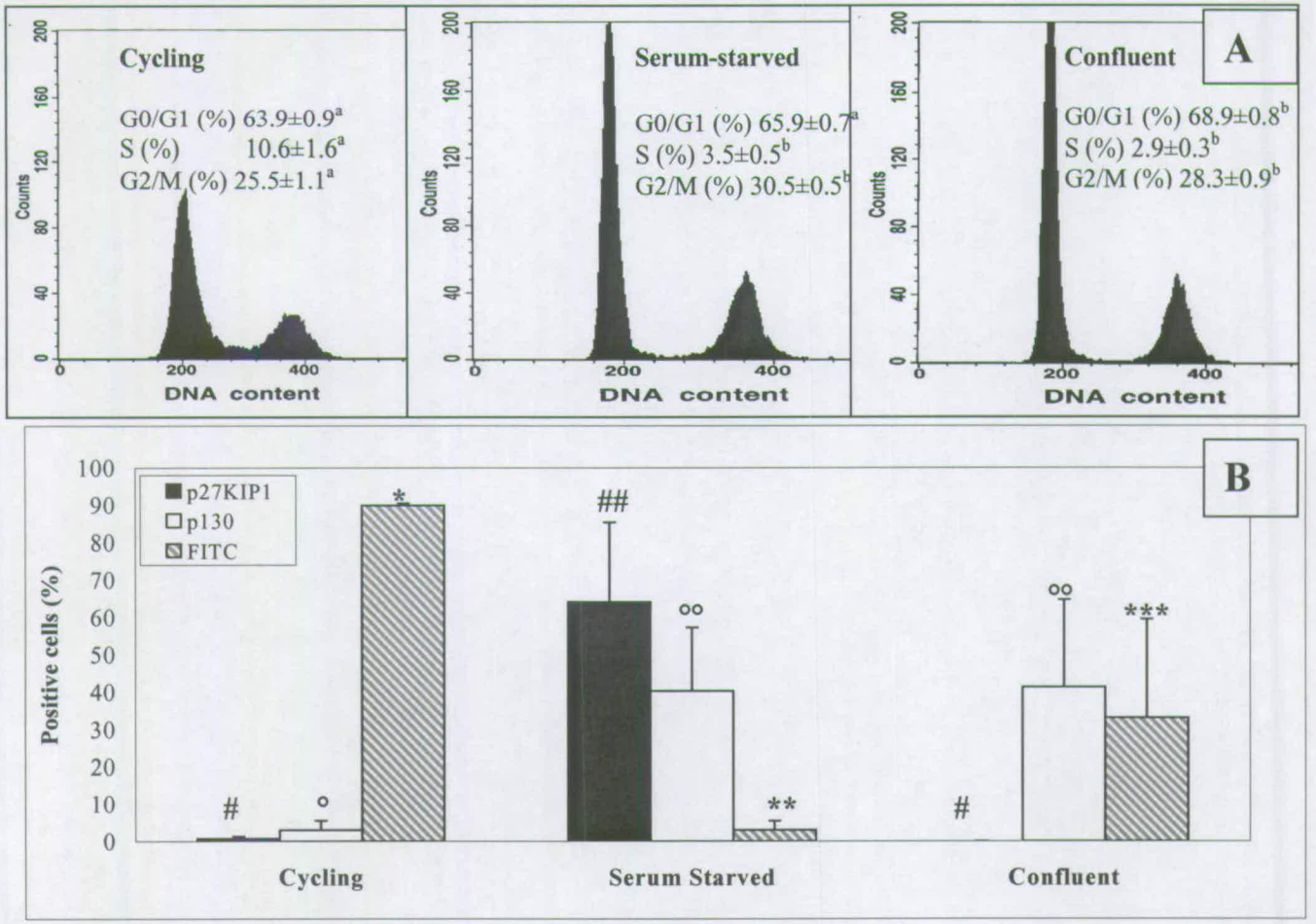

Mouse Foetal Fibroblasts, at passage 3, were assigned to three treatment groups: cycling cells, cultured for 24h with 10% FCS; serum-starved cells, cultured for 72h with 0.1% FCS; confluent cells, kept under contact inhibition for 3 days. Samples were double stained with Propidium Iodide and $p27^{KIP1}$, p130 or FITC. Propidium Iodide was used to detect cell cycle profiles (A), whereas p130 and p27 were used as positive G0 markers and FITC was used as a negative G0 marker (B). Data from three replicates are expressed as mean±SEM. Percentages within the same cell cycle category with different superscripts, and columns with the same colour and different symbols, differ significantly (one-way ANOVA, α=0.05).

Figure 3.8 Cell cycle distribution of serum-starved quiescent cells

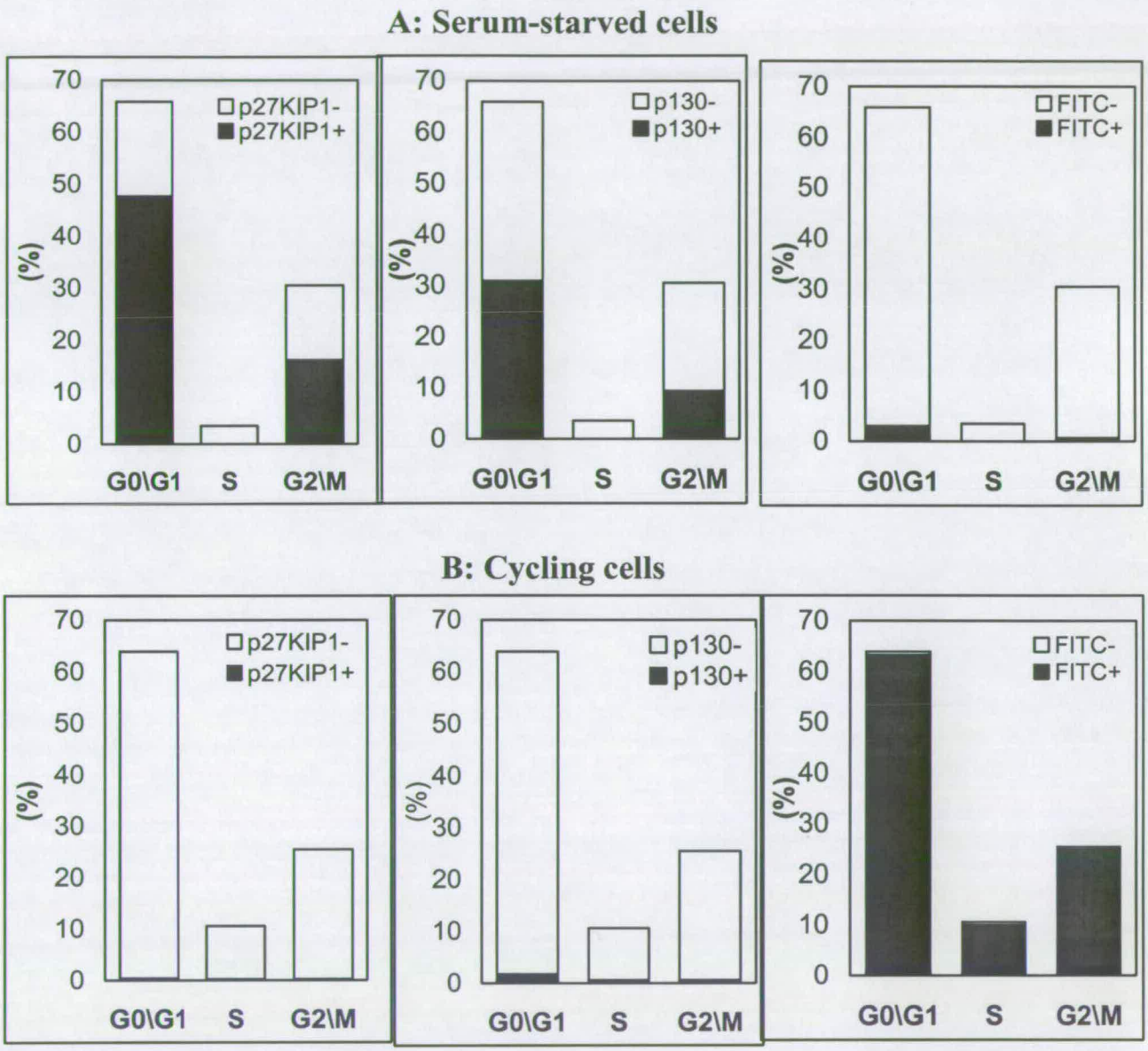

Cell cycle distribution of quiescent and non-quiescent cells was assessed in cycling cells, used as a non-quiescent control, and serum-starved cells. Cells were stained with PI/$p27^{KIP1}$; PI/p130; PI/FITC. Cells that were $p27^{+}/p130^{+}/FITC^{-}$ were considered quiescent; cells that were $p27^{-}/p130^{-}/FITC^{+}$ were considered non-quiescent. Cells were gated according to their DNA content: G0/G1 (=2N); S (=2N/4N); G2/M (=4N). Proportion of cells expressing quiescence markers, was assessed on gated cells. Data are expressed as mean percentages of three replicate experiments.

In serum-starved groups, the percentages of apoptotic cells were significantly higher than those found in cycling cells (17.4±2.9% vs 8.7±1.2%, p=0.02), whereas in contact-inhibited cells they were significantly lower (3.3±0.6%, p<0.0001).

Serum-starved cells had significantly higher percentages of $p27^{KIP1+}$ (p=0.005) and $p130^{+}$ cells (p<0.05), and significantly lower percentages of $FITC^{+}$ cells (<0.01), than cycling cells (Fig.3.7B). Cell cycle distribution of quiescent cells in the serum-starved population was also investigated (Fig.3.8B), and compared to that of cycling cells (Fig.3.8A).

Contact-inhibited cells did not express $p27^{KIP1}$ (Fig.3.7B), similarly to what was observed in cycling cells (p=0.05). The percentages of p130 were significantly higher than those found in cycling cells (p<0.05), and comparable to those found in serum-starved cells (p=0.82; Fig.3.7B). The percentages of $FITC^{+}$ cells were intermediate between those found in cycling cells (p<0.05) and those observed in serum-starved cells (p<0.05; Fig.3.7B).

Immunocytochemistry results showed differences in sub-nuclear distribution of HP1 proteins in serum-starved and cycling cells (Fig.3.9).

3.2.2.5 Discussion

Cell cycle profiles confirmed the growth-arrest state shown by PCNA staining. It also showed that 2/3 of the cells were arrested in G0/G1 and 1/3 was arrested in G2/M. This is not the result of karyotype abnormalities or of cell aggregation. It must be therefore correlated with a synchronization effect. Unlike progression through early G1 (Sherr, 1993; Baldin *et al.*, 1993), that is dependent on availability of growth factors (mitogen-dependent), transition through G2/M is mitogen-independent, and is regulated by the activity of the cyclin B/$p34^{cdc2}$ (Cdk1) protein kinase complex, otherwise known as Meiosis/Mitosis Promoting Factor (MPF) (for review on Cdks see Pines and Hunter, 1991). Progression through G2/M is also regulated by $p34^{cdc2}$ (Cdk1), associated with cyclin A. The Cdk inhibitor $p27^{KIP1}$, that is up regulated in G0 cells, is a promiscuous inhibitor: it mainly targets Cyclin E/Cdk2 and Cyclin D1/Cdk4 complexes, but it is also able to inhibit Cdk2

Figure 3.9 Sub-nuclear distribution of HP1 proteins in serum-starved and cycling cells

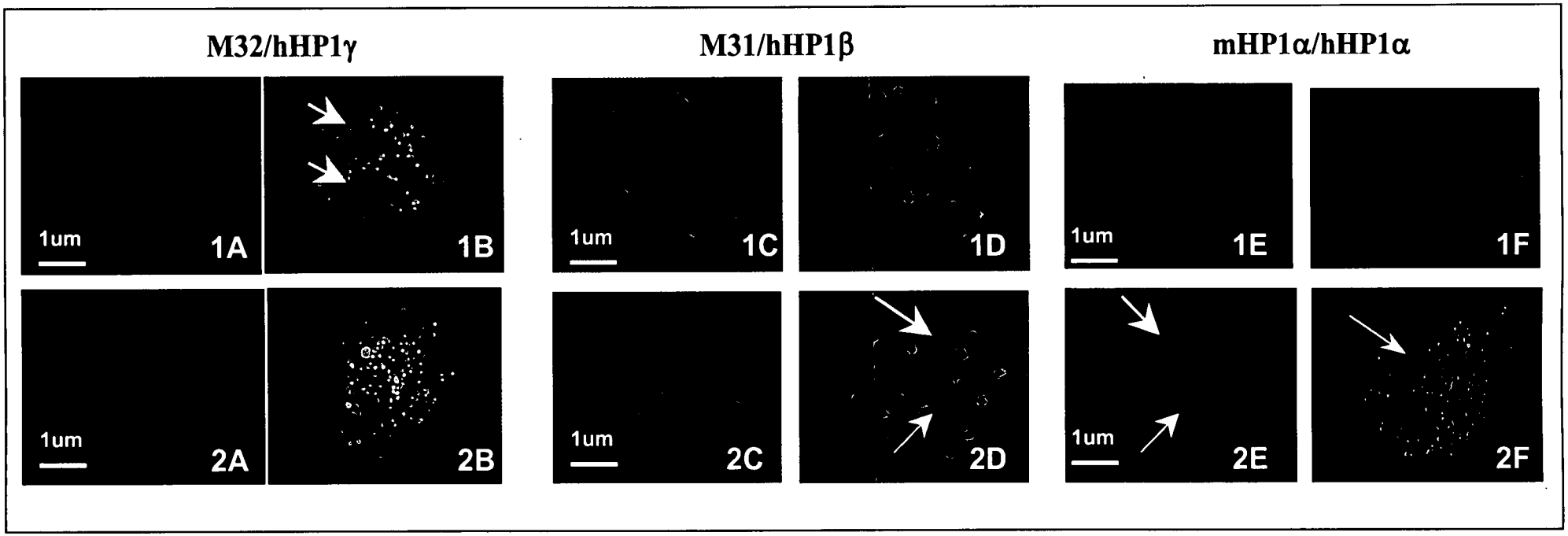

Microphotographs of nuclei of Mouse Foetal Fibroblasts, that had been cultured for 24h with 10% FCS (cycling; 1A-F), or serum-starved for 72h with 0.1% FCS (quiescent, 2A-F). Cells were fixed with paraformaldehyde 1% or 4%, processed for indirect immunofluorescence with FITC conjugated anti-M32 (1A-B; 2A-B), FITC conjugated anti-M31 (1C-D; 2C-D) or FITC conjugated anti-mHP1α (1E-F; 2E-F), recognizing mouse homologues of human hHP1γ, hHP1β and hHP1α. Finally cells were stained with the DNA dye DAPI (blue, 1A-2A, 1C-2C, 1E-2E). M32 concentrated around the nucleoli in cycling cells (1B, arrows) and had a more uniform distribution in G0 cells (2B); M31 was organized into big clusters (arrows, 2D), colocalised with clusters of heterochromatin in G0 cells (arrows, 2C) and was both organised into clusters and uniformly diffused in cycling cells (1D); mHP1α distribution was similar to that of M31, except that clusters (arrows, 2F) were smaller.

activity, when it is bound to other cyclins, and cyclin $p34^{cdc2}$ (Cdk1) activity, when it is bound to cyclin B or A (for review on Cdk inhibitors see Sherr and Roberts, 1995). Therefore, up regulation of $p27^{KIP1}$ induced by serum starvation, could potentially induce arrest in G2/M by inactivation of the cyclin B/Cdk1 complex.

Serum starvation had a negative effect on cell survival, in contrast with what previously found with Trypan blue staining, that showed no difference in the percentages of live cells between cycling and serum-starved cell populations (94-95%, p=0.35). PI might represent a more sensitive method of analysis.

Contact inhibition had no detrimental effect on cell survival, nor on karyotype, as suggested by the low percentages of polyploid cells, similar to the ones found in cycling cells. These results confirmed previous findings on cell viability and karyotype of cells contact-inhibited for three days at passage 3 (see paragraph 3.2.1.4).

According to a broad definition of quiescence, serum-starved cells were quiescent because, compared to cycling cells, they had significantly higher percentages of $p27^{KIP1+}$ and $p130^{+}$ cells, and significantly lower percentages of $FITC^{+}$ cells. The existence of a quiescent status in serum-starved cells was also confirmed by HP1 immunocytochemistry results, that showed dramatic differences in the chromatin status of cycling and serum-starved cells. Particularly important in confirming quiescent state of serum-starved cells were changes observed in the sub-nuclear distribution of M31/hHP1β, with pericentromeric localisation, since changes in centromeric chromatin have been described as a landmark of nuclear quiescence.

However, flow cytometry results also indicated that serum-starved cells constitute a variable population of G0 cells:

1) Not all serum-starved cells were quiescent. Although almost all serum-starved cells were $FITC^{+}$, only a proportion were $p27^{KIP+}$ and $p130^{+}$.

2) Percentages of quiescent cells varied according to the quiescence marker used. This observation suggests that different markers might identify sub-populations of G0 cells with different features. Whether these sub-sets of cells overlap could only be proved by simultaneous staining with all three markers.

3) The high SEM values obtained in serum-starved cells indicated a great variability within replicate experiments, carried out under the same experimental conditions, but on different populations of cells.

Cell cycle analysis of serum-starved cells showed that not all quiescent cells were diploid and not all diploid cells were quiescent. When considering only diploid cells (G0/G1), the percentages of G0 (quiescent) or G1 (non-quiescent) cells, depending on the marker used, were: with $p27^{KIP1}$, 72.5% in G0 and 27.5% in G1; with p130, 48.2% were in G0, and 51.8% were in G1; with FITC, 94.1% were in G0 and 5.9% were in G1. However, between 81% and 74% of quiescent cells were diploid (G0/G1). The remaining cells were quiescent, but with a tetraploid content of DNA, and therefore in G2/M. This implies that, under the experimental conditions used in these experiments, quiescence and diploidy were not necessarily associated.

Contact inhibition results were different from those obtained in serum-starved cells. Growth-arrest induced by cell-to-cell contact has been usually associated with increases in $p27^{KIP1}$ (St. Croix *et al.,* 1998). However, in these experiments very low percentages of contact-inhibited cells expressed $p27^{KIP1}$, a situation similar to that observed in cycling cells. The percentages of $FITC^{+}$, indicative of protein synthesis levels, were also higher than those found in serum-starved cells, although they remained lower than those observed in non-quiescent cells. The only similarity with serum-starved quiescent cells, were the high percentages of $p130^{+}$ cells. A possible explanation might be that, although cells still appeared to be normoploid under the conditions used in these experiments, they might have already been undergoing changes associated with transformation, occurring at later passages. The percentages of polyploid cells found in contact-inhibited cells, at passage 3, were comparable to those found in cycling and serum-starved cells, and karyotype of contact-inhibited cells was still normal at passage 4. However appearance of clusters of transforming cells at passage 6, in association with the shortening of the doubling time at passage 5 and 6, suggest that contact inhibition might induce transformation at later passages. Subtle changes associated with cell transformation occurring at passage 4 could explain loss of immuno-positivity for quiescence markers.

3.2.2.6 Conclusions

Serum starvation appears to be the best method to produce a well-characterised population of quiescent mouse foetal fibroblasts. However it has two main drawbacks:

- It produces a mixed population of diploid and tetraploid cells;
- It produces a mixed population of quiescent and non-quiescent cells.

Presence of high percentages of diploid and tetraploid cells is not optimal for nuclear transfer experiments. Tetraploid cells can be successfully used for mouse nuclear transfer, when reconstructed embryos are cultured in the absence of cytochalasin B, to enable pseudo-polar body extrusion and depolarisation. However, nuclear transfer with diploid cells requires the addition of cytochalasin B, since, under these experimental conditions, pseudo-polar body extrusion would induce haplodization.

Serum starvation did not produce a pure population of quiescent cells. The levels of purity could not be improved by positive selection of quiescent cells or negative selection of non-quiescent cells, given the intracellular nature of the quiescence markers in fibroblasts, that makes them accessible only after fixation.

3.3 SYNCHRONIZATION IN G1

3.3.1 Growth-arrest by G1 or G1/S blocking agents

3.3.1.1 Experimental Design

Mouse Foetal Fibroblasts were synchronized using the G1/S blocking agents hydroxyurea and methotrexate, and the G1 blocking agent mimosine and lovastatin (for Methods see Paragraph 2.5).

Experimental conditions included:

- Two time points, 24h and 48h;
- Eleven treatment groups, corresponding to four blocking agents used at two or three different concentrations:
  - Lovastatin: 5uM, 15uM, 30uM;
  - Hydroxyurea: 1mM, 2mM, 4mM;

- Methotrexate: 0.1uM, 1uM, 2uM;
- Mimosine: 400uM, 800uM.

Other four treatment groups were used as controls. Cells cultured in medium with 10% FCS, with no chemical added, were used as a culture control. Since lovastatin had been reconstituted with ethanol, control cells, cultured in medium with 10% FCS and similar concentrations of ethanol, but no lovastatin, were also included as controls (for Methods see Paragraph 2.5).

PCNA staining was used to assess growth-arrest under the different experimental conditions. Data were collected in three separate experiments.

3.3.1.2 Statistical analysis

Data were analysed using a two-way-ANOVA (Statistica 4.5, Windows 1995). Variables included:

- Percentage of $PCNA^+$ cells (dependent variable);
- Time and treatment (independent variables).

Main effects of time or treatment were assessed independently, before considering treatment and time interaction.

Analysis was also broken down in a one-way ANOVA (Statistica 4.5, Windows 1995), considering treatment effects only, at a fixed time point, 24h or 48h.

3.3.1.3 Results

The percentages of cells in S-phase found at 48h (14.8±1.9%) were significantly lower than those found at 24h (8.1±1.1%; time effect, $p<0.0001$). Treatment effect was also significant ($p<0.0001$). Lovastatin, hydroxyurea and mimosine, all significantly reduced the percentages of cells in S-phase compared to controls ($p<0.0001$). The percentages of $PCNA^+$ cells were similarly low in groups treated with lovastatin, hydroxyurea and mimosine ($p>0.05$). No significant difference was observed in the percentages of cells in S-phase found in groups treated with different concentrations of lovastatin ($p>0.6$), hydroxyurea ($p>0.3$) and mimosine ($p>0.3$). Lovastatin controls were similar to normal controls ($p>0.6$), except for the 15uM control, that had significantly lower percentages of $PCNA^+$ cells ($p=0.007$). The percentages of cells in S-phase in groups treated with 0.1uM and

Figure 3.10 Growth arrest by G1 and G1/S blocking agents

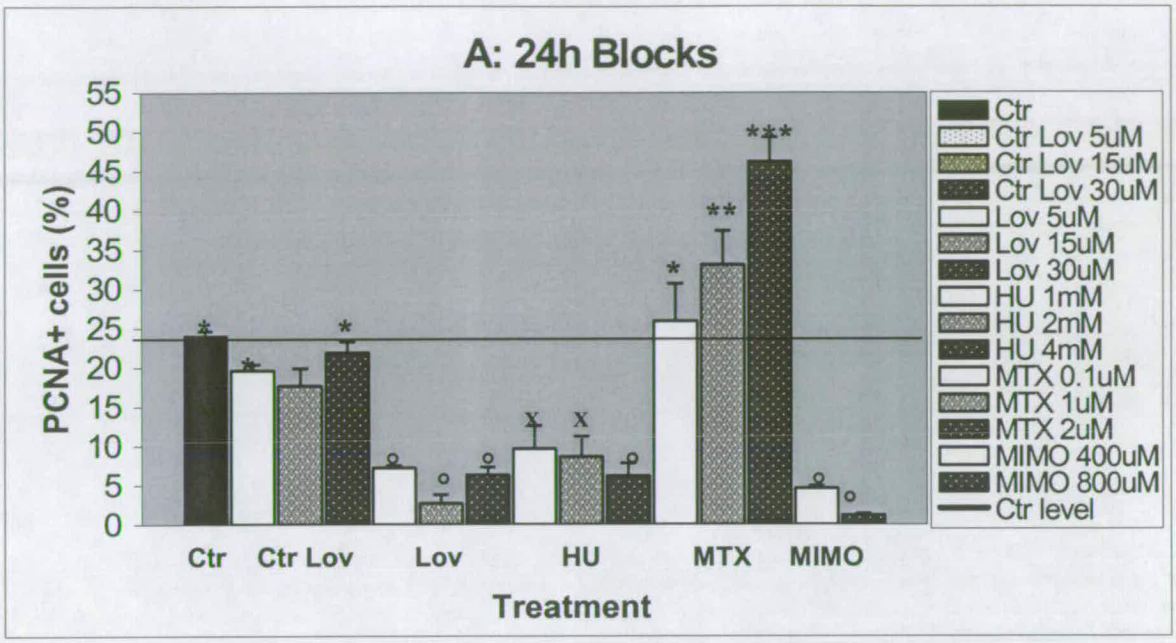

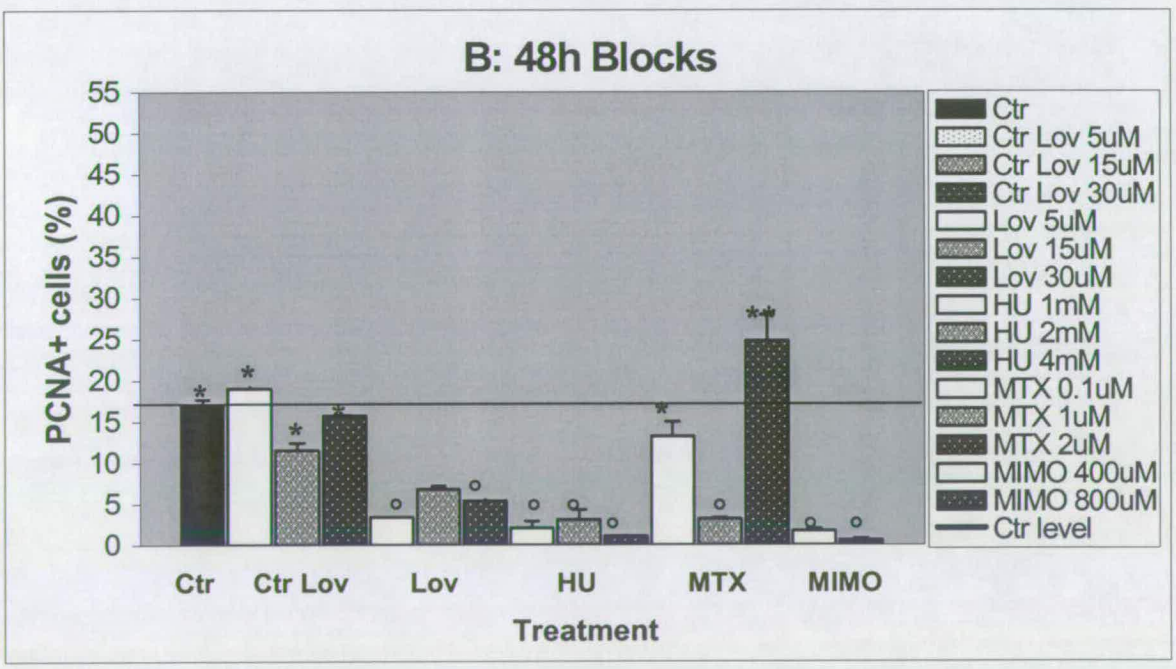

Mouse Foetal Fibroblasts were incubated for 24h or 48h, with 10%FCS alone (Ctr), or supplemented with different concentrations of the G1 blocking agents lovastatin (Lov 5-30uM), hydroxyurea (HU 1-4mM), methotrexate (MTX 0.1uM-2uM), mimosine (MIMO 400-800uM). Lovastatin was dissolved in ethanol, so controls, with similar concentrations of ethanol but with no lovastatin, were also included in the analysis (Ctr Lov 5-30uM). Cells were fixed and stained for PCNA, to assess percentages of cells in S-phase in the different treatment groups. The line indicates the level of $PCNA^+$ cells in cycling cells, cultured with 10% FCS alone (Ctr level). Data from three separate experiments are expressed as mean+SEM. Columns marked by symbols had percentages of PCNA+ cells significantly different from controls (Ctr; one-way ANOVA; treatment effect at 24h or 48h; α=0.05; Statistica 4.5, Windows 1995).

1uM methotrexate were similar (p=0.6; p=0.3) to those found in control groups or even higher, when methotrexate was used at the highest concentration (2uM; p<0.0001).

A significant reduction (p<0.0001) in the percentages of cells in S-phase was observed when cells were incubated for 24h with lovastatin, hydroxyurea and mimosine (Fig.3.10A). The lowest concentrations were as efficient as the highest ones in inducing growth-arrest in groups treated with lovastatin (p>0.1), hydroxyurea (p>0.2), and mimosine (p>0.3). The lowest percentages of $PCNA^+$ cells were observed in groups incubated for 24h with 800uM mimosine (1.2±0.2). These percentages were not significantly different from those observed in groups treated with lovastatin, regardless of the concentration, and with 4mM hydroxyurea. The percentages of $PCNA^+$ found in groups treated with 1mM and 2mM hydroxyurea (Fig.3.10A), although significantly lower than those observed in the control group (p<0.0001), were higher than those found in cells treated with 800uM mimosine (p=0.007, p=0.02).

Cells treated for 24h with methotrexate had levels of cells in S-phase similar, in the 0.1uM group (p=0.53), or significantly higher, in the 1uM (p<0.004) and 2uM (p<0.0001) groups, than controls.

Lovastatin control groups were similar to controls, except for the 15uM lovastatin control group (p=0.043).

All treated cells appeared healthy. Signs of suffering were observed only in cells treated with lovastatin.

Cells cultured for 48h, in the absence of blocking agents (control), had significantly lower percentages of $PCNA^+$ cells than cells cultured for 24h (p<0.03). Comparison of treatment groups with the control group, at 48h, gave similar results to those observed at 24h (Fig.3.10B). The lowest percentages of $PCNA^+$ cells were observed in cells treated with 800uM mimosine (0.7±0.0), and these were comparable to those observed at 24h (p=0.86). Similar percentages were obtained in groups incubated for 48h with 5uM (p=0.3) and 30uM (p=0.1) lovastatin and with hydroxyurea, regardless of the concentration (p>0.4). Only percentages observed in the 15uM lovastatin group were higher than those found in these treatment groups (p=0.047). Similarly to what was observed at 24h, the percentages of cells in S-phase

were similar to controls, in cells treated with 0.1uM methotrexate ($p=0.2$), and higher than controls, in cells treated with 2uM methotrexate ($p=0.01$). The percentages of $PCNA^+$ cells in the 1uM methotrexate group were lower than controls ($p<0.0001$), and similar to those found in control groups treated for 48h, with lovastatin ($p=0.2$), hydroxyurea ($p=0.4$) and mimosine ($p=0.4$).

The percentages of $PCNA^+$ cells found in lovastatin control groups were comparable to those found in control groups cultured for 48h ($p>0.06$). Cells in the lovastatin control and lovastatin treatment groups appeared to be suffering.

3.3.1.4 Conclusions

Incubation with blocking agents for 24h was as effective as incubation for 48h in inducing growth-arrest. Overall percentages of $PCNA^+$ cells were lower in the 48h groups compared to the 24h groups. However, at 48h, significant reductions in the percentages of $PCNA^+$ cells were observed in the culture control group whereas reductions in the percentages of $PCNA^+$ cells in treatment groups were similar tot hose observed at 24h. Time affects culture but not efficiency of growth-arrest.

Lovastatin, regardless of concentration, hydroxyurea 4mM, and mimosine 400 and 800uM, were equally effective in inducing growth-arrest. Appearance of suffering signs in lovastatin treated group, suggested possible detrimental effect of this chemical. This effect was not mediated by the presence of ethanol, used to dissolve this drug, since lovastatin controls, containing ethanol but not lovastatin, had no signs of suffering.

The most efficient and less detrimental growth-arrest in G1 was achieved by incubating cells with 4mM hydroxyurea or 400uM-800uM mimosine.

3.3.2 Absence of quiescence in G1 arrested cells

3.3.2.1 Experimental design

Dual parameter FACS analysis using Propidium Iodide and FITC was carried out on Mouse Foetal Fibroblasts, incubated for 24h in 10% FCS medium supplemented with 4mM hydroxyurea. Cells cultured for 24h in 10% FCS were used

Figure 3.11 Cell cycle and quiescence markers in cells treated with hydroxyurea

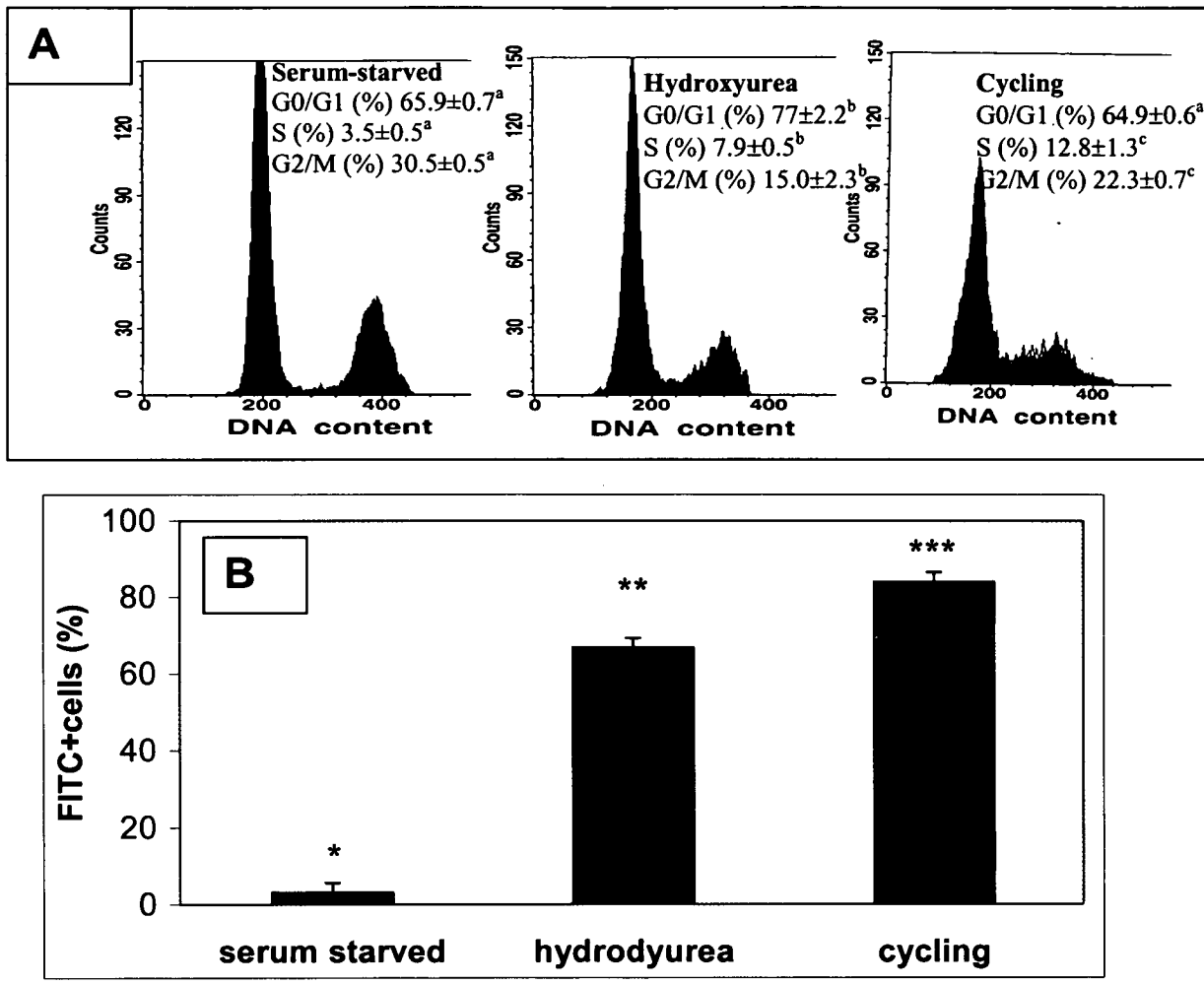

Figure 3.12 Cell cycle distribution of G1 cells, synchronized with hydroxyurea

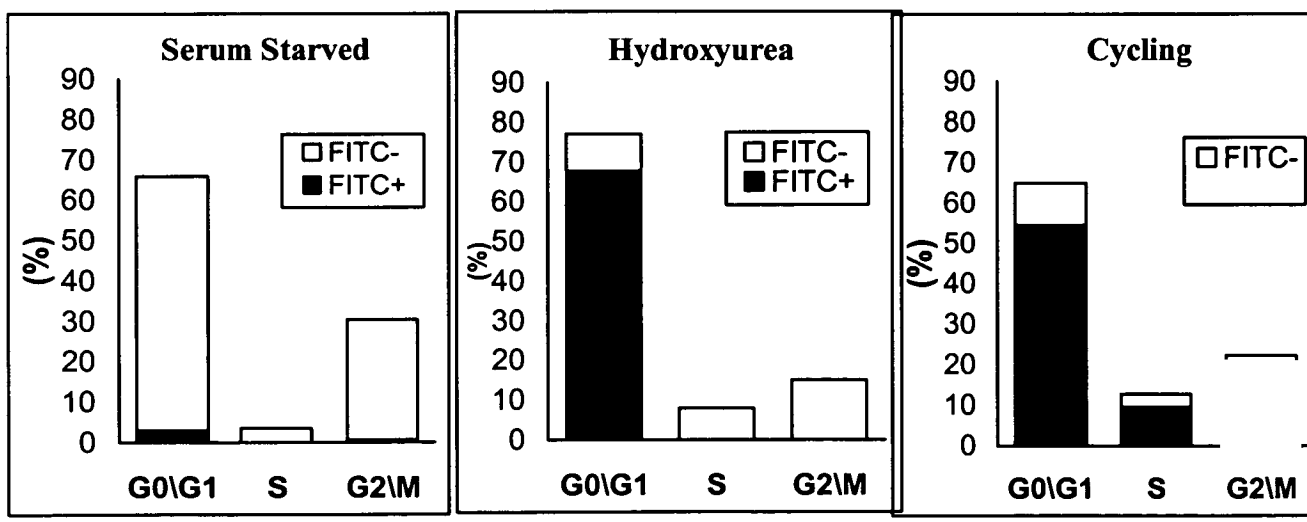

Figure 3.11 A-B Mouse Foetal Fibroblasts were cultured for 24h in 10% FCS medium alone or supplemented with 4mM hydroxyurea. Serum-starved data were obtained in previous experiments are shown here for comparison purposes. Samples were double stained with Propidium Iodide and FITC. Propidium Iodide was used to detect cell cycle profiles (A), whereas FITC was used as a negative G0 marker (B). Data from three replicates are expressed as mean±SEM. Percentages within the same cell cycle category with different superscripts (A), or columns with the same colour with different symbols (B), differ significantly (one-way ANOVA, α=0.05).

Figure 3.12 Cells were gated according to their DNA content: G0/G1 (=2N); S (=2N/4N); G2/M (=4N). The proportion of non-quiescent cells ($FITC^+$) was assessed on gated cells. Results of three replicate experiments are expressed as mean percentages.

as a control population of cycling cells. Data were also compared with those obtained from cells that had been serum-starved for three days with 0.1% FCS.

Parameters, acquired in three replicate experiments, included:

1) Cell cycle profiles, to asses cell cycle distribution of growth-arrested cells;
2) Percentages of apoptotic cells;
3) Percentages of cells with protein synthesis ($FITC^+$).

Data were analysed using a one-way ANOVA, with percentages as dependent variable and treatment as independent variable (Statistica 4.5, Windows 1995).

3.3.2.2 Results

Cells treated with hydroxyurea had significantly lower percentages of cells in S-phase than cycling cells ($p<0.02$), similarly to what was observed in serum-starved cells ($p<0.001$; Fig.3.11A). The percentages of cells in S-phase observed in groups treated with hydroxyurea were higher than the percentages observed in serum-starved cells ($p<0.02$). In cells treated with hydroxyurea, the percentages of G0/G1 (=2N) and G2/M (=4N) cells were respectively higher ($p=0.002$) and lower ($p<0.03$) than those observed in cycling cells (Fig.3.11A).

Apoptosis rates found in cells cultured for 24h with 10% FCS and 4mM hydroxyurea were higher than those found in cells cultured with 10% FCS medium alone ($p=0.03$) and higher than those found in serum-starved cells ($p=0.03$).

The percentages of $FITC^+$ cells found in the group treated with hydroxyurea were 20-fold higher than those observed in serum-starved cells ($p<0.0001$; Fig.3.11B). The percentages of $FITC^+$ cells in the hydroxyurea ($p=0.007$) and the serum-starved groups ($p<0.0001$) were both significantly lower than those observed in cycling cells (Fig.3.11B). The percentages of $FITC^+$ cells found in the diploid cell population (gate on G0/G1 cells) of the hydroxyurea treated cells (88.1±2.8%), were similar to those observed in cycling cells (95.9±1.3%; $p=0.13$).

Mean fluorescence of cells treated with hydroxyurea, considered both as a whole cell population (337±14) and as a diploid population (302±14), were higher than those found in serum-starved cells (168±36; $p<0.005$; 129±23; $p<0.002$) and similar to those found in cycling cells (309±7; $p=0.5$; 256±15; $p=0.18$).

Almost 100% of $FITC^+$ cells found in the hydroxyurea group, were diploid (Fig.3.12). In the hydroxyurea treatment group, 77±2.2% of the cells were diploid, and, of these, 88.1% were $FITC^+$ (G1) and 11.9% were $FITC^-$ (G0).

3.3.2.3 Discussion

Cell cycle analysis confirmed the growth-arrest state of cells synchronized with hydroxyurea. However, the hydroxyurea block was less effective than serum starvation in reducing the percentages of cells in S-phase. In cells treated with hydroxyurea, the decrease in the percentages of cells in S-phase was associated with a decrease in cells in G2/M, and an increase of cells in G0/G1-phase. This situation is different from the one observed in serum-starved cells, where the decrease in cells in S-phase was associated with an increase in cells in G2/M, while the percentages of diploid cells remained unchanged.

The higher apoptosis rates observed in cells incubated with hydroxyurea suggested that this treatment was more detrimental than synchronization by serum starvation.

Unlike serum starvation, growth-arrest by hydroxyurea did not significantly affect much the state of activity of synchronized cells. The percentages of $FITC^+$ cells in the hydroxyurea groups were 20-fold higher than those found in serum-starved cells. These percentages were lower (66.9%) than those found in cycling cells (84.1%), suggesting that hydroxyurea treatment might be associated, in about 20% of the cases, with a reduction in cell activity (quiescence). However, the percentages of diploid cells with active protein synthesis (G1) were as high as those found in cycling cells. The ability of hydroxyurea to induce growth-arrest in the absence of quiescence was also confirmed by the fact that the hydroxyurea treatment did not affect the levels of protein synthesis/cell (FITC mean fluorescence), unlike serum starvation where protein synthesis levels were also reduced. Most of the $FITC^+$ cells found in the HU treatment groups were diploid, possibly as a result of the overall increase of diploid cells observed in these groups.

3.3.2.4 Conclusions

The high levels of diploid cells (G0/G1) obtained with hydroxyurea treatment, associated with the high percentages of G1 cells (88.1 % of G0/G1 population), make this synchronization method ideal to produce a well-characterised G1 population of Mouse Foetal Fibroblasts. The only drawback was represented by the high rates of apoptosis induced by treatment with 4mM hydroxyurea for 24h. More detailed titration assays and improvements in the culture conditions (medium, O_2 tension) might reduce this problem.

CHAPTER 4

T-LYMPHOCYTES AS A SOURCE OF G1 KARYOPLASTS

4.1 INTRODUCTION

Cell models used to compare developmental potential of G0 and G1 karyoplasts, after transfer to a recipient MII oocyte, should have two main features: 1) exist in a well-characterised G0 and G1 state; 2) have potential for nuclear transfer.

T-lymphocytes possess both these features, therefore they represent a good cell candidate for this study. Quiescent blood cells have been previously used for nuclear transfer experiments in amphibians, cattle and mouse. In a pioneering work carried out in amphibians, transfer to recipient MII oocytes of frog erythrocytes, that are nucleated and arrested in a terminally differentiated G0 state, resulted in development to a further stage (feeding tadpoles) than that previously reached using other types of adult somatic and germ cells (DiBerardino *et al.*, 1986). In mouse it was demonstrated that nucleated G0 erythrocytes, isolated from 12-day foetuses, which have a condensed chromatin and have low levels of transcription, undergo chromatin remodelling and resumption of transcription after NT (Szöllösi *et al.*, 1998). Similar experiments were carried out using mouse thymocytes (Szöllösi *et al.*, 1986a; 1986b; 1988; Czolowska *et al.*, 1984; 1986). More recently mouse lymphocytes, isolated from the thymus, the spleen and the peritoneal cavity, after injection into enucleated MII oocytes, were able to support pre and post-implantation development to the foetal stage, though no development to term was reported (Wakayama and Yanagimachi, 2001). Development to blastocyst was only 3.1% for thymocytes, 21-22% for spleenocytes and 23-31% for cells isolated from the peritoneal cavity, identified as macrophages. Implantation rates were 0% for thymocytes, 75-91% for spleenocytes, 50-76% for macrophages (Wakayama

Yanagimachi, 2001). No development to term was observed with all three cell types. Ability of lymphoid cells to support development to term, after transfer to MII oocytes, has been since proved by two separate experiments: an experiment where a calf was cloned from peripheral blood pan lymphocytes (Galli *et al.*, 1999); an experiment in mouse where development to term was obtained from T and B-lymphocytes (Hochedlinger and Jaenish, 2002).

In addition to their potential for nuclear transfer, T-lymphocytes have the advantage of existing in a well-defined G0 and G1 state. T-cells, are naturally quiescent at isolation, but can be induced, by mitogenic stimuli, to leave the G0 state and re-enter the cell cycle in G1, through a process known as T-cell activation. The cell cycle of T-cells, compared to that of other somatic cell types, has three features that make them particularly interesting for this study: 1) activation of T-cells is an orderly sequence of well known, interdependent events, that can be easily manipulated in order to block T-cells in G1; 2) T-cells have a prolonged G1 phase (24-30h) compared to that of other somatic cells, which represents a further advantage for synchronization in G1; 3) the expression, during T-cell activation, of surface markers, that can be used as negative markers of cell quiescence and, therefore, to discriminate between G0 and G1 cells.

The activation of T-cells takes place in two stages, regulated by different stimuli and different signal transduction pathways (Ajchenbhaum *et al.,* 1993):

1) A "competence-phase", during which T-cells respond to a primary signal (mitogens, e.g. PHA, ConA) undergoing G0/G1 transition and becoming capable (competent) of responding to a second exogenous signal (IL-2) and to proliferate;
2) A "the commitment-phase", during which T-cells respond to a second signal (lymphokine, e.g. IL-2), undergoing G1/S transition and becoming committed to progress through DNA replication even in the absence of any further stimulation by mitogenic factors.

These two stages of T-cell activation are characterised by quantitative as well as qualitative differences in signal transduction (Ajchenbhaum *et al.,* 1993), in particular in patterns of activity of mitogen dependent kinases (MAPK). Stimulation of the T cell receptor (TcR) results in induction of the "competent state", that is

associated with the following molecular events (Fig.4.2): calcium mobilisation; protein kinase C (PKC) dependent internalisation of CD3; translocation of AP-1 transcription factors to the nucleus; expression of immediate early genes, within the first 3-6h following T-cell activation (c-*jun*, c-*fos*, CD25); activation of G1 phase cyclin-dependent kinases (Cdk4, Cdk6), by increased synthesis of Cdk4 and Cdk6 and by increased synthesis of cyclin D2, with which they form the cyclin D2/Cdk4 and cyclin D2/Cdk6 complexes, necessary for G1 progression. In T-cells cycling D1 is not expressed and cyclin D3 is expressed during the commitment-phase, and mainly acts as a sink for the sequestration of $p27^{KIP1}$, an inhibitor of Cdk2, the main regulator of G1/S and S-phase progression (Ajchenbaum *et al.,* 1993).

Stimulation of the interleukin receptor alpha (IL-2-RΔ) or CD25 induces a cascade of signals, leading T-cells to proliferate (Fig.4.2): sustained translocation of AP-1 transcription factors to the nucleus; increased expression of early G1 genes (c-*jun*, c-*fos*, CD25) and expression of new genes such as c-*myc* and IL-2, which further increases CD25 expression; activation of G1/S and S-phase cyclin-dependent kinases (Cdk2), by increased synthesis of G1/S (cyclin E, cyclin A) and S-phase (cyclin A) cyclins and inactivation of Cdk2 inhibitors, such as $p27^{KIP1}$, by ubiquitinization and sequestration by cyclin D3 (Ajchenbaum *et al.,* 1993).

In mature T-cells the primary signal for activation is triggered by antigen through the interaction of the T cell receptor and CD3 (TcR.CD3) complex. Antigenic stimulation can be mimicked by a variety of compounds including mitogenic lectins, such as Concanavalin A (ConA) or phytohemagglutinin (PHA) (Kimura and Ersson, 1981), by antibodies directed against components of the TcR.CD3 complex (Geppert and Lippsky, 1987) or by a combination of phorbol 12-myristate 13 acetate (PMA), a protein kinase C activator, and the calcium ionophore ionomycin (Truneth *et al.*, 1985). These activating agents will initially stimulate the TcR.CD3 complex, leading to G0/G1 transition and CD25 expression (competence-phase; Fig.4.1), and then induce IL-2 production, which not only drives T-cell proliferation but also further increases the levels of CD25 expression (commitment-phase, Fig.4.1). Stimulation of CD25 by autocrine IL-2 finally triggers G1/S transition and DNA synthesis completing the transformation of T-lymphocytes from resting (G0) cells to cycling cells (for reviews see Erard et *al.*, 1984; Malek and

Figure 4.1 T-cell activation: cell cycle profile and CD25 expression

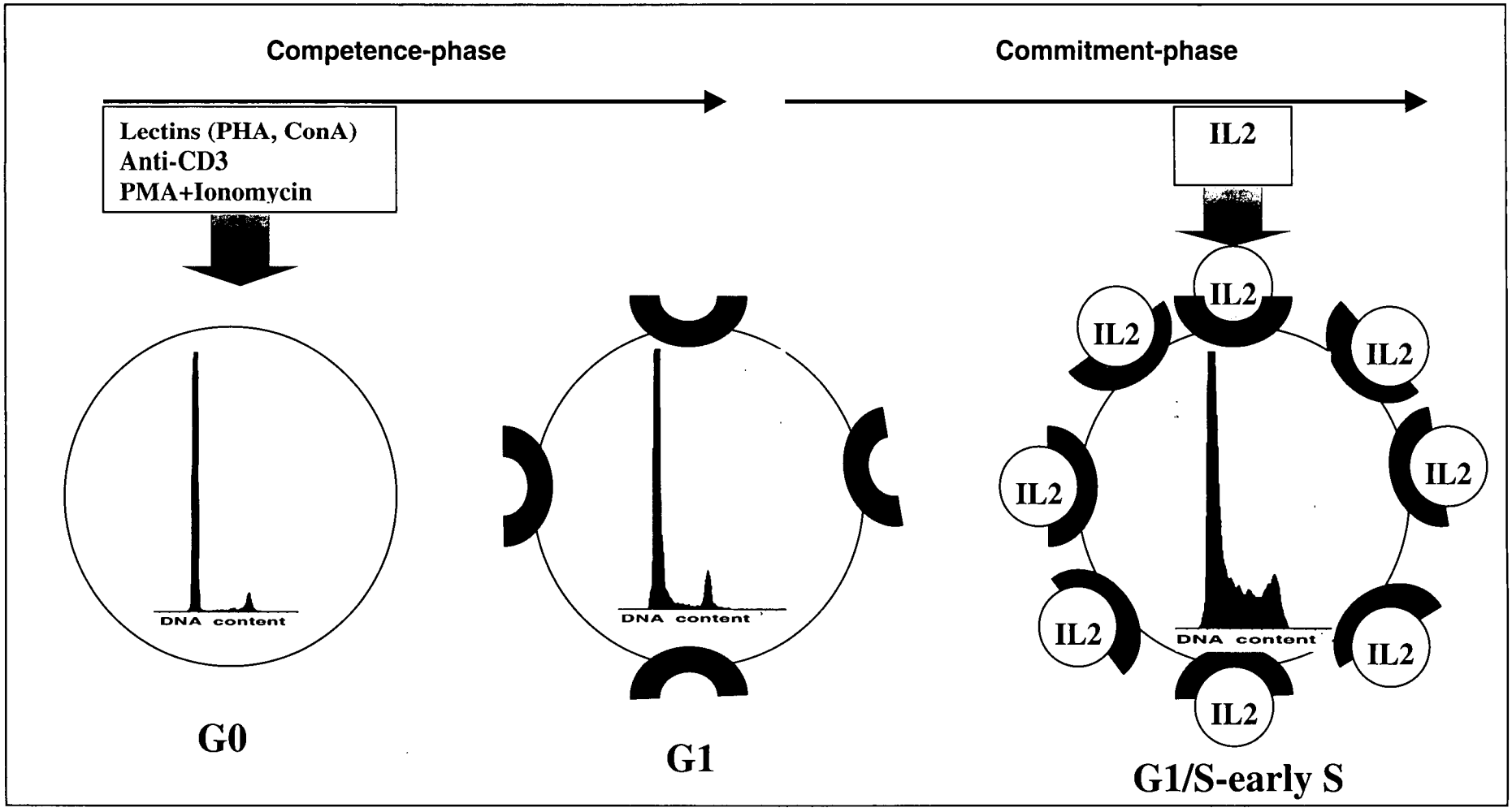

Figure 4.2 T-cell activation: molecular markers

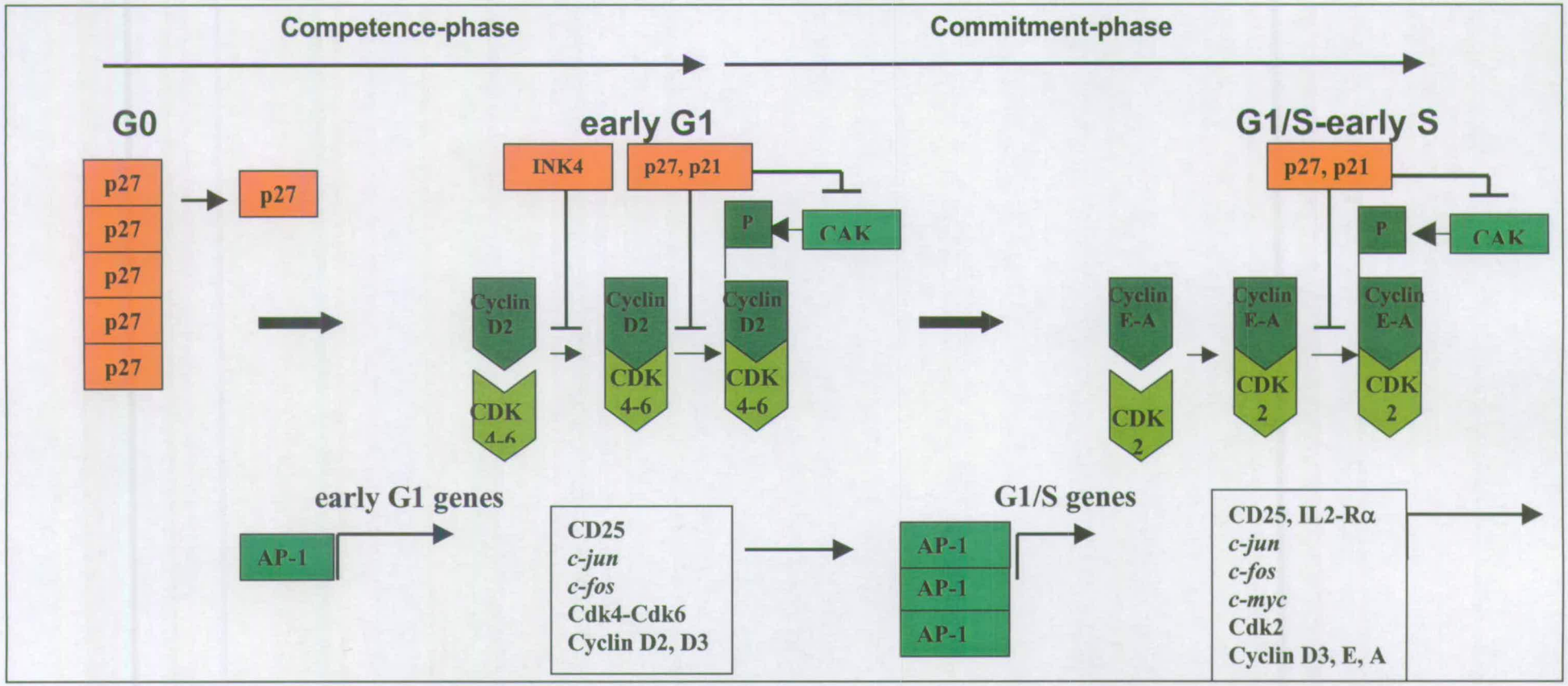

Figure 4.1 and 4.2 show cellular and molecular events of T-cell activation. T-cell activation is a two-step process: a competence–phase, triggered by mitogens (e.g. PHA, PMA+Ionomycin, ConA, anti-CD3) during which cells re-enter the cell cycle; a commitment-phase, during which cells become committed to initiate DNA replication, as a result of IL-2 and IL-2Rα interaction. The competence-phase is characterised by: CD25 expression, in the absence of DNA replication (Fig.4.1) and molecular events that regulate G0-G1 transition (Fig.4.2). The commitment-phase is characterised by: reinforced CD25 expression, release of endogenous IL2, DNA replication (Fig.4.1) and molecular events that regulate G1/S transition (Fig.4.2).

Ashwell, 1985; Bismuth *et al.*, 1985). However this cascade of events can be manipulated in order to obtain T-cells synchronized in G1. Two strategies can be used to synchronize T-cells in G1, enabling them to leave their quiescent state (G0) without reaching the cycling state:

1) Activate T-cells with submitogenic concentrations (e.g. 0.5-0.8ug/ml PHA for human T-cells) of activating agents (Modiano *et al.*, 1999; Firpo *et al.*, 1994; Proust *et al.*, 1991);

2) Activate T-cells with mitogenic concentration of growth factors (e.g. 8-10ug/ml PHA for human T-cells) in the presence of G1/S blocking agents, such as hydroxyurea (Adams *et al.*, 1967, Kim *et al.*, 1992; Ajchenbaum *et al.*, 1993).

The first strategy relies on the fact that the intensity of the primary signal can determine whether T-cells will re-enter the cell cycle and become arrested in the G1-phase or progress through the restriction point "R", at the G1/S transition, and undergo DNA replication. Although most of the molecular and cellular events that occur following T-cell activation are directly proportional to the concentration of ligand as well and the density of ligated receptors, the induction of other key events appears to take place in a "all or none" fashion and only when an activating threshold is surpassed. Induction of endogenous IL-2, which, by interaction with CD25, triggers G1/S progression and DNA replication, belongs to the latter group. This means that concentrations of activating agents below this threshold (submitogenic concentrations) will be enough to induce G0/G1 transition (competence), but not enough to induce production of autocrine IL-2, therefore, not enough to induce cell cycle progression, unless exogenous IL-2 is added (Modiano *et al.*, 1999).

The threshold between submitogenic and mitogenic concentrations is influenced by many factors and varies with the type of mitogen used, the batch of mitogen, the species considered. The mitogenic concentration must be tested under each experimental condition, by titrating the activating agent.

A second method to synchronize T-cells in G1 is to stimulate them with mitogenic concentrations of activating agents, in the presence of G1/S blocking agents, like hydroxyurea (Adams *et al.*, 1967, Kim *et al.*, 1992; Ajchenbaum *et al.*, 1993). The addition of hydroxyurea (HU) inhibits DNA replication from taking place

but it does not interfere with the activation process in itself, which represents the mechanism leading to DNA replication. In mouse it has been shown that addition of HU does not alter the expression of cell cycle regulators such as cyclin D2, cyclin D3 and cyclin E, responsible for G1 and G/S progression and only marginally reduces the synthesis of cyclin A which is responsible for S-phase progression, while maintaining the percentages of cells in S-phase below 5% (Ajchenbaum *et al.,* 1993).

The interleukin-2 receptor alpha (IL-2Rα) or CD25 can be used to discriminate between G0 and G1 cells (Fig.4.1). The interleukin-2 receptor (IL-2R) is formed by three transmembrane proteins called IL-2Rα, IL-2Rβ and IL-2Rγ or γ_c chain (Minami *et al.*, 1993; Waldman, 1989). These subunits combine to give three classes of IL-2R (Soldaini *et al.,* 1995): low affinity receptors formed only by the IL-2Rα chain (p55), devoid of signalling ability; intermediate affinity receptors, that are IL-2Rγ and IL-2Rβ heterodimers (p75), required for signalling transduction; the high affinity receptor, formed by a combination of IL-2Rα, IL-2Rγ and IL-2Rβ chains (p55/p75), responsible for the IL-2-driven T-cell proliferation. While the γ_c chain is constitutively expressed in all mature T-cells and their thymic precursors (Cao *et al.*, 1993), and the IL-2Rβ chain is expressed in some resting T-cells (Tanaka *et al.,* 1991), the IL-2Rα is undetectable in resting T-cells but is efficiently induced upon T-cell activation as cells enter the G1-phase, becoming the key regulator of IL-2 responsiveness, at the time of G1/S transition (Robb *et al.,* 1981; Fig.4.1). For this reason the IL-2Rα can be used as a marker to discriminate between G0 cells, which do not express it, from G1 cells, which start expressing it in response to TcR.CD3 complex stimulation by mitogens. Expression of IL-2Rα or CD25 can be used together with DNA content, incorporation of tritiated thymidine ([^{3}H]-thymidine) into DNA, the expression of cell cycle specific markers ($p27^{KIP1}$, cyclin D3) to assess the cell cycle stage of T-cells.

4.2 ISOLATION AND ACTIVATION OF T-CELLS FROM DIFFERENT LYNPHOID TISSUES

4.2.1 Aim

These experiments were aimed at selecting a lymphoid tissue that gave T-lymphocytes that could be:

1) Activated, with mitogenic concentration of activating agents;
2) Synchronized in G1, with sub-mitogenic concentrations of activating agents. (Firpo *et al.*, 1994; Modiano *et al.*, 1999).

Apoptosis rates in different lymphoid tissues were also compared.

4.2.2 Experimental design

All data were collected in three separate experiments.

Lymphocytes were isolated from six-week-old, female, CBA/Ca inbred mice, killed with CO_2, from three different lymphoid tissues (for Methods see Paragraph 2.7):

1) Spleen;
2) Thymus;
3) Lymph nodes;

In each experiment, lymphoid tissues were collected from two animals and pooled together, to reduce individual variability.

Cells were synchronized in G1 and activated using the lectin Phytohemagglutinin (PHA) and a protocol previously described for human lymphocytes (Firpo *et al.*, 1994). Treatment groups included:

1) Freshly isolated cells (Ctr0h);
2) Cells cultured for 48h in 10% FCS culture medium (formulation at A.2.1; Ctr48h);
3) Cells cultured for 48h in 10% FCS culture medium, supplemented with 0.8ug/ml, to induce a sub-mitogenic level of activation (P0.8);
4) Cells cultured for 48h in 10% FCS culture medium, supplemented with 8ug/ml PHA and 4nM exogenous IL-2 (P8/IL);

5) Cells cultured for 48h in 10% FCS culture medium, supplemented with 16ug/ml PHA, and 4nM exogenous IL-2 (P16/IL);

Cells in treatment groups 1 and 2 corresponded respectively to fresh and cultured quiescent cells. Cells in treatment group 3 represented putative G1 cells. Cells in treatment groups 4 and 5 represented cycling cells.

Putative G1 cells were stimulated with sub-mitogenic concentrations of PHA (0.8ug/ml), high enough to induce TcR stimulation, resulting in CD25 expression and G0/G1 transition, but not high enough to induce production of endogenous IL-2 and IL-2/CD25 interaction, necessary for G1/S transition and DNA replication (Firpo *et al.*, 1994). Cycling cell populations were stimulated with mitogenic concentrations of PHA (8-16ug/ml), that induce full T-cell activation, resulting in CD25 over expression, IL-2 production, and, as a result of CD25 stimulation by endogenous and/or exogenous IL-2, G1/S transition and DNA replication (Firpo *et al.*, 1994).

For each tissue, about $2\text{-}4x10^6$ cells were allocated to treatment group 1 (CTR0), and processed immediately. Cultured cells were seeded at a concentration of $1x10^6$/ml/well, in 24 well plates, and two wells were allocated to each treatment group (2-5). After 48h incubation at 37°C, 5% CO_2, cells from 2 wells belonging to the same treatment were pooled together, counted, and processed for flow cytometry for the following staining (for Methods see paragraph 2.9):

1) CD3-FITC/CD25-R-PE
2) CD3-FITC/PI

In these experiments only live cells expressing CD3 (T-lymphocytes) were included in the CD25 and PI analysis (live/$CD3^+$ gate; see Paragraph 2.10.2). This was done to: prevent apoptotic cells from interfering with the analysis; prevent fluctuations in T-cell percentages, among the different lymphoid tissues, from interfering with the analysis.

The following parameters were acquired (see Paragraph 2.10.2):

1) For CD25 staining (live/$CD3^+$ gate):
   a) Percentage of $CD25^+$ cells;
   b) Mean fluorescence levels.
2) For PI staining:

a) Percentage of apoptotic cells (all cells gated);

b) Cell cycle profile (live/$CD3^+$ gate), that included:

(a) Percentage of cells in G0/G1-phase;

(b) Percentage of cells in S-phase;

(c) Percentage of cells in G2/M-phase.

4.2.3 Statistical Analysis

Data were transformed as follows: percentages (%$CD3^+$, %$CD25^+$, %G0/G1, %S, %G2/M) by Logit transformation; mean fluorescence data by Log transformation (GenStat 4.21, Windows 2000). Treatment and tissue were used as independent variables and data were analysed by two-way ANOVA (Statistica 4.5, Windows 1995) with an alpha level for critical ranges of 0.05, considering:

- Tissue, as main effect, regardless of treatment;
- Treatment, as main effect, regardless of tissue;
- Treatment and tissue interaction.

Significant effects were further broken down by using a Least Significant Difference (LSD) test or planned comparison (Post-Hoc comparison test), to identify the specific source of variance (i.e. specific tissue or specific treatment or specific tissue at a given time). Where specified, a one way-ANOVA was used, on selected cases, to confirm the LSD results, considering only selected cases for the treatment or tissue variable. To discriminate a possible culture effect from the treatment effect, for each dependent variable, selected cases were included in the analysis in order to assess:

- Culture effect, comparing only treatment group 1 (Ctr0h) and 2 (Ctr48h) in the various tissues;
- Effect of treatment on cultured cells, comparing treatment groups 2-5, in the various tissues.

A one-way ANOVA was used to analyse the percentage of T-lymphocytes ($CD3^+$) found in the different lymphoid tissues.

Figure 4.3 Effect of treatment on apoptosis of T-lymphocytes

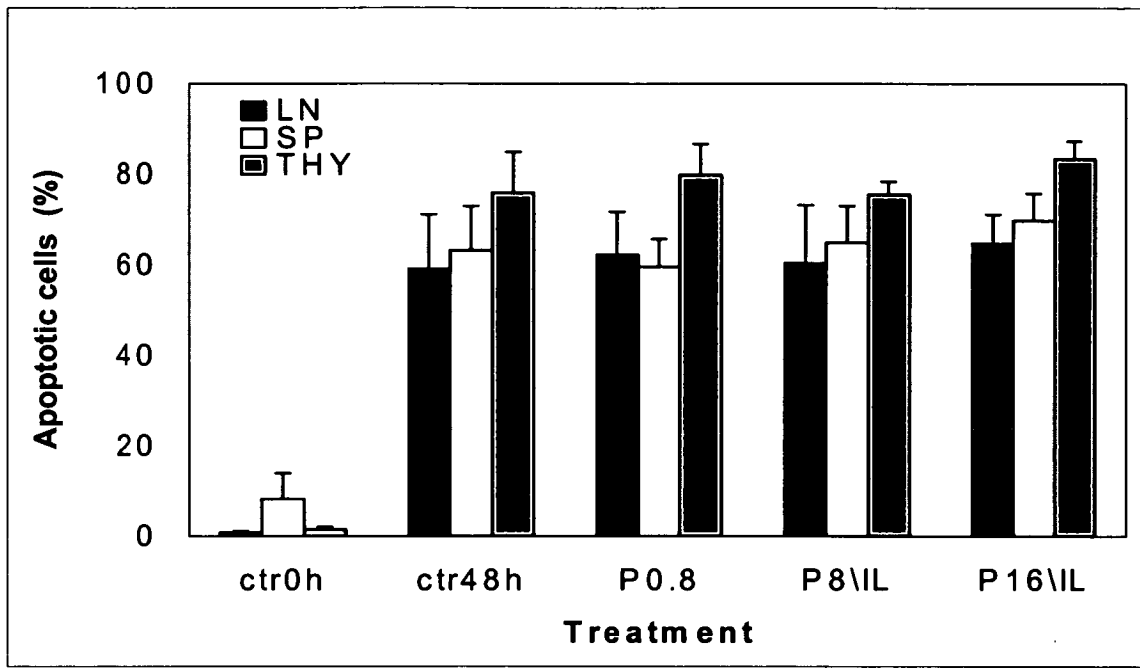

Figure 4.4 Positive effect of 2-mercaptoethanol on apoptosis

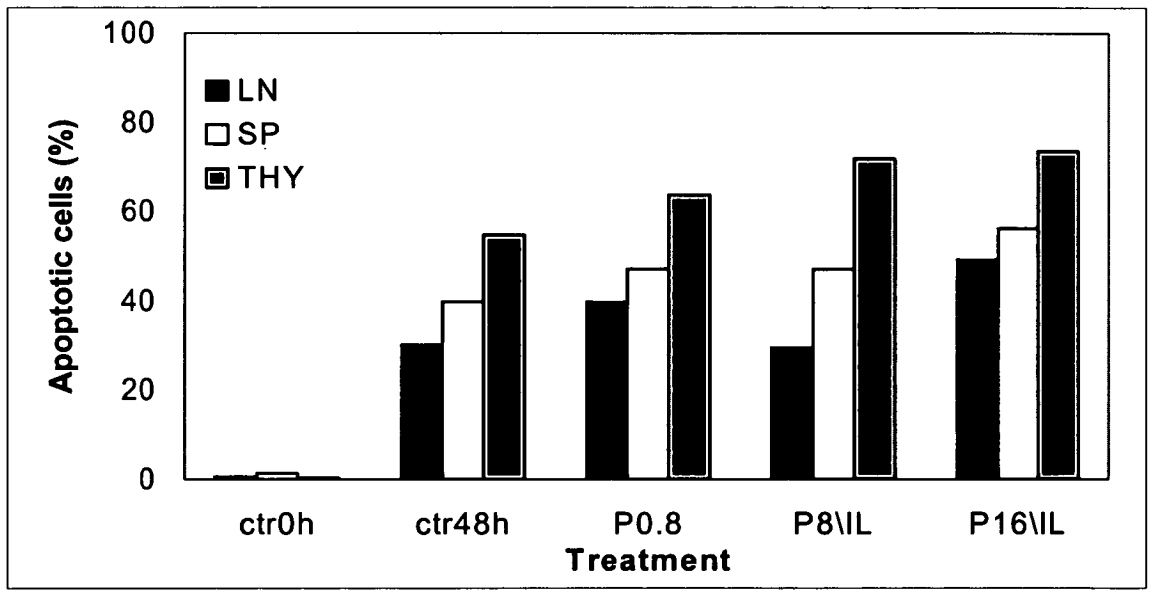

Figure 4.3 Percentages of apoptotic cells were assessed by Propidium Iodide staining and FACS analysis. Cells were stained at isolation (Ctr0h) or after culture for 48h with: medium (Ctr48h); 0.8ug/ml PHA (P0.8); 8ug/ml PHA and 4nM IL-2 (P8/IL); 16ug/ml PHA and 4nM IL-2 (P16/IL). The groups Ctr0h and Ctr48h corresponded respectively to fresh and cultured G0 cells. Results from three replicate experiments are expressed as mean percentages±SEM. **Figure 4.4** Apoptosis rates were assessed in cells cultured for 48h under the same conditions described in Figure 4.3, but in the presence of 2-mercaptoethanol. Data were collected in a single experiment.

4.2.4 Results

Culture for 48h, in the absence of activating agents, dramatically increased (time, $p<0.001$) the percentage of apoptotic cells (Fig.4.3).

The percentages of apoptotic cells remained equally high, in cultured cells, regardless of the treatment conditions (treatment, $p=0.86$; Fig.4.3). The highest apoptosis rates were observed, in all tissues, when cells were stimulated for 48h with 16ug/ml PHA in the presence of 4nM IL-2 (group P16/IL). The overall rate of apoptosis in culture, under the different conditions, differed among tissues (tissue, $p=0.03$). The death rate observed in thymocytes (range, 76%-83%) was significantly higher than that observed in cells isolated from the lymph nodes (range, 59%-65%, $p<0.005$) and the spleen (range, 63% to 70%, $p<0.05$). The lowest rate of apoptosis was observed in cells from lymph nodes (Fig.4.3).

Apoptosis rates were reduced, in all treatment groups, by addition of the anti-oxidant 2- mercaptoethanol (Fig.4.4).

Culture for 48h (Fig.4.5, A-B), in the absence of activating agents, had no effect on the percentage of $CD25^+$ cells and the mean fluorescence intensity (time, $p=0.60$ and $p=0.18$). This applied to all tissues (tissue, $p>0.4$).

In all the tissues (tissue, $p=0.17$), the percentages of $CD25^+$ cells and values of mean fluorescence intensity increased significantly in the presence of activating agents (treatment, $p<0.001$). Cells treated with 0.8ug/ml PHA (P0.8) had percentages of $CD25^+$ cells and mean fluorescence intensity similar to those observed in the absence of activating agents (Ctr48h), therefore in G0 cells ($p=0.6$ for $\%CD25^+$; $p=0.76$, for mean fluorescence). Incubation for 48h with 8ug/ml or 16ug/ml PHA and 4nM IL-2 (P8/IL; P16/IL) increased the percentages of $CD25^+$ cells ($p<0.001$) and the mean fluorescence intensity ($p<0.001$). No significant difference was observed in the level of expression of CD25 in T-lymphocytes stimulated with 8ug/ml or 16ug/ml PHA and 4nM IL-2 ($CD25^+\%$, $p=0.42$; mean fluorescence $p=76$).

Culture for 48h (Fig.4.6A) reduced the percentages of diploid cells (G0/G1) in all tissues (time, $p=0.035$; tissue, $p=0.083$). The culture effect on the percentage of

Figure 4.5 Effect of treatment on the expression of CD25 in T-lymphocytes from different lymphoid tissues

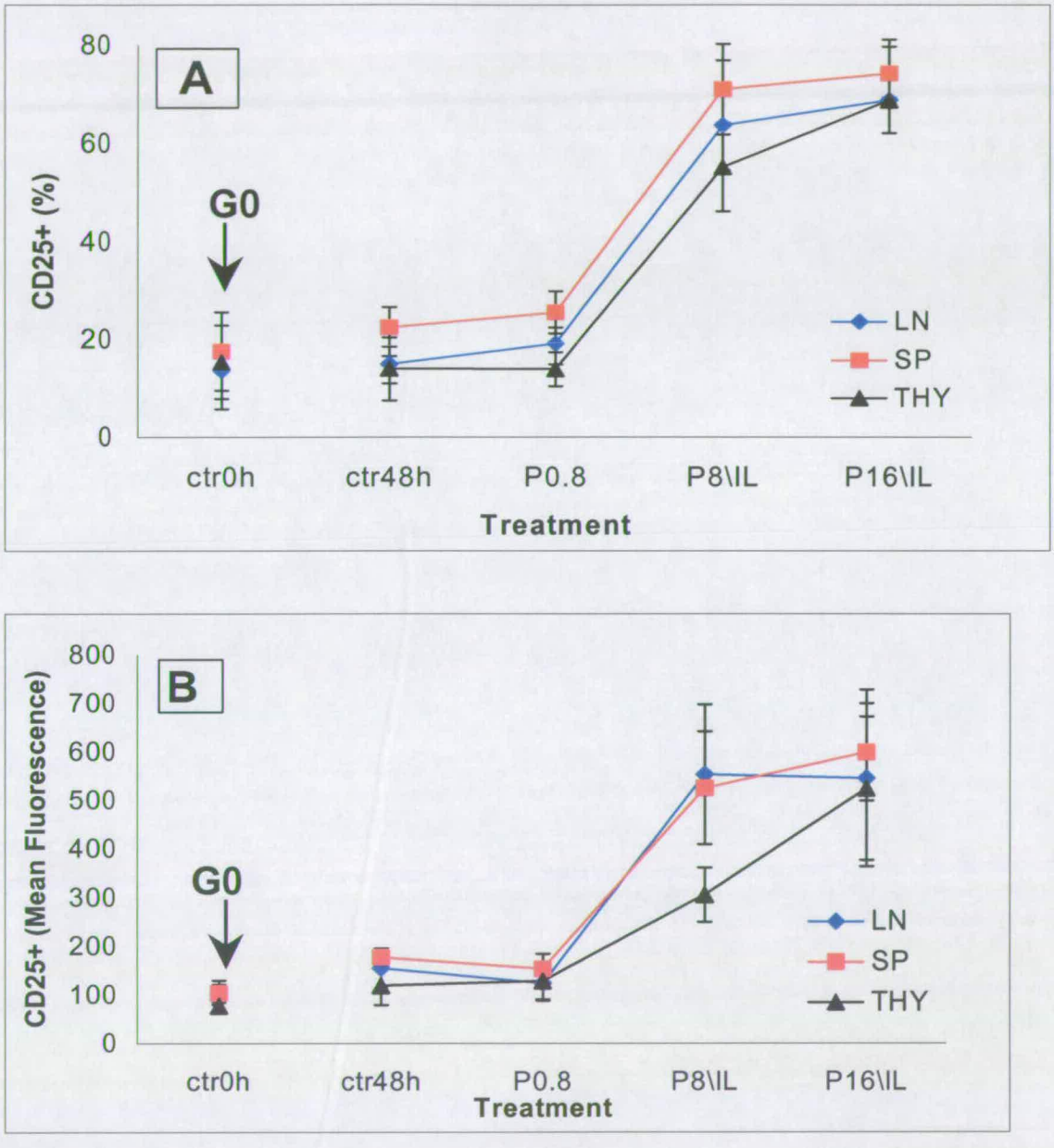

Cells were stained for CD25 and processed for FACS analysis at isolation (Ctr0h), or after culture for 48h with: medium (Ctr48h); 0.8ug/ml PHA (p0.8); 8ug/ml PHA and 4nM IL-2 (P8/IL); 16ug/ml PHA and 4nM IL-2 (P16/IL). The groups Ctr0h and Ctr48h corresponded to fresh or cultured G0 cells. Expression of CD25 was assessed as percentage of $CD25^+$ cells (A) and as mean fluorescence intensity of $CD25^+$ cells (CD25/cell; B). Data, collected in three replicates, are summarised as mean values±SEM.

Figure 4.6 Effect of treatment on the cell cycle of T-lymphocytes from different lymphoid tissues

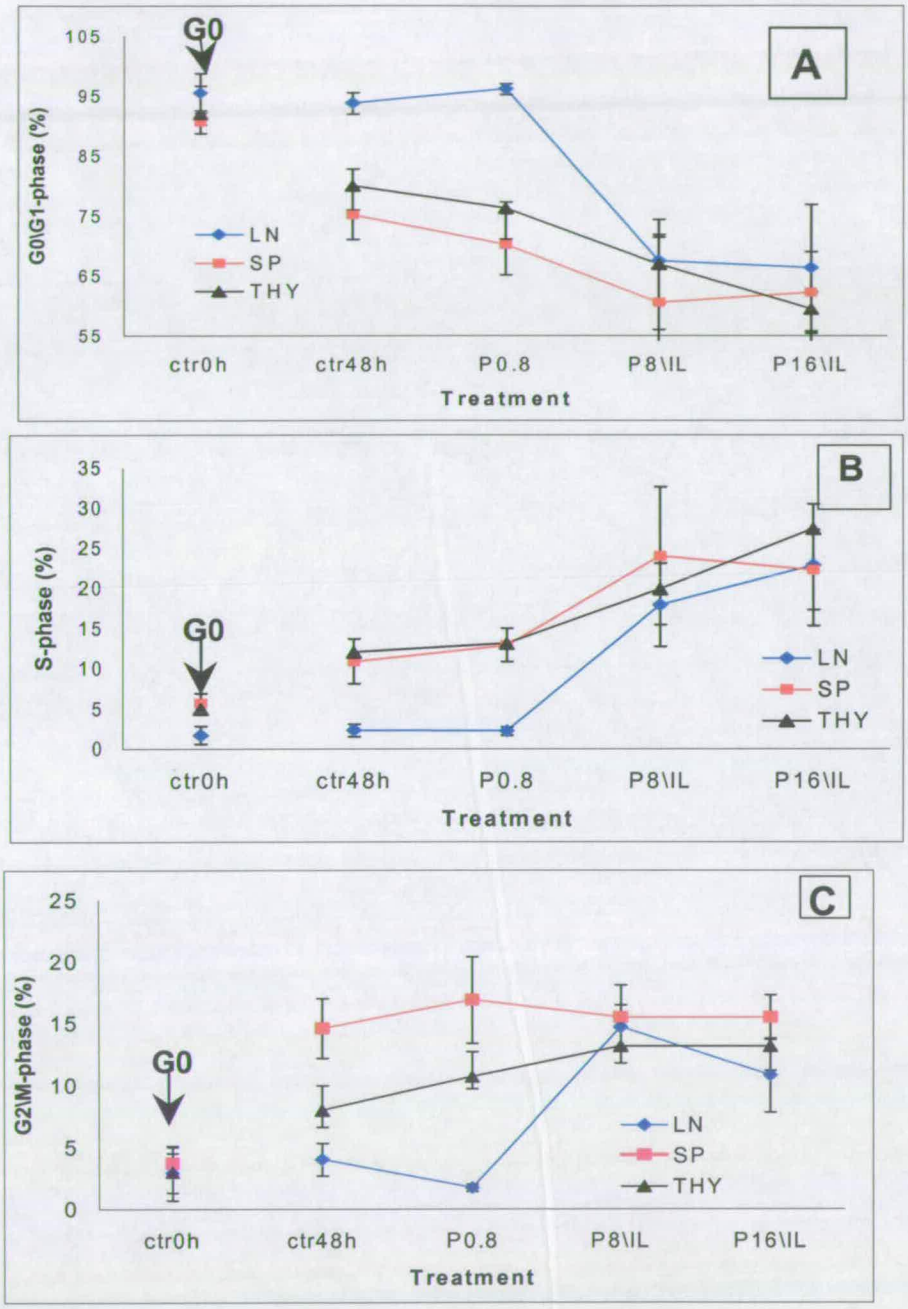

Cell cycle analysis of cells stained with Propidium Iodide (PI) and processed for FACS analysis, at isolation (Ctr0h) or after culture for 48h with: medium (Ctr48h); 0.8ug/ml PHA (p0.8); 8ug/ml PHA and 4nM IL-2 (P8/IL); 16ug/ml PHA and 4nM IL-2 (P16/IL). The groups Ctr0h and Ctr48h corresponded to fresh or cultured G0 cells. Data, collected in three replicates, are summarised as mean percentages±SEM.

diploid cells was investigated more in detail using the LSD test and a one-way ANOVA. The LSD test revealed that the source of variability, detected between 0h and 48h, using time as main effect, was the significant difference in the percentage of diploid cells observed in the lymph nodes, at time 0, and that found in the spleen ($p=0.19$) and the thymus ($p=0.12$), at 48h. However no significant difference was detected, in each tissue, before and after culture for 48h. A one-way ANOVA, considering one tissue at a time and only time as an independent variable, confirmed this observation in the lymph nodes ($p=0.20$) and, to a lesser extent, in the spleen (0.054), although it showed a significant decrease in the percentage of diploid cells in the thymus ($p=0.028$).

Cells isolated from the lymph nodes had percentages of diploid cells higher than those found in cells isolated from the thymus and the spleen, both at isolation (Ctr0h) and after 48h (Ctr48h) in culture (spleen, $p=0.02$; thymus, $p=0.03$).

The decrease observed in the percentage of diploid cells in culture, was associated with an increase in the percentage of cells in S-phase (Fig.4.6B) and G2/M-phase (Fig.4.6C), but only the latter was significant (time, $p=0.033$). A more detailed one-way ANOVA, restricting the analysis to one tissue at a time and using only time as an independent variable, confirmed that the increase in S-phase cells was minimal and not significant in the lymph nodes and spleen ($p=0.22$), and was greater and significant in the thymus ($p=0.049$). The effect of culture on the percentages of cells in S-phase was mediated by the tissue of origin (tissue, $p=0.04$). The LSD test, with tissue as a main effect, showed that cells coming from the lymph nodes had lower percentage of S-phase cells than cells isolated from the thymus and the spleen, both at isolation ($p<0.04$) and after 48h in culture ($p=0.01$). These data were also confirmed by a one-way ANOVA, considering one time point at a time and using tissue as an independent variable.

The percentages of G2/M cells increased in all tissues as a result of culture (time, $p=0.035$; tissue, $p=0.16$). When the effect of time was analysed more in detail using a one-way ANOVA, considering each tissue separately and time as an independent variable, the rate of increase in the percentages of cells in G2/M was found to be lowest and not significant in the lymph nodes, higher but still not significant in the thymus ($p=0.06$) and highest and significant in the spleen

($p<0.001$). T-cells isolated from the lymph nodes had lower percentages of G2/M cells at isolation and lower percentages after 48h in culture, compared to the spleen and the thymus.

Treatment (Fig.4.6A) significantly affected the percentage of G0/G1 cells (treatment, $p<0.001$) in a tissue specific manner (tissue, $p<0.001$). The LSD test, considering treatment as a main effect, showed that the percentages of cells in G0/G1 were not affected by the addition of 0.8ug/ml PHA (P0.8; $p=0.93$), but were significantly reduced by addition of 8ug/ml (P8/IL) or 16ug/ml PHA (P16/IL) and 4nM IL-2 ($p<0.001$). The LSD test, considering tissue as a main effect, showed tissue-specific differences ($p<0.001$). The percentage of G0/G1 cells decreased only in the lymph nodes ($p<0.001$), while it remained unchanged in the thymus and the spleen ($p>0.1$).

The effect of treatment on the percentages of T-lymphocytes in G2/M and S-phase (Fig.4.6 B-C) was similar to that observed for G0/G1 cells. Both cell cycle stages were affected by treatment ($p<0.001$) and tissue of origin ($p<0.001$). In the lymph nodes the percentages of T-lymphocytes in S and G2/M-phase, were not affected by addition of 0.8ug/ml PHA ($p=0.8$; $p= 0.1$), but they increased significantly after the addition of higher concentrations of PHA ($p<0.001$). There was no significant difference in the percentages of T-cells in S ($p=0.55$) and G2/M-phase ($p=0.31$) between groups stimulated with 8ug/ml PHA (P8/IL) or 16ug/ml PHA (P16/IL), in the presence of IL-2. In T-lymphocytes isolated from spleen and thymus, the percentages of T-cells in G2/M and S-phase were not affected by treatment ($p>0.09$), and were as high as those observed in the Ctr48h and P0.8 groups. The percentages of cells in G2/M and S-phase in observed in activated cells from the thymus and the spleen, were significantly higher than those observed in the lymph nodes in the Ctr48h and P/0.8 groups, and similar to those observed in the lymph nodes in the P8/IL and P16/IL groups, after activation.

4.2.5 Conclusions

High rates of apoptosis were observed in culture, in all tissues, regardless of the treatment and the tissue of origin, showing the extreme fragility of murine T-

lymphocytes. Addition of 2-mercaptoethanol proved to be essential in reducing death rates of mouse T-lymphocytes.

Shifts in the expression of CD25 were not influenced by culture, in the absence of mitogens, but only by culture with activating agents. This observation confirmed the strict correlation existing between the expression of this marker and the activation state of T-cells.

The results of these experiments demonstrated that the lymph nodes represented the best source of T-lymphocytes to use in this project, because they had the following features:

1) Consistently lower apoptosis rates, even in the absence of 2-ME;
2) Better level of synchronization in G0 at isolation, with higher percentages of G0/G1 cells, and lower percentages of cells in G2/M and S-phase than those found in the thymus and the spleen, associated with low levels of CD25 expression;
3) Quiescence of T-lymphocytes was not perturbed by culture, in the absence of mitogens, while culture altered the cell cycle profile of T-cells from the spleen and the thymus, decreasing the percentages of cells in G0/G1 and increasing the percentages of cells in S and G2/M;
4) T-lymphocytes isolated from the lymph nodes responded better to activation, with a perfect correspondence between the changes observed in the cell cycle profile (decrease in G0/G1 cells, increases in S and G2/M cells) and the increase observed in the level of expression of CD25. No changes were observed in the cell cycle profile of T-cells from the thymus and the spleen, during activation, possibly because it was impossible to discriminate the effect of culture from the effect of activation.
5) Lymph nodes gave a pure population of T-cells (Paragraph 2.7) that did not require a further purification step with depletion of $CD3^-$ cells.

Lower concentrations of PHA (0.8ug/ml) were unable to induce G0-G1 transition in mouse T-cells, as suggested by the absence of CD25 expression. This concentration had been previously used to synchronize human T-cells in G1.

However these results indicated that synchronization of mouse T-cells in G1 had to be achieved with other PHA concentrations or other synchronization methods.

Culture for 48h with 8ug/ml PHA was able to induce maximal T-cell activation, as indicated by the significant increase observed in the expression of CD25, in association with a significant reduction in the percentage of G0/G1 cells and a significant increase in the percentages of cells in S and G2/M. No further increases in the activation state was observed at higher PHA concentrations, suggesting that, at this concentration, cells had reached an activation plateau. This activation protocol was selected for other experiments, considering that maximal apoptosis rates had been consistently observed, in all tissues, when cells were stimulated with 16ug/ml PHA.

4.3 SYNCHRONIZATION OF T-LYMPHOCYTES IN G1 BY PHA TITRATION

4.3.1 Aim

The previous experiment failed to produce G1 cells by using submitogenic concentrations of PHA, 0.8ug/ml, that had been previously used to synchronize human T-cells in G1 (Modiano *et al.,* 1999; Firpo *et al.*, 1994; Proust *et al.,* 1991).

The aim of this experiment was to use PHA titration, in the presence or absence of IL-2, to find the submitogenic conditions at which mouse T-cells start expressing activation markers, in the absence of DNA replication (G0/G1 transition). Cells synchronized in G1 would be characterised by percentages of $CD25^+$ cells and levels of CD25 expression significantly higher than those observed in quiescent cells and similar to those found in activated cells. They would also have high percentages of G0/G1 cells, with a diploid content of DNA (2N), similar to those found in quiescent cells and significantly higher than those found in activated, cycling cells. They should also have low percentages of cells in S-phase (2/4N) and G2/M phase (4N), similar to those found in G0 populations, and significantly lower than those found in activated cycling cells. Data reported in the literature (Firpo *et al.,* 1994; Modiano *et al.*, 1999) have shown that human T-cells, stimulated with submitogenic concentrations of PHA (0.5-0.8ug/ml) have 96% of the cells in G0/G1, only 1-3% of

the cells in S and G2/M, and 12-15% of the cells expressing CD25 ($CD25^+$). These cells can be considered in G1 because they have the same cell cycle profile as quiescent cells, cultured in medium alone, with similar high percentages of G0/G1 cells (97%) and low percentages of cells in S (3%) and G2/M-phase (0%). They also have percentages of $CD25^+$ cells (12-15%) higher than those found in cultured quiescent cells (<3%), though lower than those observed in fully activated T-cells (80%-90%).

4.3.2 Experimental design

Data were collected in three separate experiments.

For each replicate, cells were isolated from the lymph nodes of four, CBA/Ca, 6 week old, female mice. For each experiment cells from each animal were pooled together, counted and assigned to various treatment groups. For each treatment group three sets of data were collected: data from the FACS analysis; data from the [^{3}H]thymidine incorporation assay; cell counts. For each replicate $4x10^6$ freshly isolated cells, were resuspended in medium containing only 10% FCS, processed and stained immediately for FACS analysis. This was considered as treatment group 1), containing freshly isolated quiescent cells (G0). The remaining cells were seeded at a concentration of $2x10^6$/well in 24 well plates, assigning 1 well/treatment group for the FACS analysis and the cell counts, or $0.2x10^6$/well in 96 well plates, assigning 3 wells/treatment group for the [^{3}H]incorporation assay. All the cells were cultured for 48h, at 37°C, 5% CO_2 in air, under the following treatment conditions:

2) Medium with 10 % FCS, considered as cultured quiescent cells (P0);
3) Medium with 10 % FCS, 1ug/ml PHA (P1);
4) Medium with 10 % FCS, 2ug/ml PHA (P2);
5) Medium with 10 % FCS, 4ug/ml PHA (P4);
6) Medium with 10 % FCS, 8ug/ml PHA (P8);
7) Medium with 10 % FCS, 16ug/ml PHA (P16);
8) Medium with 10 % FCS, 0ug/ml PHA and 4nM IL-2 (P0/IL);
9) Medium with 10 % FCS, 1ug/ml PHA and 4nM IL-2 (P1/IL);

10) Medium with 10 % FCS, 2ug/ml PHA and 4nM IL-2 (P2/IL);

11) Medium with 10 % FCS, 4ug/ml PHA and 4nM IL-2 (P4/IL);

12) Medium with 10 % FCS, 8ug/ml PHA and 4nM IL-2 (P8/IL);

13) Medium with 10 % FCS, 16ug/ml PHA and 4nM IL-2 (P16/IL).

For detailed Media composition see A.2.1, A.2.3, A.2.4. At the end of the incubation period, cells from each treatment group that had been cultured in the 24 well plates, were harvested, counted, divided into samples for FACS analysis (for Methods see Paragraph 2.9) and stained for:

- CD3-FITC/CD25-R-PE
- CD3-FITC/PI

Gates and parameters acquired were as described at paragraph 4.2.1.

For the [^{3}H]thymidine incorporation assay cells were frozen at –20°C and processed by liquid scintillation (for Methods see Paragraph 2.7).

4.3.3 Statistical Analysis

Data, categorised in the different dependent variables were transformed as follows: percentages (%CD25$^+$ cells, %G0/G1-phase cells, %S-phase cells, %G2/M-phase cells) by Logit transformation; mean fluorescence data and counts per minute (cpm) by Log transformation (GenStat 4.21, Windows 2000). Data from FACS analysis (%CD25$^+$ cells, %G0/G1-phase cells, %S-phase cells, %G2/M-phase cells, mean fluorescence) were analysed using the program Statistica 4.5 for Windows 1995, with an alpha level for critical ranges of 0.05, to perform a one-way and a two-way ANOVA, on selected groups.

The two-way ANOVA was carried out on groups 2-13, considering PHA and IL-2 as independent variables and analysing:

- PHA concentration as main effect, regardless of IL-2 presence or absence
- IL-2, presence or absence, as main effect, regardless of PHA concentration
- PHA x IL-2 interaction, to assess a possible synergic effect of these two factors

Significant effects were further broken down by using a LSD test or planned comparison (Post-Hoc comparison test) to identify the specific source of variance

(e.g. specific PHA concentration, presence or absence of IL-2, specific concentration of PHA with or without IL-2).

A one-way ANOVA and a LSD test were used on groups 1-13, considering only treatment group as an independent variable to compare the quiescent state of freshly isolated cells (group 1, G0) with that of:

- Quiescent cells cultured for 48h without mitogens (group 2, P0), to confirm that culture in itself did not affect the quiescent state and that P0 cells could be used as a good control of cell quiescence with which to compare activation state of cultured groups;
- All the other treatment groups (groups 3-13), the ones containing G1 cells in particular, to see how their activation state differed from that of freshly isolated quiescent cells and to identify the specific source of variance (e.g. specific treatment).

Data from the [^{3}H]thymidine incorporation assay were analysed using a Nested Analysis of Variance (GenStat 4.21, Windows 2000), using the following structure:

1) Block Structure: block/wells/IL-2/PHA, where:
   a) Blocks, corresponded to experiments 1-3;
   b) Wells, corresponded to wells 1-3;
   c) IL-2, corresponded to groups with or without IL-2;
   d) PHA, referred to PHA concentrations 0-16ug/ml.
2) Treatment structure (IL-2 x PHA), considering:
   a) IL-2 as main effect, regardless of PHA;
   b) PHA concentration as main effect, regardless of IL-2 presence;
   c) IL-2 and PHA interaction.

At each level of analysis, differences between specific groups of interest were assessed using a Student's T-test for the difference in means, with an alpha level of 0.05:

$$t = (\text{mean1} - \text{mean2}) / SE\ (\text{mean1} - \text{mean2})$$

using the means values and the standard error of the difference in means (SED), obtained in the tables of the Nested Analysis of Variance (GenStat 4.21, Windows 2000).

4.3.4 Results

An average of $7.3x10^6$ total cells/animal were collected, of which about 86.5±7.4%, corresponding to $6.3±1.8x10^6$ cells/animal, were $CD3^+$, T-lymphocytes.

Comparison of G0 cells (group1) with cells cultured for 48h in the absence of mitogens (P0, group2) showed that these treatment groups had similar percentages of $CD25^+$ cells (p=0.91) and mean fluorescence (p=0.78; Fig.4.8 A-B). The cell cycle profiles of the two groups were also similar (Fig.4.9 A-B), with high percentages of G0/G1 cells (p=0.18) and low percentages of cells in S-phase (p=0.82) in both groups. Cells in the P0 group only had significantly higher percentages of cells in G2/M (p=0.04; Fig.4.9C). A similar increase in G2/M cells as a result of culture had been observed in the previous experiment, in particular in T-cells derived from the spleen. The percentages of apoptotic cells observed in the treatment group P0 (Fig.4.7) were higher than those observed in the group G0 (p=0.01). These data suggested that cells cultured in the absence of mitogens represented the best control of cell quiescence with which to compare the level activation of cultured cells, since they were as quiescent as freshly isolated G0 cells, but with rates of apoptosis, that can interfere with the analysis, comparable to those of other cultured cells.

The overall rate of apoptosis in culture (Fig.4.7) was 30±4.5%, comparable to that previously observed for cells cultured with the anti-oxidant 2-mercaptoethanol (37.1±4.6%), and it remained constant regardless of treatment. The rate of apoptosis in culture was not affected by PHA concentration (p=0.54) nor by IL-2 (p=0.54), although the absence of IL-2 slightly increased the death rates from 27.7±6.0% to 32.3±6.6%. The interaction of PHA and IL-2 was also not significant (p=0.92), suggesting that there was no synergic effect of these two factors on apoptosis.

The expression of CD25, expressed both as percentage of $CD25^+$ cells and mean fluorescence, was affected by treatment in culture. The percentage of $CD25^+$ cells (Fig.4.8A) was affected by PHA concentration (p<0.001). There was a positive correlation between PHA concentration and the percentage of $CD25^+$ cells that rose

Figure 4.7 PHA titration: effect of PHA concentration and IL-2 on apoptosis

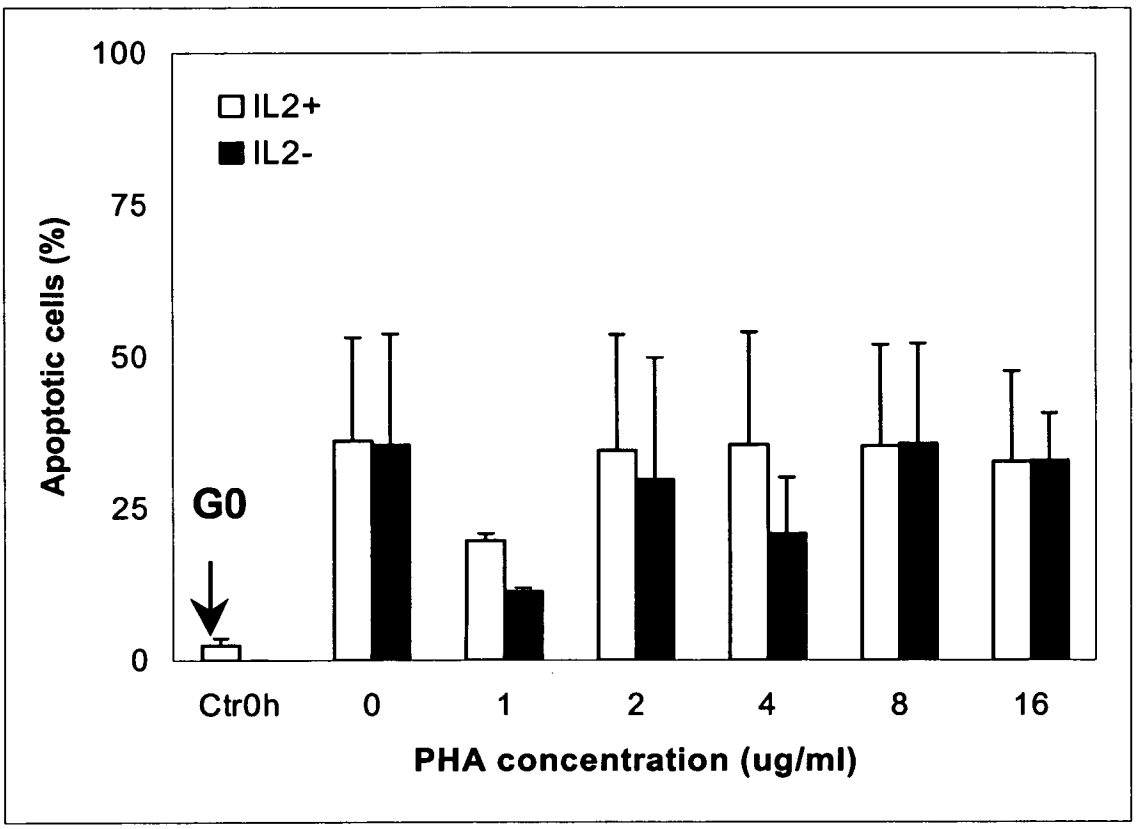

Percentages of apoptotic cells were assessed by Propidium Iodide staining and FACS analysis on cells treated for 48h, with increasing concentrations of PHA (0-16ug/ml), in the presence or absence of 4nM IL-2. Freshly isolated cells (Ctr0h) were also included as controls. Data from three replicates are expressed as Mean+SEM.

Figure 4.8 PHA titration: effect of PHA concentration and IL-2 on CD25 expression

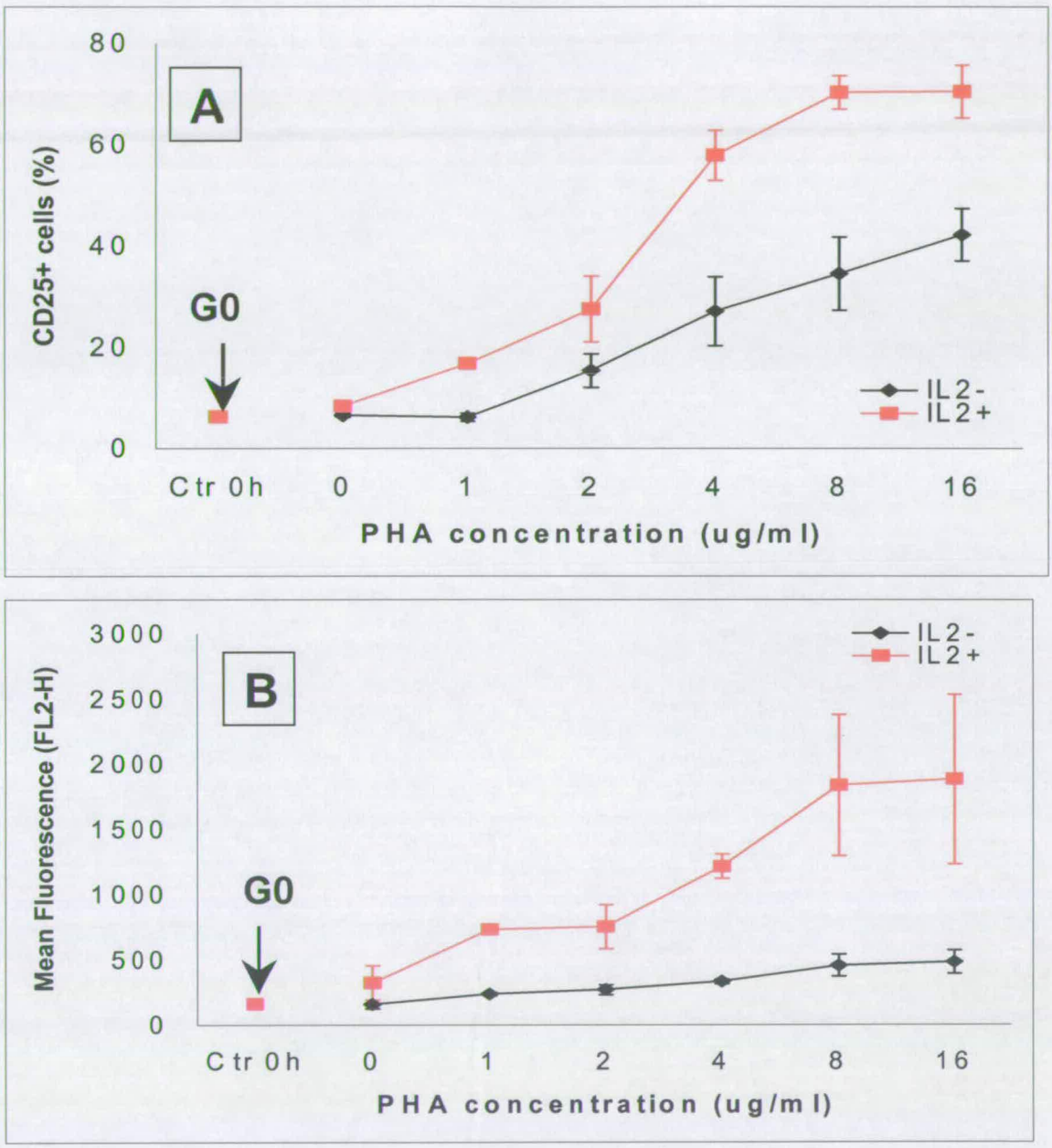

Cell were stained for CD25 and processed for FACS analysis at isolation (Ctr0h), or after culture for 48h with increasing concentrations of PHA (0-16ug/ml), in the presence or absence of 4nM IL-2. The groups Ctr0h and Ctr48h corresponded to fresh or cultured G0 cells. Expression of CD25 was assessed as percentage of $CD25^{+}$ cells (A) and as mean fluorescence intensity (CD25/cell; B). Data collected in three replicates are summarised as mean values±SEM.

Figure 4.9 PHA titration: effect of PHA concentration and IL-2 on cell cycle profile

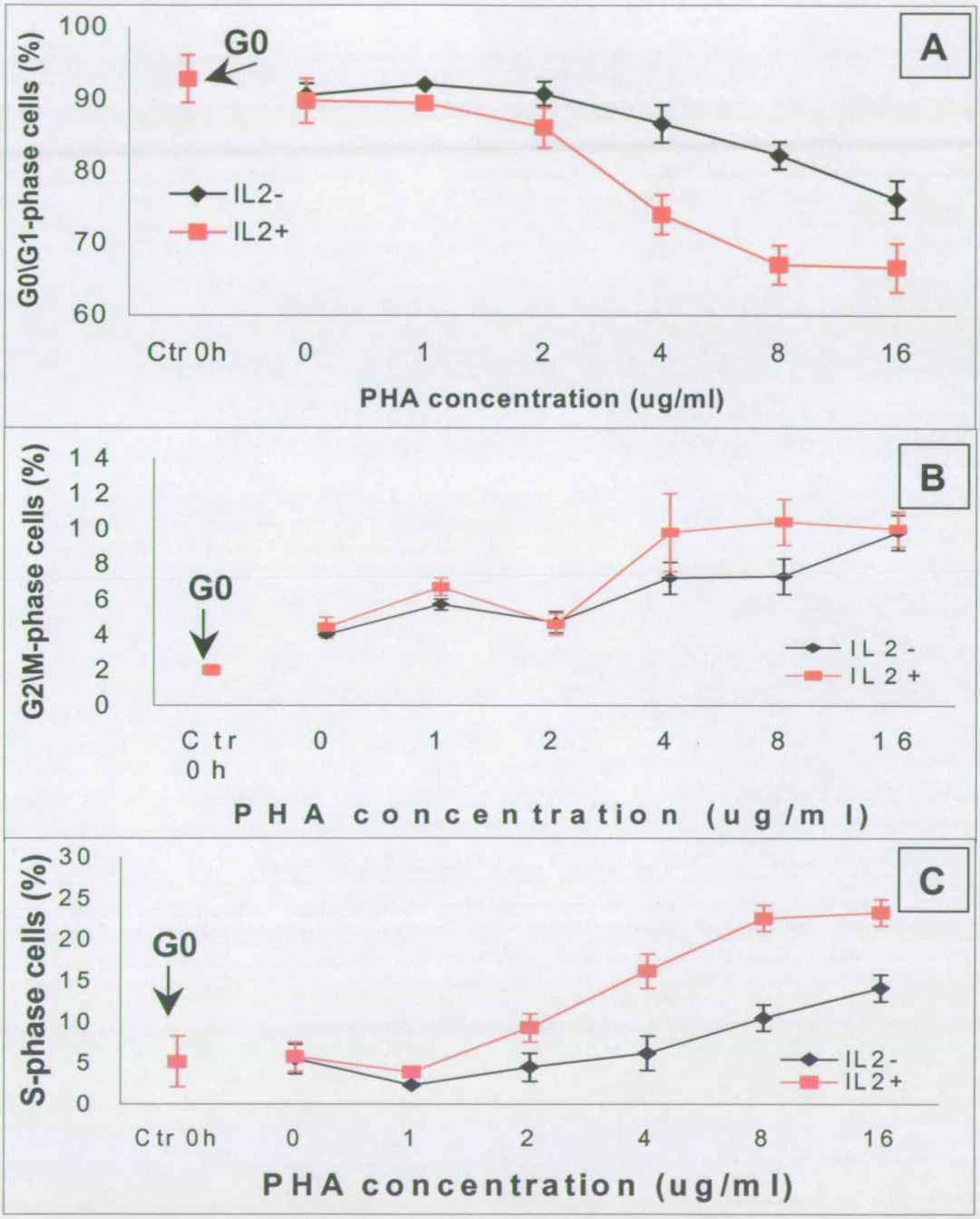

Cell cycle analysis of cells stained with PI and processed for FACS analysis, at isolation (Ctr0h), or after culture for 48h with increasing concentrations of PHA (0-16ug/ml), in the presence or absence of 4nM IL-2. The groups Ctr0h and Ctr48h corresponded to fresh or cultured G0 cells. Data from three experiments are expressed as mean percentages±SEM of G0/G1 (A), S (B) and G2/M (C) cells.

from 7.5±0.5%, in the absence of PHA, to 11.5±2.3%, at 1ug/ml, 21.5±7.5%, at 2ug/ml, 42.4±7.5%, at 4ug/ml, 52.5±8.3%, at 8ug/ml and, finally, 56.4±6.5% at 16ug/ml. The percentages of $CD25^+$ cells found in cells stimulated with 2ug/ml PHA or more, regardless of the presence of IL-2, was significantly higher than that found in quiescent cells, cultured without PHA (P0, $p<0.001$). Cells stimulated with 4ug/ml PHA had percentages of $CD25^+$ comparable to those found in cycling cells stimulated with 8ug/ml ($p>0.12$), but significantly lower than the maximal levels reached in cycling cells stimulated with 16ug/ml ($p<0.04$). The percentage of $CD25^+$ cells observed in the two cycling groups, stimulated with 8ug/ml and 16ug/ml PHA, were similar ($p=0.52$).

The presence of IL-2 also affected CD25 expression. The overall percentage of $CD25^+$ cells was significantly higher ($p<0.001$) in groups activated in the presence of IL-2 (41.9±6.2%), than in cells stimulated without IL-2 (22.1±3.8%).

When considering specific treatment groups (Fig.4.8A), the percentages of $CD25^+$ cells rose significantly ($p<0.03$) above the levels observed in cultured, quiescent cells, when cells were stimulated with 1ug/ml PHA or more, in the presence of IL-2, or with 2ug/ml PHA or more, in the absence of IL-2. Cells stimulated with 4ug/ml PHA, in the presence of IL-2, had percentages of $CD25^+$ cells similar ($p>0.19$) to those observed in cycling cells stimulated with 8ug/ml or 16ug/ml PHA and 4nM IL-2. Cells stimulated in the absence of IL-2 never reached ($p<0.008$) levels of CD25 expression similar to those of cycling cells, not even when stimulated with 16ug/ml PHA (42.3±5.2%).

Mean fluorescence intensity (Fig.4.8B), used as a measure of the levels of CD25 expression/cell, was also greatly affected by PHA concentration ($p<0.001$). Mean fluorescence was positively correlated with PHA concentration, and it gradually increased from 239±79, in the absence of PHA, to 485±103, at 1ug/ml, 511±131, at 2ug/ml, 774±187, at 4ug/ml, 1148±393, at 8ug/ml, and 1182±435 at 16ug/ml PHA. Mean fluorescence was significantly higher ($p<0.008$) than that of quiescent cells, cultured in the absence of PHA, when cells were stimulated with 1ug/ml or more PHA. Cells stimulated with 4ug/ml PHA or more had mean

fluorescence levels similar to those of cycling cells, stimulated with 8 or 16ug/ml PHA ($p>0.3$).

Mean fluorescence was also significantly affected by IL-2 ($p<0.001$). Cells cultured in the presence of IL-2 had significantly higher levels of mean fluorescence (1125±200) than cells cultured without IL-2 (322±36).

Specific treatments also influenced the level of expression of CD25 (Fig.4.8B). Mean fluorescence increased significantly from the levels observed in cultured quiescent cells, when cells were stimulated with 1ug/ml or more PHA, in the presence of IL-2 ($p<0.001$), and 4ug/ml PHA or more, in the absence of IL-2 ($p<0.036$). Mean fluorescence values were comparable ($p>0.05$) to those observed in cycling cells, stimulated with 8ug/ml or 16ug/ml PHA and 4nM IL-2, in groups cultured with 1ug/ml PHA or more, in the presence of IL-2. However the levels of mean fluorescence observed in cycling cells appeared to be much closer to those detected in cells stimulated with 4ug/ml PHA and IL-2 ($p=0.46$-0.50), rather than to those seen in cells stimulated with 4nM IL-2 and 1ug/ml ($p=0.064$-0.071) or 2ug/ml PHA ($p=0.050$-0.053). In the absence of IL-2, the levels of expression of CD25 never rose above those observed in cultured quiescent cells ($p>0.5$), not even after maximal stimulation with 16ug/ml PHA, and remained significantly lower than those observed ($p<0.006$) in cycling cells stimulated with 8ug/ml or 16ug/ml, in the presence of 4nM IL-2.

The percentage of cells G0/G1-phase was affected by PHA concentrations ($p<0.001$) and it gradually decreased as PHA concentrations increased. The percentages of G0/G1 cells were as high as 90.2±1.8% and 90.7±0.6%, in groups cultured without PHA or with 1ug/ml PHA, but gradually decreased to 88.4±1.9%, at 2ug/ml, 80.3±3.2%, at 4ug/ml, 74.6±3.5%, at 8ug/ml and 71.4±2.9%, at 16ug/ml PHA. Cells stimulated with 2ug/ml or less PHA, retained percentages of diploid cells similar to those found in cultured quiescent cells ($p>0.4$). Cells stimulated with 4ug/ml PHA had percentages of diploid cells similar to those of cycling cells stimulated with 8ug/ml PHA ($p=0.13$), but significantly higher than those of cycling cells stimulated with 16ug/ml PHA ($p=0.02$). The percentages of diploid cells observed in cycling groups stimulated with 8ug/ml or 16ug/ml were similar ($p=0.42$).

The presence of IL-2 also influenced the percentages of diploid cells, that were significantly lower ($p<0.002$) in groups containing IL-2 (78.8±2.6) compared to groups that did not contain it (86.4±1.5).

The percentage of G0/G1 cells in culture was affected by specific treatments (Fig.4.9A). The percentage of diploid cells remained similar to that observed in cultured, quiescent cells in groups where cells were stimulated with 2ug/ml PHA or less, in the presence of IL-2 ($p=0.20$), or with 4ug/ml or less, in the absence of IL-2 ($p=0.27$). Cells stimulated with 4ug/ml PHA in the presence of IL-2 had low percentages of G0/G1 cells, comparable ($p>0.29$) to those found in cycling cells stimulated with 8ug/ml or 16ug/ml PHA and 4nM IL-2. Cells stimulated with 16ug/ml PHA, in the absence of IL-2, also had low percentages of diploid cells, comparable to those observed in cycling cells stimulated with 8ug/ml or 16ug/ml PHA and 4nM IL-2 ($p>0.17$).

Treatment in culture also affected the percentages of cells in S-phase. PHA had a significant effect on the percentages of cells in S-phase ($p<0.001$). These percentages were positively correlated with PHA concentrations, starting at 5.6±1.9% and 3.1±0.4%, at 0 and 1ug/ml PHA, and then increasing steadily at 6.9±1.7%, at 2ug/ml, 11.2±2.3%, at 4ug/ml, 16.5±2.7%, at 8ug/ml, and finally 18.7±2.4%, at 16ug/ml. Groups stimulated with 2ug/ml or less PHA, still retained low percentages of cells in S-phase, comparable to those observed in groups cultured without PHA ($p>0.4$). Cells stimulated with 4ug/ml PHA or more had percentages of cells in S-phase as high as those observed in cycling cells stimulated with 8ug/ml or 16ug/ml PHA ($p>0.05$).

The percentage of replicating cells found in the T-cell population was also influenced by IL-2 ($p<0.006$). The overall percentages of cells in S-phase were 13.5±2.0%, in groups containing IL-2, and 7.2±1.1%, in groups with no IL-2.

When considering specific treatment effects (Fig.4.9 B), it was observed that the percentages of cells in S-phase remained ($p>0.24$) as low as the ones found in cultured quiescent cells in groups stimulated with 2ug/ml PHA or less, in the presence of IL-2 ($p=0.24$), or 8ug/ml PHA or less, in the absence of IL-2 ($p=0.14$). Cells stimulated with 4ug/ml PHA, in the presence of IL-2 ($p>0.47$), and cells

stimulated with 16ug/ml PHA, in the absence of IL-2 ($p>0.28$), had percentages of cells in S-phase comparable to those found in cycling cells stimulated with 8ug/ml or 16ug/ml PHA, and 4nM IL-2.

The percentages of cells in G2/M were affected by PHA concentrations ($p<0.001$). For concentrations of PHA between 0 and 2ug/ml, the percentages of cells in G2/M ranged from 4.2±0.3% to 6.2±0.4%. They then increased progressively to 8.5±1.3%, at 4ug/ml, 8.9±1.0%, at 8ug/ml and 9.9±0.7% at 16ug/ml PHA. The percentages of G2/M were similar to those observed in cultured, quiescent cells in groups stimulated with 2ug/ml or less PHA ($p>0.5$). Cells stimulated with 4ug/ml PHA or more had percentages of G2/M cells comparable to those of cycling cells, stimulated with 8ug/ml or 16ug/ml ($p>0.18$).

Addition of IL-2 also increased the percentage of G2/M from 6.4±0.5% to 7.6±0.8%, although this difference was not significant ($p=0.09$).

Comparison of specific treatment groups (Fig.4.9C) showed that percentages of G2/M cells remain similar ($p>0.8$) to those observed in cultured, quiescent cells, when cells were stimulated with 2ug/ml PHA, both with and without IL-2. The percentages of G2/M cells found in groups that had been stimulated with 4ug/ml PHA, with or without IL-2, were as high ($p>0.7$) as those observed in cycling cells, stimulated with 8ug/ml or 16ug/ml PHA and 4nM IL-2.

The [^{3}H]thymidine incorporation assay confirmed that cells cultured with 1ug/ml (9764±3269) or 2ug/ml PHA (23924±5951cpm), in the presence of 4nM IL-2, had higher ($p<0.001$) rates of incorporation, than quiescent cells, cultured in medium alone (448±124cpm). However these levels of incorporation remained lower ($p<0.001$) than the maximal levels observed in cycling cells cultured with 4ug/ml PHA or more (>46664±10624cpm), in the presence of IL-2, or with 16ug/ml PHA, in the absence of IL-2 (37250±13122cpm).

Cell counts failed to give a clear indication of the replication rates of cultured cells. A possible explanation might be that differences in cell numbers among treatment groups might have been masked by the overall apoptosis rates in culture, which were uniformly high in all treatment groups (average 30.0±4.5%).

4.3.5 Conclusions

Cells stimulated with 2ug/ml PHA and 4nM IL-2 represented the best G1 model obtained by means of PHA titration (Table 4.1). Cells in this treatment group had higher percentages of $CD25^+$ cells and higher mean fluorescence levels than those found in cultured quiescent cells, but similar, high percentages of diploid cells (Table 4.1). The percentages of cells in S-phase and G2/M-phase were also as low as those observed in cultured, quiescent cells (Table 4.1).

Although it was possible to use submitogenic concentrations of PHA and IL-2, identified by PHA titration, to synchronize cells in G1, this method turned out to be sub-optimal. The ideal G1 population should have 100 percent of the cells expressing CD25, at high levels, while remaining in a diploid state, without undergoing DNA replication. Signs of activation, at submitogenic concentrations of PHA, low enough not to trigger G1-S transition and DNA replication, are very weak. The percentages of $CD25^+$ cells and mean fluorescence levels observed in cells stimulated with 2ug/ml and IL-2 (Table 4.1) were lower than those observed in cycling cells, stimulated with 4ug/ml or more PHA and 4nM IL-2.

Cells stimulated with 1ug/ml PHA and IL-2, also had cell cycle and CD25 expression features similar to those of G1 cells. However the fact that their levels of CD25 expression were even lower than those found in cells stimulated with 2ug/ml PHA and IL-2 and the fact that their percentages of cells in G2/M were significantly higher than those found in cultured, quiescent cells (P0), made them a less suitable G1 candidate than cells stimulated with 2ug/ml PHA and IL-2.

Cells stimulated with 1 and 2ug/ml PHA and IL-2, had rates of thymidine incorporation higher than those of found in quiescent cells. This is in contrast with what observed using PI staining that showed that percentages of cells in S-phase were not increased by PHA concentrations as low as 2ug/ml, even in the presence of IL-2. This difference might depend on the greater sensitivity of the thymidine incorporation assay, and suggests that it might not be possible to completely uncouple T-cell activation from S-phase progression, by means of mere PHA titration.

These findings suggested that it might be necessary to find an alternative method to PHA titration to produce G1 cells with higher percentages of $CD25^+$ cells

Table 4.1 Summary of PHA titration results

	Treatment	$CD25^+$(%)	Fluorescence	%2N (G0/G1)	%2/4N (S)	%4N (G2/M)	cpm
G0	-	6.6±0.4 [a]	158±34 [a]	90.5±1.7 [a,b]	5.5±1.8 [a]	4.0±0.2 [b]	448±124 [a]
G1	**P2/IL**	27.6±6.5 [b]	753±168 [c]	86.1±2.8 [b]	9.3±2.3 [a]	4.6±0.6 [b]	23924±5951 [c]
Cycling	**P4/IL**	57.9±4.9 [c]	1216±95 [c]	74.0±2.7 [c]	16.2±0.6 [b]	9.8±2.2 [c]	48632±13353 [d]

Comparison of the activation state of T-cells from three treatment groups: 1) freshly isolated quiescent cells (G0); 2) cells activated for 48h with 4ug/ml PHA and 4nM IL-2 (cycling); 3) cells activated for 48h with submitogenic concentrations of PHA, 2ug/ml, and 4nM IL-2 (G1). The optimal submitogenic concentration of PHA was assessed by PHA titration. The activation state of T-cells was assessed considering their cell cycle profile (%G0/G1, %S and %G2/M cells), expression of CD25 (%$CD25^+$ cells; mean fluorescence) and [3H]thymidine incorporation rates, expressed as counts per minute (cpm). Data were collected in three replicates and are summarised as means±SEM. Data in the same columns with different superscripts are significantly different ($p<0.05$).

and higher mean fluorescence levels, associated with lower rates of thymidine incorporation.

Conclusions, regarding the activation protocol, were also drawn. When added to PHA, IL-2 increased the state of activation of T-lymphocytes (4.3.3 Results), as indicated by the reduction observed in the percentages of G0/G1 cells, and the increase observed in the percentages of cells in S and G2/M-phase, associated with the increase in CD25 expression (percentages of $CD25^+$ cells, mean fluorescence). However, no significant difference was observed in the activation state of cells stimulated with IL-2 alone, in the absence of PHA, and that of quiescent cells, both cultured (P0) or freshly isolated (G0).

PHA alone, in the absence of IL-2, was also unable to fully activate T-lymphocytes: 1) percentages of $CD25^+$ cells and mean fluorescence levels, in the absence of IL-2, never reached levels observed in cycling cells, stimulated with 4ug/ml or more PHA and IL-2, not even when stimulated with maximal concentrations of PHA; 2) cell cycle profiles and rates of thymidine incorporation similar to those observed in cycling cells, were observed only when cells were stimulated with maximal levels of PHA (16ug/ml).

These results indicated that PHA and IL-2 were both necessary to induce T-lymphocyte activation. In the presence of IL-2 and PHA, a plateau of activation, beyond which no further significant increase was observed in the activation state of T-cells, measured as levels of CD25 expression, cell cycle profile and rates of thymidine incorporation, was reached when cells were stimulated with 4ug/ml or more PHA (Table 4.1). However maximal levels of activation were reached when cells were stimulated with 8 or 16ug/ml PHA and 4nM IL-2.

4.4 SYNCHRONIZATION OF T-LYMPHOCYTES IN G1 BY HYDROXYUREA BLOCK

4.4.1 Aim

In the previous experiment PHA titration was successfully used to identify the submitogenic concentration of PHA to use for synchronization in G1 of mouse T-cells. However it also suggested that other methods should be used to produce G1

cells, with higher percentages of $CD25^+$ cells and higher mean fluorescence levels, while retaining a quiescent cell cycle profile. Activation in the presence of G1/S blocking agents, like hydroxyurea, was tested for synchronization in G1 (Adams *et al.*, 1967, Kim *et al.*, 1992).

4.4.2 Experimental design

The design of this experiment was divided into two parts:

1) Identification of optimal synchronization conditions;

2) Assessment of cytotoxic effects of the blocking conditions.

Experiments to find optimal blocking conditions were carried out in three replicates. For each replicate cells from the lymph nodes of eight, 6 week old, CBA/Ca, female mice, were isolated, pooled together, counted and assigned to a specific treatment group. Cells were cultured in culture medium containing 2-mercaptoethanol, 10% FCS (legend=M; composition A.2.1), in the presence or absence of 8ug/ml and 4nM IL-2 (legend=A; composition A.2.4-A.2.5), that induce maximal activation, as shown in previous experiments. Cells were also cultured in the absence or presence of hydroxyurea (Kim *et al,* 1992; Paragraph 2.7) at two different concentrations: 0.5mM (legend=B1) or 1mM (legend=B2). Treatment groups are summarised below:

1) Culture in medium with 10% FCS (M);

2) Culture in medium with 10% FCS, 0.5mM HU (M+B1);

3) Culture in medium with 10% FCS, 1mM HU (M+B2);

4) Culture in medium with 10% FCS, PHA and IL-2 (M+A);

5) Culture in medium with 10% FCS, PHA, IL-2, and 0.5mM HU (M+A+B1);

6) Culture in medium with 10% FCS, PHA, IL-2, 1mM HU (M+A+B2);

Previous experiments (Paragraph 4.2-4.3) had shown that culture in itself, in the absence of activating agents, did not alter the quiescent state of T-lymphocytes, isolated from the lymph nodes. Therefore, only cultured cells were used as a quiescence control (group1) in this analysis, while freshly isolated, quiescent cells were omitted. Cells, in each treatment group, were cultured for 24h or 48h.

Each treatment group was analysed for:

1) FACS analysis;

2) [^{3}H]thymidine incorporation;

3) Cell counts.

Cells were seeded in two, 24 well plates, at a concentration of $2x10^6$/well/ml, assigning 1 well/treatment group. Cells cultured for 24h were seeded in one plate and cells cultured 48h were seeded in the other plate. Cells were also seeded in two 96 well plates, at a concentration of $0.2x10^6$/well/100ul, assigning 3 wells/treatment group. Cells cultured for 24h were seeded in one plate and cells cultured for 48h were seeded in the other plate. At the end of the incubation period, 24h or 48h after seeding, cells in the 24 well plates were harvested, counted and processed for FACS analysis (Paragraph 2.7). At the end of the incubation period, cells in the 96 well plates were frozen at –20°C and processed together to detect rates of [^{3}H]thymidine incorporation (Paragraph 2.9).

To further confirm that the selected protocol for synchronization in G1 had no detrimental effect, cells, that had been treated for 24h with the highest concentration of hydroxyurea (HU), were activated for another 24h with 8ug/ml PHA and 4nM IL-2, to assess their ability to re-enter the cell cycle. The state of activation of T-cells was assessed by FACS analysis, [^{3}H]thymidine incorporation, and cell counts. Experiments were set up by culturing cells, for 24h, in 24h well plates, at a concentration of $2x10^6$ cell/well/ml, for FACS analysis and cell counts, assigning 1 well/sample. Alternatively cells were cultured in 96 well plates, at a concentration of $0.2x10^6$/well/100ul, for [^{3}H]thymidine incorporation, assigning 3 wells/sample. Cells were cultured in triplicate samples, and each of the three samples, belonging to the same treatment group, was placed on a separate plate. All samples were cultured, for 24h, under the following treatment conditions:

1) Medium alone (M);
2) Medium with hydroxyurea 1mM (M+B2);
3) Medium with activating agents (M+A);
4) Medium with activating agents and hydroxyurea 1mM (M+A+B2).

After 24h, one plate, containing a sample from each of the four treatment groups, was left in culture and incubated, under the same conditions for further 24h, and harvested at 48h. A second plate was harvested at 24h. Samples on the third plate, from all treatment groups, were harvested, washed twice in PBS and once with medium, and replated, at the same concentration, with activating agents, regardless

of the previous treatment condition, and incubated for further 24h. At harvest, each plate was processed for FACS analysis and cell counts, or frozen at –20°C and processed for [^{3}H]thymidine incorporation.

Samples processed for FACS analysis were stained with anti-CD3-FITC/anti-CD25-R-PE and anti-CD3-FITC/PI (for Methods see Paragraph 2.9).

Although these studies are mainly focused on T-lymphocytes, previous experiments (Paragraphs 4.2-4.3) had confirmed that cells from the lymph nodes were mainly $CD3^+$ (i.e. T-lymphocytes). This level of purity in the lymph nodes is such that no further purification steps, to deplete unwanted $CD3^-$ cells, would be required in future NT experiments, and the cell population isolated from the lymph nodes could be used as a whole. Therefore, although it would have been possible to restrict the analysis to T-lymphocytes, gating cells which were both live and $CD3^+$ (live/$CD3^+$ gate), only live cells were included in the CD25 and PI analysis (live gate; see Paragraph 2.10.2), omitting the CD3 gating for T-lymphocytes.

The following parameters were acquired (see Paragraph 2.10.2):

1) For CD25 staining (live gate):
   a) Percentage of $CD25^+$ cells;
   b) Mean fluorescence levels.
2) For PI staining:
   a) Percentage of apoptotic cells (all cells gated);
   b) Cell cycle profile (live gate), that included:
      (a) Percentage of cells in G0/G1-phase;
      (b) Percentage of cells in S-phase;
      (c) Percentage of cells in G2/M-phase;

The [^{3}H]thymidine incorporation assay was performed as previously described (for Methods see Paragraph 2.7).

4.4.3 Statistical Analysis

Data, categorised in the usual dependent variable categories, were transformed as follows for analysis (GenStat 4.21, Windows 2000): percentages (%$CD25^+$ cells, percentages of cells in G0/G1, S and G2/M) with the Logit

transformation; continuous numerical values (mean fluorescence, cpm) with the Log transformation.

Data were analysed using a Nested Analysis of Variance and a one-way ANOVA.

The Nested Analysis of Variance, with an alpha level for critical ranges of 0.05, was used on the different treatment groups, to assess variance in the quiescence state deriving from different culture treatments, containing activating and/or blocking agents. In this case variance was considered only relatively to a cultured control of cells quiescence: cells cultured in the absence of activating agents, with or without blocking agents (M, M+B1, M+B2). The analysis was carried out on two levels:

1) General level, considering individual treatment groups:
   a) Block Structure: block/time/condition, with:
      - Block, including replicate 1, replicate 2, replicate 3;
      - Time, including 24h or 48h;
      - Condition including M, M+B1, M+B2, M+A, M+A+B1, M+A+B2;
   b) Treatment structure: time x condition, with:
      - Time, as main effect;
      - Condition, as main effect;
      - Time and condition interaction;

2) Detailed level, braking variation into variation depending on activating agents (A) and variation depending on blocking agents (B). Furthermore, two levels were assigned to factor A, corresponding to culture medium with (A1) or without (A0) 8ug/ml PHA and 4nM IL-2. Three levels were assigned to factor B corresponding, respectively to 0mM (B0), 0.5mM (B1) and 1mM hydroxyurea (B2).
   a) Block Structure: block/time/condition (A x B), with:
      - Block, including replicate 1, replicate 2, replicate 3;
      - Time, including 24h or 48h;
      - Condition, including all the possible combinations of A and B: A0B0 (M), A0B1 (M+B1), A0B2 (M+B2), A1B0 (A), A1B1 (A+B1), A1B2 (A+B2);
   b) Treatment structure: (time x A x B), with:

- Time, as main effect;
- A, as main effect, regardless of B;
- B, as main effect, regardless of A;
- A and time interaction, regardless of B;
- B and time interaction, regardless of A;
- A and B and time interaction;

In the experiments assessing the detrimental effects of hydroxyurea, the block structure used for the Nested Analysis of Variance included also variance between wells, because a great variability among wells was observed: block/**well**/time/condition or block/**well**/time/condition (A x B).

At each level of analysis, differences between specific groups of interest were assessed using a Student's T-test for difference in means, with an alpha level of 0.05: t=(mean1-mean2)/SE (mean1-mean2). Means and SED (Standard Error of Difference in Means) were obtained from the tables of the Nested Analysis of Variance (GenStat 4.21, Windows 2000).

A one-way ANOVA, considering treatment as independent variable, (Statistica 4.5, Windows 1995) was also carried out on all groups, including cultured groups and freshly isolated cells (G0), with an alpha level for critical ranges of 0.05. This was done to compare variance of the quiescent state found in cultured treatment groups, not only relatively to cultured quiescent cells, but also relatively to the quiescent state of T-cells at isolation (G0).

4.4.4 Results

An average of $6.2\pm3.2\text{x}10^6$ total cells were isolated from the lymph nodes of each animal. About 89.7±1.7 % of total cells, corresponding to $5.5\pm2.8\text{x}10^6$/animal, were $CD3^+$ (i.e. T-lymphocytes).

Time in culture affected apoptosis (time, p=0.044). Overall apoptosis rates in culture, considering all culture conditions, were 4-fold higher at 48h (23.9±2.9) than they were at 24h (5.6±1.9).

Cells that had been cultured for 48h in medium alone, in the absence of activating and/or blocking agents (M), had higher rates of apoptosis than cells that had been cultured for 24h under the same conditions ($0.01<p<0.05$; Fig.4.10). Cells

Figure 4.10 Effect hydroxyurea synchronization on apoptosis

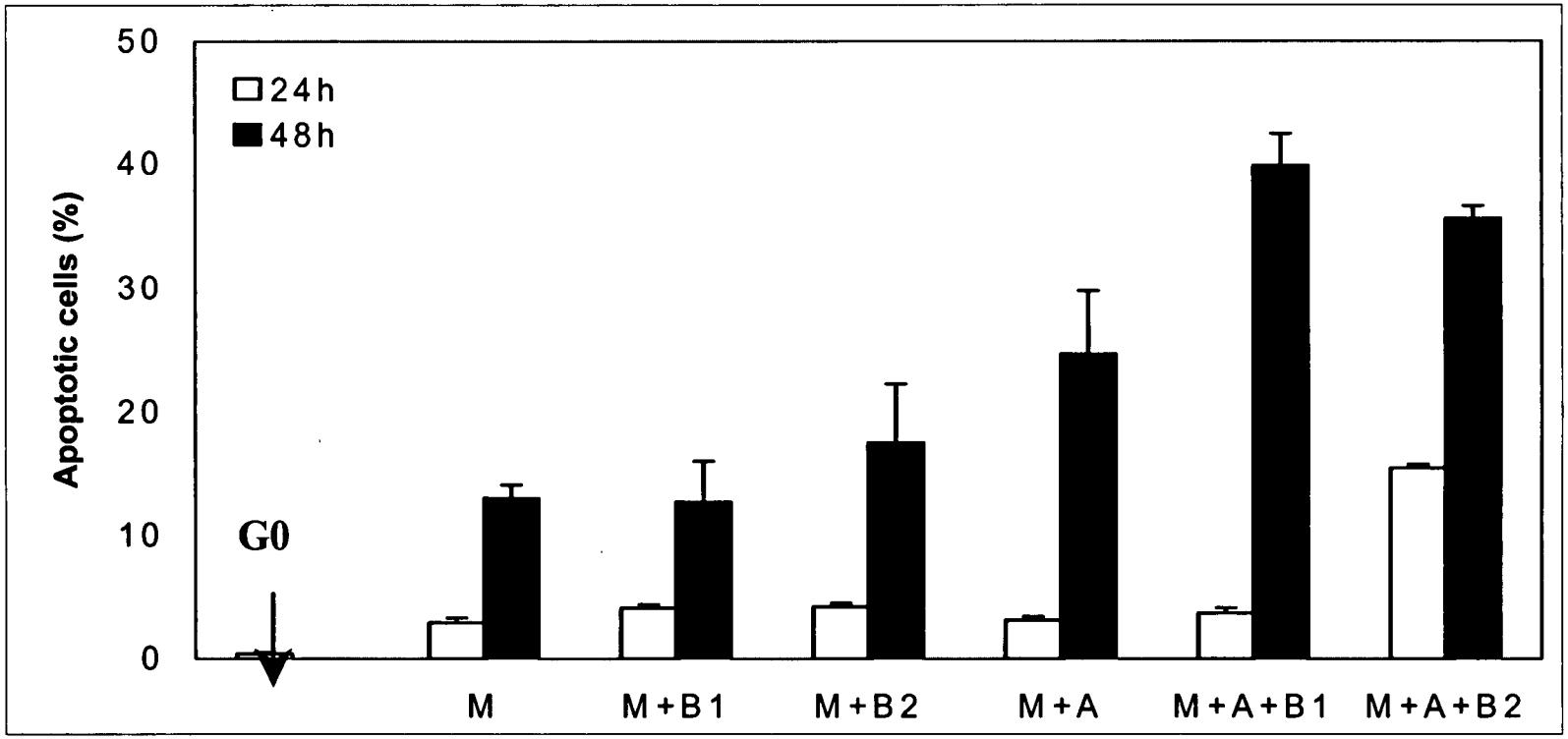

Cells were assessed for apoptosis by PI staining and FACS analysis, at isolation, or after culture for 24h or 48h in: 10% FCS medium (M); M supplemented with the activating agents PHA 8ug/ml and IL-2 4nM (M+A); M or M+A supplemented with the blocking agent hydroxyurea (B) at two different concentrations, 0.5mM (B1) or 1mM (B2). Cells in the group M were a quiescence, culture control, cells in group M+A were cycling cells; cells in M+A+B were "putative G1 cells". Data were collected in three replicates and are summarised as mean±SEM.

that had been cultured for 24h in M had very low death rates (Fig.4.10), though they were significantly higher than those observed in freshly isolated G0 cells ($p<0.001$).

Treatment conditions in culture (condition, $p=0.005$) influenced rates of cells death, adding their effect to the effects of time, rather than synergizing with it (time x condition, $p=0.147$). Apoptosis in culture could be affected by three factors: 1) presence of activating agents (A); 2) presence of blocking agents (B); 3) interaction of activating and blocking agents (A x B).

Activating agents, with or without B, increased apoptosis (A, $p<0.001$), but this effect appeared to be mediated by time (time x A, $p=0.027$). Compared to M, incubation with A for 24h, in the presence or absence of B, did not increase cell death rates ($0.1<p<0.5$), but it increased apoptosis at 48h ($p<0.001$). Similarly incubation with A, in the absence of blocking agents (B), did not increase apoptosis at 24h ($p>0.5$), but it did at 48h ($0.001<p<0.01$).

Blocking agents, in the presence or absence of activating agents, had no effect on cell survival in culture (B, $p=0.05$), at least at the concentrations used in these experiments. Their effect was independent from time in culture (time x B, $p=0.626$). In the absence of activating agents, incubation with blocking agents, at both concentrations, for 24h (B1 at 24h, $0.1<p<0.5$; B2 at 24h, $0.1<p<0.5$) and 48h (B1 at 48h, $p>0.5$; B2 at 48h, $p>0.5$) did not increase apoptosis rates, compared to controls, cultured in medium alone (Fig.4.10). Rates of apoptosis observed in groups containing B1 were higher at 48h than at 24h ($0.05<p<0.1$), and significantly higher at 48h that at 24h in groups containing B2 ($0.01<p<0.05$). However, a comparable increase in death rates was observed as a result of culture in medium alone (M) for 24h and 48h ($0.01<p<0.05$).

Interaction of activating and blocking agents did not increase apoptosis (A x B, $p=0.55$), at both time points (time x A x B, $p=0.289$). However the effect of their interaction depended on the concentration of hydroxyurea (Fig.4.10): activation in the presence of lower concentrations of hydroxyurea (A+B1), did not increase apoptosis, at 24h ($p>0.5$) and 48h ($0.1<p<0.5$); activation in the presence of higher concentrations of hydroxyurea (A+B2), increased apoptosis at 24h in a marginal way ($0.01<p<0.05$). Activation in the presence of higher concentrations of hydroxyurea

Figure 4.11 Synchronization with hydroxyurea: effect on the cell cycle profile

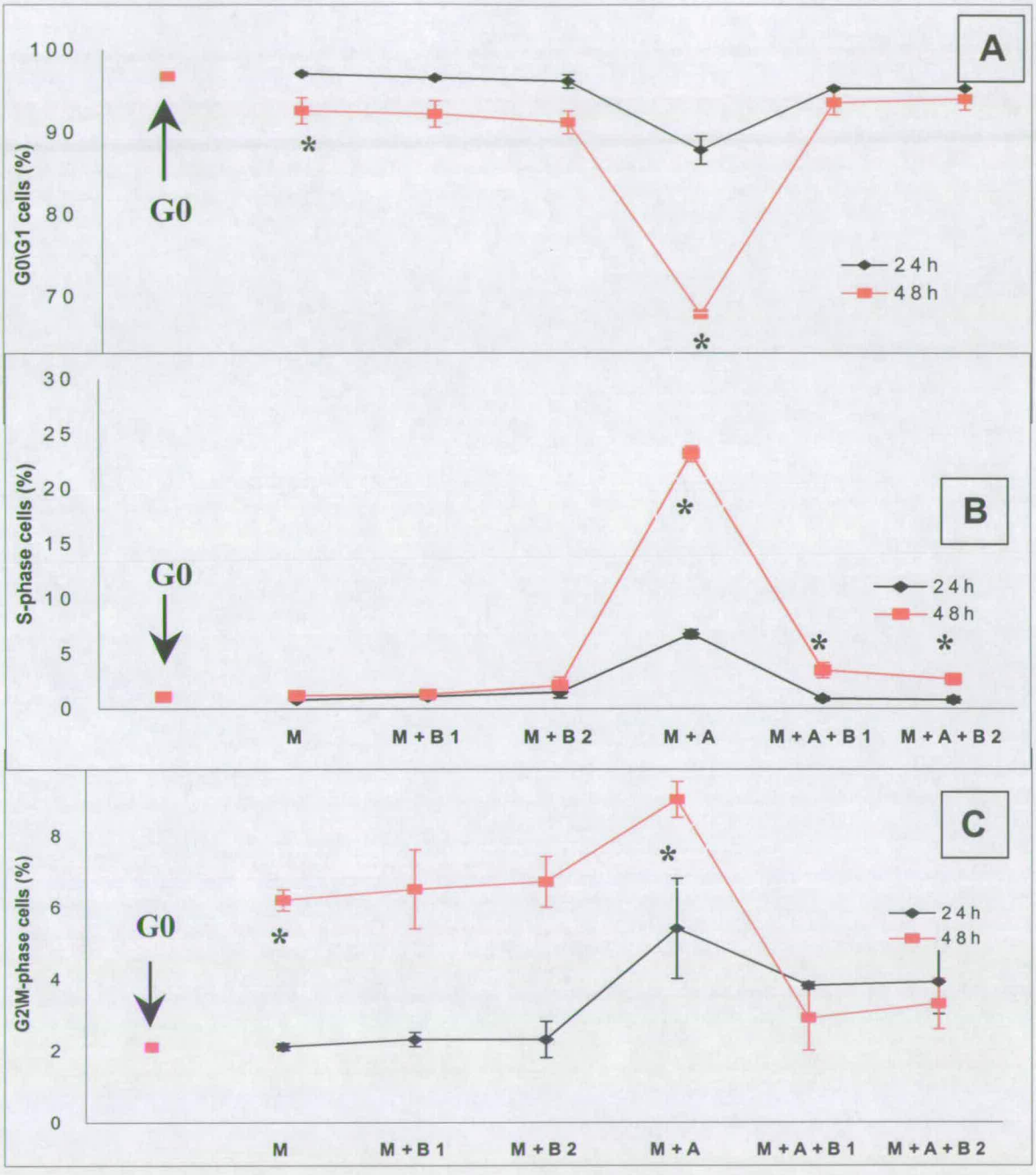

Cell cycle analysis (%G0/G1, A; %S, B; %G2/M, C) of cells stained with PI, at isolation (G0), or after culture for 24h or 48h in: medium (M); M with the activating agents PHA 8ug/ml and 4nM IL-2 (M+A); M or M+A supplemented with the blocking agent hydroxyurea (B) at two different concentrations, 0.5mM (B1) or 1mM (B2). Cells in the group M were a quiescence, culture control, cells in group M+A were cycling cells; cells in M+A+B were "putative G1 cells". Data were collected in three replicates and are summarised as mean±SEM. (*) Significantly different.

(A+B2) did not increase apoptosis at 48h ($0.1<p<0.5$), possibly masked by the culture effect (M at 24h vs M at 48h, $0.01<p<0.05$).

The percentages of G0/G1 cells were influenced by time in culture (G0/G1, $p=0.048$). The overall percentages of G0/G1 cells, considering all treatment conditions, were higher at 24h (97.7±0.8) than at 48h (88.6±2.2). The percentages of G0/G1 cells found in groups that had been cultured for 24h in medium alone (M) remained as high as those found in freshly isolated, quiescent cells ($p=0.78$; Fig.4.11A). Culture for 48h in medium alone, decreased the percentages of G0/G1 cells, compared to cultured and freshly isolated quiescent cells ($p<0.001$; Fig. 4.11 A).

Treatment affected the percentages of G0/G1 cells (condition, $p<0.001$) and their effect was mediated by time (time x condition, $p<0.031$). Activating agents (A, $p<0.001$), in the presence or absence of blocking agents, affected the percentages of G0/G1 cells, regardless of time (time x A, $p=0.11$). Incubation with activating agents alone (A; Fig.4.11A), for 24h and 48h, decreased the percentages of G0/G1 cells ($p<0.001$) compared to quiescent cells cultured for 24h and 48h in medium alone.

The percentages of G0/G1 cells observed in cells that had been activated for 48h were lower than those obtained after activation for 24h ($p<0.001$).

Presence of blocking agents during culture altered the effect of activation on the percentages of G0/G1 cells (A x B, $p<0.001$) in a time-dependent manner (time x A x B, $p<0.001$). The percentages of G0/G1 cells found in groups activated 24h in the presence of both concentrations of hydroxyurea, were higher than those observed in activated cells ($p<0.001$; for B1 and B2; Fig.4.11 A), and similar to those found in quiescent cells, that had been cultured in medium alone for 24h ($p>0.5$, for A+B1 and A+B2) and to freshly isolated quiescent cells ($p=0.16$, for A+B1; $p=0.23$, for A+B2). At 24h, the percentages of G0/G1 cells, found in the two groups activated with the lower and higher concentrations of hydroxyurea were also mutually similar ($p>0.5$). The percentages of G0/G1 cells found in groups that had been activated for 48h, in the presence of both concentrations of hydroxyurea, were higher than those observed in activated cells ($p<0.001$, for A+B1 and A+B2), and comparable to those found in quiescent cells, cultured in medium alone for 48h ($0.1<p<0.5$, for A+B1 and

A+B2), though not as high as those found in freshly isolated, G0 cells ($p=0.024$, for A+B1; $p=0.042$ for A+B2). However the percentages of G0/G1 cells found in cells activated for 48h, in the presence of both concentrations of hydroxyurea, apart from being mutually similar ($p>0.5$), were also similar to those found at 24h, in the same treatment groups ($0.1<p<0.5$).

Time in itself had no significant effect on the percentages of cells in S-phase ($p=0.076$). The overall percentages of replicating cells found at 24h, regardless of treatment conditions, were similar to those found at 48h ($p>0.5$; Fig.4.11B). Cells cultured in medium alone, in the absence of any treatment, had low percentages of cells in S-phase, both at 24h and 48h of culture ($0.1<p<0.5$), similar to those found in freshly isolated quiescent cells ($p=0.89$, at 24h; $p=0.39$, at 48h).

The treatment condition had a significant effect on the percentages of cells in S-phase (condition, $p<0.001$) and this effect was mediated by time (time x condition, $p=0.012$). The presence of activating agents, regardless of the presence of blocking agents, influenced the percentages of replicating cells (A, $p<0.001$) in a time-dependent manner (A x time, $p<0.001$). Incubation with activating agents, in the absence of blocking agents, for 24h and 48h, increased the percentages of cells in S-phase ($p<0.001$), compared to culture controls. The percentages of S-phase cells, after activation for 48h, were higher than those found at 24h ($0.01<p<0.001$).

Hydroxyurea altered the effect of activating agents on the percentages of cells in S-phase (A x B, $p<0.001$). The effect of blocking agents was mediated by the length of the activation period.

The percentages of cells in S-phase found in groups activated for 24h in the presence of both concentrations of hydroxyurea were lower than those found in activated cells ($p<0.001$, for A+B1 or B2). At 24h (Fig.4.11B), the percentages of replicating cells found in the groups activated with blocking agents, regardless of the concentration, remained as low as those found in cultured ($p>0.5$, for A+B1 or B2) and freshly isolated, quiescent cells ($p=0.93$, for A+B1; $p=0.94$, for A+B2). At 48h (Fig.4.11B), the percentages of replicating cells found in the groups activated in the presence of blocking agents, were higher than those observed in the culture control, though to a lesser extent in groups incubated with 1mM hydroxyurea ($0.01<p<0.05$)

rather than with 0.5mM hydroxyurea ($0.001<p<0.01$). These percentages were also higher than those found in G0 cells ($p=0.004$, for A+B1; $p=0.015$; for A+B2). However, the overall percentages of replicating cells found at 48h, in groups activated in the presence of blocking agents, were, anyway, very low (2.7-3.5%).

The percentages of cells in S-phase observed in groups activated in the presence of blocking agents, at both concentrations, were mutually similar at 24h ($p>0.5$) and at 48h ($p>0.5$). However, groups with the same concentrations of blocking agents, at different time points, differed significantly ($0.01<p<0.001$).

The percentages of cells in G2/M, considering all treatment groups, were not influenced by time (time, $p=0.079$) and were similar at 24h (3.3±0.4%) and at 48h (5.8±0.6%). However, the percentages of G2/M cells were affected by treatment. Cells cultured 24h had percentages of G2/M cells similar to those found, at isolation, in G0 cells ($p=0.92$). However, cells cultured in medium alone, for 48h had higher ($p=0.002$) percentages of G2/M cells than those observed in cultured and freshly isolated, G0 cells (Fig.4.11C). At 48h, the percentages of G2/M cells were higher those observed in cells cultured for 24h, even in groups where cells were incubated with medium and blocking agents ($00.1<p<0.01$ for M+B1; $p<0.001$, for M+B2). These percentages were similar to those observed in cells cultured 48h, in medium alone ($p>0.5$).

The percentages of G2/M cells were affected by the treatment condition (condition, $p=0.007$) in a time-dependent manner (condition x time, $p<0.001$). Incubation for 24h with activating agents, in the absence of blocking agents, increased the percentages of G2/M cells compared to the culture control ($0.001<p<0.01$) and to freshly isolated quiescent cells ($p=0.016$). Incubation for 48h, with activating agents, in the absence of blocking agents, increased the percentages of G2/M cells, compared to those found in G0 cells, at isolation ($p=0.002$). However the increase induced by activation was similar to that observed at 48h as a result of culture alone ($0.1<p<0.5$) in the absence of activating agents. The culture effect might have masked a possible activation effect. The percentages of G2/M cells observed in cells activated for 48h were significantly higher than those observed at 24h ($0.01<p<0.05$).

Blocking agents inhibited the increase in the percentages of G2/M cells induced by activation (A x B, $p=0.009$).

Activation for 48h in the presence of hydroxyurea, regardless of concentration, reduced the percentages of G2/M cells to levels lower than those obtained in activated cells ($p<0.001$; Fig.4.11C). Furthermore, these percentages were even lower than those observed in cells cultured in medium alone ($p<0.001$), and similar to those observed in freshly isolated, G0 cells ($p=0.25$ for A+B1; $p=0.54$ for A+B2).

Activation in the presence of hydroxyurea, for 24h, reduced the percentages of G2/M cells from 5.4% to 3.8-3.9%, though this decrease was not significant ($0.1<p<0.5$, Fig.4.11C). The percentages of G2/M cells found in cells that had been incubated for 24h with activating and blocking agents, also remained very low (3.8%-3.9%), though they appeared to be significantly different ($0.001<p<0.01$, A+B1; $0.01<p<0.05$, A+B2; t-test) from those observed in the culture control (2.1%). However, a one-way ANOVA showed no significant difference with freshly ($p=0.07$-0.11) and cultured quiescent cells ($p=0.06$-0.09).

The percentages of G2/M cells found in groups activated for the same time but with different concentrations of hydroxyurea, were mutually similar ($p>0.05$). Groups activated with the same concentration of HU, but for different times were also similar (for B1, $0.001<p<0.01$; for B2, $p<0.001$).

The percentages of $CD25^+$ cells (Fig.4.12A), increased slightly, as an effect of culture, from 5.4±0.3%, observed in freshly isolated cells (G0), to 10.8±1.1% and 11.8±0.3%, for cells cultured respectively for 24h and for 48h. However this increase was not significant ($p=0.06$) and it was not affected by time in culture (10.8±1.1 vs 11.8±0.3, $p>0.5$).

The different treatment conditions in culture had a significant effect on CD25 expression (condition, $p<0.001$), in a time-dependent manner (condition x time, $p<0.001$), at least for some treatments. Incubation with activating agents, for 24h and 48h, in the absence of blocking agents, increased the percentages of $CD25^+$ cells compared to the culture control ($p<0.001$) and freshly isolated, quiescent cells

Figure 4.12 Effect of hydroxyurea on CD25 expression

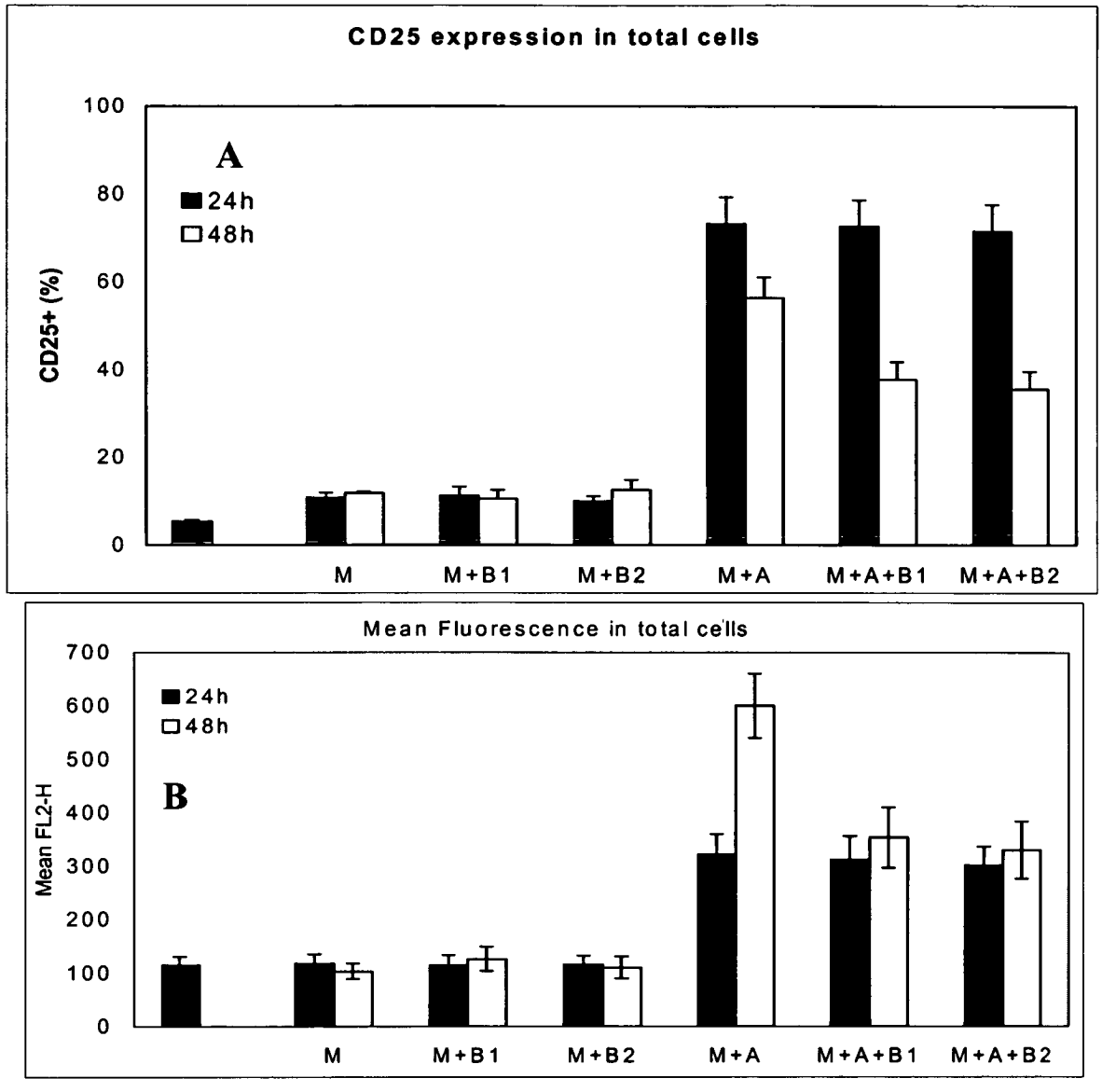

Cell were stained for CD25 and processed for FACS analysis at isolation (G0), or after culture for 24h 48h with: medium (M); M with the activating agents PHA, 8ug/ml, and IL-2, 4nM, (M+A); M or M+A supplemented with the blocking agent hydroxyurea (B) at two different concentrations, 0.5mM (B1) or 1mM (B2). Cells in the group M were a quiescence, culture control, cells in group M+A were cycling cells; cells in M+A+B were "putative G1 cells". Expression of CD25 was assessed as percentage of $CD25^{+}$ cells (A) and as mean fluorescence intensity (CD25/cell; B). Data, collected in three replicates, are summarised as mean values ± SEM.

($p<0.0001$). The percentages of $CD25^+$ cells were higher after activation for 24h than for 48h (73.3% vs 56.3%), although this difference not significant ($0.1<p<0.5$).

The presence of blocking agents did not affect the percentage of $CD25^+$, both in the presence or absence of activating agents ($p=0.111$). In the absence of activating agents, the proportion of $CD25^+$ cells remained as low as those found in the culture controls, where only medium was added, regardless of the concentration and of the length of the culture period ($p>0.5$, at 24h; $0.1>p>0.5$, at 48h with B1, and $p>0.5$ with B2). The percentages of $CD25^+$ cells found in groups incubated with the same concentration of hydroxyurea, but for a different length of time, were similar ($p>0.5$). Groups incubated with different concentrations of hydroxyurea but for the same length of time, were also similar.

The percentages of $CD25^+$ cells found in all groups incubated with hydroxyurea, without activating agents, regardless of time, were comparable to those found in G0 cells ($p>0.05$), the only exception being cells cultured for 48h with 1mM HU ($p<0.04$).

Blocking agents had no significant effect on the expression of CD25 during activation (A x B, $p=0.219$), but this was depended upon the time spent in culture.

The percentages of $CD25^+$ cells observed in groups activated for 24h in the presence of hydroxyurea, were higher than those found in cultured ($p<0.001$) and freshly isolated quiescent cells ($p<0.001$) and remained as high as those found in groups activated without hydroxyurea ($p>0.5$, Fig.4.12 A).

The percentages of $CD25^+$ cells, observed in groups activated for 48h in the presence of hydroxyurea, were higher than those found in cultured ($p<0.001$) and freshly isolated, quiescent cells ($p<0.001$), but they were also lower than those found in groups activated without hydroxyurea ($p<0.001$, Fig.4.11 A). The percentages of $CD25^+$ cells found in groups activated for 48h with hydroxyurea were also lower than those observed in cells activated for 24h in the presence of the same concentration of hydroxyurea ($p<0.001$).

Cells cultured for 24h or 48h, in medium alone, had the same levels of mean fluorescence ($p>0.5$) and these levels were also similar to those observed in freshly isolated, quiescent cells ($p=0.84$, Fig.4.12B).

The different treatment conditions in culture had a significant effect on mean fluorescence expression (condition, $p<0.001$). Incubation with activating agents (A, $p<0.001$), regardless of the presence or absence of blocking agents (A x B, $p=0.338$), dramatically increased mean fluorescence levels. Activation, for 24h and 48h, in the absence of blocking agents, increased mean fluorescence levels, compared to culture controls ($p<0.001$; Fig.4.12 B) and to freshly isolated, quiescent cells ($p<0.003$, at 24h; $p<0.0001$, at 48h). The increase in mean fluorescence levels observed after activation for 48h was greater than that observed after activation for 24h ($0.01<p<0.05$; Fig.4.12B).

The addition of blocking agents did not affect the expression of CD25 ($p=0471$), both in the presence or absence of activating agents. During incubation with blocking agents, in the absence of activating agents, the levels of mean fluorescence remained as low as those found in the culture controls, where only medium was added, regardless of the concentration of hydroxyurea and of the length of the culture period ($p>0.5$, for all groups). The levels of mean fluorescence, observed under these experimental conditions, were also similar to those found in freshly isolated G0 cells ($p>0.8$). The levels of mean fluorescence found in groups incubated with the same concentration of hydroxyurea, but for a different length of time were similar ($p>0.5$). Groups incubated with different concentrations of hydroxyurea but for the same length of time were also similar ($p>0.5$).

The presence of blocking agents did not interfere with the expression of CD25 during activation (A x B, $p=0.338$). However the outcome was affected by the length of the incubation period. Cells activated for 24h, in the presence of hydroxyurea, regardless of the concentration, had mean fluorescence levels higher than those found in freshly isolated ($p<0.001$) and cultured quiescent cells ($0.01<p<0.001$). The levels of mean fluorescence, at both concentrations of hydroxyurea, were also as high as those found in activated cells ($p>0.5$; Fig.4.12B).

Cells activated for 48h in the presence of hydroxyurea, regardless of the concentration, had mean fluorescence levels higher than those found in freshly isolated ($p<0.001$) and cultured quiescent cells ($p<0.001$; Fig.4.12B). However, their levels of mean fluorescence, at both concentrations of hydroxyurea, were not as high those found in cells activated for 48h ($0.05<p<0.01$, for A+B1 and A+B2), though

comparable to those found after activation for 24h, in the presence or absence of hydroxyurea ($p>0.5$, Fig.4.12 B).

Results of the [^{3}H]thymidine incorporation assay, expressed as counts per minute±SEM, confirmed that incubation with activating agents increased dramatically thymidine incorporation rates, both at 24h (16163±5887cpm, $p<0.0001$ and at 48h (56575±13668cpm; $p<0.0001$), compared to culture controls (390±143cpm, at 24h; 519±150cpm, at 48h). Replication rates at 48h were significantly higher than those observed at 24h ($p<0.001$). The addition of hydroxyurea was able to maintain replication levels as low as those observed in cultured, quiescent cells (390±143) only when added at the higher concentration of 1mM and when the cells were activated for no longer than 24h (318±112, $p>0.5$).

Cell counts results, expressed as population doublings±SEM, showed that, apart from cells cultured in the presence of activating agents for 24h (1.13±0.17, PDs) and 48h (1.34±0.5, PDs), that had higher cell numbers than controls (0.8±0.11, at 24h; 0.61±0.12, $p<0.049$) all the other groups, including cells activated with hydroxyurea (0.71±0.09, at 24h; 0.80±0.8, at 48h), had replication rates similar to controls ($p>0.5$) and appeared to be in a growth arrest state.

Cytotoxicity experiments showed that, after replating the percentages of cells in G0/G1, found in cells that had been previously activated in the presence of hydroxyurea, decreased from 97.7% to 77.9%, and the percentages of cells in S-phase and G2/M-phase increased from 0.5% to 13.7% and from 1.8% to 8.4%. This cells cycle profile was similar to that observed, after replating, in cells, that had been previously activated for 24h, without hydroxyurea, and to that of cells that had been continuously activated for 48h (Table 4.2). The percentages of $CD25^+$ cells remained at high levels (78.3%), comparable to the maximal levels found in cells that had been activated for 24h (81.3%). The levels of mean fluorescence were slightly lower than those observed in cells activated for 48h, but higher than the levels reached after activation for 24h.

Rates of [^{3}H]thymidine incorporation in cells rescued from the hydroxyurea block (153164cpm, for 1mM HU; 180323cpm, for 0.5mM HU) were comparable to

those of cells that had been activated for 24h, before being replated and activated for other 24h (166276cpm). These rates were also higher than those observed in cells that had been activated for 24h (38875) or 48h (113863).

Results of cell counts showed that cells that had been activated for 24h in the presence of 0.5mM or 1mM HU and then replated and activated for additional 24h had higher population doublings (1.38-1.48 PDs) than cells in the control groups, that had been cultured for 24h,in medium with (0.62-0.84 PDs) or without (0.73 PDs) hydroxyurea, before they were replated. These population doublings were also higher than those observed in cells that had been activated for 24h (1.08) or 48h (0.97).

4.4.5 Discussion

Due to the fragility of mouse lymphocytes in culture, selection of treatment conditions with minimal effects on apoptosis is crucial. Culture increased apoptosis, in a marginal way at 24h, and dramatically, at 48h. Activation did not increase apoptosis at 24h, but increased death rates at 48h, although this might have been a result of the culture effect.

Blocking agents, in the absence of activating agents, did not increase apoptosis, at both concentrations, compared to culture controls. Higher death rates were observed at 48h, in the presence of blocking agents, especially at higher concentrations, however this was a result of culture: increases in death rates had been observed also in absence of blocking agents; death rates observed at 48h, with or without blocking agents, were the same. Activation in the presence of blocking agents had a marginal effect at 24h, when the highest concentration of hydroxyurea was used. This concentration might have been detrimental also at 48h, but it was masked by the culture effect.

Taking all these considerations into account, the most successful treatment to reduce apoptosis of mouse T-cells would be to activate them with hydroxyurea for no longer than 24h.

Culture for 24h did not alter the quiescent state of cells. However culture for 48h, in medium alone, decreased the percentage of G0/G1 and increased the percentage of G2/M cells. The former effect had not been observed in previous experiments (Paragraph 4.2-4.3). This difference may have resulted from the fact that

in previous experiments cell cycle analysis had been restricted to T-lymphocytes. Analysis carried out on T-lymphocytes ($CD3^+$/live, gate), confirmed this suggestion: no difference was observed in the percentages of G0/G1 cells observed in $CD3^+$ cells cultured for 24h or 48h in medium alone (M, $p0.1<p<0.05$). However, the percentages of G0/G1, at 48h, were higher than those found in freshly isolated, quiescent cells ($p<0.01$), whereas they remained similar, at 24h ($p=0.2$).

Activation for 24h and 48h reduced the percentage of G0/G1 cells. The effect observed at 48h was stronger, but might have been a result of the culture effect.

Analysis of the effects of activation and blocking agents on the percentages of G0/G1 cells showed that hydroxyurea, at whatever concentration, was able to maintain high levels of diploid cells during activation, under all experimental conditions. The only difference observed was that, at 48h, the percentages of diploid cells were not as high as those found in freshly isolated cells. However, this might have been a result of the culture effect, more intense at 48h than at 24h (M at 48h vs M at 24h, $p<0.001$), on which hydroxyurea had no effect (24h M vs 48h M+B1 or B2, $0.01<p<0.001$; 48h M vs 48h M+B1 or B2, $0.1<p<0.5$; 48h M vs 24h M, $p<0.001$).

Activation increased the percentages of replicating cells. This effect was more accentuated at 48h than at 24h. Hydroxyurea was more effective in containing increases in the percentages of replicating cells in cells activated for 24h. At 48h hydroxyurea was less effective, although percentages always remained quite low (3.5%-2.7%).

Activation increased the percentages of G2/M cells, both at 24h and 48h. Activation for 24h or 48h in the presence of hydroxyurea, maintained the percentages of G2/M cells at acceptable levels, since percentages never rose above 3.9%, even if the levels found in cultured or freshly isolated quiescent cells were even lower.

Increases in the percentages of $CD25^+$ cells and in CD25 mean fluorescence were observed only as a result of activation, and not of culture, confirming that CD25 expression cannot be triggered by aspecific stimuli, but only as part of the T-cell activation pathway. Maximal percentages of $CD25^+$ cells were found in cells activated for 24h, both in the presence or absence of hydroxyurea, since addition of

blocking agents did not interfere with the activation status of T-cells. The situation after activation for 48h was less favourable since the percentages of $CD25^+$ cells, in the absence of hydroxyurea were lower than those found at 24h, and became even lower after addition of hydroxyurea. This may have been the result of higher rates of apoptosis observed in cells activated for 48h (24.7±5.1%), especially in the presence of 0.5mM (39.8±2.6%) and 1mM (35.6±1.0%) HU.

Activation increased dramatically mean fluorescence levels, at 24h and 48h, with a stronger effect observed at the latter time point. Hydroxyurea did not alter the level of mean fluorescence of cells activated for 24h, confirming that it did not interfere with the activation process. Though maximal levels of mean fluorescence were found in cells activated for 48h, after addition of hydroxyurea, these levels remained comparable to those found in cells activated, with or without hydroxyurea, for 24h. However these results might have been affected by the high death rates observed under those experimental conditions

Cytotoxicity experiments confirmed that the effect of hydroxyurea was completely reversible.

4.4.6 Conclusions

Activation in the presence of hydroxyurea represented the best method to produce G1 karyoplasts from T-lymphocytes: the addition of hydroxyurea during activation blocked the undesired cell cycle effects of activation, keeping the percentages of G0/G1 cells at high levels and inducing replicative arrest, but without interfering with the activation state of T-cells (Table 4.2).

Activation with HU for 24h and 48h produced G1 cells with similar cell cycle profiles: the percentages of G0/G1 cells were equally high at 24h (95%) and at 48h (94%); the percentages of cells in S-phase and G2/M-phase were low at 24h and at 48h, though the percentages of cells in S-phase were significantly lower at 24h (0.8% vs 2.7-3.5%) and the percentages of cells in G2/M were significantly lower at 48h (3.8-3.9% vs 2.9-3.3%). However when using [^{3}H]thymidine incorporation to assess replication rates, effective growth arrest was observed only when cells were activated for 24h in the presence of 1mM HU.

Table 4.2 Summary of synchronization in G1 by hydroxyurea

	Cycling (24h)	G1 (24h)	G0 (24h)
Apoptosis	3.1±0.3 [a]	15.4±0.3 [c]	0.4±0.1 [d]
[^{3}H]-Tdr (SI)	47.76±8.76 [a]	0.93±0.05 [c]	1±0 [c]
G0/G1	87.8±1.7 [a]	95.3±1.0 [c]	96.8±0.4 [c]
S	6.9±0.4 [a]	0.8±0.3 [c]	1.0±0.4 [c]
G2/M	5.4±1.4 [a]	3.9±0.9 [c*]	2.1±0.1 [c]
CD25$^+$	73.3±6.0 [a]	71.6±6.0 [a]	5.4±0.3 [d]
Fluorescence	322±39 [a]	302±75 [a]	116±16 [d]

Results from three replicates are expressed as mean percentages±SEM, except for Fluorescence, where data are expressed as mean fluorescence intensity (Mean FL2-H) ±SEM and [^{3}H]-Thymidine incorporation, where data are expressed as mean stimulation index (SI) ± SEM, obtained by dividing counts per minute (cpm) found in treatment groups by those found in control group. All data were analysed with a Nested Analysis of Variance and a one-way ANOVA (paragraph 4.4.3). Data in the same row with different superscripts are significantly different ($p<0.05$). Cells with border of same colour contain similar results.

Activation for 24h, even in the presence of HU, was enough to induce high activation levels, in terms of CD25 expression, in the G1 population. This was the result of two factors: 1) T-cells achieved very high levels of activation, already at 24h; 2) the activation state of T-cells was not affected by the presence of hydroxyurea. The effects of activating agents, on the cell cycle, were stronger at 48h than at 24h, since, after activation for 48h, lower percentages of G0/G1 cells, and significantly higher percentages of S and G2/M cells were observed. However, the effects of activating agents on CD25 expression were similar at 24h and 48h. The percentages of $CD25^+$ cells and the levels of expression of CD25/cell were very high at 24h and 48h, though the percentages of $CD25^+$ cells were higher at 24h, and mean fluorescence was significantly higher at 48h. The presence of hydroxyurea did not alter at all the activation state of cells activated for 24h, whereas in cells activated for 48h with HU the percentages of $CD25^+$ cells decreased to levels lower than those obtained at 24h and mean fluorescence decreased to levels comparable to those observed at 24h. The concentration of hydroxyurea did not affect at all the activation state of T-cells, at both time points.

Finally, apoptosis rates were lower at 24h, ranging from 2.9% to 15%, than at 48h where it ranged from 13% to 39.8%. At 48h cell death rates increased as a result of culture (13.0%), as a result of activation (24.7%) and as a result of activation in the presence of blocking agents (35.6-39.8%), though blocking agents did not have a significant effect.

The outcome of this experiment (Table 4.2) was that activation for 24h, with 8ug/ml PHA and 4nM IL-2, in the presence of 1mM HU, was identified as the optimal method to produce cells in G1, because, though they had slightly higher apoptosis rates than cells activated for 24h with 0.5mM HU, they were the only ones that had the same thymidine incorporation rates (0.93±0.05, SI) and the same cell cycle profile (95.3±1.0, %G0/G1) as cultured quiescent cells. The cells in this treatment group also had percentages of $CD25^+$ (71.6±6.0%) as high as those found in cells that had been activated for 24h (73.3±6.0%) and even higher than those of cells that had been activated for 48h (56.3±4.7%). These putative G1 cells also had

levels of mean fluorescence (302±75) as high as those of cells activated for 24h (322±39) and of cells activated for 48h with hydroxyurea (330±54), though lower than that of cells that had been activated for 48h without hydroxyurea (600±60). Cells that had been activated for 24h with 0.5mM hydroxyurea, had similar features as cells activated 24h with 1mM HU: a cell cycle profile similar to that of quiescent cells; high percentages of $CD25^+$ cells (72.7±5.9); high levels of mean fluorescence (313±43). Their apoptosis rates were even lower than those of cells activated with 1mM hydroxyurea (3.7% vs 15%), however their main disadvantage was that they had a high stimulation index (1.56±0.20 SI) indicating that hydroxyurea 0.5mM was not enough to contain completely DNA replication, and that higher concentrations of HU were required. Cells activated for 48h with hydroxyurea, cannot be used as G1 cells mainly for three reasons: their extremely high levels of apoptosis, at both concentrations of hydroxyurea (35.6%-39.8%); their low percentages of $CD25^+$ cells (35.5%); their high replication rates 2.56-fold higher than those observed in cultured quiescent cells.

Finally, the cytotoxicity assay showed that T-lymphocytes stimulated with 1mM hydroxyurea, for 24h, were able to resume the cell cycle without any side effects. In conclusion, hydroxyurea did not impair the ability of T-cells to undergo normal DNA replication and cell cycle progression, as clearly demonstrated by their high rates of $[^3H]$thymidine incorporation, even higher than those seen in cells activated for 24h or 48h without HU, and by their cell cycle profile, typical of actively replicating cells.

4.5 PURIFICATION OF G1 CELLS BY POSITIVE SELECTION OF $CD25^+$ CELLS

4.5.1 Aim

It was decided to further purify G1 cells, produced by HU block, expressing CD25 ($G1/CD25^+$). This experiment had two aims: 1) use magnetic activated cell sorting (MACS) to positively select cells expressing CD25; 2) check that the separation procedure did not trigger S-phase progression in T-cells.

4.5.2 Experimental Design

Three experiments were set up to compare three different separation protocols. In each experiment $22x10^6$ cells isolated from the lymph nodes of 8 female CBA/Ca, 6 week old mice, seeded at a concentration of $2x10^6$/well in 24 well plates, for 24h, with 8ug/ml PHA and 1mM hydroxyurea, were harvested, labelled with PE-conjugated rat anti-mouse CD25 antibody (IgG) and separated using three different protocols (for Methods see Paragraph 2.8):

1) Incubation with anti-Rat IgG magnetic microbeads, separation with one positive selection column (MS^+) and elution of $CD25^+$ cells;
2) Incubation with anti-Rat IgG magnetic microbeads and separation with two positive selection columns (MS^+) as follows: separation on a first column and elution of the first fraction of $CD25^+$ cells; separation of the $CD25^+$ cells on a second column and elution of a second fraction of $CD25^+$ cells; The two fractions of $CD25^+$ cells were then pooled together.
3) Incubation with anti-PE magnetic microbeads, separation with one positive selection column (MS^+) and elution of $CD25^+$ cells

The following cell samples from each experiment were counted and processed for FACS analysis:

1) Freshly isolated, G0 cells;
2) Activated cells, cultured with 8ug/ml PHA and 4nM IL-2;
3) Total G1 cells, cultured with 8ug/ml PHA, 4nM IL-2 and 1mM HU;
4) Total G1 cells, after labelling and before separation;
5) G1/$CD25^+$ cells, after separation;
6) G1/$CD25^-$ cells, after separation.

Samples from each treatment group were stained with CD3-FITC/CD25-R-PE or CD3-FITC/ PI (for Methods see Paragraph 2.9). Gates and parameters acquired were the same as previously described (Paragraph 4.4.2).

4.5.3 Results

All results are summarised in Table 4.3. and Table 4.4.

Table 4.3 Efficiency of positive selection of G1/CD25$^+$ cells obtained with different selection methods

Microbeads/ N columns	Seeded (x10^6)	Harvested /seeded (%)	Processed /harvested (%)	Selected /processed (%)	G1/CD25$^+$ /selected (%)	G1/CD25$^+$ (x10^6)
Anti-Rat-IgG/ 1 column	22	(63.6)	(75.0)	(88.6)	(8.6)	0.80 (3.6)*
Anti-Rat-IgG/ 2 columns	22	(59.1)	(84.6)	(66.7)	(8.2)	0.77 (3.5)*
Anti-PE/ 1 column	22	(47.3)	(75.2)	(72.8)	(52.8)	2.40 (10.9)*

Cells were synchronized in G1, by activation for 24h with 8ug/ml PHA and 4nM IL-2, in the presence of 1mM hydroxyurea. Cells in G1 were labelled with anti-CD25-PE antibody, and G1/CD25$^+$ cells were positively selected using anti-Rat IgG or anti-PE microbeads and one or two positive selection columns. Data, collected in a single experiment, are expressed as cells x10^6 or as percentages.

Table 4.4 Features of G1/CD25$^+$ cells obtained with different selection methods

	CD3$^+$ (%)	CD25$^+$ (%)	Fluorescence	Apoptosis (%)	G0/G1 (%)
Anti-Rat IgG/1 column					
G1/All	94.55	67.26	294	3.77	92.48
G1/CD25$^+$	98.64	96.83	1288	4.56	97.11
G1/CD25$^-$	98.25	78.54	292	3.56	94.03
Anti-Rat IgG/2 columns					
G1/All	91.16	66.59	381	9.63	89.59
G1/CD25$^+$	83.12	93.81	1144	11.5	97.07
G1/CD25$^-$	96.94	54.60	226	5.15	93.53
Anti-PE/1 column					
G1/All	92.14	62.51	428	22.11	95.10
G1/CD25$^+$	98.23	90.20	823	10.5	93.40
G1/CD25$^-$	95.89	61.50	430	8.13	96.28

Analysis of apoptosis rates, proportion of T-cells (CD3$^+$), cell cycle distribution and CD25 expression (% CD25$^+$ cells, mean fluorescence) of cells synchronized in G1 by activation for 24h with 8ug/ml PHA and 4nM IL-2, 1mM hydroxyurea (G1/All), and positively selected using anti-Rat IgG or anti-PE microbeads and one or two positive selection columns (G1/CD25$^+$). Features of cells in the negative fractions were also assessed (G1/CD25$^-$). Data, collected in a single experiment are expressed as percentages or as mean fluorescence intensity (Mean FL2-H).

4.5.4 Discussion

Cell yield decreased as a result of culture, processing and MACS separation (Table 4.3). About 56.7±6.9% of seeded cells were recovered after culture, 78.3±4.5% of harvested cells were recovered after cell processing and 76.0±6.2% of processed cells, including both positive and negative fractions, were recovered after separation on MS^+ columns. Although the separation protocol did not influence the total cell yield, ranging from 66.7% to 88.6%, separation with anti-PE microbeads gave a greater yield of G1/$CD25^+$ cells than separation using anti-Rat IgG microbeads, that was 10.9% of seeded cells ($2.4x10^6/22x10^6$; Table 4.4).

All separation protocols gave G1/$CD25^+$ fractions with high percentages of $CD25^+$ cells and high levels of expression of CD25/cell (Fluorescence), higher than those observed in G1 cells before separation (G1/All; Table 4.4). The only difference was that G1/$CD25^+$ cells, isolated with anti-PE beads, expressed CD25 (Fluorescence) at a slightly lower level than G1/$CD25^+$ cells isolated with anti-Rat beads (Table 4.4). This suggests that anti-PE microbeads had a greater affinity for cells expressing CD25, selecting also T-cells that expressed CD25 at very low levels (i.e. low mean fluorescence). This would also explain the greater yield obtained with the anti-PE beads compared to anti-Rat IgG beads.

4.5.5 Conclusions

A highly pure G1/$CD25^+$ population was isolated, regardless of the separation technique used (Table 4.5). The percentages of $CD25^+$ cells and of diploid cells (2N) found in the G1/$CD25^+$ population were always >90% and >93%. The levels of expression of CD25 (823-1288) were not only higher than those observed in G0 cells (137) but also higher than those observed in total G1 cells (294-428), suggesting that only cells expressing a certain amount of CD25 on their surface were positively selected. The G1/$CD25^+$ fraction also represented an almost pure population of T-lymphocytes (>90% $CD3^+$ cells). Rates of apoptosis remained low and ranging between 4.56% and 11.50% of total cells.

Although the cell cycle features (Table 4.4) of positively selected G1/$CD25^+$ cells were similar, regardless of the separation method used, the yield was different (Table

Table 4.5 Summary of synchronization in G1 by hydroxyurea block and selection of $CD25^+$ cells

Parameter	G0 (24h)	G1 (24h)	*G1/$CD25^+$ (24h)	Cycling (24h)
Apoptosis	11.4±2.3	11.8±9.4	10.5	12.4±7.2
$CD3^+$	83.5±7.2	92.6±1.7	98.2	89.2±4.2
G0/G1	95.2±1.9	92.4±2.8	93.4	81.2±3.4
$CD25^+$	11.8±3.5	65.5±2.6	90.2	63.9±10.3
Fluorescence	121±39	368±69	823	447±96

Cells isolated from the lymph nodes were cultured for 24h in: 10% FCS culture medium (G0); 10% FCS culture medium with 8ug/ml PHA and 4nM IL-2 (Cycling); activated in the presence of 1mM hydroxyurea (G1); synchronized in G1 and then purified by $CD25^+$ cell selection with anti-PE microbeads and one positive selection column. Data from three experiments are expressed as Mean±SEM. Some data (*) were obtained from a single experiment. Parameters include: percentages of $CD3^+$ cells (T-cells); percentages of diploid cells (G0/G1); percentages of $CD25^+$ cells and CD25 mean fluorescence (CD25 expression/cell).

4.3). Separation with anti-PE beads gave a greater yield of $CD25^+$ cells compared to anti-Rat IgG beads, considered both as total cell numbers ($2.4x10^6$ vs $0.8x10^6$) and as percentage of seeded cells (10.9% vs 3.5-3.6%). Anti-PE beads were selected for future experiments, because they gave a G1/$CD25^+$ population of similar purity than anti-Rat IgG microbeads, but with greater efficiency.

CHAPTER 5

T-LYMPHOCYTES AS A SOURCE OF G0 KARYOPLASTS

5.1 INTRODUCTION

During differentiation epigenetic changes of the genome restrict the potential for gene expression, in a cell type specific manner. During reprogramming the cell type specific epigenetic patterns established during differentiation must be erased in order for the genome to acquire totipotency. Recent evidence suggests that low nuclear transfer efficiency might result from incomplete or incorrect removal of these epigenetic patterns during reprogramming (Kang *et al.*, 2001; Humpherys *et al.*, 2001; Inoue *et al.*, 2002). Quiescence greatly affects the epigenetic status of chromatin with possible consequences on the reprogramming process.

Up to now only abnormal DNA methylation patterns have been studied in cloned embryos foetuses and placentas. Cloned pre-implantation cattle embryos displayed insufficient (Kang *et al.*, 2001) and ectopic demethylation of genomic DNA, with most of the abnormalities localised in the trophectoderm (Kang *et al.*, 2002). Mice cloned using ES cells and their placentas had significantly higher weights than controls and abnormal levels of expression of imprinted genes, mostly lower than controls (H19, Peg1/Mest, Meg1/Grb10; Humpherys *et al.*, 2001). Abnormal patterns of expression of parental imprinted genes (Igf2, H19) were observed in placentas from cloned pups (Humpherys *et al.*, 2001). Foetuses cloned using Sertoli and cumulus somatic cells, retained normal weights and had normal patterns and levels of expression of imprinted genes (Inoue *et al.*, 2002). However, their placentas where abnormally enlarged and, though retaining normal patterns of expression of imprinted genes, foetal tissues had lower levels of expression of some imprinted (Peg1/Mest, Meg1/Grb10, Meg3/Gtl2) and non-imprinted genes (Igfbp2, Igfbp6, Vegfr2/Flk1, Esx1) compared to controls (Inoue *et al.*, 2002).

There is contradictory evidence whether quiescence might affect methylation patterns of gene expression. Serum-starved human normal fibroblasts (NHF) had significantly higher levels of methylation (50% vs 0-15%) of CpG in the O-6-methylguanine-DNA methyltransferase (MGTMT) gene than non-quiescent cells (Pieper *et al.*, 1999). Furthermore, serum starvation and contact inhibition, conditions known to induce cell quiescence in somatic cells, resulted in reduced methylation levels and increased transcription levels of the imprinted genes H19 and Igf2, in ES cells (Baqir and Smith, 2000). However, other evidence in cattle suggests that there is no difference in the overall methylation level of genomic DNA of serum-starved and cycling foetal fibroblasts (50-100% CpG methylated in the Bov-B gene; Kang *et al.*, 2001).

This chapter focused on investigating other epigenetic changes, that play an important role in the regulation of gene expression both during development and quiescence, that have not been investigated yet in relation to nuclear transfer: chromatin remodelling and acetylation.

Nuclear chromatin condensation and spatial organisation changes during the cell cycle (Juan and Darzynkiewicz, 1998; Bridger *et al.*, 2000). Chromatin appears to be very condensed during mitosis whereas it is maximally decondensed at the time of entrance in S-phase. Chromatin of G0 cells presents a high level of condensation, even if not as high as cells in M-phase. Quiescence-related changes in chromatin condensation are particularly dramatic in T-cells, the cell model of choice of these experiments, as demonstrated directly by Acridine Orange staining and indirectly by changes in T-cell nuclear size and composition. Changes in chromatin condensation correlate with changes in DNA *in situ* sensitivity to denaturation and have been detected in T-cells using Acridine Orange (AO), a metachromatic fluorochrome, which differentially stains in green non-denatured (double-stranded) DNA, with a higher level of condensation, and in red denatured (single stranded) DNA, with a lower level of condensation (Juan and Darzynkiewicz, 1998). This assay has shown that quiescent T-cells have significantly higher levels of red fluorescence, associated with decondensed chromatin, and significantly higher levels of green fluorescence, associated with condensed chromatin than activated T-cells (Juan and Darzynkiewicz, 1998).

These differences in chromatin condensation associate with changes in the transcriptional activity, as detected under the same experimental conditions using a modified AO staining and flow cytometry. Under different experimental conditions AO can be used to distinguish G0 and G1 cells based on their RNA content. Total RNA content is largely composed of ribosomal RNA, and is therefore an estimate of ribosome synthesis and ultimately of protein synthesis. At appropriate concentrations and stringent ionic conditions AO intercalation into double stranded DNA results in green fluorescence, whereas it results in red fluorescence when it intercalates to single stranded RNA (Juan and Darzynkiewicz, 1998).

Quiescent lymphocytes, upon activation, also undergo dramatic changes in their nuclear size and morphology, also associated with changes in the rate of DNA replication and/or transcription. Two separate studies clearly show the correlation existing between state of activation and nuclear size (Setterfield *et al.,* 1983) and state of activation and chromatin conformation (Pompidou *et al.*, 1984). In these two studies human peripheral blood lymphocytes (99% T-cells, <1% monocytes, <1% B-cells) were stimulated with Concanavalin A (Con A) or phytohemagglutinin (5ug/ml) over a chase period of 48h-72h. Nuclear volume (Setterfield *et al.,* 1983) was measured, whereas chromatin condensation (Pompidou *et al.,* 1984) was evaluated using nuclear refringency (image intensity analysis: quantifies the shift in chromatin condensation in the cell population) and electron microscopy (semi-quantitative ultrastructural analysis: percentage of cells with condensed or decondensed chromatin). These studies identified three nuclear morphotypes on the basis of activation state, nuclear size and chromatin conformation: I) unstimulated (resting T-cells); II) partially activated (competent T-cells); III) fully activated (lymphoblastic cells) nuclei. Resting cells (morphotype I) have a small nucleus that constitutes nearly all the cell volume. Semi-quantitative ultrastructural analysis >60% G0 cells display a condensed chromatin conformation characterised by dense masses (compact chromatin bodies), that in rat have been shown to correspond to a haploid number of chromosomes (Lopez-Velazquez *et al.,* 1996). Most bodies are localised at the periphery, in contact with the nuclear envelope. The largest body always contains the nucleolus-associated chromatin and is positioned around the nucleolus. There is a certain level of variability in the distribution pattern of compact chromatin

bodies among G0 lymphocytes, but interestingly lymphocytes may share identical distribution patterns with different cell types of individuals of the same species (Lopez-Velazquez *et al.,* 1996). Resting lymphocytes usually have one, large nucleolus displaying a ring-like figure (Pompidou *et al.,* 1984).

Upon T-lymphocyte activation cellular and nuclear size increase dramatically and chromatin becomes gradually dispersed (Setterfield *et al.*, 1983). During early activation (<24h, morphotype II) the nucleus starts enlarging, reaching a 6-fold increase by the late activation stage (24h-72h, morphotype III). The increase in nuclear volume mainly results from a 10-fold increase in the volume of the proteinaceous intechromatinic region, and, to a lesser extent, from the 1.5-fold increase in volume and spatial dispersion of chromatin (Setterfield *et al.*, 1983). Cycloheximide and alpha-amanitin block nuclear structural and functional activation by preventing matrix expansion showing the strict association existing between these events. During early activation (morphotype II), within 30 min of mitogenic stimulation, chromatin partially and transiently disperses, as chromatin bodies begin to disaggregate. This event is marked by a 6.7% reduction in nuclear refringency index (NRI) and 16% cells condensed. Within 60 min this situation is reversed: NRI goes back to control levels, and by the acquisition by >60% of the cells of a condensed chromatin structure. During late activation (morphotype III) complete and prolonged chromatin decondensation takes place, marked by a 11% reduction in NRI with 15% of the cells displaying a condensed chromatin structure, and a 33% reduction in NRI with 7% of the cells displaying a condensed chromatin structure by 48h (Setterfield *et al.*, 1983).

Early nuclear structural activation events are temporarily coupled with transcriptional activation but not DNA replication events (Setterfield *et al.*, 1983). The appearance of morphotype II is associated with a 55% increase in [^{3}H]uridine incorporation. Late nuclear structural activation events are temporarily coupled with initiation of DNA replication. The appearance of morphotype III is associated with a 7-13-fold increase in [^{3}H]thymidine incorporation. Pre-treatment with 1ug/ml actinomycinD (actD), which binds DNA preventing transcription, blocks chromatin dispersion. These data support the association between chromatin conformation and DNA transcription and/or replication, without proving any causal-effect relationship.

The mechanisms behind cell cycle regulated chromatin changes are largely unknown. However there is some evidence that non-histone proteins might mediate heterochromatin repression during quiescence. Proteins belonging to the Polycomb group (e.g. BMI1) and zinc finger proteins (e.g. Ikaros, Eos, Pegasus, Ailos), mainly expressed in T-lymphocytes, are cell cycle regulated (Voncken *et al.*, 1999; Avitahl *et al.*, 1999; Georgopoulos, 2002). Furthermore, quiescent cells also contain larger amounts of histone H1° instead of histone H1. The reprogramming factor nucleoplasmin has a greater affinity for histone H1° and this might also represent an advantage for reprogramming (Kikyo and Wolffe, 2000). Histone post-translational modifications, such as histone H4 acetylation (Pogo *et al.*, 1966) and histone H3 phosphorylation (Patskan and Baxter, 1985) are also associated with exit of T-cells from quiescence.

Chromatin conformation is one of the regulatory mechanisms involved in the restriction of genomic potential during differentiation (Leitch, 2000). These epigenetic restrictions have to be removed to re-establish totipotency. Experiments carried out in *Xenopus* showed that chromatin remodelling complexes play an important role in reprogramming the patterns of gene repression of somatic nuclei after transfer to recipient oocytes (Dimitrov and Wolffe, 1996; Kikyo and Wolffe, 2000; Kikyo *et al.*, 2000). The reprogramming process involves the appearance of a more open and transcriptionally active chromatin structure mediated by the activity of remodelling complexes and by the removal of repressive chromatin structures established during differentiation. Particularly important seems to be the activity of complexes that create a more open and transcriptionally active chromatin structure, such as the complexes of the SNF/SWI family containing the ATP-ase ISWI, often coupled to acetyltransferases. On the contrary, complexes inducing closed chromatin structure, deacetylation and CpG-methylation (e.g. MeCP2/Rdb3/Sin3) do not seem to be involved in the reprogramming process (Kikyo and Wolffe, 2000). Removal of proteins that accumulate during differentiation is also important for the reprogramming of cloned embryos. Histone H1 is removed during reprogramming (Bordignon *et al.*, 1999; 2001). However removal of other proteins, associated with differentiation, may also be important. These include the Polycomb-group (Pc-G) of proteins (Kikyo and Wolffe, 2000), that sustain developmentally regulated

expression (e.g. homeotic genes, *Drosophila*; Hox gene clusters, mammals) and the zinc-finger proteins (e.g. Ikaros, Eos, Pegasus, Ailos) that mediate lineage commitment and differentiation of haematopoietic stem cells into lymphocytes (Georgopoulos, 2002).

Post-translational modifications of histones, which are affected by quiescence, also contribute to the restriction of gene expression during embryo development and differentiation, and might play an important role in nuclear reprogramming. In particular, dramatic changes in the acetylation status of histone H4 (Adenot *et al.,* 1997; Worrad *et al.,* 1995), at lysines 5, 8, and 12 (H4.Ac5; H4.Ac8; H4.Ac12), histone H3 (Stein *et al.,* 1997), at lysines 9 and/or 18 (H3.Ac9/18) and histone H2A (H4.Ac5), take place in the mouse embryo around the time of zygotic gene activation and during differentiation (Ma *et al.,* 2001; Wiekowski *et al.,* 1997). These changes have been mapped in detail in mouse and will be described in detail in the next chapter. However acetylation patterns have yet to be described in cloned embryos.

Experiments in this chapter focused on the effects of quiescence on the expression and sub-nuclear localisation of proteins belonging to the heterochromatin protein 1 (HP1) group, and on the acetylation status of histone H4. HP1 proteins were selected because they belong to the same family as the Pc-G proteins (Jones *et al.,* 2000), which are both cell cycle regulated (Voncken *et al.,* 1999) and developmentally regulated. The regulation of HP1 proteins in relation to quiescence and embryo development is still unknown and so is its possible involvement in nuclear reprogramming. A single form of HP1 was first isolated in *Drosophila melanogaster* (James and Elgin, 1986). However screening with CD probes has revealed multiple variants in higher eukaryotes (Singh *et al.,* 1991). Mammalian HP1 comprises three distinct isotypes termed hHP1α, hHP1β, hHP1γ in humans and mHP1α, M31, M32 in mice. The different isotypes are structurally very similar but are distributed in different regions of the nucleus (Jones *et al.,* 2000). Descriptive studies using specific antibodies showed that HP1α and HP1β are predominantly found in pericentromeric constitutive heterochromatin, suggesting they might play a role in centromere function as previously described in HP1-like proteins in fission yeast and *Drosophila.* On the contrary, HP1γ is distributed in a fine-grain pattern

throughout the nucleoplasm, which suggested its possible association with heterochromatin complexes within euchromatin and its exclusion from constitutive heterochromatin. The effect of T-cell quiescence on histone H4 acetylation has partially been investigated (Pogo, 1966; Knosp *et al.*, 1991). However the aim, of the experiments in this chapter was to use specific antibodies, developed to investigate changes in histone H4 acetylation during early embryo development, in mouse (Worrad *et al.,* 1995), to correlate specific changes in acetylation induced by cell quiescence with changes observed during reprogramming, after nuclear transfer.

Changes observed in HP1 proteins and histone H4 acetylation, were also correlated with specific activation markers.

Markers of T-cell activation included:

1) *CD25 or IL-2Rα,* negative marker of quiescence, that is not expressed in G0 T-lymphocytes but is expressed upon activation (see Chapter 4; Soldaini *et al.*, 1995);

2) *Proliferating cell nuclear antigen (PCNA),* negative marker of quiescence, that is maximally expressed during the S–phase of the cell cycle and has been described in activated T-cells (Kurki *et al.,* 1987);

3) *Cyclin D3,* negative marker of quiescence, that is not expressed in G0 T-lymphocytes but it is up regulated after activation as shown using Western-blots (Ajchenbaum *et al.,* 1993);

4) $p27^{KIP1}$, that is down regulated as G0 T-lymphocytes become activated (Polyak *et al.,* 1994b). The protein $p27^{KIP1}$ is also over expressed in serum-starved mouse fibroblasts (Rivard *et al.,* 1996; Chapter 3). This protein is the only known positive marker of cell quiescence in T-lymphocytes, since p130, of the retinoblastoma family, is only found in serum-starved mouse fibroblasts (Coats *et al.,* 1999; Paragraph 1.4.1).

5.2 EFFECT OF QUIESCENCE ON CHROMATIN CONFORMATION

5.2.1 Aims

Use specific antibodies to describe qualitative (sub-nuclear localisation) and quantitative (levels of expression) differences in mouse HP1 proteins (mHP1α, M31, M32) between quiescent and non-quiescent cells. Correlate changes observed in chromatin conformation during activation with specific activation markers: $p27^{KIP1}$, CD25, PCNA and cyclin D3.

5.2.2 Experimental design

Experiments were carried out in three replicates, unless stated otherwise For each replicate T-cells were isolated from the lymph nodes of eight, six week old, female mice of the inbred strain C57BL/6, pooled together and counted (6.7±0.4 $x10^6$ cells/animal; 73.4±12.4% $CD3^+$ cells). A total of 21-30$x10^6$ cells were used in each experiment, of which 5-8$x10^6$ cells were used fresh (fresh G0 cells), and 16-22 $x10^6$ were cultured in 24 well plates, at a concentration of 2$x10^6$/well. Three treatment conditions were considered:

1) Fresh quiescent cells (G0 fresh);
2) Quiescent cells, cultured for 24h in 10% FCS medium (A.2.1; G0 cultured) cells;
3) Cells activated for 24h with 10% FCS medium, supplemented with 8ug/ml PHA (A.2.3) and 4nM IL-2 (A.2.4; Cycling).

Cells from each treatment group were assigned to different staining groups (Table 5.1) and processed for FACS analysis (Paragraph 2.9 and 2.10.2) or for immunocytochemistry (Paragraph 2.11). Number of replicates varied among staining conditions (Table 5.2). In cells processed for mHP1α/DAPI, M31/DAPI, M32/DAPI parameters defining morphological and total fluorescence features were acquired (Paragraph 5.12). Parameters defining features of clusters of fluorescence were also acquired for M31/DAPI staining, since this protein colocalises with pericentromeric

Table 5.1 Experimental design for chromatin experiments: staining/treatment group

Experiment	Analysis	Staining	G0 (fresh)	G0 (cultured)	Cycling
Activation markers	FACS	$CD25^+$, PI	X	X	X
	FACS	$p27^{KIP1}$/PI	X	-	X
	IF	PCNA/DAPI	X	X	X
	IF	D3/DAPI	X	-	X
Chromatin markers	IF	mHP1-α/DAPI	X	-	X
	IF	M31/DAPI	X	X	X
	IF	M32/DAPI	X	-	X
Chromatin/Activation	IF	M31/PCNA/DAPI	X	-	X
	FACS/IF	M31/CD25/DAPI	X	X	X

Table 5.2 Experimental design for chromatin experiments: staining/replicate

Experiment	Analysis	Staining	Replicate			
			1	2	3	4
Activation markers	FACS	$CD25^+$, PI	X	X	X	-
	FACS	$p27^{KIP1}$/PI	X	-	-	-
	IF	PCNA/DAPI	X	X	X	-
	IF	D3/DAPI	X	-	-	-
Chromatin markers	IF	mHP1-α/DAPI	X	X(?)	X	X(?)
	IF	M31/DAPI	X	X	X	X
	IF	M32/DAPI	X	X(?)	X	X(?)
Chromatin/Activation	IF	M31/PCNA/DAPI	-	-	X	-
	FACS/IF	M31/CD25/DAPI	-	-	X	-

Table 5.1 Cells were assigned to three treatment groups: freshly, isolated, quiescent cells (G0 fresh); quiescent cells cultured for 24h in 10% FCS medium (G0 cultured); cells activated for 24h with 8ug/ml PHA and 4nM IL-2 (Cycling). In some cases only one quiescent group was included in the analysis.

Table 5.2 Staining were performed in 1-4 experiments. In some replicates gave inconsistent results (?), and were excluded from the analysis.

heterochromatin, and concentrates into clusters. The mHP1α protein should also be organised in clusters, similarly to what observed for M31 (Kourmouli *et al.*, 2000). However, in these experiments mHP1α clusters were not as clear as the ones observed with M31 staining, maybe due to a background problem. M32 associates with non-constitutive heterochromatin and is evenly distributed throughout the nucleus, in a fine grain distribution (for review on HP1 proteins see Paragraph 5.1).

When analysing both total nuclear fluorescence and clusters of fluorescence, mean fluorescence and peak fluorescence were used as positive markers of chromatin condensation and SD of mean fluorescence was used as a negative marker of chromatin condensation. Fluorescence intensity was considered a measure of the level of expression of HP1 proteins. The area of fluorescence was a measure of the level of expression and the level of condensation of HP1 proteins. The number of clusters was used as measure of the tendency of M31 to concentrate in the pericentromeric regions. Cluster numbers ≤1 indicated a dispersed nuclear distribution.

The results of the M31 staining obtained in three replicates, were always very consistent. On the contrary staining for M32 and mHP1α appeared to be less consistent, and in one replicate, no data were collected. When repeated for a fourth time M31 gave results consistent with previous experiments whereas M32 and mHP1α still gave inconsistent results for inexplicable reasons. As a consequence of this results from M31 were collected in four replicates and results from M32 and mHP1α staining, could be collected only in two replicates.

In the first replicate different markers of T-cell activation were tested, trying to identify markers which gave us the clearest result and could be used in following experiments in combination with the chromatin staining.

Staining for activation markers were performed as follows:

1) Staining for CD25 and Propidium Iodide (PI; for Methods see Paragraph 2.9), for FACS analysis;
2) Double staining for $p27^{KIP1}$/PI (Methods Paragraph 2.9), for FACS analysis;
3) Double staining for cyclin D3/DAPI (for Methods see Paragraph 2.11), for immunocytochemistry;

4) Double staining PCNA/DAPI (Methods Paragraph 2.11), for immunocytochemistry.

CD25-R-PE and PI staining were performed only on live cells, using gates (live gate; Paragraph 2.10.2) and parameters as in previous experiments (see Paragraph 4.4).

For $p27^{KIP1}$/PI double staining parameters acquired included:

1) Percentages of $p27^+$ cells, calculated in the whole population of live cells (live gate; Paragraph 2.10.2);
2) Percentages of $p27^+$ cells, calculated only in diploid cells (G0/G1 cells gate; see Paragraph 2.10.2).

Double staining with PI made it possible to calculate the percentages of diploid, quiescent ($p27^+$) cells (G0) and diploid, non-quiescent ($p27^-$) cells (G1).

For cyclin D3 and PCNA (Methods see Paragraph 2.11), analysis was performed using parameters and gates described elsewhere (Paragraph 2.12).

Only the activation markers that gave us the best results in the first replicate would be used in the following two replicates as activation controls and would be correlated with the chromatin changes observed during activation.

In the last replicate, the two activation markers selected in previous experiments were correlated with changes observed in the M31 staining. In view of the inconsistency of earlier results, M32 and mHP1α were not correlated with activation markers.

Staining included (for Methods see Paragraph 2.11):

- M31-FITC/PCNA-TXR/DAPI
- M31-FITC/CD25-PE/DAPI

For each staining, three images and a total of 40 cells were acquired from two slides. Analysis was carried out using the parameters and gates described elsewhere (Paragraph 2.12).

5.2.3 Statistical analysis

All data were transformed using a log transformation (mean fluorescence, peak, integral intensity), except data expressed as percentages, which were transformed using a Logit transformation. Choice between non-transformed and transformed data was made by comparing the normality of their distributions using residual fit plots (GenStat 4.21, Windows 2000). Treatment groups were compared using Student-t test for independent samples (Statistica 4.5, Windows 1995). A Chi-square test was used to compare proportion of cells expressing $p27^{KIP1}$.

5.2.4 Results

Morphological features T-cells changed dramatically according to their activation state (Fig.5.1). Quiescent cells, either fresh or cultured, were significantly smaller than cycling cells, activated for 48h. Since most of the cell area of T-cells is occupied by the nucleus, changes in cell size mainly reflected changes in the size of the nucleus. The percentage of cell area occupied by the nucleus was very high in all groups, ranging from 70.8%, in activated cells, to 81.4% and 82.8%, respectively in cultured and freshly isolated, quiescent cells. Similarly cell: nuclear ratios were very low ranging from 1.23 an 1.26, respectively in fresh and cultured quiescent cells, to 1.44 in cycling cells. As a result of this, not only the cell size, but also the nuclear size of quiescent T-cells, either fresh or cultured, was significantly smaller than that of cycling cells. Culture of T-cells in the absence of mitogens also increased their cell size and nuclear size, however this increase was of a significantly lower magnitude than that triggered by mitogenic activation. Finally, although the increase in cell size induced by T-cell activation was associated with a significant increase in nuclear size, it was also the result of an increase in cytoplasm volume, as shown by the increase in the cell: nuclear ratio (1.44) significantly higher than that of quiescent cells (1.23-1.26). This might have resulted from the increase in cytoplasmic (protein synthesis) as well as nuclear activities (replication/transcription) associated with T-cell activation.

Figure 5.1 Cell morphology of quiescent (G0) and cycling lymphocytes

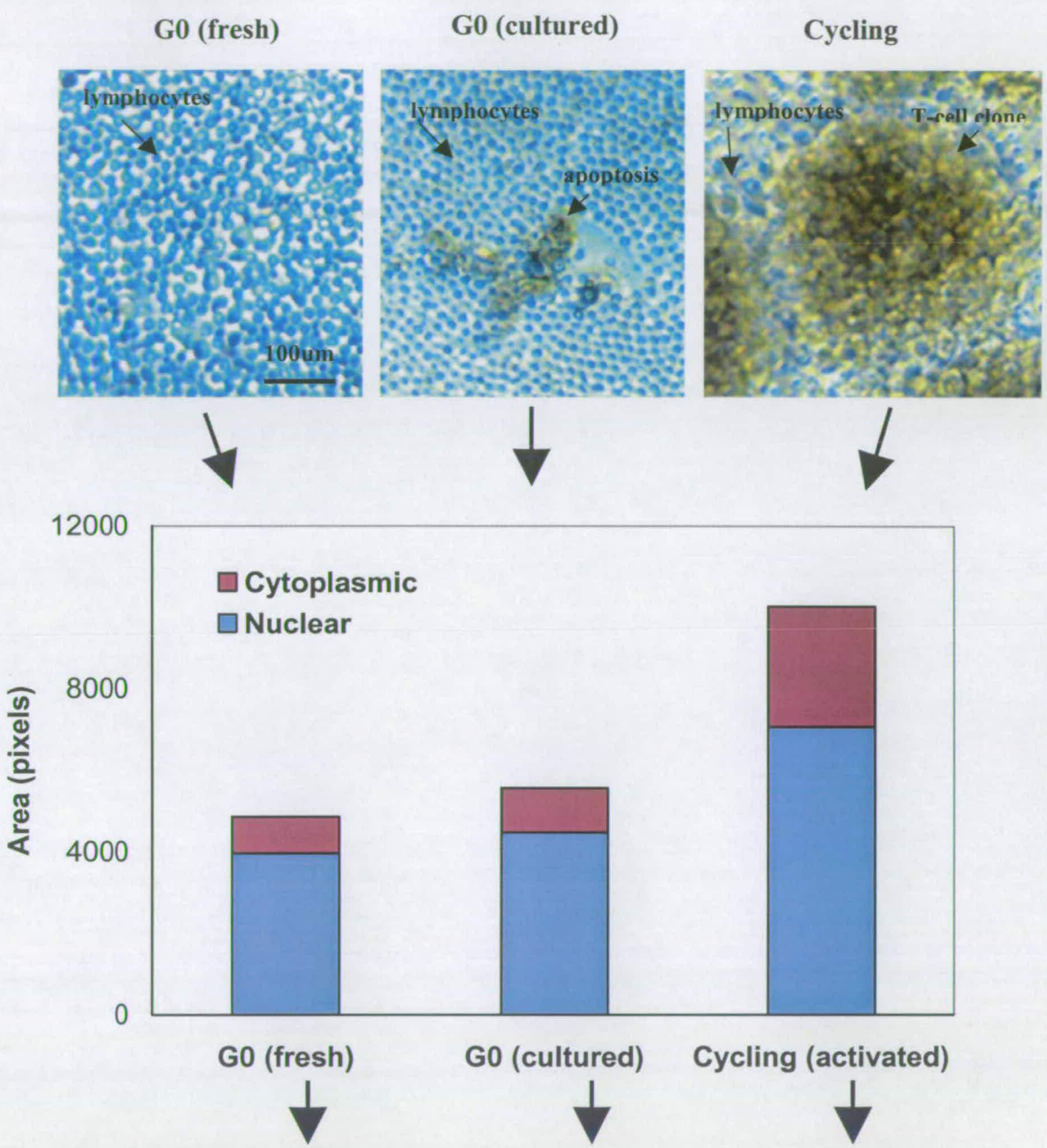

Nuclear area (%)	82.8±1.6[a]	81.4±1.8[a]	70.8±1.4[b]
Cell/Nucleus	1.23±0.03[a]	1.26±0.03[a]	1.44±0.03[b]
Nuclear area	3962±55[a]	4472±100[b]	7054±280[c]
Cell area	4864±75[a]	5565±143[b]	10022±386[c]

Brightfield images comparing freshly isolated T-cells (G0 fresh), quiescent T-cells that had been cultured for 48h in 10% FCS medium (G0 cultured), and T-cells that had been activated for 48h with 8ug/ml PHA and 4nM IL-2 (Cycling). Data were obtained analysing 40 cells from 3 images collected in three experiments and are expressed as mean±SEM (t-test for independent samples). Data within rows with different superscripts differ significantly ($p<0.05$).

Immunostaining for M31 (Fig.5.2), the mouse homologue of human HP1β, showed that the nucleus of quiescent cells, either cultured or freshly isolated, contained clusters of M31, colocalised with patches of condensed chromatin (DAPI). On the contrary both M31 and the chromatin (DAPI) were dispersed in the nucleus of activated cells. This observation was confirmed by image analysis (for Methods see Paragraph 2.11). Analysis of total nuclear fluorescence showed that quiescent cells had significantly lower fluorescence intensity, therefore less M31 content, than activated cells (Fig. 5.2). This was probably a result of the smaller size of their nucleus (Fig. 5.1). However, M31 appeared to be more concentrated in quiescent cells, as confirmed by their significantly higher values of mean fluorescence, SD and peak fluorescence compared to activated cells (Fig. 5.2). Cultured quiescent cells contained the same quantity of M31 as freshly isolated quiescent cells (Fig.5.2) but in a larger nucleus (Fig. 5.1). This explains why the mean intensity and peak intensity of cultured quiescent cells was intermediate between that of freshly isolated and activated cells and their SD was lower (Fig.5.2). These data suggest that culture in itself might have a marginal effect on chromatin condensation, though not as high as that induced by activation. Cluster analysis confirmed the tendency of chromatin and M31 to condense into clusters in quiescent cells and be dispersed in activated cells (Fig. 5.2). Data showed that quiescent cells contained an average of 3.2-4.0 clusters of M31, whereas activated cells only contained a diffused form of M31 (cluster n° ≤1). The intensity of the fluorescence of clusters of M31 was similar in all groups, but concentrated over a significantly smaller area in quiescent cells (30.3%-34.5%) compared to activated cells (40.9%; Fig.5.2). As a consequence of this M31 clusters found in quiescent cells had a higher mean fluorescence and peak fluorescence compared to activated cells (Fig.5.2). Cultured quiescent cells had a peak cluster intensity intermediate between that of freshly isolated and activated cells and a lower SD, suggesting, once more, a possible effect of culture on chromatin condensation. In conclusion the analysis of the clusters of M31 confirmed what observed when considering total nuclear fluorescence.

The protein mHP1α, mouse homologue of human hHP1α, also appeared to be more concentrated in quiescent cells and dispersed in activated cells (Fig.5.3). In contrast to earlier reports (Kourmouli *et al.*, 2000), mHP1α appeared to be only

Figure 5.2 Chromatin conformation of T-cells: immunostaining for M31

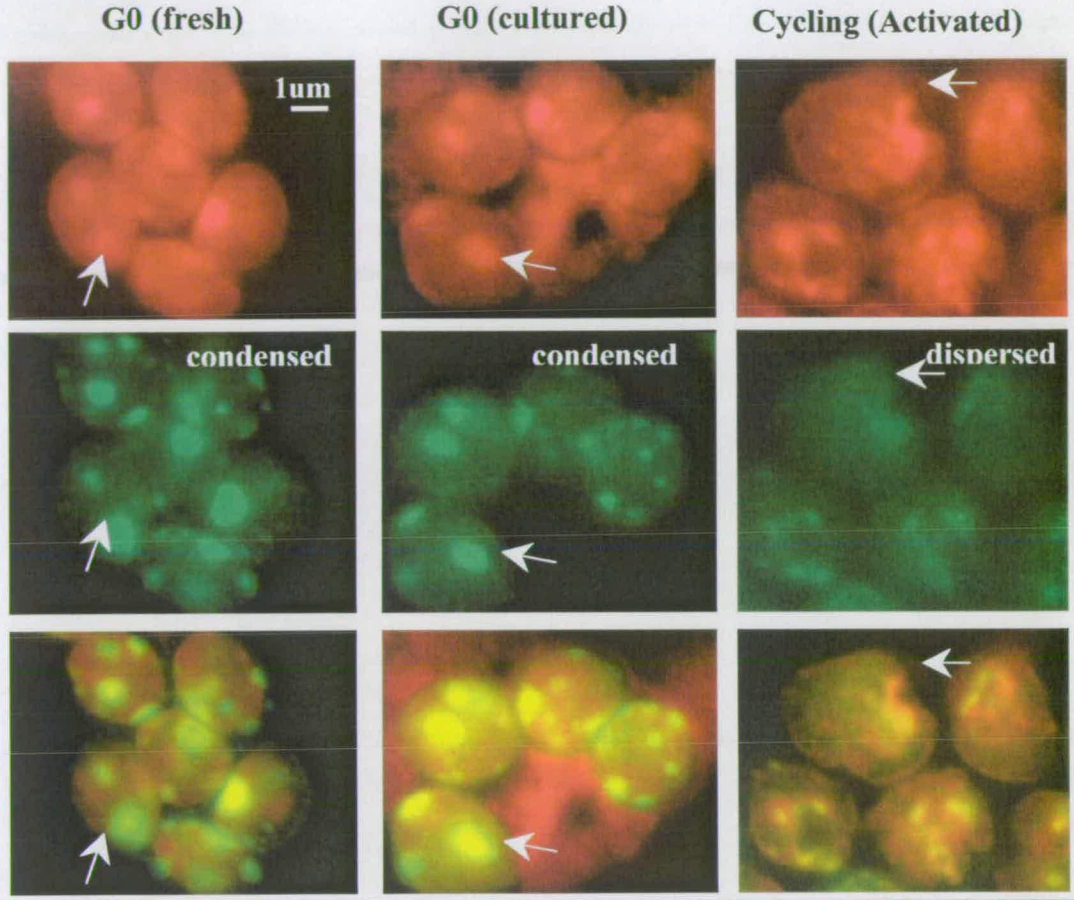

Nuclear Fluorescence	G0 (fresh) 1	G0 (cultured) 2	Cycling 3	1 vs 3	2 vs 3	1 vs 2
%area FL	100.00±0.00	100.00±0.01	100.00±0.00	p>0.5	p>0.5	p>0.5
Mean	93.2±5.1	83.6±3.6	79.5±3.8	p=0.037	p=0.498	p=0.120
SD	39.2±1.8	19.6±1.3	33.1±1.8	p<0.0001	p<0.0002	p<0.0001
Intensity	367814±19350	372969±19974	545615±28894	p<0.0001	p<0.0001	p=0.590
Peak	240.3±4.8	216.2±5.5	181.6±6.3	p<0.0001	p<0.0001	p=0.003
Cluster Fluorescence						
Cluster n°	3.2± 0.2	4.0±0.3	0.1±0.1	p<0.0001	p<0.0001	p=0.034
% area Fl	34.5±4.1	30.3±3.1	40.9±3.9	p=0.271	p=0.040	p=0.415
Mean	152±2	132±3	80±7	p=0.696	p=0.333	p=0.485
SD	39.2±1.8	19.6±1.3	33.1±1.8	p<0.0001	P<0.0002	p<0.0001
Intensity	213574±24632	189902±22429	230368±34368	p=0.881	p=0.980	p=0.088
Peak	240±5	220±5	153±8	p<0.0001	p<0.0001	p=0.012

Epifluorescent images of T-cells double stained with FITC-conjugated anti-M31 antibody (αM31-FITC) and DAPI, represented with a pseudo colour red. M31 was condensed into large clusters (pericentromeric heterochromatin) in freshly isolated G0 cells and dispersed in cycling T-cells, activated with 8ug/ml PHA and 4nM IL-2. T-cells cultured for 48h in medium alone (G0 cultured) were included as controls. Data summarised in the table were obtained from 40 cells (x63 objective) acquired from 3 images (for Methods see Paragraphs 2.11-2.12, Fig.2.7). Data, collected in three experiments, are expressed as mean±SEM (t-test for independent samples; α=0.05; GenStat 4.5, Windows 1995).

partially organised in large clusters, colocalised with areas of heterochromatin (DAPI), and partially organised in smaller clusters, scattered throughout the nucleus. For this reason cluster analysis was omitted. Analysis of nuclear fluorescence confirmed the tendency of mHP1α to be more condensed in quiescent cells compared to activated cells. Quiescent cells had a significantly lower intensity, therefore mHP1α content, than activated cells, possibly as a result of their smaller nuclear size (Fig.5.3). However quiescent cells had significantly higher peak fluorescence and a higher mean fluorescence and SD compared to activated cells (Fig.5.3). These data suggested the tendency of mHP1α to exist in a concentrated form in quiescent cells and in a dispersed form in non-quiescent cells.

Immunostaining for M32 (Fig. 5.4), the mouse homologue of human hHP1γ, showed that M32 had the tendency to organise in small clusters, with the appearance of speckles, scattered throughout the nucleus. These speckles were very clear in quiescent cells, where the chromatin and M32 were more condensed, but disappeared in activated cells, where the chromatin and M32 were more dispersed. Image analysis showed that quiescent cells had significantly lower fluorescence intensity, therefore M32 content, than activated cells (Fig. 5.4). This may be due to the lower nuclear size of quiescent cells compared to activated cells (Fig. 5.1). However M32 appeared to be more concentrated in quiescent cells as demonstrated by the significantly higher mean fluorescence, peak fluorescence and SD values, found in G0 cells compared to activated cells.

The analysis of activation markers confirmed efficiency of CD25 and Propidium Iodide (PI) staining (Chapter 4) as T-cell activation controls. Freshly isolated and cultured quiescent cells had significantly higher percentages of G0/G1 cells than activated cells and significantly lower percentages of cells in S-phase compared to activated cells (Table 5.3). The percentages of G2/M cells found in freshly isolated cells, were also significantly lower than those found in activated cells and similar to those observed in cultured quiescent cells (Table 5.3). In quiescent cells, both freshly isolated and cultured, the percentages of $CD25^+$ cells and CD25 mean fluorescence were significantly lower than those found in activated cells, indicating a very good level of activation in this set of experiments (Table 5.3). There was no significant difference in the percentage of $CD25^+$ cells and mean

Figure 5.3 Chromatin conformation of lymphocytes: immunostaining for mHP1α

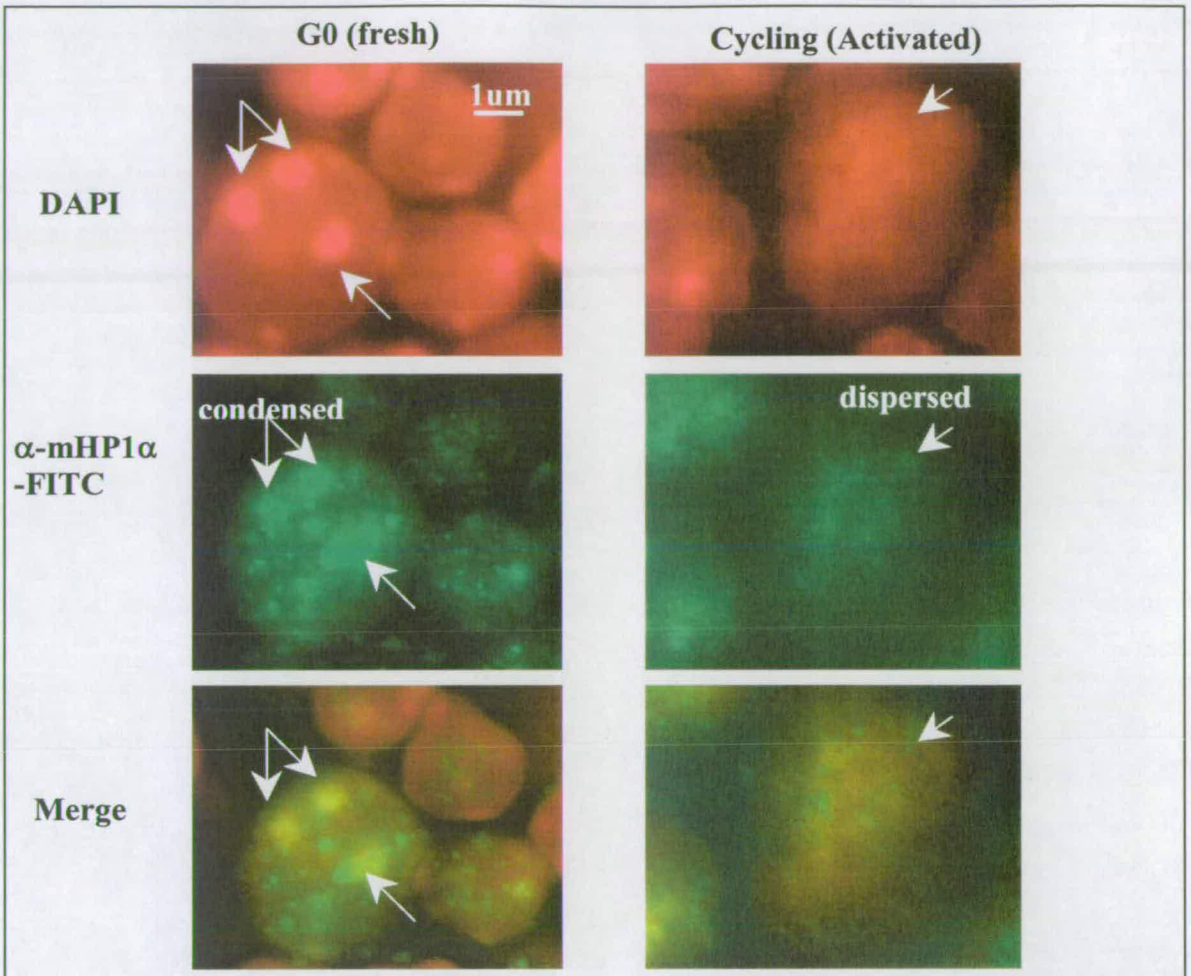

Cell morphology	G0 (fresh)	Cycling	p
Nuclear Area	44502±143	7811±364	p=0.013
Cell Area	5607±171	10495±478	p<0.0001
Nucleus (%)	78.5±0.6	74.8±1.2	p=0.012
Cell/Nucleus	1.28±0.01	1.35±0.03	p=0.013
Nuclear Fluorescence			
Intensity	267374±28032	431243±29171	p<0.0001
Mean Intensity	59±4	56±3	p=0.77
SD	21.0±1.5	17.5±1.3	p=0.089
Peak	181±8	129±7	p<0.0001
Area Fluorescence	100.0±0.0	100.0±0.0	p>0.5

Epifluorescent images of T-cells double stained with FITC conjugated anti-mHP1α-antibody (αmHP1α-FITC), and DAPI represented with a pseudo colour red. mHP1α is condensed in large clusters (pericentromeric heterochromatin) and small speckles in) in freshly isolated G0 cells and dispersed in cycling T-cells, activated with 8ug/ml PHA and 4nM IL-2. Data summarised in the table were obtained from 40 cells (x63 objective) acquired from 3 images (for Methods see Paragraphs 2.11-2.12, Fig.2.7). Data, collected in three experiments, are expressed as mean±SEM (t-test for independent samples; α=0.05; GenStat 4.5, Windows 1995).

Figure 5.4 Chromatin conformation of lymphocytes: immunostaining for M32

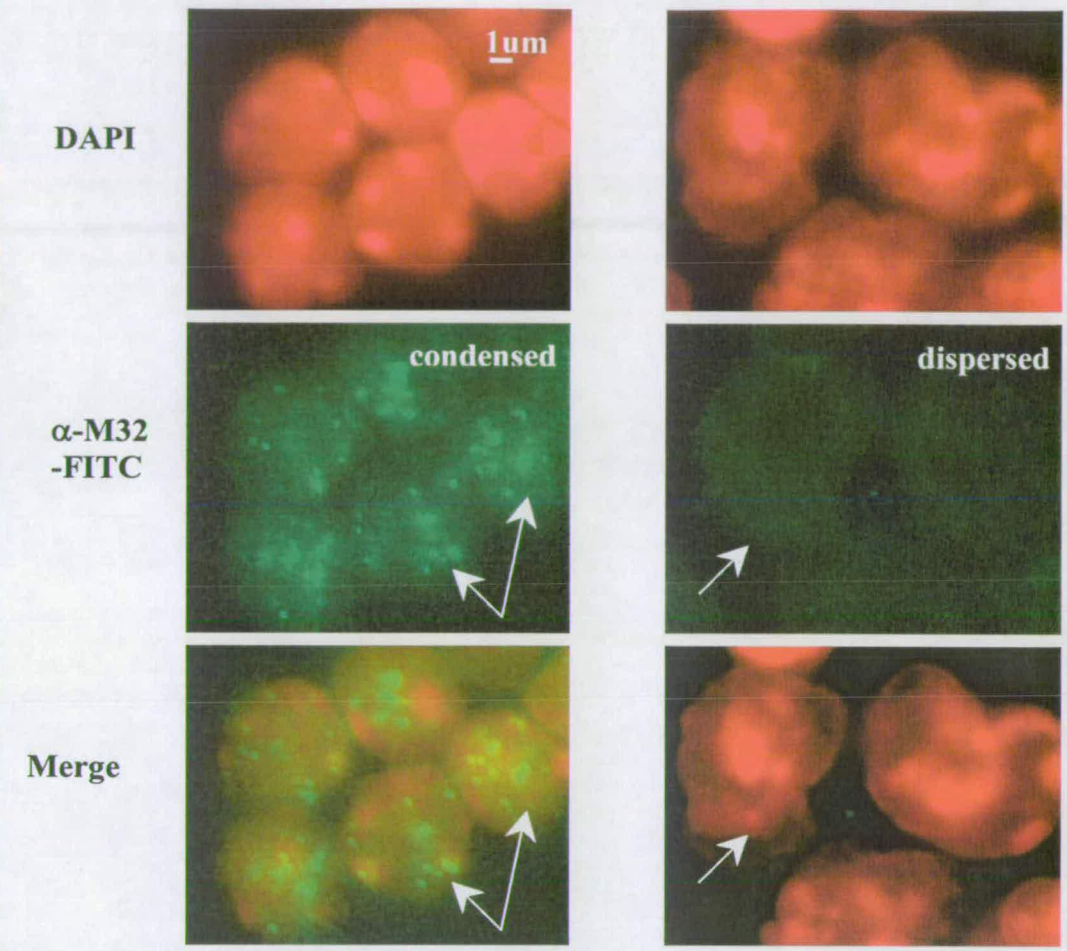

Cell morphology	G0 (fresh)	Cycling	p
Nuclear Area	4199±153	7413±281	p<0.0001
Cell Area	5396±291	12432±488	p<0.0001
Nucleus (%)	79.1±0.9	61.3±2.1	p<0.0001
Cell/Nucleus	1.27±0.02	1.72±0.07	p<0.0001
Nuclear Fluorescence			
Intensity	122138±6260	311981±59147	p<0.0001
Mean Intensity	62.7±3.4	17.0±1.1	p<0.0001
SD	21.3±1.5	5.5±0.8	p<0.0001
Peak	166.6±8.9	53.0±7.1	p<0.0001
% area fluorescence	99.9±0.3	100.0±0.0	p>0.5

Epifluorescent images of T-cells double with FITC conjugated anti-M32 antibody (αM32-FITC) and DAPI, represented with a pseudo colour red. M32 is condensed into speckles (facultative heterochromatin) in freshly isolated G0 cells and dispersed in cycling T-cells, activated with 8ug/ml PHA and 4nM IL-2. Data summarised in the table were obtained from 40 cells (x63 objective) acquired from 3 images (for Methods see Paragraphs 2.11-2.12, Fig.2.7). Data, collected in three experiments, are expressed as mean±SEM (t-test for independent samples; α=0.05; GenStat 4.5, Windows 1995).

fluorescence between freshly isolated and cultured quiescent cells, although they seemed to have higher percentages of G2/M and S-phase cells, and lower percentages of G0/G1 cells (Table 5.3).

Results of the double staining with anti-$p27^{KIP1}$/PI showed that the percentages of $p27^+$ cells were significantly higher in freshly isolated, quiescent cells than in activated cells (Table 5.4). This difference was even greater when considering only the diploid cell population (G0/G1; Table 5.4). In this case 88.9% of diploid, quiescent cells (G0/G1) were in G0 ($p27^+$) and 11.1% appeared to be in G1 ($p27^-$). Of the diploid cells (G0/G1), in the activated cell population, 40.5±% were in G0 ($p27^+$) and 59.5% were in G1 ($p27^-$). The p27 staining showed a reduction of quiescent cells after activation. However, the percentages of $p27^+$ (65.2%) found in activated cells appeared to be exceedingly high, especially when compared to the percentage of $CD25^-$ cells found in the same cell population (11.1%). This might result from the fact that intracellular staining is not ideal for FACS analysis because of high background problems leading to false positives.

PCNA appeared to be a very reliable marker of T-cell activation (non-quiescence): quiescent cells, both fresh and cultured, had significantly lower percentages of $PCNA^+$ cells compared to cycling cells (Fig.5.5). There was no difference in the percentage of $PCNA^+$ cells found in cultured and freshly isolated, quiescent cells (Fig.5.5).

The percentages of $D3^+$ cells were significantly lower in cultured quiescent cells compared to activated cells (Fig.5.5). Quiescent cells also had significantly lower values of intensity associated with lower values of mean fluorescence, and peak fluorescence suggesting that G0 cells contained less cyclin D3 than activated cells (Fig.5.5). Analysis of cyclin D3 nuclear and cytoplasmic fluorescence, showed that G0 cells contained less cyclin D3 in the nucleus, where the cyclin is present in an active form, while maintaining similar levels of cyclin D3 in the cytoplasm, where the protein is not active (Fig.5.5). This observation together with the high percentages of $D3^+$ cells found in the G0 cell population, suggests that, when using cyclin D3 as a negative marker of quiescence, discriminating between $D3^+$ and $D3^-$ cells may not be enough and may require further discrimination of $D3^+$ cells with or

Table 5.3 Activation control for chromatin experiments: CD25 and PI staining

	G0 (fresh) 1	G0 (cultured) 2	Cycling 3	1 vs 3	1 vs 2	2 vs 3
CD25+ (%)	3.7±0.5	11.4±4.1	88.8±3.4	<0.0001	=0.14	<0.0001
Fluorescence	62.9±10.5	65.7±14.8	290.4±6.7	<0.0001	=0.87	<0.0001
G0/G1 (%)	93.7±0.3	82.8±2.2	57.9±1.9	<0.0001	=0.027	<0.0005
S (%)	0.7±0.1	5.6±0.9	28.8±1.6	<0.0001	=0.014	<0.0001
G2/M (%)	5.6±0.3	11.5±1.3	13.3±0.3	<0.005	=0.040	=0.26
Apoptosis	1.1±0.6	31.5±5.7	18.3±0.2	<0.0001	<0.0001	=0.28

Results from three replicate experiments (10000 events/replicate). Data are expressed as Mean±SEM (t-test for independent samples, α=0.05).

Table 5.4 Activation control for chromatin experiments: $p27^{KIP1}$/PI staining

	G0 (fresh)	Cycling (activated)	p
p27+ (% Total cells)	87.6	65.2	p<0.001
p27+ (% G0/G1 cells)	88.9	40.5	p<0.001
G0/G1 (%)	90.2	65.3	p<0.001
S (%)	1.1	22.0	p<0.001
G2/M (%)	8.7	12.7	p>0.05

Results from a single experiment (10000 events). Data are expressed as Mean±SEM (Chi-square test, α=0.05).

Figure 5.5 Activation control for chromatin experiments: PCNA and cyclin D3

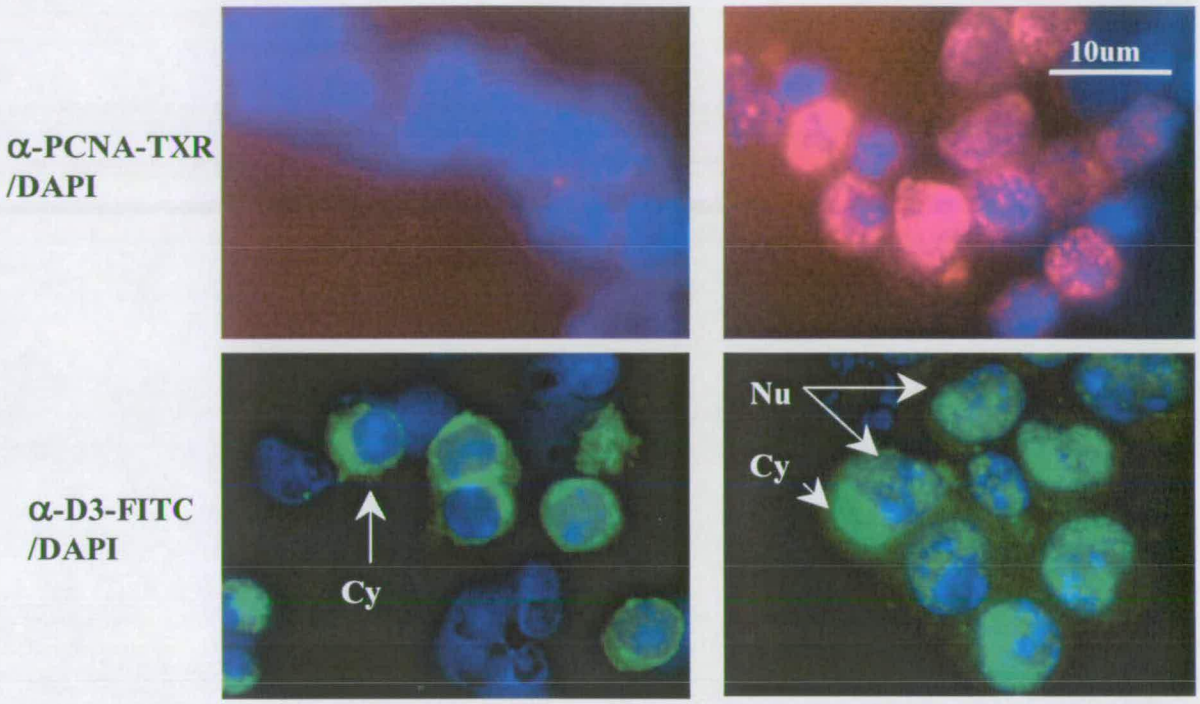

	G0 (fresh)	G0 (cultured)	Cycling (activated)	p 1 vs 3	p 1 vs 2	p 2 vs 3
PCNA+ (%)	0.6± 0.1	2.5± 0.6	40.7± 2.1	<0.0001	=0.13	<0.0001

		G0 (cultured)	Cycling (activated)	p
D3+ (%)		24.0±2.4	38.8±1.9	p<0.02
Cell	Intensity	145464±20256	493291±52024	p<0.001
	Mean	48.5±6.2	87.7±6.5	p<0.001
	SD	26.2±2.7	38.2±3.1	p<0.005
	Peak	164.1±13.5	208.3±9.1	p=0.017
	%Area Fl	94.6±2.5	100.0±0.0	p=0.053
Nucleus	Intensity	92422±13280	394272±43834	p<0.001
	Mean	47.1±6.0	104.2±7.6	p<0.001
	SD	17.1±2.4	30.5±2.3	p<0.001
	Peak	132.8±14.1	205.7±9.6	p<0.001
	%Area Fl	98.0±1.3	100.0±0.0	p=0.138
Cytoplasm	Intensity	53042±7709	99019±11504	p<0.001
	Mean	52.1±6.8	56.2±5.7	p=0.109
	%Area Fl	90.1±4.0	97.1±2.5	p<0.001

T-cells double stained with FITC conjugated anti-cyclin D3 (α-D3-FITC) antibody or Texas red conjugated anti-PCNA (α-PCNA-TXR) and DAPI. Quiescent cells are $PCNA^-$, with cyclin D3 only in the cytoplasm (Cy). Activated cells are $PCNA^+$, with cyclin D3 in the nucleus (Nu) or in the whole cell. Data summarised in the tables are expressed as mean±SEM (1-way ANOVA, for $\%PCNA^+$ and $\%D3^+$; t-test for independent samples, for others; $\alpha=0.05$). Fluorescence values were acquired on 40 cells taken from 3 images obtained in 1 (D3) or 3 experiments (PCNA). Percentages of PCNA+ and cyclin D3+ cells were calculated on 200 counts/ 3 fields/slide, with 1 slide/replicate.

without nuclear staining. For these reasons PCNA appeared to be a more direct and less subjective marker of T-cell activation.

The activation markers CD25 and PCNA were selected and were correlated with the chromatin marker M31 that had given the most consistent results.

Results of the FACS analysis of cells double stained with M31 and CD25 (Fig.5.6) confirmed that quiescent cells, both fresh and cultured, had lower percentages of $CD25^+$ cells, and lower levels of CD25 expression/cell (mean fluorescence), than activated cells (Fig.5.6A). Microscopic evaluation (Fig.5.6B) of CD25 expression also confirmed that G0 cells had lower percentages of $CD25^+$ cells (4/40, 10%) than activated cells (21/40, 52.5%). Discrepancies between the percentages of $CD25^+$ cells obtained by FACS analysis and by microscopic evaluation, especially in the activated group (78.9% vs 52.5%), may be due to damage of the CD25 surface marker during fixation of samples for FACS analysis. Changes in CD25 expression were associated with changes in chromatin status (Fig.5.6B and Table 5.5A). Quiescent cells were mostly $CD25^-$ and, at the same time, were characterised by patches of condensed chromatin and clusters of M31 (high intensity/small nuclear area; high mean fluorescence, peak fluorescence and SD; high cluster number). Activated cells were mainly $CD25^+$ and characterised by dispersed chromatin and dispersed M31 distribution (high intensity/large nuclear area; low mean fluorescence, peak fluorescence and SD; no clusters). To further prove the correlation between CD25 expression and chromatin status, chromatin features of $CD25^+$ and $CD25^-$ cells, were compared (Table 5.5B). Results showed that $CD25^-$ cells had a chromatin status (condensed) and a nuclear distribution of M31 similar to that of G0 cells (high intensity/small nuclear area; high mean fluorescence, peak and SD; high cluster number). Results also showed that $CD25^+$ cells had a chromatin status (dispersed) similar to that found in activated cells (high intensity/large nuclear area; low mean fluorescence, peak fluorescence and SD; no clusters).

Results of the double staining with M31 and PCNA confirmed the good level of activation in this experiment (Fig.5.7-Table 5.6). Only 5% of freshly isolated quiescent cells were $PCNA^+$, while 60% of activated cells were $PCNA^+$ (Table 5.6A). All the fluorescence parameters of the PCNA-TXR staining (intensity, mean, peak, SD) were also significantly lower in quiescent cells than in activated cells (Table

Figure 5.6 Immunostaining for M31/CD25 in lymphocytes

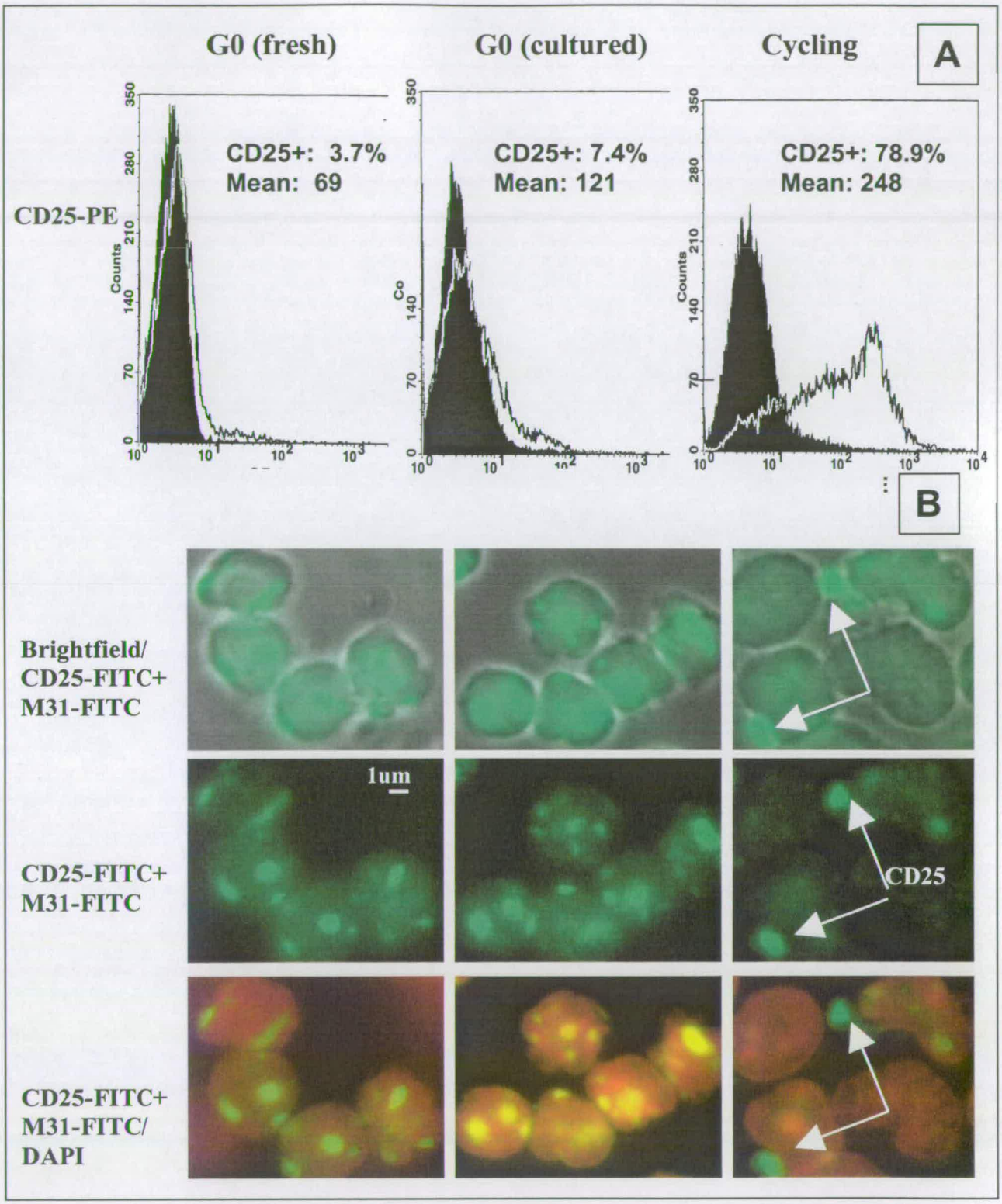

Figure 5.6A CD25 expression assessed by FACS analysis.
Figure 5.6B Triple staining for FITC conjugated anti-M31 antibody (αM31-FITC), PE-conjugated anti-CD25 (αCD25-PE) antibody and DAPI, represented here with a pseudo-colour red. G0 cells do not express CD25 and have M31 condensed in large clusters (pericentromeric heterochromatin). Activated cells express CD25 and dispersed M31.

Table 5.5A Results of M31/CD25 staining: comparison of G0 and cycling cells

Cell morphology	G0 (cultured) 1	G0 (fresh) 2	Cycling 3	1 vs 3	2 vs 3	1 vs 2
Nuclear Area	4363±111	4603±154	9511±549	<0.0001	<0.0001	=0.435
Cell Area	5645±126	6456±148	13320±710	<0.001	<0.001	<0.001
Nucleus (%)	77.3±0.8	70.8±1.3	71.8±1.4	<0.003	=0.471	<0.002
Cell/Nucleus	1.30±0.01	1.43±0.03	1.41±0.03	<0.002	=0.615	<0.0003
Nuclear fluorescence						
FITC-Intensity	422389±14199	383921±19231	431358±42339	=0.21	=0.16	=0.88
FITC-Mean Intensity	97.9±3.2	86.5±4.5	46.3±3.4	<0.0001	<0.0001	=0.060
FITC-SD	40.5±1.4	38.9±1.5	18.7±1.5	<0.0001	<0.0001	=0.0455
FITC-Peak	235±3.8	216±5.5	131±9.9	<0.0001	<0.0001	=0.210
Clusters (n°)	3.30±0.30	2.80±0.20	0.20±0.02	<0.0001	<0.0001	<0.123

Table 5.5B Results of M31/CD25 staining: comparison of $CD25^+$ and $CD25^-$

Cell morphology	$CD25^-$	$CD25^+$	p
Nuclear Area	6066±377	8854±865	<0.002
Cell Area	8256±559	12182±1132	<0.0002
Nucleus (%)	75.3±1.0	72.9±1.5	=0.203
Cell/Nucleus	1.34±0.02	1.39±0.03	=0.249
Nuclear Fluorescence			
FITC-Intensity	407222±18199	470108±58276	=0.196
FITC-Mean Intensity	78.0±4.5	59.0±6.0	=0.0179
FITC-SD	32.7±1.9	22.7±2.2	<0.003
FITC-Peak	193.2±9.1	159.7±14.1	=0.0488
Clusters (n°)	2.49±0.29	0.39±0.03	<0.0001

Table 5.5A-Table 5.5B Results of triple staining with αM31-FITC, αCD25-PE and DAPI. Data were obtained from 40 cells acquired from 3 images (x630) collected in one replicate experiment. Data are expressed as mean±SEM, and were analysed using a t-test for independent samples (α=0.05).

5.6A). Results (Table 5.6A) showed that fresh, quiescent cells were mainly $PCNA^-$ and, at the same time, were characterised by patches of heterochromatin (DAPI) associated with clusters of M31-FITC, as indicated by the nuclear fluorescence parameters (high intensity/small nucleus, high mean fluorescence, peak, SD and number of clusters). Activated cells (Table 5.6A) were mostly $PCNA^+$ and characterised by dispersed chromatin and dispersed M31-FITC distribution as indicated by the nuclear fluorescence parameters (high intensity/large nucleus, low mean fluorescence, peak and SD, absence of clusters). To further prove the correlation between PCNA expression and chromatin status, chromatin features of $PCNA^+$ and $PCNA^-$ cells, were compared (Table 5.6B). $PCNA^-$ cells coupled low PCNA-TXR expression levels (low intensity, mean, peak, SD) with a condensed M31-FITC distribution, similar to that of G0 cells (low intensity/small nuclear area; high mean fluorescence, peak and SD; high cluster number). $PCNA^+$ cells coupled high PCNA-TXR expression levels (high intensity, mean, peak, and SD) with a dispersed M31 distribution, similar to that found in activated cells (high intensity/large nuclear area; low mean fluorescence, peak fluorescence and SD; no clusters).

5.2.5 Conclusions

Previous nuclear transfer experiments suggested that smaller cells might have a greater potential for NT than larger ones (development to term 2.2% vs 0.7%; Wakayama *et al.,* 1999). These experiments confirmed that cell size, at least in the lymphocyte model, depends on the nuclear size that is greatly affected by the activation state. Quiescent cells had a smaller nucleus, and therefore a smaller cell size, than activated cells. This is due to the fact that nuclear size is affected by ploidy: diploid cells (G07G1) have a smaller nucleus than cycling cells (S, G2/M). Quiescent cells are mainly diploid while activated cells have high percentages of cells in G2/M and S-phase. Nuclear size might also be affected by the dramatic differences in chromatin conformation observed in quiescent and activated cells.

Immunostaining with anti-HP1 antibodies (anti-mHP1α, anti-M31, anti-M32) showed a lower level of expression (lower fluorescence intensity) of these

Figure 5.7 Immunostaining for M31/ PCNA in lymphocytes

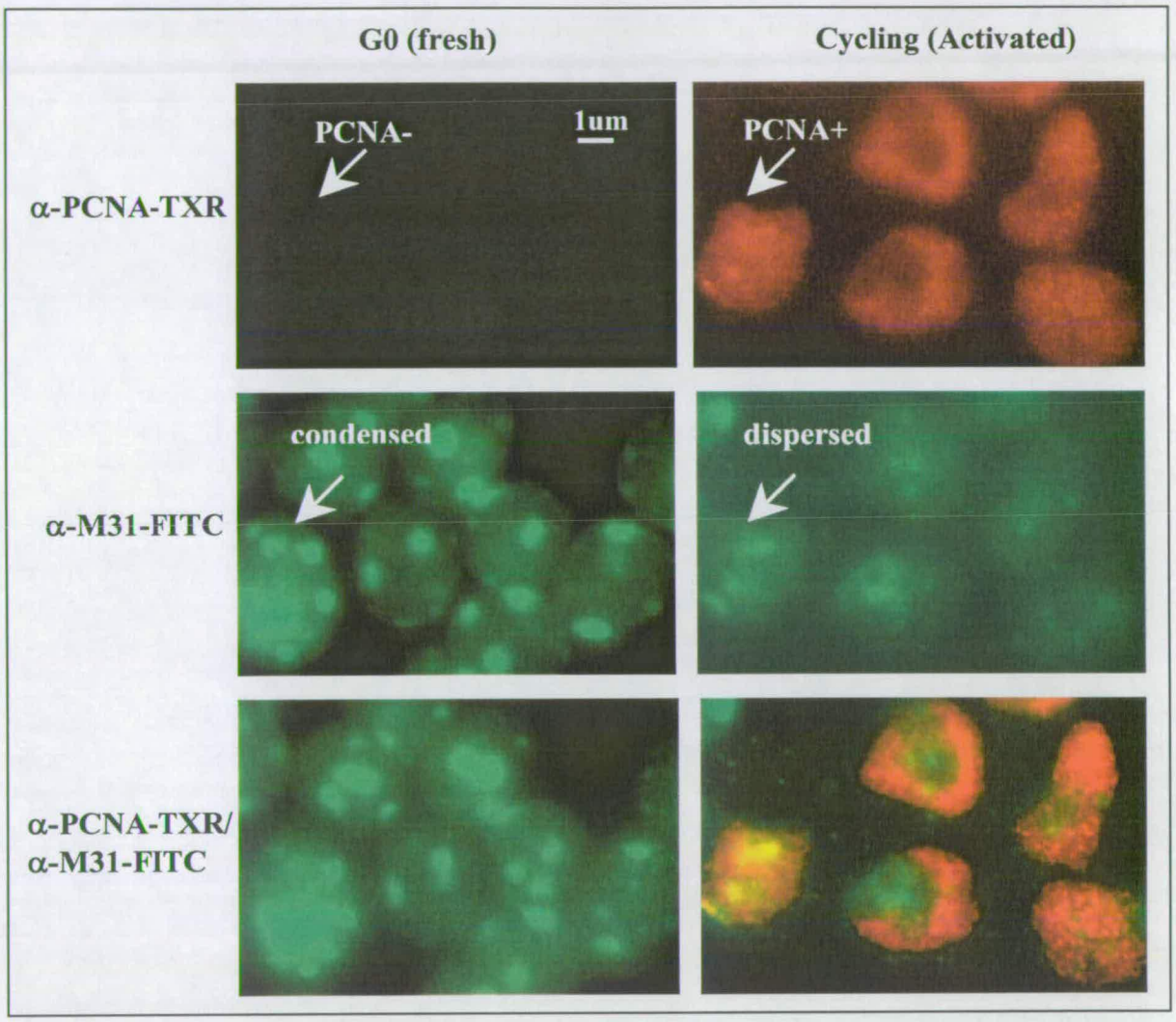

Cells triple stained with FITC conjugated anti-M31 antibody (αM31-FITC), TXR-conjugated anti-PCNA (αPCNA-TXR) antibody and DAPI. G0 cells are PCNA- and with M31 condensed in large clusters (pericentromeric heterochromatin). Activated cells are $PCNA^{+}$ and with dispersed 31.

Table 5.6A Results of M31/PCNA staining: comparison of G0 and Cycling cells

Cell morphology	G0 (fresh)	Cycling	p
Nuclear Area	4022±145	7283±501	<0.0001
Cell Area	5303±212	10015±682	<0.0001
Nucleus (%)	76.6±1.2	72.8±0.9	0.0059
Cell/Nucleus	1.32±0.03	1.38±0.02	0.052
M31 fluorescence			
Intensity	310918±20317	317177±22929	0.649
Mean Intensity	77.8±4.2	49.2±4.2	<0.0001
SD	32.9±1.7	23.4±2.3	<0.0002
Peak	199.4±6.4	136.3±9.7	<0.0001
Clusters (n°)	2.92±0.29	0.17±0.09	<0.0001
PCNA fluorescence			
Intensity	62671±38720	342767±45655	<0.0001
Mean Intensity	11.2±4.6	42.5±4.1	<0.0001
SD	4.9±1.3	13.0±1.2	<0.0001
Peak	29.6±7.5	90.5±7.2	<0.0001
PCNA+ (%)	5%	60%	-

Table 5.6B Results of M31/PCNA staining: comparison of $PCNA^+$and $PCNA^-$cells

Cell morphology	$PCNA^-$	$PCNA^+$	p
Nuclear Area	4314±248	8433±502	<0.0001
Cell Area	5772±345	11578±689	<0.0001
Nucleus (%)	75.4±0.9	73.1±1.2	0.128
Cell/Nucleus	1.34±0.02	1.38±0.02	0.246
M31 fluorescence			
Intensity	293306±17742	357126±27548	0.0462
Mean Intensity	73.3±4.3	42.9±2.5	<0.0002
SD	32.5±1.9	19.0±1.6	<0.0001
Peak	188.7±7.9	124.4±7.9	<0.0001
Clusters (n°)	2.24±0.29	0.12±0.08	<0.0001
PCNA fluorescence			
Intensity	32800±6899	555628±59170	<0.0001
Mean Intensity	11.2±4.6	42.2±4.1	<0.0001
SD	4.9±1.3	13.0±1.2	<0.0001
Peak	29.6±7.5		90.5±7.9

Table 5.6 A-B show data acquired from cells triple stained with αM31-FITC, αPCNA-TXR and DAPI. Data were obtained from 40 cells acquired from 3 images (x630) collected in one replicate experiment. Data are expressed as mean±SEM, and were analysed using a t-test for independent samples (α=0.05).

proteins in G0 cells compared to activated cells. However, as confirmed by image analysis, quiescence induced dramatic changes in the distribution patterns of these proteins. In G0 cells, HP1 proteins had a tendency to concentrate in clusters, whereas in activated cells they have a dispersed distribution. These studies showed that the nucleus of quiescent cells is characterised by large clusters of M31 and mHP1α proteins, colocalised with patches of pericentromeric, constitutive heterochromatin, and smaller clusters (speckles) of M32, colocalised with areas of non-constitutive heterochromatin. After activation, as nuclear size increased and chromatin decondensed, M31, mHP1α and M32 also acquired a dispersed distribution. The differences in chromatin status observed in quiescent and non-quiescent cells are likely to be one of the regulatory mechanisms involved in gene silencing during quiescence.

Staining with the four activation markers of choice, three positive markers of activation led to the following conclusions:

1) All markers showed a significant difference between quiescent and non-quiescent cells, confirming the good activation level achieved in these experiments;
2) Percentages of cells expressing positive markers of activation (CD25, cyclin D3, PCNA) and their levels of expression were significantly lower in quiescent cells than in activated cells;
3) Percentages of cells expressing the negative marker of activation ($p27^{KIP1}$) was significantly higher in quiescent cells compared to activated cells and this difference was even greater when only diploid cells (2N) were included in the analysis;
4) CD25 and PCNA were considered as the most reliable markers of activation and were correlated with markers of chromatin status;

The shifts observed in the activation markers during exit from quiescence and re-entry into the cell cycle were associated with changes in chromatin status.

Quiescent cells contained smaller quantities of HP1 proteins (M31, mHP1α, M32) compared to activated cells but in a more condensed form, which tended to associate with areas of condensed chromatin (DAPI).

Quiescent cells, fresh and/or cultured, were characterised by clusters of M31 and in some cases mHP1α, colocalised with patches of pericentromeric, constitutive heterochromatin (DAPI). The nucleus of quiescent cells also contained small clusters of M32, with speckled appearance, possibly colocalised with areas of non-constitutive heterochromatin (DAPI).

Activated cells were characterised by a dispersed chromatin status of pericentromeric, constitutive heterochromatin and non-constitutive heterochromatin. Changes in chromatin status were associated with dispersion of all three HP1 proteins (M31, mHP1α, M32).

Results of the triple staining for M31/CD25/DAPI and M31/PCNA/DAPI showed a negative correlation between activation and chromatin condensation and confirmed the strict correlation existing between the state of activation of lymphocytes and the chromatin status. Quiescent cells could be characterised as being $CD25^-$/ $M31^{condensed}$ and $PCNA^-/M31^{condensed}$, whereas activated cells could be characterised as being $CD25^+/M31^{dispersed}$ and $PCNA^+/M31^{dispersed}$. This correlation was otherwise confirmed by selecting $PCNA^-$ and $CD25^-$ cells or $PCNA^+$ and $CD25^+$ cells and checking the M31 distribution. This confirmed once more the association $CD25^-/PCNA^-/M31^{condensed}$ and the association $CD25^+/PCNA^+/M31^{dispersed}$.

These experiments highlighted the potential of M31 to act as a marker of the chromatin changes induced by quiescence. M31 was therefore selected to assess the impact of these changes on nuclear transfer.

5.3 EFFECT OF QUIESCENCE ON HISTONE H4 ACETYLATION

5.3.1 Aim

Assess the effect of quiescence on acetylation status of histone H4 on specific lysines (K5, K12), using specific antibodies (anti-H4.Ac5, anti-H4.Ac12) that are able to detect changes in acetylation associated with zygote gene activation in mouse embryos. The antibody H4.Ac2-4, that recognizes acetylation of lysines 2-4 and had not been previously described in the literature, was also used in these

experiments. Changes in acetylation were correlated with changes observed in the activation markers, CD25 and PCNA.

5.3.2 Experimental design

Experiments were carried out in three replicates. For each replicate T-cells were isolated from the lymph nodes of 4-8, six week old female mice of the inbred strain C57BL/6 (5.9±0.5 x10^6 cells /animal; $CD3^+$, 77.8±14.6%).

A total of 19-21x10^6 cells were used in each replicate, of which 2.5-4.5 x10^6 cells were used fresh (fresh, quiescent cells) and 16x10^6 were cultured in 24 well plates, at a concentration of 2x10^6/well. Treatment groups included (Table 5.7):

1) Fresh, quiescent cells (G0 fresh);
2) Quiescent cells, cultured 24h in 10% FCS medium (A.2.1; G0 cultured) cells; cells activated 24h with 10% FCS medium, supplemented with 8ug/ml PHA (A.2.4) and 4nM IL-2 (A.2.5; Cycling).

For some staining only one quiescent group was included (Table 5.7).

For H4.Ac2-4, H4.Ac5, H4.Ac12 staining (Methods see Paragraph 2.11), nuclear area and features of nuclear fluorescence were analysed (Analysis see Paragraph 2.12).

Only two activation markers were used in these experiments: PCNA staining (Methods see Paragraph 2.11); CD25 and PI staining (Methods see Paragraph 2.12). Gates and parameters used for analysis were as previously described (Paragraphs 2.10-2.11). For CD25 and PI analysis was carried out on total live cells (live gate) omitting CD3 gating (see Paragraph 4.4).

An attempt was made to assess cells for activation and acetylation simultaneously by double staining them with PCNA/H4.Ac5 or H4.Ac12 or H4.Ac2-4 and counter staining with DAPI. However, it was not possible to stain cells in this way. Negative interactions between anti-acetylated H4 and antibodies for functionally correlated molecules (RNA polymerase II; Worrad *et al.*, 1995) have been described before. Acetylation is highly dependent on DNA replication, and is reduced by inhibitors of DNA synthesis (Worrad *et al.*, 1995). DNA replication and

Table 5.7 Experimental design for acetylation experiments: staining/treatment groups

Experiment	Analysis	Staining	G0 (fresh)	G0 (cultured)	Cycling
Activation control	FACS	$CD25^+$ and PI	X	X	X
	IF	PCNA/DAPI	X	X	X
H4 Acetylation	IF	H4.Ac2-4	-	X	X
	IF	H4.Ac5	-	X	X
	IF	H4.Ac12	-	X	X

Cells from were assigned to three treatment groups: freshly isolated, quiescent cells (G0 fresh); quiescent cells, that had been cultured for 24h, in 10% FCS medium (G0 cultured); cells that had been activated for 24h with 8ug/ml PHA and 4nM IL-2 (Cycling). Samples were processed either for Immunocytochemistry (IF) or FACS analysis (See Paragraph 2.9-2.11 for Methods).

acetylation sites are also spatially correlated. In these experiments a similar nuclear distribution at the periphery of the nucleus (ring-like) has been observed in $PCNA^+$ cells (Fig. 5.7, cycling cells) and cells stained for acetylation, especially H4.Ac2-4 and H4.Ac12 (Fig.5.8). These observations suggest that negative interaction might be possible. No attempt was made to correlate CD25 and H4 acetylation markers.

5.3.3 Statistical analysis

All data were transformed using a log transformation (mean fluorescence, peak, integral intensity), except data expressed as percentages, which were transformed using a Logit transformation. Choice between non-transformed and transformed data was made by comparing the normality of their distributions using residual fit plots (GenStat 4.21, Windows 2000). Treatment groups were compared using Student-t test for independent samples (Statistica 4.5, Windows 1995; α=0.05).

5.3.4 Results

Activation controls showed that T-cells responded very well to the activation protocol (Table 5.8; Table 5.9). Quiescent cells, fresh or cultured, was had lower percentages of $CD25^+$ cells, lower levels of CD25 expression and higher percentages of diploid cells (G0/G1), than activated cells. Culture increased cell death rates regardless of the culture conditions (Table 5.8). However the percentages of apoptotic cells in culture were similar to those observed in previous experiments, if not lower (Fig. 4.9).

PCNA staining also confirmed that quiescent cells, either fresh or cultured, were only occasionally $PCNA^+$ (0.5-0.0%), while high percentages of activated cells were $PCNA^+$ (Table 5.9).

There was a dramatic difference in the acetylation level of histone H4, between quiescent and activated cells (Fig.5.8). Immunostaining with FITC conjugated antibodies recognizing acetylated histone H4 (H4.Ac2-4, H4.Ac5, H4.Ac12) resulted in a dull, green fluorescence staining in quiescent cells and a very bright, green fluorescence in activated cells. A peripheral nuclear distribution, similar to that described in mammalian embryos (Worrad *et al.*, 1995) at the time of zygote

Table 5.8 Activation control in acetylation experiments: CD25 and PI staining

	G0 (fresh) 1	G0 (cultured) 2	Cycling 3	p 1 vs 3	p 1 vs 2	p 2 vs 3
Apoptosis	1.1±0.6	19.8±2.1	17±2	<0.002	<0.002	=0.75
CD25 (%)	4.5±0.9	9.0±1.0	64±13	<0.005	=0.42	<0.02
Fluorescence	95.2±4.7	82.1±5.5	595±120	<0.0005	=0.57	<0.0003
G1 (%)	95.5±0.6	89.8±3.9	68.2±3.9	<0.002	=0.14	<0.001
S (%)	0.9±0.1	2.8±1.6	22.0±2.5	<0.001	=0.29	<0.004
G2/M (%)	3.3±0.7	7.4±2.4	9.7±1.4	<0.03	=0.12	=0.37

Data were obtained analysing 10000 events/replicate in three replicate experiments. Data are expressed as Mean±SEM (t-test for independent samples, α=0.05).

Table 5.9 Activation control in acetylation experiments: PCNA staining

	G0 (fresh)	G0 (cultured)	Cycling	1 vs 3	1 vs 2	2 vs 3
PCNA+ (%)	0.5±0.0	0.0±0.0	35.7±0.6	<0.0001	0.52	<0.0001

Data were obtained analysing 200 cells/3 fields/replicate in three replicate experiments. Data are expressed as Mean±SEM (t-test for independent samples, α=0.05).

Figure 5.8 Staining for histone H4 acetylation in T-lymphocytes

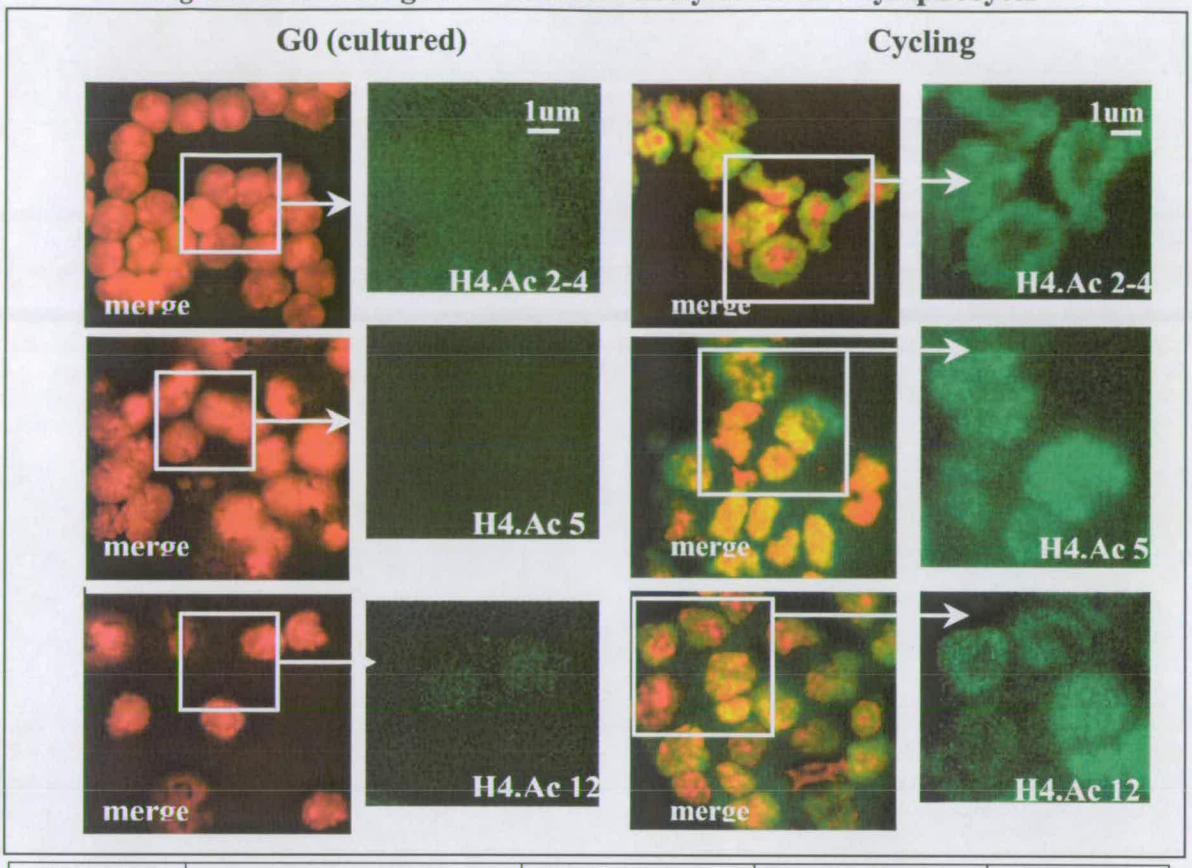

Staining	Parameter	G0 (cultured)	Cycling	p
H4.AC2-4	Nuclear area (pixels)	4579±99	8815±384	<0.001
	Intensity	43630±4590	961768±60717	<0.001
	Mean	9.5±0.9	110.4±5.4	<0.001
	SD	3.1±0.1	32.4±1.6	<0.0001
	Peak	28.2±4.9	206.0±7.0	<0.001
	Area Fluorescence (%)	92.1±1.7	100.0±0.0	<0.001
H4.AC5	Nuclear area (pixels)	4219±220	4119±304	=0.431
	Intensity	36500±5632	122347±14503	<0.001
	Mean	9.5±1.2	26.8±2.5	<0.001
	SD	4.9±0.3	3.4±0.3	<0.02
	Peak	32.7±5.3	50.0±4.4	<0.001
	Area Fluorescence (%)	81.5±5.0	99.7±0.3	<0.001
H4.Ac12	Nuclear area (pixels)	3829±195	3863±184	=0.901
	Intensity	21535±3840	100003±8391	<0.001
	Mean	5.3±0.8	25.6±1.6	<0.001
	SD (Mean1)	3.0±0.4	5.9±0.3	<0.0001
	Peak	23.9±3.9	62.1±3.9	<0.001
	Area Fluorescence (%)	72.2±5.7	99.±0.3	=0.003

Figure 5.8 shows cells double stained with FITC conjugated αH4.Ac2-4, αH4.Ac5, and αH4.Ac12 and DAPI (merge). G0 cells are deacetylated and activated cells are hyperacetylated. Data in the table are expressed as mean±SEM (t-test for independent samples, α=0.05) and were obtained from 40 cells acquired from 3 images (x400), collected in three replicate experiment.

gene activation, was observed in activated cells (Fig. 5.8). This pattern was particularly clear when cells were stained with anti-H4.Ac2-4 and anti H4.Ac12 antibodies. Histone acetylation is associated with transcriptional activation, therefore the observation that G0 cells are deacetylated whereas activated cells are hyperacetylated complies with the observation that quiescent cells are transriptionally comparatively inert whereas cycling cells are transriptionally active. In all three staining (H4.Ac2-4, H4.Ac5, H4.Ac12), all the fluorescence parameters (intensity, mean, peak, SD of mean) considered were significantly lower in quiescent cells compared to activated cells (Fig.5.8).

5.3.5 Conclusions

Changes in the activation status of lymphocytes are associated with changes in the acetylation status of histone H4 on lysines K2-4, K5, K12. Quiescent cells are $CD25^-/PCNA^-$ and deacetylated, whereas activated cells are $CD25^+/PCNA^+$ and hyperacetylated. Some of the antibodies used in this set of experiments (H4.Ac5/12) have been used to detect changes in acetylation patterns occurring in mouse embryos at the time of zygote gene activation (ZGA). Therefore they can be used to investigate the impact of quiescence-induced changes in H4 acetylation on the time of ZGA in cloned embryos.

CHAPTER 6

EFFECT OF QUIESCENCE ON NUCLEAR TRANSFER

6.1 INTRODUCTION

The main aim of the experiments described in this chapter was to investigate if and how quiescence of donor cells might affect development of cloned embryos.

There have been suggestions that quiescence of donor nuclei might improve development of cloned embryos. The first mammals cloned from somatic cells were produced using serum-starved, quiescent cells (Campbell *et al.*, 1995; 1996b; Wilmut *et al.*, 1997). Most successful somatic cell nuclear transfer experiments, in a variety of mammalian species, have been performed carried out using cultured or freshly isolated quiescent cells (Chapter 1, Table 1.1). However, up to date, there is still no conclusive evidence proving a direct link between quiescence and nuclear transfer efficiency.

In the experiments described in this chapter donor T-cells synchronized in G0 and G1 were used to investigate the effects of quiescence on the pre- and post-implantation development of cloned embryos. The effect of quiescence on timing of Premature Chromosome Condensation (PCC) was also included in these developmental studies.

PCC refers to the condensation of donor chromatin into chromosomes, within 2-3h after reconstruction, followed by chromatin decondensation, nuclear swelling and pronuclear (PN) formation. Earlier experiments in rabbits and mouse showed that PCC is a morphological expression of nuclear reprogramming and is strictly correlated with the developmental potential of cloned embryos (Collas *et al.*, 1992a, 1992b; Collas and Robl, 1991; Cheong *et al.*, 1994). Mouse nuclear transfer (NT) experiments with donor blastomeres at the 2-cell stage showed that both PCC

and non-PCC embryos were able to support development to blastocyst but only PCC embryos were able to support development to term in 12.5% of cloned embryos (Cheong *et al.,* 1994). Other studies in rabbits indicated that cell cycle stage of donor cells influenced PCC (Collas *et al.,* 1992a) and that a strict correlation existed between cell cycle-mediated abnormalities observed during PCC and low developmental potential of transplants (Collas *et al.,* 1992a, 1992b; Collas and Robl, 1991). G1 transplants had significantly higher rates of development to blastocyst (71%) and normal PCC morphology, with metaphase plates characterised by normal spindle morphology and chromosomes aligned at the equator of the spindle. On the contrary, S transplants had low developmental potential (15%) and abnormal PCC morphology with chromosomes located outside the spindle, adjacent to the front poles, and abnormal spindle morphology. The most common spindle abnormalities included microtubules radiating from the poles and/or the sides and multiple spindles (2-3). These studies suggested that donor cell cycle has a significant effect on very early stages of development of cloned embryos, such as PCC. These effects can result in chromosome and spindle abnormalities in transplant embryos that are responsible for impaired development during later stages of development (Collas and Robl, 1991). Abnormal features of PCC have also been described in cloned mouse embryos reconstructed using cumulus cell (Wakayama *et al.*, 1998). In this case some of the embryos were unable to form a regular metaphase plate, correctly aligned at the equator, and single, condensed chromatids appeared to be attached to a single pole of the spindle.

There is also some indirect evidence suggesting that quiescence might affect nuclear transfer efficiency by altering epigenetic status and gene expression in cloned embryos. Cloned embryos derived from quiescent cells have lower levels of expression of interferon Tau (IF-τ) gene, correlated with poor embryo quality (Wrenzicky *et al.*, 2001). Furthermore, contact inhibition, a condition known to induce quiescence in cultured cells, reduced the methylation levels of imprinted genes (Baqir and Smith, 2000), often abnormally hypermethylated in cloned embryos (Inoue *et al.,* 2002; Humpherys *et al.*, 2001).

The experiments described in this chapter focused on histone H4 acetylation and chromatin conformation, and addressed the question whether epigenetic changes induced by quiescence in donor cells (Chapter 5) affected the epigenetic status of cloned embryos, after nuclear transfer, with potential effects on embryo development.

Changes in chromatin conformation contribute in establishing epigenetic constraints during embryo development and differentiation (Leitch, 2000). Before fertilisation maternal chromatin is condensed in chromosomes with a nucleosomal structure and sperm chromatin, where most or all histones are replaced by protamines, appears as a highly compacted structure. At this stage maternal and paternal genomes are also transcriptionally inactive. After fertilisation, as a result of exposure to the ooplasm of MII oocytes and gradual replacement of protamines with histones, the sperm chromatin decondenses (Perreault, 1992). After a transient re-condensation and female pronucleus formation, the male pronucleus is formed. A phase of pronuclear swelling is followed by condensation into chromosomes at syngamy and, finally, karyo and cytokinesis (Adenot *et al.*, 1991).

Heterochromatin gene silencing also plays a pivotal role in cell type specific restriction of gene expression, as embryonic cells differentiate into somatic cells. Chromatin changes taking place during early embryo development and differentiation are mediated by remodelling networks, involving histone and non-histone silencing proteins. In early embryos sperm protamines and the embryonic linker histone B4 are exchanged with core histones H2A and H2B and the somatic linker histone H1 (Clarke *et al.,* 1998), mediated by the remodelling factor nucleoplasmin (Hiyoshi *et al.*, 1991). As shown in *Xenopus*, eggs store large amounts of SWI/SNF-like complex containing a BRG1-like remodelling factor (Gelius *et al.,* 1999). Early mouse embryos contain large amounts of SWI/SNF-like complexes containing BRM (SNF2 alpha) and BRG1 (SNF2 beta) remodelling factors (Dauvillier *et al.,* 2001), mainly involved in vasculogenesis. Changes in chromatin non-histone silencing proteins play an important role in differentiation. In Xenopus embryos Polycomb proteins (xPcG1), involved in heterochromatin gene repression, accumulate as cells differentiate. There is a negative correlation between accumulation of xPcG1 and cell totipotency, expressed as their ability to produce

swimming tadpoles after nuclear transfer (Kikyo and Wolffe, 2000). Other transcription factors are involved in the differentiation of specific tissues specific manner. The activity of some zinc-finger proteins (e.g. Ikaros, Eos, Pegasus, Ailos) is, for example, restricted to chromatin changes that mediate lineage commitment and differentiation of haematopoietic stem cells into lymphocytes (Georgopoulos, 2002).

During reprogramming epigenetic restrictions to gene expression established during differentiation, including heterochromatin repression, have to be erased. There is increasing evidence supporting the central role played by remodelling networks in nuclear reprogramming (Kikyo and Wolffe, 2000; Renard, 1998; Cheong *et al.*, 1994). Recent data demonstrated that nuclear swelling is the morphological expression of an exchange between cytoplasm and donor nucleus of molecules with chromatin remodelling properties (Kikyo and Wolffe, 2000). At the time of nuclear swelling about 85% of the proteins contained in the donor nucleus are lost and replaced by proteins coming from the recipient oocyte cytoplasm (Kikyo *et al.,* 2000). When *Xenopus* epithelial cells are transferred to recipient oocytes H1 and H1° linker histones are replaced by B4 embryonic linker histone and by the chromatin structural protein HMG1 (Dimitrov and Wolffe, 1996). Loss of immunoreactivity to H1 has been described also in cattle and it has been suggested as a marker of reprogramming (Bordignon *et al.,* 1999; 2001). Removal of H1 and its replacement with B4/HMG1 is mediated by nucleoplasmin, in a reverse manner to what is observed during normal embryo development. The ATP-ase ISWI, contained in several SNF/SWI-like remodelling complexes, is also incorporated, as H1 is lost. On the contrary the MeCP2/Rdb3/Sin3 that targets deacetylation and heterochromatin silencing to regions of methylated DNA, does not seem to be involved in nuclear reprogramming (Kikyo *et al.,* 2000).

Post-translational modifications of histones, that are affected by quiescence, also contribute to the restriction of gene expression during development and differentiation and might play an important role in nuclear reprogramming.

In mouse, both maternal and paternal mature gametes are hypoacetylated (histone H4<3 acetylated lysines). However during early embryo development

(Adenot *et al*, 1997), before zygote gene activation (ZGA), paternal and maternal chromatin are differentially acetylated. The oocyte stores large quantities of diacetylated histone H4, which are preferentially incorporated into the sperm after fertilisation. Therefore, during G1 of the first cell cycle, the male pronucleus is hyperacetylated and transcriptionally more active than the female pronucleus, as confirmed by the fact that reporter genes are preferentially expressed when injected into the male pronucleus (Ram and Shultz, 1993). Differences in acetylation reflect differences in chromatin structure previously described in this paragraph. At the end of G1 of the first cell cycle, female and male pronuclei exhibit equivalent acetylation and chromatin structure. In the mouse, the time of zygote gene activation, which starts at the G2/S of the 1-cell stage (Latham *et al.*, 1992) and is maximal at the 2-cell stage (Schultz, 1993), is marked by the appearance of a typical acetylation pattern at the periphery of the nuclei. This peripheral staining pattern was observed when embryos were assessed for acetylation of H4 at lysines 8, 5, 12 (H4.Ac5/8/12; Worrad *et al.*,. 1995) and acetylation of histone H3 (Stein *et al.*, 1997) on at lysines 9 and/or 18 (H3.Ac9/18). However it was not observed when embryos were assessed for acetylation of histone H4 at lysine 16 (H4.Ac16; Worrad *et al.*, 1995), suggesting different histone isoforms may play different roles during embryo development. Apart from this correlation between histone acetylation and transcriptional activation (ZGA), histone H4 deacetylation is often found in association with CpG methylation (Newell-Price *et al.*, 2000), suggesting a possible implication in cell differentiation, genomic imprinting and X chromosome inactivation. Some imprinted genes, such as the U2af1-rs1 in mouse, appear to be both methylated and deacetylated (Gregory *et al.*, 2001; 2002). Furthermore, the level of acetylation of the inactive X chromosome is lower than the active X chromosome (Jeppesen and Turner, 1993). These data suggest that erasure of patterns of acetylation/deacetylation should also be a prerequisite of nuclear reprogramming.

In conclusion the general aim of the experiments described in this chapter was to investigate the possible effect of quiescence on the epigenetic status of donor cells and its possible implications on nuclear reprogramming. The main focus was on the possible effect of quiescence on the expression and sub-nuclear localisation of

the chromodomain proteins belonging to the heterochromatin 1 (HP1) group, and on the acetylation status of histone H4. The HP1 proteins are very similar to the Polycomb group of proteins (Jones *et al.*, 2000), which are both cell cycle regulated (Voncken *et al*, 1999) and developmentally regulated. The regulation of HP1 proteins in relation to quiescence and embryo development is still unknown and so is its possible involvement in nuclear reprogramming. Effect of quiescence on histone acetylation has partially been investigated using electrophoresis (Pogo *et al.*, 1966). However the present aim is to use specific antibodies, developed to investigate changes in histone H4 acetylation during early embryo development in mouse (Worrad *et al.*, 1995) to correlate more specific changes in acetylation induced by cell quiescence with changes observed during reprogramming, after nuclear transfer.

6.2 METHODS

Donor T-cells in G0 and G1 were produced using a protocol optimised in previous experiments (Paragraphs 4.4-4.5; Methods Paragraph 2.13.1). Cell yield, cell cycle and activation features of G0 and G1/CD25$^+$ donor cells were assessed in the first three Nuclear Transfer experiments. Cell counts (mean±SEM) showed that in each NT experiment, an average of 34.7±13.0 x10^6 cells were seeded, 16.8±7.4 x10^6 cells were harvested; 10.0±12.1 x10^6 were processed and 5.5±6.7 x10^6 (54.5%) were selected and used as G1/CD25$^+$ donor cells. FACS analysis confirmed quiescent state of G0 donor cells, and non-quiescent state of G1/CD25$^+$ donor cells (Fig.6.1; Table 6.1).

Donor T-cells were injected into enucleated MII oocytes (for Methods see Paragraph 2.13.2). Reconstructed embryos were cultured in M16 medium for 72h, till the morula/blastocyst stage, and assessed for *in vitro* development (8 replicates; Methods see Paragraph 2.13.4) or fixed, at selected time points, and processed for immunocytochemistry (5-6 replicates; Methods see Paragraph 2.14).

Double staining for chromatin (DAPI) and microtubules (FITC-anti-β-tubulin, Methods see Paragraph 2.14), was used to assess timing of Premature Chromosome Condensation and spindle morphology.

Figure 6.1 Preparation of donor T-cells

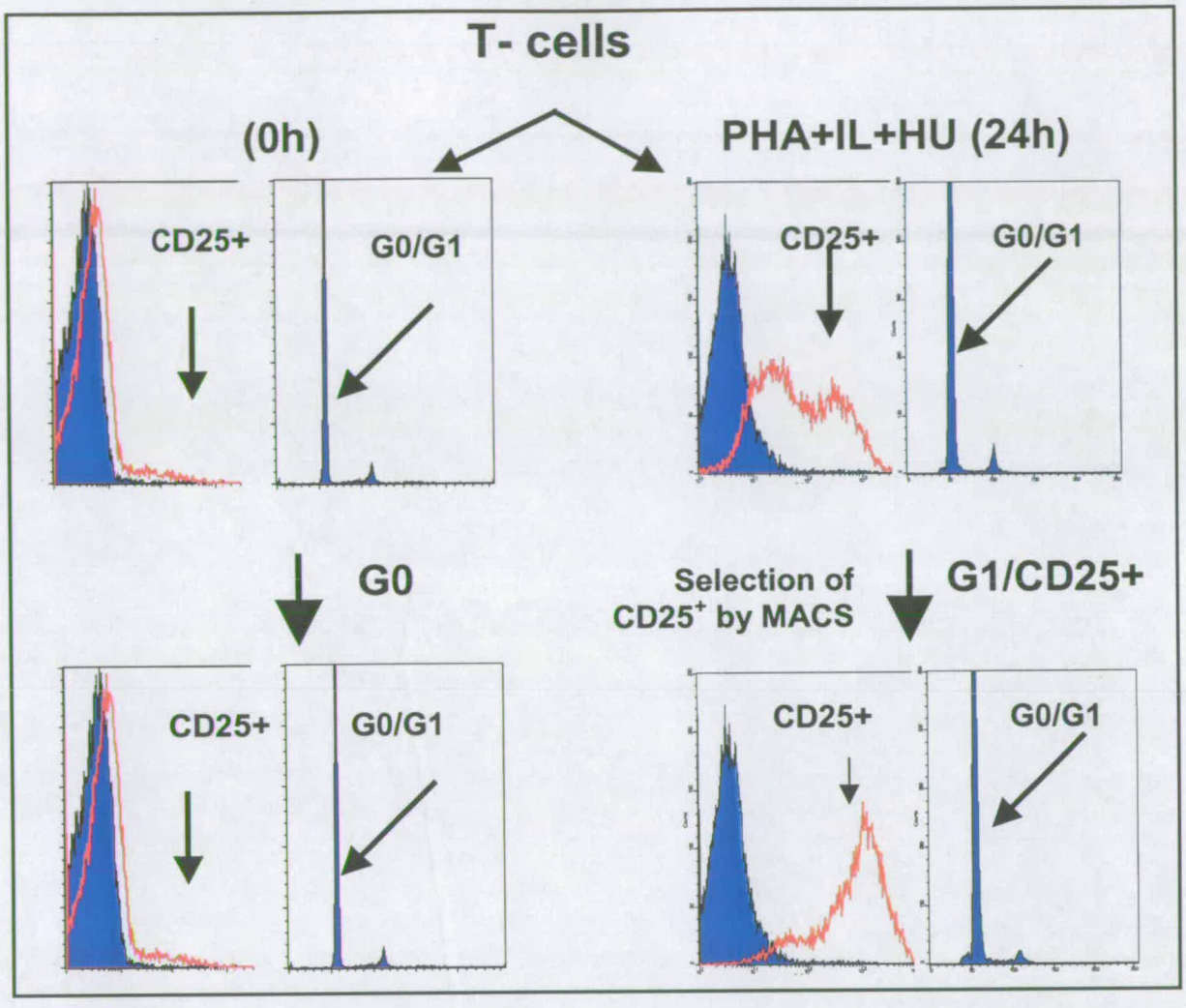

Table 6.1 Cell cycle features of G0 and G1 lymphocytes used in NT experiments

Parameter	G0	G1/CD25$^+$	p
CD3+	85.7±2.6^a	97.4±0.9^b	<0.05
CD25 (%)	17.6±4.1^a	93.3±1.8^b	<0.0001
CD25 Mean FL	97±24^a	474±151^b	0.03
G0/G1 (%)	98.4±0.2^a	94.8±1.4^b	>0.05
S (%)	0.5±0.2^a	0.7±0.2^a	0.55
G2/M (%)	1.2±0.2^a	4.4±1.2^{ab}	0.077
Apoptosis	1.1±1.1^a	8.0±1.1^b	0.04

Figure 6.1 G0 donor cells were freshly isolated lymphocytes (G0, fresh). G1 donor cells, were isolated from cultured 24h in medium supplemented with 1mM hydroxyurea (HU), 8ug/ml phytohemagglutinin (PHA) and 4nM interleukin 2 (IL-2). At the end of the incubation period G1 cells were harvested and CD25$^+$ cells were positively selected using magnetic cell sorting (G1/CD25$^+$).

Table 6.1 FACS analysis of donor cells stained with Propidium Iodide (cell cycle analyses) and anti-CD25 antibody. Results from three replicates experiments expressed as Mean±SEM. Data were transformed using a log (Mean Fluorescence) or logit transformation (%) and analysed using a T-test for independent samples (α=0.05).

To assess changes in histone H4 acetylation, in epigenetic studies, control fertilised embryos, cloned embryos and MII oocytes were double stained for chromatin and histone H4 acetylation (DAPI/anti-H4.Ac double staining; Methods see Paragraph 2.14), using a panel of polyclonal antibodies recognizing different acetylated isoforms of histone H4: anti-histone H4 acetylated on lysine 5 (anti-H4.Ac5), lysine 8 (anti-H4.Ac8), lysine 12 (anti-H4.Ac12), lysine 16 (anti-H4.Ac16). Patterns of expression of these antibodies had been previously described in detail in cells (Thorne *et al.*, 1990; Turner and Fellows 1989, Turner *et al.,* 1989) as well as mouse embryos (Adenot *et al.,* 1997; Worrad *et al.,* 1995; Ma *et al.,* 2001; Wiekowski *et al.,* 1997), but never in NT embryos. Sheep anti-serum to histone H4 acetylated on lysine 2-4 (anti-H4.Ac 2-4), the patterns of expression of which had never been described before, was also used. Samples were then incubated with the corresponding FITC-conjugated secondary antibodies and mounted using Vectashield antifade containing DAPI (Methods see Paragraph 2.14).

Triple staining for chromatin, H4 acetylation and DNA replication (DAPI/anti-H4.Ac/PCNA triple staining) was also carried out on control, fertilised embryos collected and fixed at selected time points, but with very limited results (Methods see Paragraph 2.14).

Changes in chromatin conformation mediated by HP1 proteins, in epigenetic studies, were assessed by triple staining for chromatin, M31 and DNA replication (DAPI/M31/PCNA, triple staining), carried out on whole mounts of MII oocytes, control, fertilised embryos and NT embryos (Methods see Paragraph 2.14).

For *in vivo* developmental studies (2 replicates), 2-cell embryos or morula/blastocyst stage embryos were transferred respectively to the oviducts or uterus of Swiss Webster foster mothers (Methods see Paragraph 2.13.4). Caesarean section of recipient females was carried out 19.5 days post coitus, to look for signs of implantation and foetal development.

Nuclear transfer experiments with mouse embryonic stem cells were carried out in three replicates, in the same weeks in which T-cell nuclear transfer experiments were performed (Methods see Paragraph 2.13.6). The data from these

experiments were included to show efficiency rates of the nuclear transfer system used in our laboratory, in terms of rates of *in vitro* and *in vivo* development after reconstruction.

Fertilised B6D2F1 embryos were used, in four experiments, as a control for epigenetic changes occurring during normal embryo development. Fertilised embryos, collected around the time of pronuclear formation (10-13 h.p.c.), were fixed and processed for immunostaining at selected time points (Methods see Paragraph 2.13.5-2.14).

MII oocytes were also included as activation controls (Methods see Paragraph 2.13.3) and immunostaining controls.

6.3 EFFECT OF QUIESCENCE ON PREMATURE CHROMOSOME CONDENSATION

6.3.1 Aim

Investigate if quiescence has an effect on the timing of premature chromatin condensation (PCC) and on the morphology of the chromosomes and the spindle at the time of PCC.

6.3.2 Experimental Design

Experiments were carried out in two replicates. In each replicate embryos were reconstructed by injecting G0 and G1/CD25$^+$ lymphocytes (2 treatment groups) derived from the lymph nodes of C57BL/6 mice, into MII oocytes of B6D2F1 (C57BL/6 x DBA/2) mice. In each replicate 30 embryos belonging to each of the two treatment groups, derived from G0 or G1-cells, were placed in culture in microdrops (15 embryos/30ul drop) of complete M16 medium immediately after reconstruction. In each replicate, 3 embryos per treatment group were collected at 10min, 30min, 1h, 2h, 3h after reconstruction. Embryos were fixed and double stained with FITC conjugated anti-tubulin antibody (β-tubulin-FITC), which stains in green the microtubules in the mitotic spindle, and Propidium Iodide (PI), that stains in red the

DNA. Embryonic chromatin was classified as being: condensed; organised in a metaphase plate; organised in individualized chromosomes. Furthermore, chromosomes could have a normal or abnormal appearance. Embryos could either have a spindle or not, and the spindle could have normal or abnormal features. In general early embryo development progressed through three stages: 1) condensed chromatin with asters but no spindle; 2) metaphase plate, associated with a mitotic spindle; 3) chromosomes migrating to the two poles of the mitotic spindle. Digitalized images were acquired using a confocal microscope (Nikon EFD3), a x 20 objective, and the Confocal Assistant™ program (Version 4.02; Todd Clark Brelje) and were edited using Adobe Photoshop program (Windows 2000).

6.3.3 Results

Results of double staining for β-tubulin-FITC/PI suggest that events associated with early embryo development occur at an earlier time in G1-derived rather than G0-derived NT embryos (Fig.6.2-6.3). After 10min (Fig.6.2/1B) from reconstruction G1-derived embryos already had multiple asters, and by 30 min (Fig.6.2/2B) microtubules started organizing in a mitotic spindle, even if the chromatin was still condensed. In G0-derived embryos multiple asters were visible 30min after reconstruction (Fig.6.2/2A) and microtubules only appeared in association with the metaphase plate, 1h after reconstruction (Fig.6.2/3A). At 1h after reconstruction the situation was similar in both groups, with the 50% (3/6) of the embryos still with condensed chromatin, 33.3% (2/6) with metaphase plates and only 16.7% (1/6) with individualized chromosomes (Fig.6.3). However, 2h after reconstruction, in the G1-derived embryos, individualized chromosomes, migrating to the opposite poles of the mitotic spindle, were the predominant feature (4/6, 66.6%) and the only feature (6/6, 100%) at 3h after reconstruction (Fig.6.3). On the contrary, in the G0-derived embryos, 50% (3/6) of the embryos were still at the metaphase plate stage at 2h after reconstruction, and chromosomes became the most represented feature (3/6, 50%) only 3h after reconstruction (Fig.6.3). Approximately 1/3 of G0-derived embryos still had a condensed nucleus, that had not undergone PCC yet, 3 hours after reconstruction (Fig.6.3). In the G1-group all embryos

Figure 6.2 Double staining with anti-tubulin-FITC and Propidium Iodide in G0- and G1- derived NT embryos

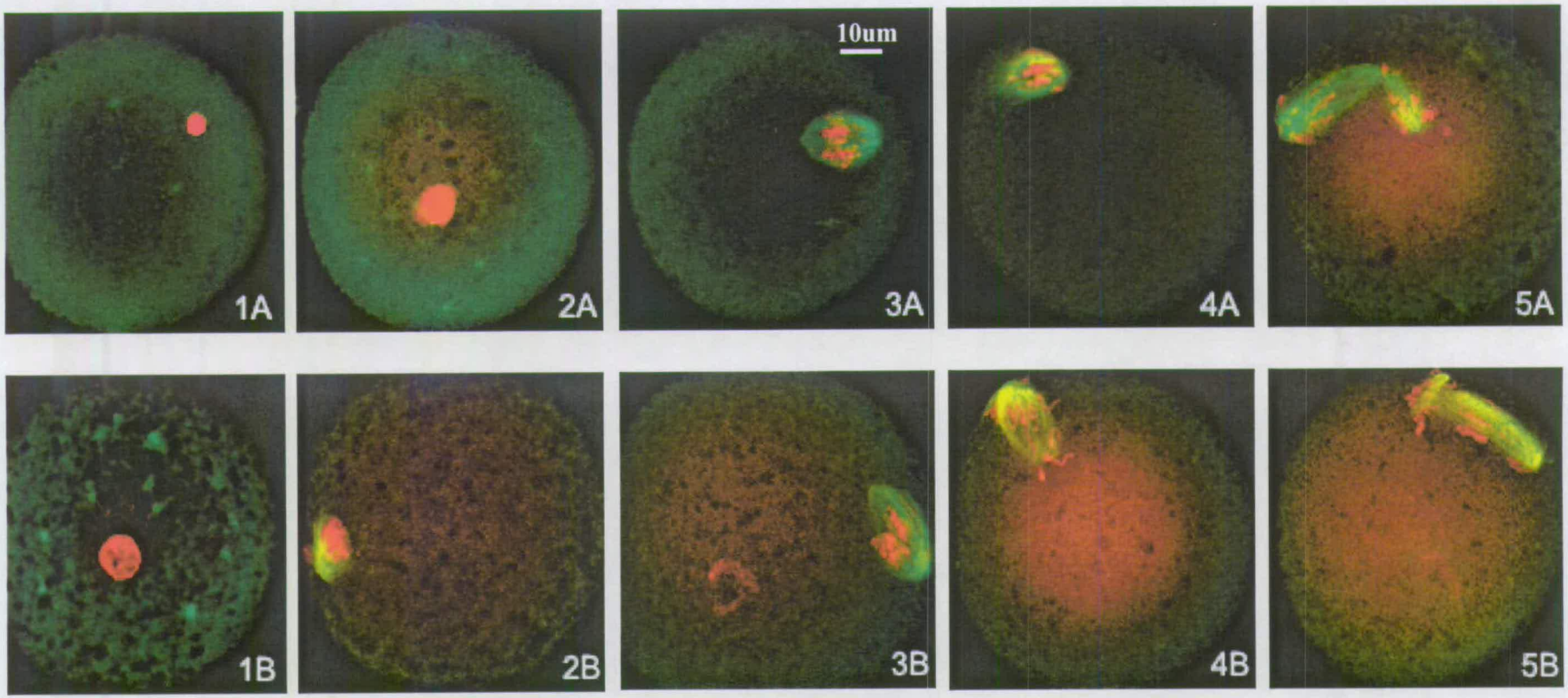

G0- (A) and G1- (B) derived NT embryos stained with anti-tubulin-FITC (green) and Propidium Iodide (red) to assess chromatin conformation and spindle morphology. Embryos were fixed and processed after 10 min, 30 min, 1 hour, 2hours and 3 hours after transfer to an enucleated MII oocyte. Chromatin (red) could be condensed (1A/B, 2A/B), organised in a metaphase plate (3A/B, 4A) or in individualised chromosomes (4B, 5A/B). Chromosomes usually looked abnormal, with their chromatids laying outside the mitotic spindle in a disorganised way. The first sign of spindle formation was the appearance of the asters (A). The Spindle (green) could have a normal (3A/B, 4A/B) or abnormal (5A/B) appearance. Images were taken using a confocal microscope and a x20 objective.

Figure 6.3 Premature Chromosome Condensation (PCC) in G0 and G1-derived NT embryos

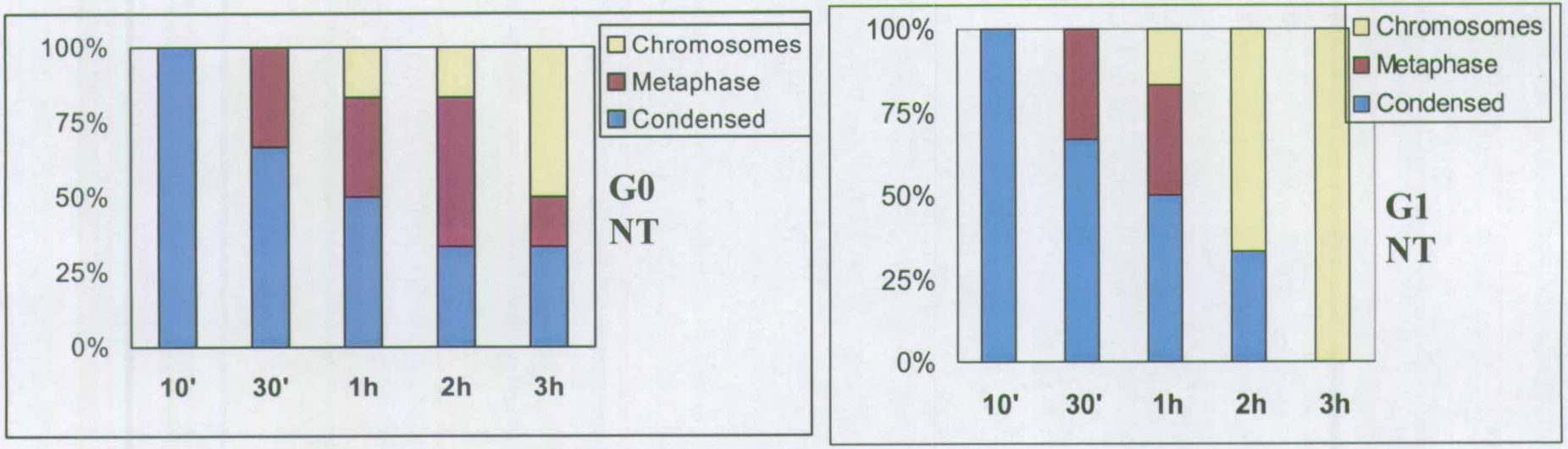

At each time point 6 embryos (replicates=2), embryos fixed and were double stained with DAPI (DNA staining) and FITC-anti-tubulin (spindle) antibodies at selected time point after reconstruction. Based on DNA staining, chromatin organisation levels: 1) condensed; 2) organised in a metaphase plate, with individualised chromosomes just about visible.

underwent full PCC by 3 hours after reconstruction. Finally 100% of individualized chromosomes (Fig.6.2/4B, Fig.6.2/5A-5B), regardless of the cell cycle stage of the donor cells, had abnormal features and were usually associated with abnormal spindles (double spindle, Fig.6.2/5A-5B).

6.3.4 Conclusions

This study showed that quiescence affected the timing of early embryonic events after NT, with regard to PCC. A longer delay (≥3h) between reconstruction and activation might be required if the cells are in a quiescent state, whereas a shorter delay (2h) should be enough for completion of PCC in G1-derived embryos.

In this experiment failure to undergo PCC in 33.3% of G0-derived embryos, even at 3h after reconstruction might be associated with cell membrane retention. Failure to break the membrane of donor cells before injection is more likely to occur with G0 cells as opposed to G1 cells because their smaller size makes it technically more demanding.

Finally, abnormalities in chromosome and spindle morphology, both in G0 and G1-derived embryos, may account for some of the abnormalities in nuclear/cell segregation observed (abnormal karyokinesis and cytokinesis) observed in later stages of development (see Appendix B.1).

6.4 EFFECT OF QUIESCENCE ON THE DEVELOPMENT OF CLONED EMBRYOS

6.4.1 Aims

Compare:

1) *In vitro* developmental potential of G0 and G1-derived NT-embryos (activation, cleavage, 4-cell, morula/blastocyst rates);
2) *In vivo* developmental potential of G0- and G1- NT embryos performing 2-cell stage and blastocyst stage embryo transfers.

6.4.2 Experimental Design

A total of 8 replicate Nuclear Transfer experiments were performed using G0 or G1/CD25$^+$ donor cells derived from the lymph nodes of CBA/Ca (5 replicates), C57BL/6 (1 replicate) or (C57BL/6xCBA) F1 (2 replicates). Donor T-cells were injected into MII oocytes of B6D2F1 (C57BL/6 x DBA/2) mice. Embryos were cultured in M16 to assess *in vitro* development. When possible, blastocysts were fixed and stained with DAPI to assess cell numbers.

In three replicate experiments, using G0-donor cells, and 4 replicate experiments, using G1- donor cells, NT embryos at the 2 and blastocyst stage were transferred to Swiss Webster recipient females to check for implantation sites and development to term.

6.4.3 Statistical analysis

In vitro development data were analysed using the Chi-square test and a Fisher's exact test for 2x2 contingency, in groups where expected frequencies were less than 5. A one-tailed test was performed since, during development, percentages were only expected to decrease (GenStat 4.21, Windows 2000; α=0.05).

6.4.4 Results

In vitro developmental studies (Table 6.2) showed that survival rates after injection were similarly very high in G0 and G1- derived embryos ($p>0.05$). Embryos reconstructed with G0 and G1-lymphocytes also had similar activation rates ($p=0.26$) and similar rates of development to the 4-cell ($p=0.57$), morula ($p=0.17$) and blastocyst stages ($p=0.065$; Table 6.2). The only difference was that G1-derived embryos had significantly higher cleavage rates than G0-derived embryos ($p<0.0001$). Survival rates after injection were significantly lower than those obtained with ES-cells, at least when using donor T-cells in G0 ($p=0.01$). Unlike ES-derived embryos ($p=0.1$), activation rates of T-lymphocyte derived NT embryos were lower than those observed in parthenogenetic and fertilised control embryos, at least when using G0-derived NT embryos ($p<0.0001$). Activation rates

Table 6.2 *In vitro* development of G0- and G1- derived NT embryos

Donor cell	Enucleated	Injected (%)	Activated (%)	2-cell/activated (%)	4-cell/activated (%)	M+BL/activated (%)	BL/activated (%)
Lymphocytes (G0)	436	405 (92.9)[a]	342 (84.4)[a]	249 (72.8)[a]	43/243 (17.7)[a]	12/243 (4.9)[a]	1/243 (0.4)[a]
Lymphocytes (G1)	618	583 (94.3)[ab]	507 (87.0)[ab]	430 (84.8)[b]	65/348 (18.7)[a]	27/348 (7.8)[a]	8/348 (2.3)[a]
Controls (parthenogenetic)	86	-	86 (100)[c]	84 (97.7)[c]	-	81/86 (94.2)[b]	74/86 (86.0)[b]
ES (HM-1)	471	455 (96.6)[b]	441 (96.9)[c]	238 (53.9)[e]	-	143/441 (32.4)[d]	-
Thymocytes[1]	-	176	168 (95.5)	-	-	5/168 (3.0)	-
Spleenocytes[1]	-	80	49 (57.5)	-	-	11 (13.7)	-
Macrophages[1]	-	308	187 (60.7)	-	-	58 (31.0)	-

Results from 8 replicate experiments with G0- and G1-lymphocytes isolated from the lymph nodes of (C57BL/6xCBA) F1, C57BL6 and CBA/Ca female mice (~50-80 embryos/replicate). In the table are also included: data of parthenogenetically activated oocytes of B6D2F1 mice (~10/replicate); data from fertilised embryos (4 replicates); data from NT experiments carried out in the same period with HM-1 ES cells (100 embryos/replicate; 4 replicates); data regarding NT experiments carried out in other laboratories using lymphoid cells isolated from the thymus the spleen and the peritoneal cavity of B6D2F1 females ([1]Wakayama *et al.*, 2001). Of the NT blastocysts we obtained 1/1 G0-derived blastocyst and 5/8 G1-derived blastocyst were fixed to assess cell numbers and 3/8 of G1-derived blastocysts were transferred to the uteri of recipient females for in vivo development (see tab. 6.7). Values within columns with different superscripts differ significantly. Chi-square test or Fischer's exact test for 2x2 contingency (one-tailed), where expected frequencies were less than 5 (α=0.05). Only data acquired in our laboratories were included in the analysis.

Table 6.3 *In vivo* developmental potential of NT embryos

Stage	Enucleated	Injected (%enucleated)	Activated (%injected)	2-cell (% activated)	M+BL (% activated)	Transferred (recipient)	Implantation sites	Live
Lymphocyte (G0)	52	44 (84.6)	42 (95.4)	25 (59.5)	-	25 (1)	-	0
Lymphocyte (G0)	40	35 (87.5)	35 (87.5)	12 (34.3)	-	12 (1)	-	0
Lymphocyte (G0)	103	80 (77.7)	79 (98.7)	62 (78.5)	-	62 (3)	0**	0
Lymphocyte (G1)	62	58 (93.6)	50 (92.6)*	44 (88.0)	6 (12.0)	3 (1)	0***	0
Lymphocyte (G1)	103	81 (78.6)	81 (100)	62 (76.5)	-	26 (1)	-	0
Lymphocyte (G1)	149	116 (77.8)	114 (98.3)	103 (90.3)	-	29 (1)	-	0
Lymphocyte (G1)	57	53 (93.0)	43 (81.1)	37 (86.0)	-	37 (1)	-	0
ES	387	374	364	194	110	102 (6)	0	0
Thymocytes[1]	NA	176	168 (95.5)	NA	5/168 (3.0)	0	-	0
Spleenocytes[1]	NA	80	49 (57.5)	NA	11/80 (13.7)	11 (2)	10 (90.9)	0
Macrophages[1]	NA	308	187 (60.7)	NA	58/308 (31.0)	52 (5)	26 (50.0)	0

Results of embryo transfer experiments with G0-derived (3 replicates) and G1-derived (4 replicates) NT embryos. Experiments with ES cells (HM1) are the result of three replicate experiments.

*Calculated 50/54, instead of 50/58 because 4 were lost.

** Female sacrificed on day 11. Uterus red and oedematous but no implantation signs.

*** Female sacrificed on day 21, but no implantation signs.

§ Implantation and development to term from HM-1 and R1 ES-cell lines were obtained one month after these experiments (Gao *et al.*, 2002).

[1] Wakayama *et al.*, 2001.

of T-lymphocyte NT embryos were also significantly lower than those observed in ES-derived embryos ($p<0.0001$). Cleavage rates of T-lymphocyte derived embryos were lower than those observed in parthenogenetic ($p<0.001$) and fertilised control embryos, but higher than those obtained with ES-derived NT embryos ($p<0.001$). Rates of development beyond the 2-cell stage were lower than those observed both in control embryos and NT embryos derived from ES-cells ($p<0.0001$). The rates of development to morula/blastocyst obtained when using T-lymphocytes were higher that those obtained in previous studies (Wakayama and Yanagimachi, 2001), with similar cell types (e.g. thymocytes). However rates of development to morula/blastocyst obtained with spleenocytes and macrophages were higher than the ones obtained in these experiments with T-cells isolated from the lymph nodes (Table 6.2).

Blastocyst cell numbers appeared to be lower in NT G1- (n=5; 29.0±5.6) and G0-derived (n=1; 34) embryos than in parthenogenetically activated control embryos (n=29; 38.4±9.6).

No development to term or implantation was obtained under any condition, using G0 and G1-T-lymphocytes (Table 6.3). Although neither implantation nor development to term was obtained using ES-cells, in experiments carried out at the time of T-cell nuclear Transfer, pups were obtained from HM-1 cells just one month later.

6.4.5 Discussion

Quiescence did not affect the *in vitro* developmental potential of nuclear transfer embryos. Only cleavage rates of G0-derived NT embryos were significantly lower than those of G1-derived NT embryos. This difference might be due to the fact that the plasma membrane of G0 cells, due to their smaller size, is more difficult to disrupt at the time of injection. Disruption of the donor cell membrane and direct exposure of the donor chromatin to the ooplasm is thought to be crucial for a successful reprogramming (Galli *et al.,* 1999). Previous NT experiments using cattle lymphocytes have linked membrane retention to developmental failure of cloned (Galli *et al.,* 1999). The previous observation that 33% of G0-derived embryos failed

to undergo PCC and retained a condensed chromatin conformation even 3h after reconstruction, while 100% of G1-derived embryos undergoes PCC within 3h from reconstruction (Paragraph 6.3.1), also suggests that technical problems leading to plasma membrane retention may result in lower cleavage rates of G0-NT embryos.

The overall developmental potential of T-lymphocytes, regardless of their cell cycle stage, was low. The high efficiency rates of the enucleation, injection and activation protocols (see Methods 2.13 and Table 6.2) used in these experiments suggests that the choice of donor cell, rather than technical problems, was entirely accountable for the developmental failures observed. Furthermore the *in vitro* development rates obtained with T-lymphocyte derived NT embryos were comparable or even higher those reported in the literature for similar cell types (Wakayama and Yanagimachi, 2001). In particular thymocytes, the majority of which are T-lymphocytes, gave higher activation percentages but lower rates of development to blastocyst stage than the T-lymphocytes isolated from lymph nodes, used in these experiments. This might be due to the fact that thymocytes are in a cycling state, with high percentages of S-phase cells, whereas the cells used in these experiments were synchronized in a G0 or G1 diploid state, therefore less likely to undergo DNA damage after transfer to MII oocytes with high MPF levels. Better developmental rates than the ones obtained in these experiments were achieved only with haematopoietic cell types. Spleenocytes and macrophages, both gave lower activation rates and higher rates of development to the morula/blastocyst stage than the cells isolated from the lymph nodes, used in these experiments. The different nature of the cells used in these experiments might account for the differences observed in the developmental potential of cloned embryos. Cells isolated from the lymph nodes are mostly T-lymphocytes while the spleen contains both T-lymphocytes and B-lymphocytes. As for macrophages, they do not even share the same lineage as lymphocytes, and they belong to the myeloid lineage. Therefore the greater developmental potential observed in these experiments might be due to the presence of B-cells and macrophages.

Comparison of NT embryos derived from T-lymphocytes and ES-cell highlighted some interesting differences. Survival rates after injection were significantly higher for ES-cell derived embryos than for T-lymphocyte embryos.

Rates of pronuclear (PN) formation observed in ES-derived NT embryos were comparable to those of those found in activation controls and higher than those obtained from T-cells. The larger size (~15um) of ES-cells compared to that of T-lymphocytes (~6-8um) might be accountable for this difference, resulting in a lower incidence of membrane retention. Interestingly, T-lymphocytes had very high cleavage rates, significantly higher than those observed in ES-cell derived embryos. The situation was reversed at later stages of development when ES-cell derived NT embryos gave significantly higher rates of development to the morula/blastocyst stages.

Due to the low rates of *in vitro* development and low blastocyst yield, only a limited number of transfers with cloned embryos, mostly at the 2-cell stage, were performed. Regardless of the cell cycle stage, T-lymphocytes isolated from the lymph nodes, used in these experiments, were not able to support development to term. Later reports also confirmed the inability of T-lymphocytes, isolated from the thymus, T and B-cells and macrophages to support development to term (Wakayama and Yanagimachi, 2001). However the question whether haematopoietic cells are able to support development to term still remains controversial. Cattle lymphocytes, isolated from peripheral blood, were able to support development to term of cloned embryos (Galli *et al.*, 1999). Furthermore, recent reports showed that mouse T- and B-lymphocytes were able to support development to term of cloned embryos (Hochedlinger and Jaenisch, 2002). However, pups were only obtained using a complex technique that coupled nuclear transfer and tetraploid aggregation. In this specific experiment ES-cells isolated from the inner cell mass of lymphocyte-derived cloned embryos were injected into tetraploid blastocysts and the resulting embryos were then transferred to recipient females. This suggests that, although possible, reprogramming of haematopoietic cells might require extreme technical solutions, able to enhance their otherwise limited plasticity.

6.5 EFFECT OF QUIESCENCE ON EPIGENETIC STATUS OF CLONED EMBRYOS

6.5.1 Epigenetic status of control, fertilised embryos

6.5.1.1 Experimental design

Control fertilised embryos were collected in four separate experiments (Methods see Paragraph 2.13.5), assessed for *in vitro* development (Table 6.4) and fixed at selected time points (Table 6.5). The time points were chosen around the time of zygotic gene activation, when major changes in transcriptional activation and gene expression are associated with dramatic changes in patterns of histone H4 acetylation (Adenot *et al.,* 1997; Worrad *et al.,* 1995) and chromatin conformation (Adenot *et al.,* 1991; Perreault, 1992). Triple labelling with anti-M31 antibody (MAC 353), anti-PCNA antibody and DAPI was used to assess changes in chromatin conformation (DAPI) mediated by the non-histone protein M31, the mouse homologue of the human hHP1β protein, and onset of DNA replication activity (PCNA) in mouse fertilised embryos. Double staining for chromatin (DAPI) and histone H4 acetylation, on lysines 2-4/5/8/12, was used to detect shifts in histone H4 acetylation patterns. The antibody MAC 353 had never been used before to study chromatin changes taking place during embryo development. The antibodies anti-H4.Ac5/8/12 had been previously used in mouse fertilised embryos (Worrad *et al.,* 1995) and are able to mark the time of zygote gene activation with the appearance of a typical staining pattern at the periphery of the nucleus, as opposed to uniform nuclear staining. The antibody anti-H4.Ac16 had also been used previously in mouse fertilised embryos (Worrad *et al.,* 1995) but unlike the other antibodies it retains a uniform distribution throughout embryo development. The antibody anti-H4.Ac2-4 had never been used before in developmental studies.

Control embryos were used to: establish immunolabelling protocols on whole embryo mounts (M31/PCNA; H4.Ac2-4/5/8/12/16); study changes in chromatin (M31/PCNA) and histone acetylation (H4.Ac2-4) occurring during

Table 6.4 *In vitro* development of fertilised embryos processed for immunocytochemistry

strain	PN (% embryos)	2-cell (%PN)	4-cell (% 2-cell)	M (% 4-cell)	BL (% M)
Total	506/562 (90.0)	313/349 (89.7)	214/226 (94.7)	128/129 (99.2)	98/98 (100)
Fixed	157	87	85	30	40

Table 6.5 Developmental stages at which control embryos were processed for immunostaining for chromatin and acetylation status

	Post-fertilisation (hours)	Post hCG (hours)	Post PN (hours)	Stage	Chromatin staining	Acetylation staining
Day 0, 12.30-13.30	5	17/18	0	PN (early)	M31/PCNA	Ac2-4, Ac5, Ac8, Ac12, Ac16
Day 0, 20.30	11-12	25	6/7	PN (late)	M31/PCNA	Ac2-4, Ac5, Ac8, Ac12, Ac16
Day 1, 16.30	32-33	45	28	2-cell	M31/PCNA	Ac2-4, Ac5, Ac8, Ac12, Ac16
Day 2, 10.00	51	63	46	4-cell	M31/PCNA	Ac2-4, Ac5, Ac8, Ac12, Ac16
Day 3, 10.00	65	87	70.	M	M31/PCNA	Ac2-4, Ac5, Ac8, Ac12, Ac16
Day 4, 10.00	89	111	94	BL	-	-
Unfertilised eggs	-	-	-	MII	M31/PCNA	Ac2-4, Ac5, Ac8, Ac12, Ac16,

Tables 6.4-6.5 Results of four replicate experiments. Animals were injected with hCG and mated at 19.30. Fertilisation takes place 10-13 hours post hCG/mating, so around 5.30-8.30 (day 0). Embryos were collected around the time of pronuclear formation, 4-5 hours after fertilisation, approximately at 13.0-13.30 (day 0) and then cultured *in vitro*. Only in one instance embryos were collected earlier, at 10-10.30 (day 0). As a result of this a lot of embryos were not fertilised (*). Cultured control embryos were assessed for development (Tab. 6.8) and fixed and processed for immunostaining at selected time points (Tab. 6.9). In the table we have omitted that a total of 7 embryos, 6 at the two cell stage and 1 at the 4-cell stage, were used as staining controls and were incubated with the secondary antibodies in the absence primary antibodies: GAR-FITC (n=2); GAR-TXR (n=2); TXR/FITC-anti-rat (n=2); GAS-FITC (n=1).

development, that had never been described before; select antibodies and protocols to use efficiently on nuclear transfer embryos.

6.5.1.2 Statistical Analysis

Data were analysed using a Pearson Chi-square test. In groups where expected frequencies were less than 5, data were analysed using a Fisher's exact test for 2x2 contingency (GenStat 4.21, Windows 2000). In particular a modified, non-randomised version of this test, namely the mid-P-value test (Hirji *et al.,* 1991), was used, since it is considered less conservative and with an actual level of significance closer to the nominal value, as compared with the classical test. Furthermore, because the percentage of embryos positive for a specific marker was expected to either increase or decrease, a two-tailed test was performed.

6.5.1.3 Results

Shifts in the percentages of $PCNA^+$ and $M31^+$ cells occurred simultaneously (Fig.6.4-6.6). Before fertilisation, 100% (12/12) MII oocytes were $M31^-/PCNA^-$ (Fig.6.4 F-M). After fertilisation, at the early pronuclear stage, 16h after hCG, 66.6% (8/12) of the embryos was $M31^+/PCNA^+$ (Fig.6.4 G-N). The percentage of $M31^+/PCNA^+$ increased significantly (16/16, p=0.024) by the late pronuclear stage, 24h post hCG (Fig.6.4 H-O), and then remained constantly high, at the 2 (12/12), 4 (14/14) and morula (5/5) stages. Similarly to what previously seen in quiescent and non-quiescent T-cells (Paragraph 5.2), M31 had two different distribution patterns: a "diffused" nuclear distribution, where M31 was uniformly spread throughout the nucleus; a "condensed" distribution, where M31 was organised in clusters, colocalised with patches of condensed chromatin (DAPI). The "condensed" M31 distribution resembled the distribution patterns observed in quiescent T-cells (Fig.6.5), previously described (Paragraph 5.2). Apart from quantitative changes in the percentages of $M31^+$ cells, occurring around the time of zygote gene activation, qualitative changes in the distribution patterns of M31 were also observed (Fig.6.6). At the early and late pronuclear stages only the "diffused" distribution was observed (8/8; 16/16). The only difference between the early and late pronuclear stages was that the proportion of "diffused" $M31^+$ cells (8/12 vs

Figure 6.4 Immunostaining for M31/PCNA/DAPI in control embryos

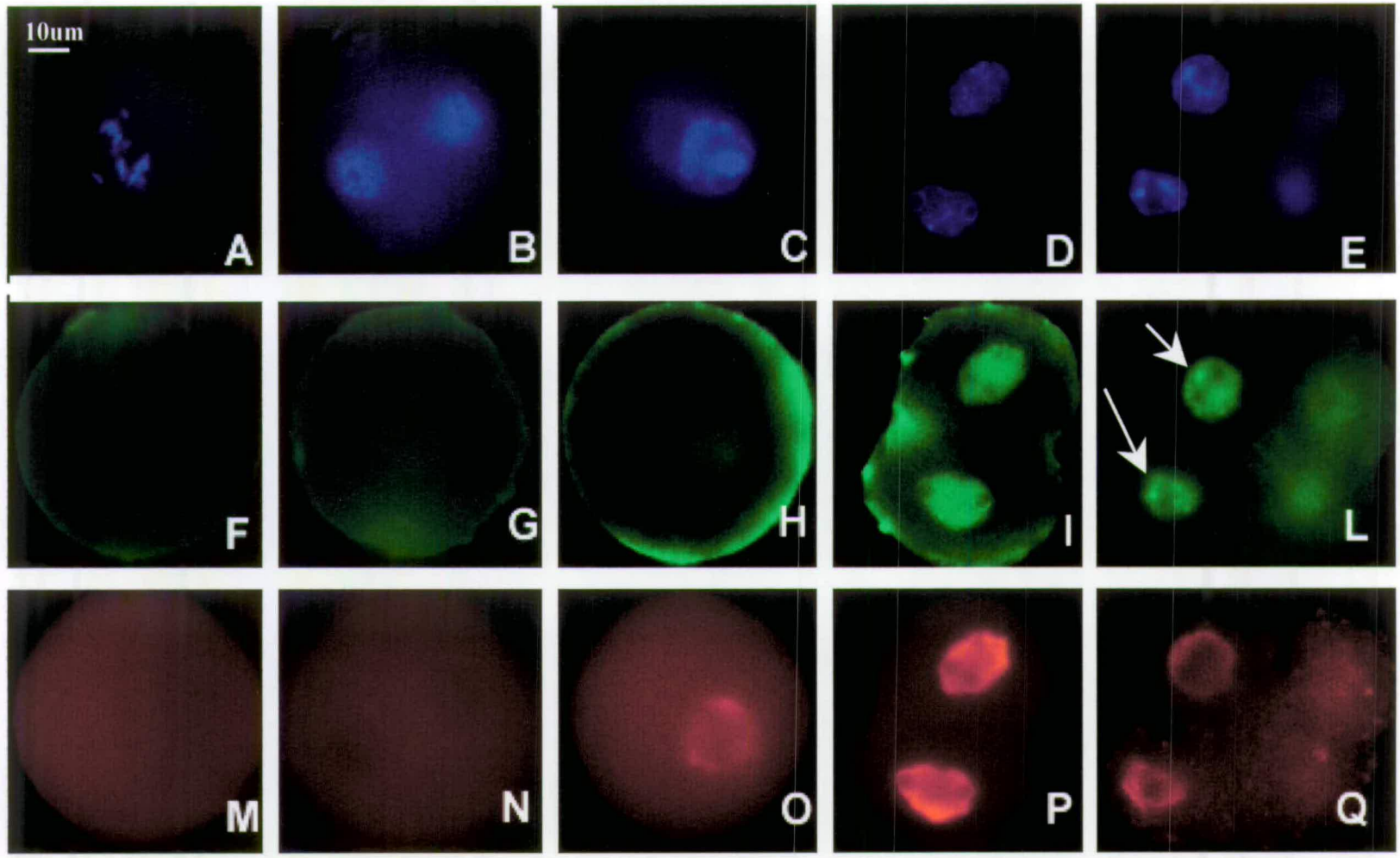

A-E DAPI staining; F-L anti M31-FITC staining; M-Q PCNA staining; A, F, M, MII oocyte; B, G, N, 1-cell stage (16h post-hCG); C, H, O, 1-cell stage (24h post-hCG); D, I, P, 2-cell stage (45h post-hCG); E, L, Q, 4-cell stage (64h post-hCG). Conclusions: M31 staining becomes clear at the onset of zygotic gene activation (ZGA). After ZGA, at the 4-cell stage, nuclear distribution of M31 looks like that of quiescent chromatin. Arrows indicate appearance of clusters of M31 at the 4-cell stage, showed in more detail in Fig.6.5.

Figure 6.5 After ZGA, 4-cell embryo nuclei look like nuclei of quiescent cells

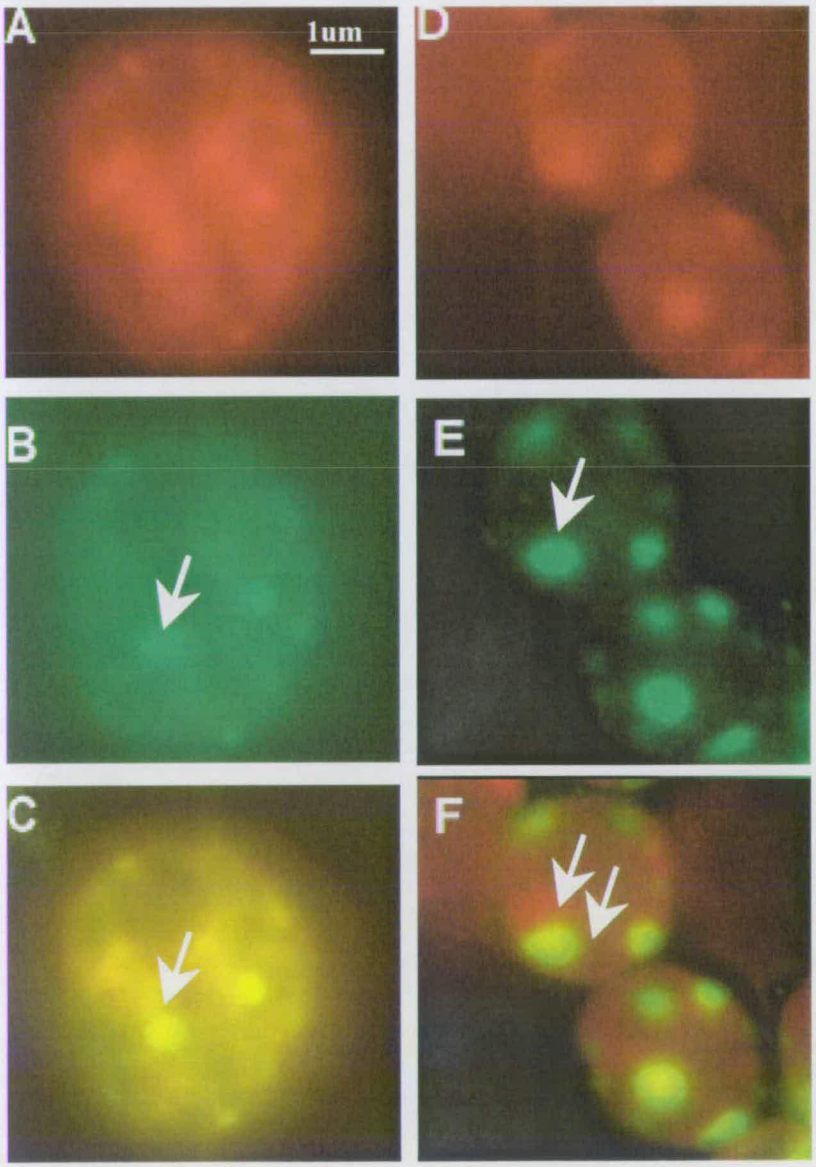

A-C, nuclei of 4-cell embryo; D-F nuclei of G0 T-cells. A, D, DAPI staining in red pseudo colour; B, E anti-HP1 beta –FITC staining; C, F merged images of DAPI/HP1-beta staining. Conclusion: after ZGA, HP1-beta colocalises again with patches of condensed chromatin (arrows).

Figure 6.6 Results of M31/PCNA immunostaining in control embryos

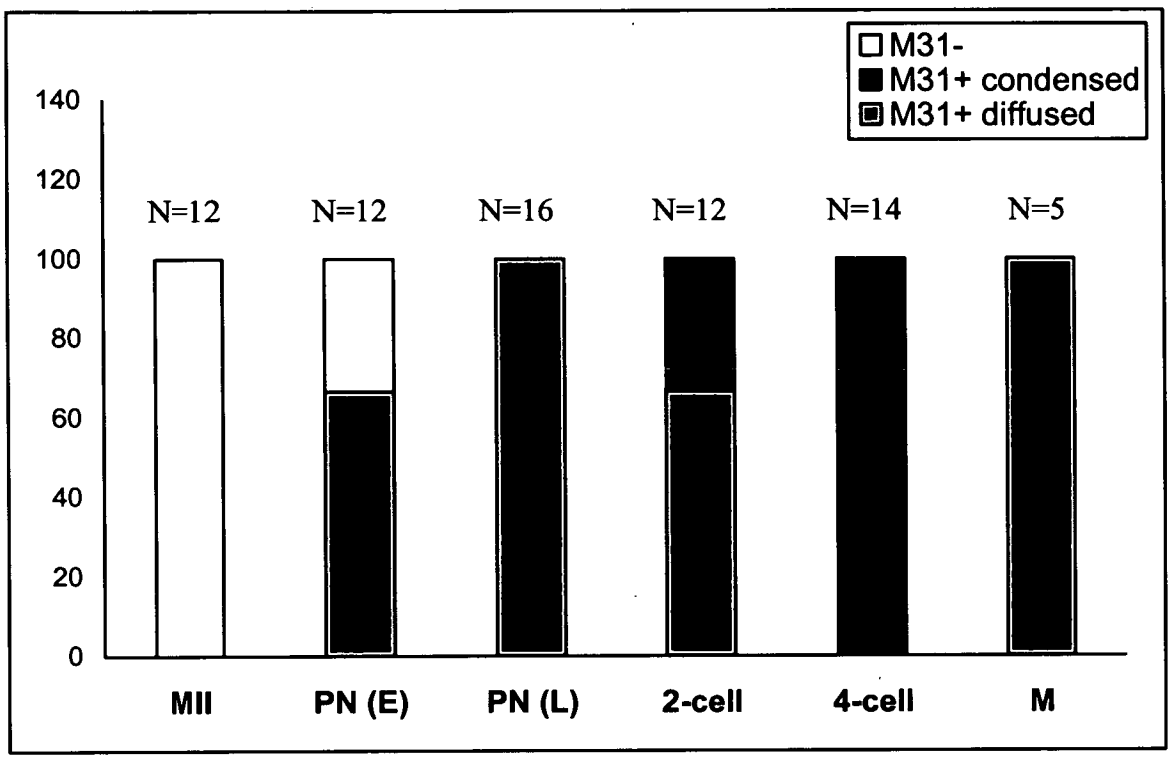

Results of triple staining of control fertilised embryos with DAPI/anti-M31/PCNA (4 experiments). Embryos were classified according to the presence ($M31^+$) or absence ($M31^-$) of M31 staining. $M31^+$ embryos were also classified according to the sub-nuclear as distribution of M31: "condensed", with M31 organised in clusters, colocalised with pericentromeric heterochromatin; "diffused", with M31 uniformly diffused in the nucleus. Results of PCNA staining are presented elsewhere (Paragraph 6.5.1).

16/16) was significantly higher in the latter (p=0.024). The main changes in M31 distribution were observed at the 2 and 4-cell stages, around the time of zygote gene activation. The overall proportion of $M31^+$ remained constant between the late PN stage and the 2-cell stage, remained constant (16/16 vs 12/12). However, a significant decrease in the proportion of $M31^+$ cells with "diffused" distribution (16/16 vs 8/12, p=0.024) and the appearance $M31^+$ cells with "condensed" distribution (4/12) were observed at this stage. This trend was maintained at the 4-cell stage where a further decrease in the proportion of $M31^+$ cells with "diffused" distribution (8/12 vs 0/14, $p<0.001$) and a further increase in the percentage of $M31^+$ cells with "condensed" distribution (4/12 vs 14/14, 33.4 vs 100%, $p<0.001$) occurred. The appearance of clusters of M31 was restricted to the 2 and 4-cell stages, since it was no longer detectable at the morula stage (0/5). Changes in the distribution patterns were also observed for the PCNA staining, but these were not quantified. Briefly PCNA appeared to concentrate at the periphery of the nucleus, with a ring-like structure, at the PN, 2-cell stage and in some of the nuclei at the 4-cell stage, whereas it had a uniformly diffused distribution in at the morula stage and in some of the nuclei at the 4-cell stage.

Staining for acetylation on lysines 8 and 16 (anti-H4.Ac8/16) gave inconsistent results that were excluded from the statistical analysis (data not shown). Immunolabelling of mouse fertilised embryos with anti-H4Ac.5 and anti-H4Ac.12 (Fig.6.7) gave similar results to those previously described (Worrad *et al.,* 1995). For each of these antibodies changes in the proportion of cells positive for acetylation staining (total Ac^+), as well as qualitative changes observed in the distribution patterns of these antibodies, were assessed (Fig.6.8). Staining of Ac^+ cells could be classified according to two different distribution patterns (Worrad *et al.,* 1995): a "diffused" distribution pattern, when the staining was uniformly distributed in the nucleoplasm; a "peripheral" distribution pattern, when the staining was restricted to the nuclear periphery (Fig.6.7 4C-5C, 3D-5D). Results (Fig.6.8) obtained with anti-H4Ac.5 and anti- H4Ac.12 were very similar. Before fertilisation, MII oocytes appeared to be deacetylated on lysines 5 (0/6) and 12 (0/6). After fertilisation, at the early PN stage, the proportion of $Ac5^+$ and $Ac12^+$ cells increased, though not significantly (p=0.27), to 4/14 (28.6%) and 3/12 (25%). Between the

Figure 6.7 Immunostaining for histone H4 acetylation in control embryos

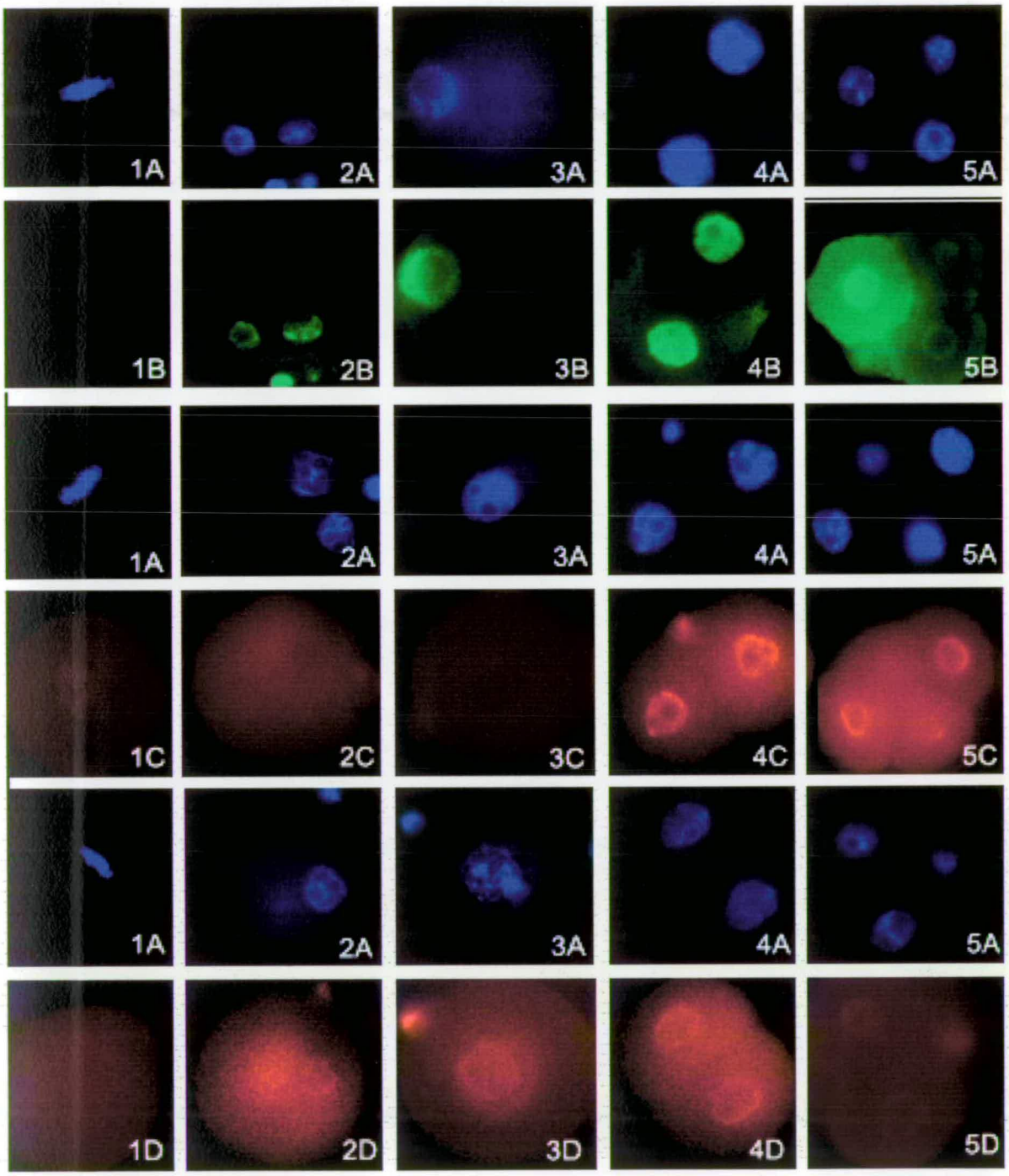

DAPI staining (A); anti-H4 (Ac 2-4)-FITC staining (B); anti H4 (Ac5)-TXR staining (C); anti H4 (Ac12)-TXR (D). 1) MII oocytes; 2) 1-cell embryos at an early PN stage 16h after hCG); 3) 1-cell embryos 7-8h after PN formation (24h after hCG); 4) 2-cell stage (after 45h after hCG); 5) 4-cell stage (64h after hCG). Peripheral nuclear staining was observed for H4.Ac5 (4C-5C) and H4.Ac12 (4D), at the 2 and 4-cell stages (Ac5), and H4.Ac2-4, at the pronuclear stage (2B-3B). These data confirmed that patterns of acetylation of histone H4 on lysines 5 and 12 could be used as markers of zygote gene transcriptional activation.

Figure 6.8 Results of immunostaining for histone H4 acetylation in control embryos

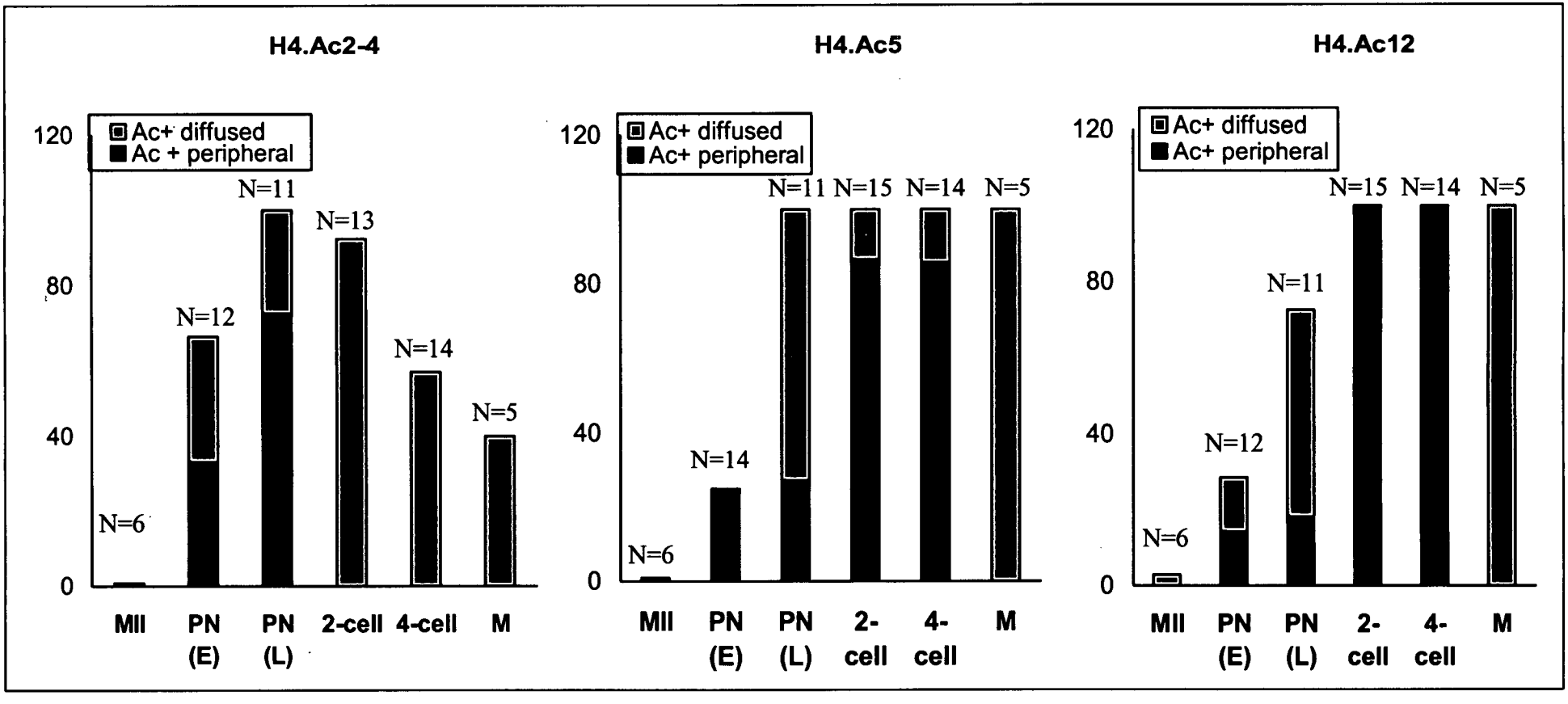

Control, fertilised embryos were fixed and double stained with DAPI and antibodies recognising histone H4 acetylated on lysines 2-4 (H4.Ac2-4), 5 (H4.Ac5) and 12 (H4.Ac12). Embryos were classified according to the presence (Ac^+) or absence (Ac^-) of acetylation staining. AC^+ embryos were also classified according to the sub-nuclear acetylation patterns: "peripheral", with acetylation staining concentrated at the periphery of the nucleus, in a ring-like structure; "diffused", with acetylation staining uniformly diffused in the nucleus. Appearance of peripheral acetylation staining for Ac5 and Ac12 has been correlated with onset of Zygote Gene Activation.

early and late PN stages the proportion of $Ac5^+$ and $Ac12^+$ cells increased significantly ($p<0.001$) to 11/11 (100%) and 8/11 (72.7%). Acetylation on lysine 12 reached a plateau (100% $AC12^+$) at the 2-cell stage, at a slightly later stage than acetylation on lysine 5 (late PN stage). At the 4-cell and morula stages, the percentages of $Ac5^+$ and $Ac12^+$ embryos remained high (14/14; 5/5).

MII oocytes were negative for acetylation staining on lysine 5 and lysine 12. Early PN stage was characterised by very low percentages of "peripheral" and "diffused" $Ac5^+$ (3/12; 0/12) and $Ac12^+$ cells (2/14; 2/14). The late PN stage was characterised by an overall increase in the percentages of $Ac5^+$ and $Ac12^+$ cells, mainly resulting from a significant increase in the proportion of "diffused" $Ac5^+$ (0/12 vs 8/11; $p=0.040$) and $Ac12^+$ (2/14 vs 6/11; $p=0.048$), while the proportion of "peripheral" $Ac5^+$ (3/12 vs 3/11; $p=0.91$) and $Ac12^+$ (2/14 vs 2/11; $p=0.81$), cells remained unchanged. At the 2 and 4-cell stages the trend was inverted: the proportion of "peripheral" $Ac5^+$ and $Ac12^+$ (13/15, 15/15; $p=0.002$; $p<0.001$) at the 2 and 4-cell stages (12/14; 14/14, $p=0.005$, $p<0.001$) were significantly higher than those observed at the late PN stage while the proportion of "diffused" $Ac5^+$ and $Ac12^+$ at the 2 (2/15; 0/15; $p=0.004$, $p=0.002$) and 4-cell stages (2/14, 0/14; $p=0.003$, $p=0.005$) were significantly lower than those observed at the late PN stage. At the morula stage, though all of the embryos were acetylated, they only displayed the "diffused" distribution (5/5) while the "peripheral" distribution was no observed at this stage (0/5).

Results of the staining with the anti-H4.Ac2-4 antibody (Fig.6.7-6.8), suggested a possible involvement of acetylation on lysines 2-4 at an earlier stage of development, than acetylation on lysines 5 and 12. Similarly to what was observed with anti-H4.Ac5 and anti-H4.Ac12 antibodies, changes in the proportion of $Ac(2-4)^+$ embryos and qualitative changes observed in the distribution patterns of this antibody were observed. Also for this antibody a "diffused" distribution pattern (Fig.6.7 4B-5B), characterised by a uniform nuclear staining, and a "peripheral" distribution pattern, with staining restricted to the nuclear periphery (Fig.6.7 2B-3B), were observed. The proportion of $Ac(2-4)^+$ cells increased significantly between the MII stage, before fertilisation, and the early PN stage (0/6 vs 8/12, $p=0.011$), reaching a peak at the late PN stage (11/11). These data were similar to what

observed with anti-H4.Ac12/Ac5 antibodies. The proportion of Ac(2-4)$^+$ cells decreased slightly at the 2 cell stage (12/13, p=0.542) and, by the 4-cell (8/14, p=0.017) and morula stages (2/5, p=0.18), reached levels significantly lower than those observed at the late PN stage and comparable to those observed at the early PN (p=0.648; p=0.374) stage. This trend was different from what observed with anti-H4.Ac5 and anti-H4.Ac12, where acetylation levels never decreased after reaching a plateau, respectively at the late PN and 2-cell stages.

When considering distribution patterns of the anti-H4.Ac(2-4)$^+$ staining (Fig.6.8), it was observed that the proportion of cells displaying the "peripheral" pattern increased significantly between the MII stage (0/6), before fertilisation, and the early PN stage (4/12, p=0.011), reaching maximal levels at the late PN stage (8/11). However, at later stages of development, the "peripheral" distribution pattern was no longer observed (0/13; 0/14; 0/5). On the contrary the "diffused" distribution pattern was present in a low proportion of cells at the early and late PN stages (4/12-3/11) and reached a peak (12/13) at the 2-cell stage. At the 4-cell (8/14) and morula stages (2/5) the proportion of "diffused" Ac(2-4)$^+$ embryos gradually decreased to levels comparable to those observed at the early (p=0.26; p=0.81) and late PN stages (p=16; p=65) and significantly lower than the ones observed at the 2-cell stage, at least at the morula stage (p=0.046).

6.5.1.4 Conclusions

These experiments showed that important changes occur in the chromatin status and the acetylation status of fertilised mouse embryos, around the time of zygote gene activation (late-PN/2-cell stage). Results of the M31 staining in fertilised embryos showed that transition between early and late PN stages is characterised by a significant increase in the percentages of "diffused "M31$^+$ cells. At the 2 and 4-cell stages, the diffused distribution pattern gradually decreased, while the condensed pattern appeared. Clusters of M31 seemed to be temporally restricted to the 2 and 4-cell stages. Appearance of these clusters might be correlated with the establishment of gene silencing patterns associated with differentiation. There are no reports in the literature showing changes in non-histone proteins during early development in the mouse, so these data represent the first ones of this kind.

PCNA staining suggested that DNA replication started at the early PN stage (5h post-fertilisation, 17/18h post-hCG, 0h post-PN formation) and by the late PN stage all of the cells were $PCNA^+$ and remained so in all the following stages analysed. However, these results are inconclusive since the cross-linking reagents used in these experiments fix the soluble form of PCNA, constitutively expressed throughout the cell cycle (see Paragraph 2.11).

Staining for acetylation of histone H4 on lysines 5 and 12 gave very similar results, and different from the ones obtained when assessing acetylation on lysine 4. The acetylation staining with anti-H4.Ac5 and anti-H4.Ac12 showed that the late PN stage is characterised by an overall increase of H4 acetylation on lysines 5 and 12, mainly due to a significant increase in the percentage of cells with a "diffused" $Ac.5^+$ and $Ac.12^+$ staining pattern. Though the overall levels of histone H4 acetylation on lysines 5 and 12 remained unchanged at the 2-cell stage, an inversion in the distribution patterns, with a significant increase in $H4.Ac5^+$ and $H4.Ac12^+$ peripheral staining, and a significant decrease in "diffused" staining pattern were observed. The situation at the 4-cell stage was comparable to the one observed at the 2-cell stage with similar, high percentages of $Ac5^+$ and $Ac12^+$ cells with "peripheral" staining pattern and similar, low percentages of cells with "diffused" staining pattern. Beyond the 4-cell stage only high percentages of $H4.Ac5^+$ and $H4.Ac12^+$ cells with "diffused" distribution patterns, similar to those observed at the late PN stage were detected. These data suggest that acetylation of histone H4 on lysines 5 and 12 at the periphery of the nucleus, though present also at earlier stages, is a main feature of the 2-cell stage. This is not surprising considering that appearance of peripheral staining after immunolabelling for H4.Ac5/12 has been correlated with transcriptional activation (Worrad *et al,* 1995), occurring in mouse at the late PN/2-cell stage. However previous reports also indicated that this staining pattern disappeared by the 4-cell stage while the data of these experiments suggest its persistence till the 4-cell stage. This discrepancy might arise from the fact that at the 4-cell stage only some nuclei (1/4, 2/4) appear to be acetylated on lysines 5 and 12, at the periphery of the nucleus. This discrepancy might stem from subjective differences on the classification of these partially stained embryos.

The anti-H4.Ac2-4 staining gave different results from those obtained with anti-H4.Ac5 and anti-H4.Ac12 staining. Overall acetylation on lysines 2-4 reached a peak at the late PN stage, remained high at the 2-cell stage and then decreased. Acetylation on lysines 5 and 12 reached a peak at the later, 2-cell stage and then remained high, at least till morula stage. Similar staining patterns to those observed on lysines 5 and 12, a peripheral and a diffused pattern, were also observed but with different shifts in distribution patterns. High percentages of cells with peripheral distribution of H4.Ac2-4 staining were restricted to the early and late PN stages, instead of the 2 and 4-cell stages. The increase in this pattern was more evident at the late PN stage, when percentages reached a peak. The 2-cell stage was characterised by high percentages of $Ac(2\text{-}4)^{+}$ cells with a "diffused" distribution pattern significantly higher then the ones observed at earlier stages of development. Beyond the 2-cell stage these percentages decreased to levels similar to the ones observed at the PN stages.

Observations regarding acetylation of histone H4 at lysines 2-4 (H4.Ac2-4) have never been described before. Only changes in histone H3 acetylation (Stein *et al.*, 1997) at lysines 9 and/or 18 (H3.Ac9/18) and histone H4 acetylation (Adenot *et al.*, 1997; Worrad *et al.*, 1995) at lysines 5, 8, 12 (H4.Ac5/8/12) had been described during mouse embryo development. These findings suggest that acetylation Ac2-4 can be used as a marker of early ZGA events (late PN), Ac5/12 marker of late activation events (2-cell stage). One of the aims of these experiments was to select appropriate acetylation markers, associated with transcriptional activation, to use in conjunction with M31/PCNA to study epigenetic reprogramming in lymphocyte-derived nuclear transfer embryos. Considering the limited availability of material from nuclear transfer experiments, it was decided to use only the anti-H4.Ac5/12 antibodies. The main reason for this was that dramatic chromatin changes, highlighted by changes in M31 sub-nuclear distribution, mainly occurred at the 2 and 4-cell stages when changes in Ac5 and 12 also occur.

Table 6.6 *In vitro* development of NT embryos processed for immunostaining for chromatin and acetylation status

Cell cycle stage		Injected	PN (%injected)	2-cell (%PN)	4-cell (%2-cell)	M (% 4-cell)	BL (%M)
G0	Total (%)	195	61/176 (34.7)	49/61 (80.3)	12/33 (36.4)	-	-
G0	Fixed	19	-	16	12	-	-
G1	Total (%)	183	133/161 (82.6)	114/133 (85.7)	24/89 (27.0)	-	-
G1	Fixed	22	-	25	24	-	-
Control	Total (%)	41	40/41 (97.5)	40/40 (100)	40/40 (100)	40/40 (100)	40/40 (100)

Table 6.7 Developmental stages at which NT embryos were processed for immunostaining for chromatin and acetylation status

	Stage	Post-activation (h)	Post-hCG (h)	Post-PN (h)	Chromatin staining	Acetylation staining
Day 0, 10.00-10.30	Condensed	-3/2.5	15/15.5	- 7.5/8	M31/PCNA	-
Day 0, 11.00-13.00	1-cell (M)	-2/0	16/19	-5/7	M31/PCNA	-
Day 0, 18.00	PN (early)	5	22.5	0	-	-
Day 0/1, 00.00-1.00	PN (late)	11-12	29	6/7	-	-
Day 1, 22.00	2-cell	33	50.5	28	M31/PCNA	H4.Ac5, H4.Ac12
Day 2, 16.00	4-cell	51	68.5	46	M31/PCNA	H4.Ac5, H4.Ac12

Tables 6.6-6.7 Experiments were carried out in two replicates using donor oocytes and C57BL/6 donor lymphocytes. Animals were injected with hCG at 19.30. The next day embryos were reconstructed around 10.00-12.00 (day 0) and activated 1-3 hours after reconstruction (13.00, day 0) by culture in Sr2+ for 5 hours (13.00-18.00). Pronuclei were visible towards the end of the activation period (18.00, day 0). Embryos were assessed for development (Tab. 6.6) and fixed and processed for immunostaining (Tab. 6.7). Developmental potential of NT embryos was not assessed beyond the 4-cell stage in this experiment because all the developing embryos were fixed earlier stages of development. Embryos were stained at two time points before activation, between 0 and 3 hours after reconstruction (10.00-13.00, day 0), and at two time points after activation (2-cell, 4-cell).

6.5.2 Immunostaining of nuclear transfer embryos

6.5.2.1 Experimental design

Embryos reconstructed from G0 and G1 cells (Methods see Paragraph 2.13; Table 6.6), in two separate experiments, were fixed at selected time points and processed for immunolabelling (Methods see Paragraph 2.14; Table 6.7) at two time points shortly after reconstruction, to assess changes in M31 distribution and histone H4 acetylation immediately after transfer (1-cell/condensed, 0-30' after reconstruction; 1-cell/PCC, 1-3h after reconstruction) and detect immediate chromatin remodelling events after NT. Embryos were also stained at the 2-cell and 4-cell stage (Table 6.7), to assess chromatin-remodelling events taking place around the time of ZGA. Results obtained at the 2- and 4-cell stages were compared with those obtained at similar stages in fertilised, control embryos.

6.5.2.2 Statistical Analysis

Because sample sizes were very small and in most cases expected frequencies were less than 5, they were analysed using a Fisher's exact test for 2x2 contingency (GenStat 4.21, Windows 2000). In particular, the mid-P-value test was performed since it is less conservative and with an actual level of significance closer to the nominal value than the classical test (Hirji *et al.*, 1991). Furthermore, because the percentages of embryos positive for a specific marker were expected to either increase or decrease, a two-tailed test was used.

6.5.2.3 Results

Results of triple staining for M31/PCNA/DAPI of G0 and G1-NT embryos, showed that between 0-3h min after reconstruction and at the 2-and 4-cell stages are shown respectively in (Fig.6.9A-6.9B). During the first 0-30 min after reconstruction G1-derived embryos (Fig.6.9A, 3A-3C) still appeared to be $M31^+$ (4/5), with a diffused distribution pattern, while none (0/5) of G0-derived embryos (Fig.6.9A, 1A-1C) were $M31^+$. Between 1-3h after reconstruction, when embryos are reaching PCC stage, and chromatin is organised in individualized chromosomes, both G0

Figure 6.9A Immunostaining for M31/PCNA/DAPI in NT embryos: 0- 3h after reconstruction

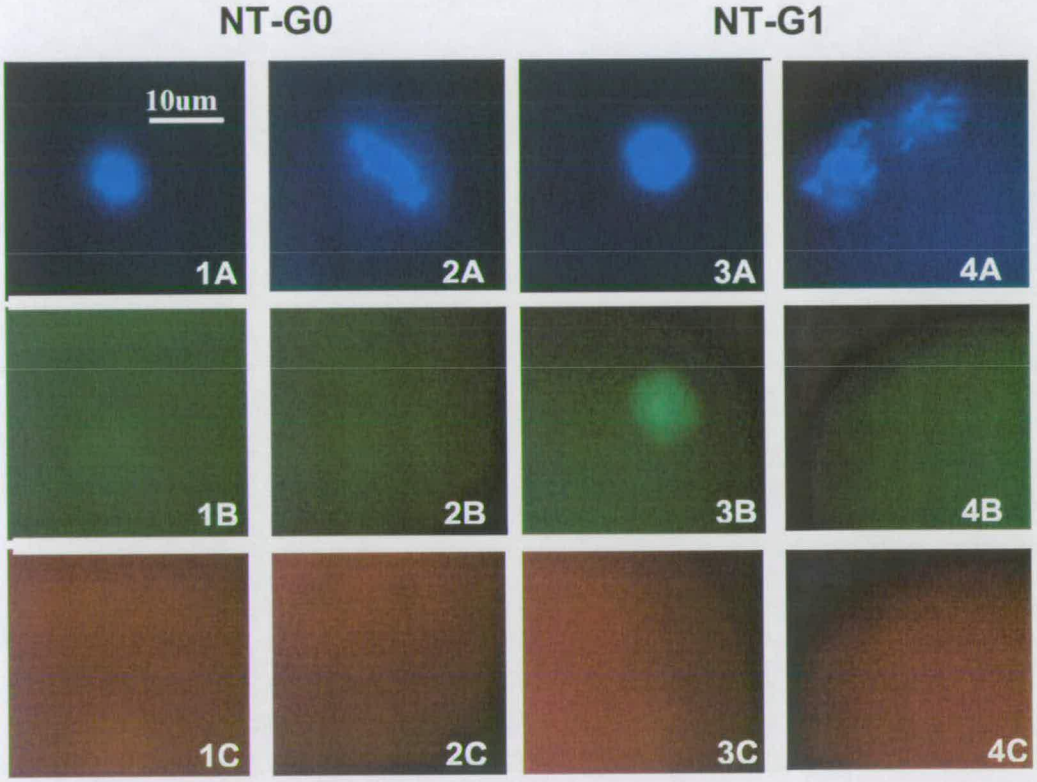

NT embryos were triple stained with DAPI (blue, A), M31-FITC (green, B) and TXR-PCNA (red, C) to assess respectively chromatin structure, M31 sub-nuclear localisation and presence of DNA replication. G0 (1-2) and G1 (3-4) NT embryos were fixed 0-30min (1, 3) after reconstruction, when chromatin is still condensed, and 2-3h (2, 4) after reconstruction, at the PCC stage.

Figure 6.9B Immunostaining for M31/PCNA/DAPI in NT embryos: 2 and 4-cell stages

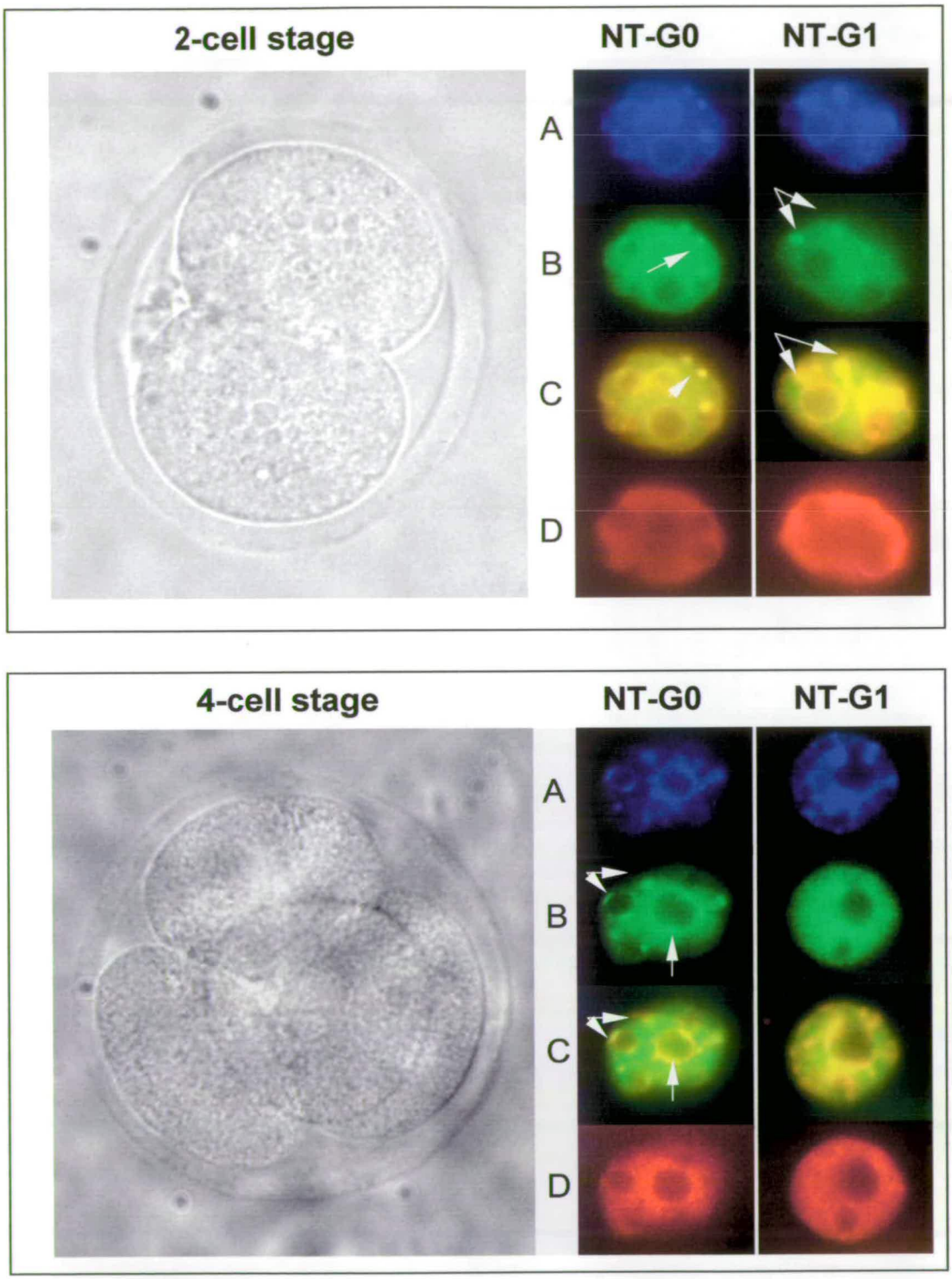

G0 and G1-NT embryos were fixed at the 2- and 4-cell stage and triple stained with DAPI (blue, A), M31-FITC (green, B) and TXR-PCNA (red, D). Figure C shows a merged image of FITC-M31 (green) and DAPI, represented in this picture with a pseudo-colour red. The yellow colour corresponds to areas of colocalisation of M31 and heterochromatin. Arrows point to M31 clusters.

Figure 6.10 Comparison of M31/PCNA immunostaining in control and NT embryos

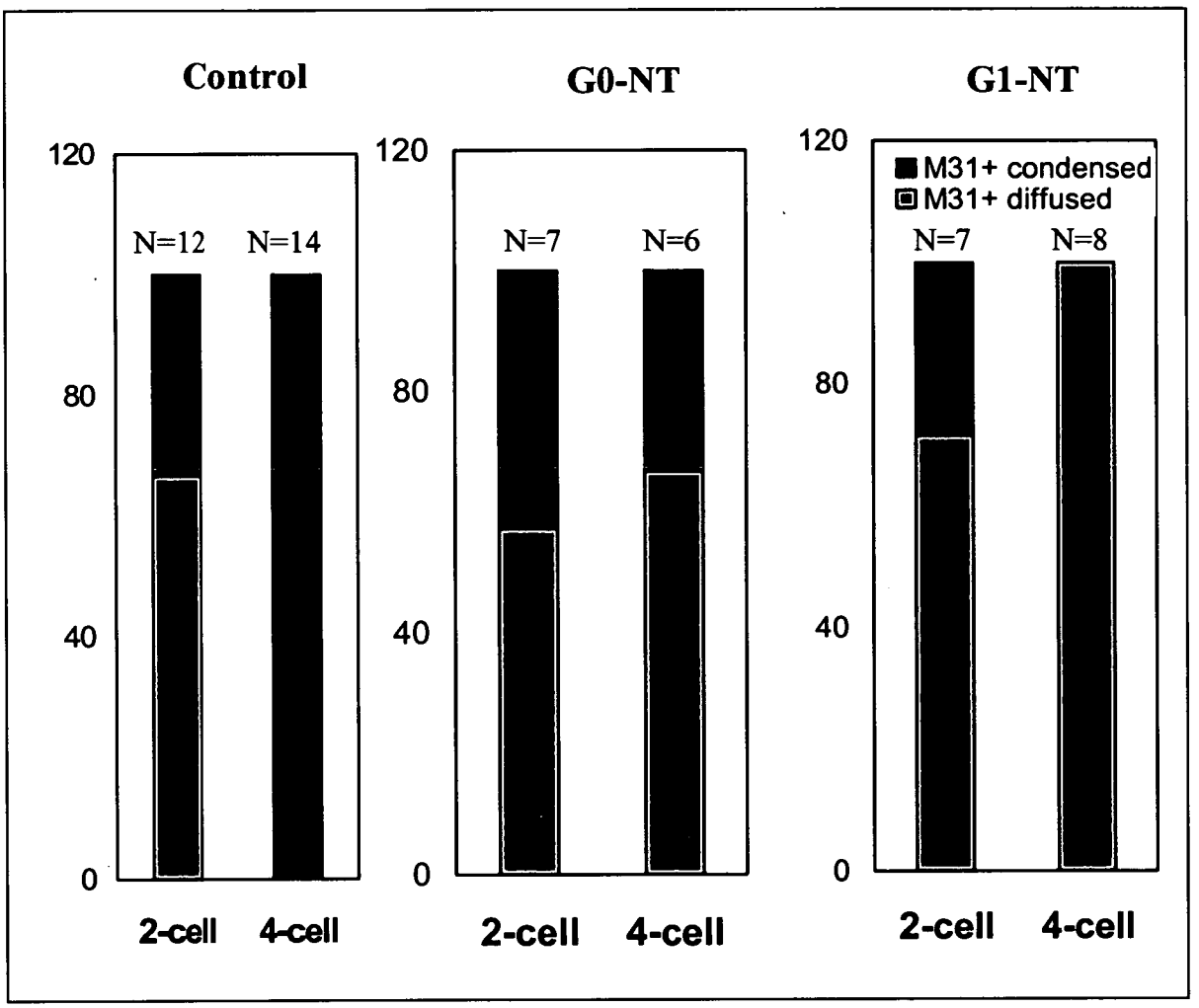

Data from two nuclear transfer experiments were compared with the results obtained with fertilised embryos. Classification was similar to that described for Figure 6.6.

(Fig.6.9A, 2A-2C; 6/6) and G1-derived (Fig.6.9A, 4A-4C; 6/6) NT embryos were $M31^-$ (Fig.6.10). Embryos in all groups were, as expected, $PCNA^-$ since DNA replication only begins at later stages of development.

At the 2-cell stage (Fig.6.9B-Fig.6.10), when ZGA is expected, both G0-derived (7/7) and G1-derived (7/7) embryos were $M31^+/PCNA^+$. In a percentage of G0 (3/7, 42.8%) and G1-NT embryos (2/7 28.5%) $M31^+$ was organised in clusters, localised at the periphery of the nucleus. These clusters resembled closely the "condensed" M31 distribution observed at the 2-cell stage in fertilised embryos (4/12, 33.3%, p=0.708 with G0-NT; p=0.806 with G1-NT). The remaining G0 (4/7, 57.2%) and G1-NT (5/7, 71.6%) embryos were characterised by a "diffused" sub-nuclear distribution for M31, again similar to the one observed in fertilised embryos (8/12, 66.6%, p=0.708 with G0-NT; p=0.806 with G1-NT).

At the 4-cell stage M31 distribution patterns observed in NT embryos, regardless of their cell-cycle stage, were very different than those observed in fertilised control embryos. Fertilised embryos at the 4-cell stage were characterised by a "condensed" M31 distribution pattern (14/14, 100%). Both G0 (2/6, 33.3%, p=0.003) and G1-derived NT embryos (0/8, 0%, p<0.001) had significantly lower percentages of 4-cell embryos with a "condensed" distribution pattern. The percentages of "condensed" M31 distribution found in G0- derived embryos (2/6, 33.3%), though significantly lower than the ones found in fertilised embryos, were higher the those found in G1-derived embryos where this patterns was not observed (0/8, 0%, p=0.07). The percentages of $PCNA^+$ embryos at the 2 and 4-cell stages were equally high in G0 (7/7; 5/6), G1-derived NT embryos (7/7; 8/8) and fertilised embryos (12/12; 14/14).

Results of double staining for DAPI and for histone H4 acetylation on lysines 5 (H4.Ac5) or 12 (H4.Ac12) showed that (Fig.6.11A-6.11B) during the first 0-30 min after reconstruction both G0 (Fig.6.11A, 1A-1B; 5/5) and G1-derived embryos (Fig.6.11A, 3A-3B; 5/5) appeared to be intensively acetylated on lysines 5 and 12. At the PCC stage the situation remained unchanged, with hyperacetylated chromosomes forming the metaphase plates of G0 (Fig.6.11A, 2A-2B; 5/5) and G1-derived embryos (Fig.6.11A, 4A-4B; 5/5). These data were surprising considering that quiescent and non-quiescent T-cells had different acetylation states at the time of

transfer: the former being transcriptionally inactive and deacetylated, and the latter being hyperacetylated and transcriptionally active.

At the 2-cell stage and at the 4-cell stage (Fig.6.11B-Fig.6.12), the overall percentages of G0 (5/5; 3/3) and G1-NT embryos (9/9; 9/9) hyperacetylated on lysines 5 and 12 of histone H4 were comparable to those of fertilised embryos (15/15; 14/14) However distribution patterns observed in H4.Ac5$^+$ and H4.Ac12$^+$ were dramatically different between G0-NT, G1-NT and fertilised embryos. At the 2-cell stage all G1-derived NT embryos had a "peripheral" (9/9) and H4.Ac12$^+$ (9/9) staining pattern for H4.Ac5$^+$ (9/9) and H4.Ac12$^+$ (9/9), similarly to what observed in control embryos (13/15, 86.7%, p=0.380; 15/15, p=1). G0-derived NT embryos had percentages H4.Ac5$^+$ (0/5) and H4.Ac12$^+$ (0/5) with "peripheral" staining significantly lower than the ones observed in fertilised (p=0.001 for Ac5; p<0.001 for Ac12) and G1-derived embryos (p<0.001 for Ac5 and Ac12). At the 4-cell stage the situation was inverted: all G0-derived embryos had a "peripheral" staining pattern for H4.Ac5 (3/3) and H4.Ac12 (3/3), comparable to what observed in fertilised embryos (12/14 for H4.Ac5, p=0.669; 14/14 for H4.Ac12, p=1); G1-derived embryos had percentages of embryos with "peripheral" staining patterns for H4.Ac5 (3/9, 33.3%) and H4.Ac12 (1/6, 16.7%) significantly lower than those observed in fertilised (p=0.018 H4.Ac5; p<0.001 for H4.Ac12) and G0-derived embryos (p=0.091 for H4.Ac5; p=0.048 for H4.Ac12).

6.5.2.4 Conclusions

The results of these experiments showed that quiescence affected both chromatin status and histone H4 acetylation status of cloned embryos. Differences in the non-histone protein M31 were observed between G0-NT and G1-NT embryos in the first 30min after reconstruction, when G1-NT embryos are M31$^+$ and G0-NT embryos are M31$^-$. At PCC stage, 1-3h after reconstruction, both G0-NT and G1-NT embryos were M31$^-$ as expected since M31 is usually not associated with DNA during the M phase. At the 2- cell stage the situation was similar in G0-NT, G1-NT and controls. This stage was characterised in all groups, by the majority of embryos displaying a "diffused" M31 pattern and by the appearance of clusters of M31 ("condensed" pattern) at the periphery of the nucleus,

Figure 6.11A Immunostaining for histone H4 acetylation of NT embryos: 0-3h after reconstruction

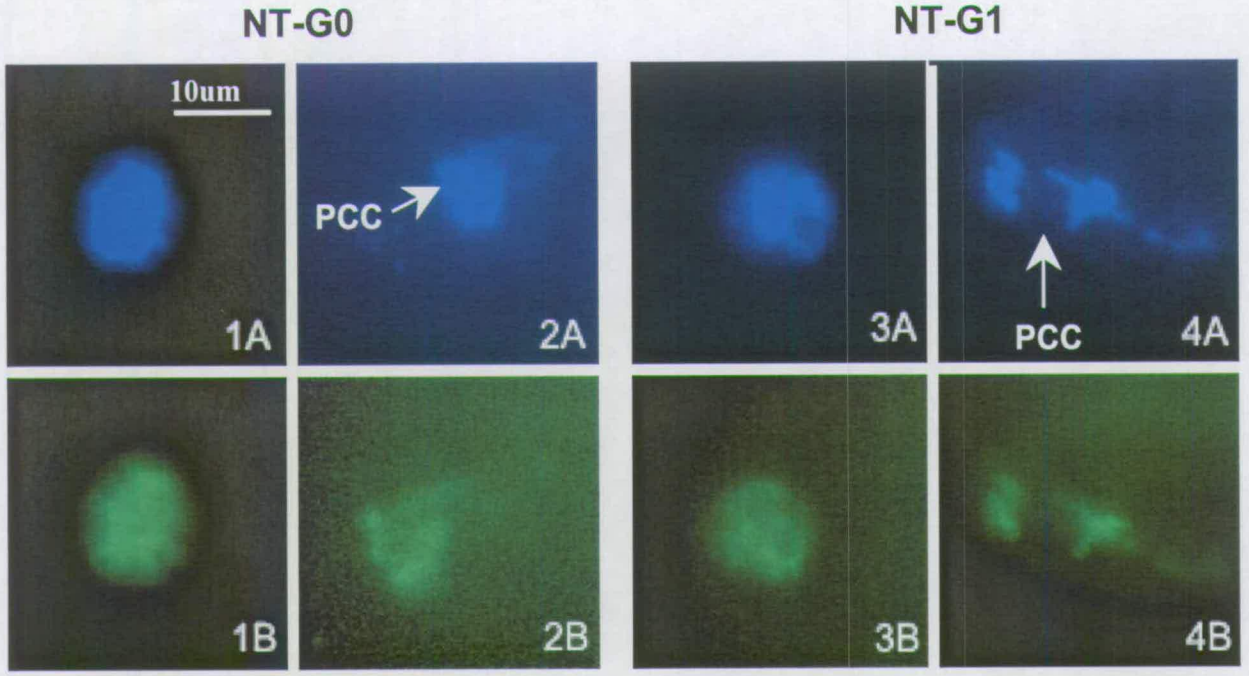

Nuclear Transfer embryos reconstructed using G0 (1-2) or G1 T-lymphocytes (2-3) were fixed after 0-30 minutes after reconstruction (1, 3), when nuclei were still condensed, and 1-3h after reconstruction (2, 4), when chromatin was organised in chromosomes (PCC-stage). Embryos were stained with the DNA staining DAPI (blue, A) and FITC anti-H4.Ac5 to detect acetylation on lysines 5 of histone H4. These images show that regardless of their acetylation status before transfer (deacetylated for G0, hyperacetylated for G1) G0 and G1 cells become immediately acetylated after transfer to a recipient MII oocyte.

Figure 6.11B Immunostaining for histone H4 acetylation of NT embryos: 2- and 4-cell stages

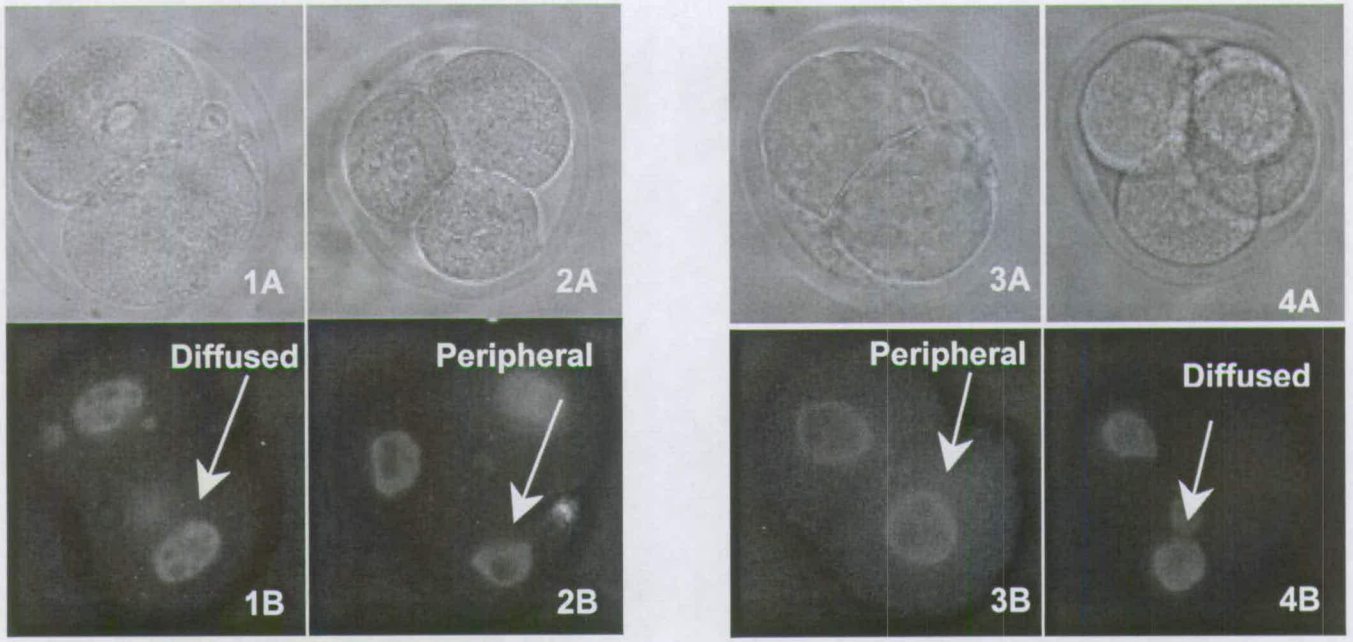

G0-(1-2) and G1- (3-4) derived embryos were fixed at the 2-cell (1-3) and 4-cell (2-4) stages. Images "A" show brightfield images. Images "B" show nuclei of embryos stained with FITC conjugated anti-H4.AC5 or antiH4. Ac12 antibodies, represented here in grey. G0-derived embryos had a uniformly "diffused" (D) sub-nuclear distribution at the 2-cell stage and a "peripheral" (P) staining distribution at the 4-cell stage. On the contrary G1-derived embryos had a peripheral" staining distribution at the 2-cell stage and a "diffused" sub-nuclear distribution at the 4-cell stage.

Figure 6.12 Comparison of immunostaining for histone H4 acetylation in control and NT embryos

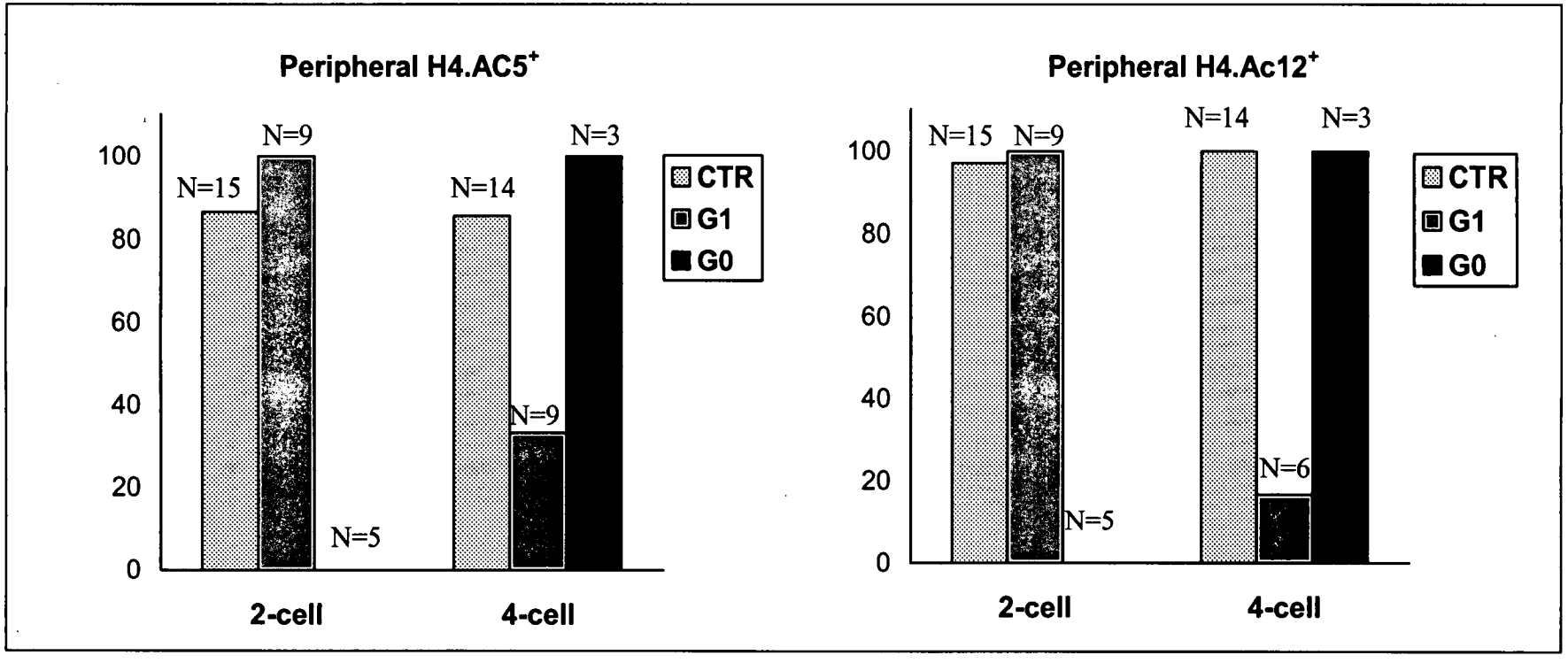

Control fertilised and G0 and G1-derived NT embryos were double stained with DAPI and antibodies recognising histone H4 acetylated on lysines 5 or 12. Percentages of embryos characterised by peripheral acetylation staining, correlated with transcriptional activation, found in the different treatment groups were compared.

where histone acetylation and transcription also take place. Dramatic differences between NT embryos, regardless of their cell cycle stage, and fertilised embryos were observed at the 4-cell stage. All controls, at the 4-cell stage, were characterised by the M31 "condensed" distribution pattern. A similar distribution pattern was observed only in a limited number of G0-NT embryos (2/6, 33.3%) and was not observed in G1-NT embryos (0/8). The results of PCNA staining suggested that this difference in chromatin status did not correlate with differences in replicative potential since equally high percentages of $PCNA^+$ embryos were observed in all groups. However the fixation method used in these experiments was not ideal to carry out this investigation: organic solvents would have been more appropriate than cross-linking reagents to fix the insoluble form of PCNA expressed in a cell cycle-dependent manner (see Paragraph 2.11).

During the first 3h after reconstruction the acetylation status of histone H4 appeared to be similar in G0 and G1-derived embryos. Regardless of their cell cycle stage and their acetylation status before transfer, both G0 and G1-nuclei became hyperacetylated on lysines 5 and 12 of histone H4. This observation is in contrast with the differences observed in cultured cells (Chapter 4) where quiescent cells were deacetylated and activated cells were hyperacetylated (Chapter 5) on histone H4.

At the 2 and 4- cell stages the situation of G0- derived and G1-derived NT embryos appeared to be dramatically different. When diploid, non-quiescent cells were transferred to recipient MII oocytes (G1), appearance of the "peripheral" distribution pattern for the anti-H4.Ac5/12 staining, was synchronous with that observed in control fertilised embryos and occurred at the 2-cell stage. On the contrary, when quiescent, diploid nuclei (G0), used as donor cells, appearance of this "peripheral" distribution pattern was delayed to the 4-cell stage. Appearance of the "peripheral" staining patterns after staining with anti-H4.Ac5 and anti-H4.Ac12 in fertilised mouse embryos had been associated with transcriptional activation (Worrad *et al.*, 1995). The results of the experiments in this chapter suggest that quiescence delays timing of ZGA in NT embryos while in the absence of quiescence, timing of ZGA in cloned embryos remains synchronous with that observed in fertilised embryos.

CHAPTER 7

GENERAL DISCUSSION

Since the first mammal was cloned using quiescent somatic cells (Wilmut *et al.*, 1997), there have been strong suggestions that quiescence plays an essential role in Nuclear Transfer (NT). Quiescent, somatic cells, either freshly isolated or made quiescent by serum starvation or contact inhibition, have been used to clone mice (Wakayama *et al,* 1998; Wakayama and Yanagimachi, 1999; Ogura *et al.,* 2000), goat (Baguisi *et al.,* 1999), muflon (Loi *et al.,* 2001) and cow (*Kato et al.,* 1998; Wells *et al.,* 1998a; Wells *et al.,* 1999; Zakhartchenko *et al.,* 1999b; Galli *et al.,* 1999; Kubota *et al.,* 2000). Nuclear transfer is still very inefficient technique, being low post-implantation development one of the limiting factors. Recent evidence in cattle shows that quiescence improves development to term of cloned embryos (Wells, 2002). Mechanisms on how quiescence might affect quality of cloned embryos and their potential to support development to term are still unknown. A possible explanation is that quiescence affects gene expression in cloned embryos, down-regulating expression of genes related to poor embryos quality (Wrenzicky *et al.*, 2001). Regulation of gene expression by quiescence could occur by altering the epigenetic status of donor cells and cloned embryos. The hypothesis sustained in this thesis is that quiescence affects the epigenetic status of donor cells and of cloned embryos, with consequences on embryo development.

Production of well characterised quiescent and a non-quiescent cell population was an essential step in proving this theory. Up to now quiescence of donor cells used for NT had never been confirmed, and "presumptive G0" cells (Wrenzycki *et al.*, 2001) had been used as donors. In these experiments specific markers, previously identified by Northern and Western blot analysis were used to confirm quiescence of donor cells. FACS analysis and immunoforescence were the techniques of choice because they offered the unique possibility, compared to molecular biology tools previously used, to assess expression of specific markers on single cells within a population, rather than in cell extracts. The first cell model used

to produce donor cells synchronized inG0 and G1 were Mouse Foetal Fibroblasts. Two synchronization methods were used to synchronize cells in G0 and several nuclear markers (p130, p27KIP1, cyclin D1) and FACS analysis were used to confirm level of synchronization in a diploid quiescent state. Results of these experiments showed that serum starvation induces reversible growth arrest in cultured cells, associated with up regulation of positive markers of quiescence ($p27^{KIP1}$, p130) and down regulation of negative marker of quiescence, like the protein synthesis marker FITC. The opposite situation was observed in cycling cells, used as negative control of quiescence. FACS analysis showed that serum starvation alters the percentages of cells expressing quiescence markers, rather than the levels of expression/cell. However not all serum-starved cells expressed quiescence markers and high SEM values also suggested a certain degree of variability within experimental population of cells, belonging to the same cell line and treated with the same protocol. Serum starvation can be used to synchronize cells in G0 but this level of synchronization varies depending on the marker used for assessment (97% $FITC^-$, 64% $p27^{KIP1+}$, 40% $p130^+$).

Another observation was that serum starvation-induced growth arrest, was associated with a significant increase in the percentage of G2/M cells (~30%) while the percentages of diploid cells remained unchanged (~65%). This result could not be due to presence of cell aggregates, excluded from the analysis by DDM, nor of cells with abnormal karyotype, as confirmed by karyotyping results. Expression of markers of quiescence was observed in a high percentage of G0/G1 (48-96% G0) as well as in G2/M cells (0-50%). About 74-100% of quiescent cells were in G0/G1 and 0-26% of them was in G2/M. It was concluded that serum starvation produces a diploid/tetraploid population of quiescent cells. Contact inhibition has been previously used to induce a "presumptive" quiescence in cultured cells. PCNA staining cell cycle analysis confirmed growth arrest under contact inhibition conditions. However only expression of p130 was comparable to that of serum-starved cells, whereas FITC and $p27^{KIP1}$ expression, was similar to that observed in cycling cells, and FITC expression intermediate between that of cycling and serum-starved cells. Changes in morphology, replication time and karyotype observed in cells kept under contact inhibition for different length of time, suggest that this

synchronization method carries, at least in mouse fibroblasts, a high risk of genotypic instability (transformation). Partially abnormal patterns of expression of quiescence markers might be part of the transformation process. Previous reports (Rhodes *et al.*, 1994) had shown that serum starvation of v-mos transformed NIH 3T3 fibroblasts induced growth arrest, as confirmed by reduction in bromodeoxyuridine and [^{3}H]thymidine incorporation, and cell cycle profile. However transformed NIH 3T3, unlike wild NIH 3T3 fibroblasts, were unable to express quiescence markers (e.g. gas1), and arrested in a G1 stage (Rhodes *et al.*, 1994) rather than a G0 stage.

G1 can be defined as a diploid, but non-quiescent cell cycle stage. Various methods were used to synchronize Mouse Foetal Fibroblasts in G1. The most effective methods, in inducing growth arrest, were incubation, for 24h, with 800uM Mimosine or 4mM hydroxyurea. More detailed analysis showed that growth arrest by hydroxyurea, induced reductions not only in the percentages of cells in S-phase, but also of cells in G2/M, while the percentages of diploid cells (~77%, G0/G1) increased. FITC staining also confirmed that most diploid cells, were in a non-quiescent state (G1, (~88%).

These results offer the first insight into the level of synchronization achieved in fibroblasts, commonly used as donors in nuclear transfer experiments, using custom synchronization methods. It also shows that serum starvation may not be optimal for synchronization in G0, because the variable level of synchronization in G0 and the high percentages of cells in G2/M. Because markers of quiescence available for fibroblasts are all intracellular, and can be detected only in fixed and permeabilised cells, they cannot be used to improve level of synchronization in G0. The only possible approach would be to produce cell lines transgenic for p27 or p130 and Green Fluorescent Protein (GFP).

Finally, although tetraploid cells can be used for NT, the protocol is different from that used for diploid cells: NT with G0/G1 cells requires presence of cytochalasin B, to inhibit pseudo-polar body extrusion and haploidisation; NT with G2/M cells does not require cytochalasin B, since diploidy can only be achieved through pseudo-polar body extrusion. This suggests that presence of a diploid/tetraploid population in serum-starved cells may not represent an optimal experimental condition for Nuclear Transfer (NT):

T-lymphocytes were also used as a second cell model to produce well-characterised cells in G0 and G1. This cell type was chosen for the unique possibility it offered of using surface, negative markers of quiescence (interleukin-Receptor α or CD25; Transferrin receptor γ), alongside intracellular markers observed in other cell types. T-lymphocytes, that are quiescent at isolation, also display dramatic changes in chromatin status and histone post-translational modifications, associated with exit from quiescence (activation). Growth arrest of freshly isolated of T-cells was confirmed by low percentages of cells in S-phase, associated with very high the percentages of diploid cells (G0/G1, ~90%). Quiescence status was confirmed by the low percentages of cells expressing CD25 (~96% $CD25^-$) and the relatively high percentages of cells expressing $p27^{KIP1}$ (~88% $p27^{KIP1+}$). Detailed analysis of one of these markers, $p27^{KIP1}$, also confirmed that, almost all diploid cells were quiescent (~90% G0) and almost all of the quiescent cells were diploid (~91%). In this cell model, quiescence and diploidy appeared to be strictly associated.

T-lymphocytes were also used to investigate effects of quiescence on the epigenetic status of somatic cells. Previous studies, using general markers of chromatin condensation (e.g. Acridine Orange, Juan and Darkinzinkiewicz, 1998), had shown that chromatin is highly condensed in human peripheral T-lymphocytes, that are in G0, and decondenses upon activation. In the present study the mouse homologues of human HP1 proteins, were used as specific landmarks of chromatin conformation. More precisely, M31 and mHP1α, respectively mouse homologues of human hHP1β and hHP1α, were used to investigate changes affecting constitutive, pericentromeric heterochromatin; M32, the mouse homologue of human hHP1γ, was used to investigate changes affecting non-constitutive heterochromatin. Immunofluorescence and previously characterised antibodies (AFRC MAC 353; M235; MAC 385) were used to investigate changes the sub-nuclear localisation and in the levels of expression of HP1 homologues, induced by T-cell activation. Changes in HP1 proteins correlated with cell quiescence had never been investigated before. The results obtained showed that in quiescent, T-lymphocytes M31 and mHP1α, was organised in large clusters, colocalised with areas of condensed chromatin (putative pericentromeric chromatin), whereas M32 was condensed into smaller aggregates, appearing like fluorescent speckles (putative non-constitutive

heterochromatin). Smaller aggregates were also visible in quiescent cells stained for mHP1α. Fluorescence was used to quantify level of HP1 condensation and overall level of protein expression. Tendency of mouse HP1 proteins to concentrate in G0 cells, correlating with tendency of chromatin to condense, was confirmed by the high levels of mean fluorescence, and peak fluorescence observed G0 cells. The high levels of SD of mean fluorescence also indicated high levels of condensation, by indicating a non-uniform HP1 nuclear distribution, ranging from a very dispersed form to a very condensed one. After activation, as cells re-entered the cell cycle, chromatin became dispersed and so did all three HP1 isoforms, as indicated by the lower mean fluorescence, peak fluorescence and SD of mean fluorescence observed in non-quiescent cells. Results showing negative correlation between CD25 or PCNA expression and condensation of M31 further confirmed the HP1-mediated effect of quiescence on chromatin conformation, in particular pericentromeric chromatin conformation.

Quiescence also induces histone post-translational modifications, such as histone acetylation (Pogo *et al.*, 1966; Knosp *et al.,* 1991) and phosphorylation (Patskan and Baxter, 1985). Quiescence-mediated changes in histone acetylation were of particular interest to this project, for two reasons: 1) they are strictly correlated with chromatin changes; 2) they play a pivotal role during early embryo development. Models correlating chromatin changes and changes in overall histone acetylation have been previously described (Newell-Price *et al.*, 2000). This correlation has been also confirmed by experiments showing how Trichostatin A, and inhibitor of histone deacetylases, increases the levels of histone acetylation as well as inducing chromatin decondensation (Maison *et al.*, 2002). This correlation is evident in quiescent cells, such as T-lymphocytes or serum-starved fibroblasts, where chromatin is very condensed (Juan and Darkinzinkiewicz, 1998; Bridger *et al.*, 2000) and level of acetylation are low (Pogo *et al.*, 1966; Knosp *et al.*, 1991). Changes in the levels of histone H4 acetylation in quiescent and non-quiescent cells were detected using a panel of antibodies that are also able to map changes in histone H4 acetylation patterns occurring at the time of zygote gene activation. The levels of acetylation on all the lysines residues considered on histone H4 (K2-4, K5, K12) appeared to be hypoacetylated in quiescent cells and hyperacetylated in non-

quiescent cells. These changes were observed under the same conditions used to study changes in chromatin conformation.

Activation of T-lymphocytes in the presence of hydroxyurea, followed by positive selection of $CD25^+$ cells, produced a well-characterised population of G1 cells, with very high percentages (>93% in nuclear transfer experiments) of diploid and non-quiescent cells.

T-lymphocytes, either in G0 or G1 were used as donor cells in Nuclear Transfer experiments, to assess effect of quiescence on epigenetic status and developmental potential of cloned embryos. Results showed that quiescence did not affect *in vitro* developmental potential of cloned embryos. However quiescence affected epigenetic status of cloned embryos. As shown by M31 staining, both G0 and G1-NT embryos had the same chromatin patterns as control embryos at the 2-cells stage. However, at the 4-cell stage, between 0%-33% of NT embryos had chromatin patterns (M31 clusters in perinucleolar localisation), similar to control embryos. These percentages were higher in G0-NT embryos (33%) than in G1-NT embryos (0%), suggesting that condensed, G0 might be more favourable to chromatin remodelling than G1. Quiescence also delayed

Regardless of their acetylation status before NT, both quiescent and non-quiescent nuclei became hyperacetylated immediately after NT. Differences in histone H4 acetylation were observed at the 2 and 4-cell stage, when the majority of NT embryos reconstructed using T-lymphocytes as donor cells failed to display the typical peripheral acetylation pattern associated with transcriptional activation. Regardless of their cell cycle stage, between 0-33% of NT-embryos had H4.Ac5 acetylation patterns similar to controls and between 0-17% of NT-embryos had H4.Ac12 acetylation patterns similar to controls. Differences in abnormal acetylation patterns were observed between G0-NT and G1-NT embryos: presence of G0 nuclei delayed appearance of the peripheral staining pattern at the 4-cell stage, in 100% of NT embryos; presence of G1 nuclei induced early disappearance at the 4-cell stage, of peripheral acetylation pattern in 67-83%. These results suggest that quiescence might delay the time of transcriptional activation in cloned embryos. Histone H4 acetylation is strictly dependent on DNA replication (Worrad *et al.,* 1994; 1995). Abnormal spatial and temporal regulation of histone acetylation may underline

abnormalities in DNA replication (Worrad *et al.*, 1994; 1995). However, it was not possible to assess this correlation. Fixation with cross-linking reagents used in these experiments, was optimal for immunostaining of the other nuclear proteins studied, but only preserved the soluble form of PCNA, constitutively expressed in cells, in a cell cycle-independent manner (see pages 53, 222, 234).

The low percentages of NT-embryos, derived from T-lymphocytes, with normal chromatin status and acetylation patterns similar to controls suggests a poor potential for nuclear transfer of this particular cell type. The poor rates of development to blastocyst obtained in experiments using T-cells, regardless of the cell cycle stage, supports this idea (Wakayama and Yanagimachi, 2001). Recent reports have shown that, T and B-lymphocytes can also be reprogrammed to support development to term (Hochedlinger and Janenisch, 2002). However, also in this case, efficiency was extremely low, and development to term, using T and B-lymphocytes, was achieved only by combining the nuclear transfer and the tetraploid aggregation technique. The abnormalities observed in acetylation and chromatin status of embryos cloned from T-cells in these experiments might be an early indication of this poor attitude for reprogramming of this particular cell type.

The present study shows that quiescence does affect epigenetic status of cloned embryos with no immediate effect on pre-implantation development, but possible effects on post-implantation development.

It also suggests that further investigation in cloned embryos, of histone post-translational modifications, such as H3/H4 acetylation, histone H3 phosphorylation and methylation, and changes in chromatin conformation, mediated by histone as well as non histone proteins, is needed to give us a better understanding of the mechanisms undermining development of cloned embryos.

APPENDIX A

MEDIA AND STOCK SOLUTIONS

A.1 MEDIA AND STOCKS FOR T-MOUSE FOETAL FIBROBLASTS

A.1.1 Culture Medium: 10% FCS DMEM

Component	ml/500ml	Product
L-glutamine 200mM	5	Life Technologies 25030-024
Foetal Calf Serum (FCS)	50	Globepharm
Na-pyruvate Mem 100mM	5	Life Technologies 11360-039
Mem non-essential amino acids	5	Life Technologies 1140-035
DMEM (Dulbecco's Modified Eagle's Medium)	435	Gibco 1965-039

Medium was filtered with 0.22uM disposable filters. It was stored at 4°C, for up to a week. Medium was warmed at 37°C, in waterbath, each time, before use. Medium used for first 24h after cell isolation, was also supplemented with 0.2% (v/v) of 50mg/ml gentamicin (Gibco, 15750-037). Serum starvation media, with 0.1% and 0.5% FCS were prepared as 10% FCS medium, only adding respectively 500ul or 2.5mlFCS.

A.1.2 Phosphate Buffer Saline (PBS)

Phosphate Buffer Saline (PBS), with Ca^{2+} and Mg^{2+}, was prepared by dissolving five OXOID tablets (BR14a; OXOID Ltd., Basingstoke, UK) in ddH_2O, and autoclaving at 115°C, for 20min. PBS was stored at room temperature.

A.1.3 0.25%Trypsin/0.04%EGTA

Component	g/lt	Product
NaCl	6.3	BDH 102414J
Na_2HPO_4 $2H_2O$	0.12	BDH 103834G
KH_2PO_4	0.216	BDH 102032W
KCl	0.333	BDH 101983K
D^+-glucose	0.9	BDH 101174Y
Tris	2.7	BDH 103154M
Trypsin 2.5% (w/v) 10x	2.5 (100ml)	Life Technologies 25090-028
Ethylene Glycol-bis Tetraacetyc Acid (EGTA) 10x	0.4	Sigma E4378
Polyvinyl Alcohol (PVA)	0.1	Sigma P8136
ddH_2O	Up to 1lt	-

All components, except Trypsin, EGTA and PVA, were dissolved in 800ml ddH2O. Then, Trypsyn, EGTA and PVA were added and pH was adjusted to 7.6, using 1N HCl. Volume was finally adjusted to 1lt. Solution was autoclaved, dispensed in 5ml aliquots and stored at-20°C, for several moths. After thawing, solution was stored at 4°C, and it was stable for a couple of weeks. For use, trypsin/EGTA solution was warned up at 37°C, in waterbath. A 3min incubation was usually enough to lift cells.

A.1.4 β-galactosidase staining

Fixative

Stock	ml	Final concentration (w/v)	Product
Formaldehyde 40% (w/v)	2.5ml	2%	BDH 101134A
Glutaraldehyde 25% (w/v)	0.4	0.2%	Aldrich G4004
ddH_2O	47.1	-	-

Glutaraldehyde was stored at 4°C. Formaldehyde was stored at room temperature. Fixatives were prepared under chemical hood, on day of experiment.

Stocks for β-galactosidase staining

Stock	Component	MW	Product
X-gal 50mg/ml	100mgX-gal in 2ml Dimethylformamide	-	Promega V394A
Na_2HPO_4 $2H_2O$ 1M	88.99g Na_2HPO_4 in 500ml ddH_2O	177.99	BDH 103834G
Citric acid H_2O 3M	315.21g Citric acid In 500ml ddH_2O	210.14	BDH 444452P
Potassium ferrocyanide 0.5M	105.6g Potassium ferrocyanide $3H_2O$ in 500ml ddH_2O	422.4	Sigma, PQ387
Potassium ferricyanide 0.5M	82.30g Potassium ferricyanide in 500ml ddH_2O	329.2	Sigma, P8131
NaCl 1M	29.22g NaCl in 500ml ddH_2O	58.44	BDH 102414J
$MgCl_2$ 1M	101.65g $MgCl_2$ in 500ml ddH_2O	203.3	Sigma M8266

All stock solutions were filtered with 0.22 disposable filters, and stored at room temperature. Potassium ferricyanide and Potassium ferrocyanide, are light sensitive, so they were always kept in the dark.

β-galactosidase staining

Stock	ml	Final concentration
X-gal 50mg/ml	0.2	1mg/ml
Na_2HPO_4/citrate acid 1M (pH6)*	0.4	40mM
Potassium ferrocyanide 0.5M	0.1	5mM
Potassium ferricyanide 0.5M	0.1	5mM
NaCl 1M	1.5	150mM

$MgCl_2$ 1M	0.02	2mM
ddH_2O	Up to 10ml	-

*The 3M citric acid stock was used to adjust the pH of the Na_2HPO_4 1M stock to 6. Staining solution was prepared on day of experiment. Initially 7.5ml ddH_2O were added. After adjusting pH of staining solution to 6, volume was brought up to 10ml.

A.1.5 Chemicals and controls for synchronization in G1

Hydroxyurea (Sigma H8627): 0.1M stock solution was prepared by diluting 76.05mg/10ml PBS and, then, filtering. Stock was prepared on day of experiment. Working dilutions were obtained by diluting the stock in the medium as follows: 10ul/ml (1mM), 20ul/ml (2mM), 40ul/ml (4mM).

Mimosine (Sigma, M0253): a 10mM stock solution prepared dissolving 25mg/12.6ml PBS. Mimosine is insoluble in aqueous solutions. Dissolved first in 9 ml PBS, add HCl 1N, until dissolved (~1.2ml). Then ad 1N NaOH until pH is 7.36. Add PBS to 12.6ml volume. Filter and store at 4°C for up to a month. Working dilutions of 400uM and 800uM obtained diluting exactly 40ul/ml (use 960ul medium), 80ul/ml in medium (use 920ul medium).

Lovastatin (Calbiochem, 438195): a 5mM stock solution was prepared by dissolving 25mg/12.5 ml. Dissolve in 0.5ml ethanol 100%, at 55°C. Add 391ul NaOH 1N. Leave at room temperature, to dissolve, for 30-50min.Add 9-10ml PBS, and adjust pH to 7.2 using HCL 1N (~0.54ml). Add PBS to reach 12.5ml volume. Filter, aliquot and store at–20°C. Lovastatin is light sensitive. Working dilutions of 5uM, 15uM, 30uM obtained diluting 1ul/ml, 3ul/ml, 6ul/ml in medium.

Lovastatin controls: a stock was prepared by diluting 500ul ethanol/12.5ml PBS. The stock was then diluted, in medium, at the following working concentrations: 1ul/ml (control 5uM lovastatin), 3ul/ml (control 15uM lovastatin), 6ul (control 30uM lovastatin).

Methotrexate (Sigma, M8407): a 50uM stock was prepared by diluting 10mg/4.4ml PBS. The 10mg of methotrexate had to be first dissolved in 300ul NaOH 1N (pH 12.5). After adding 3.5ml PBS, pH was adjusted to 7.2 using HCl 1N (~200-

240ul). Finally PBS was added to a final volume of 4.4ml. Stock was aliquotted and stored at –20°C. For working dilutions, 50uM stock was diluted as follows: 2ul/ml (f.c. 0.1uM or 10^{-7}M); 20ul/ml (f.c. 1uM or 10^{-6}M); 40ul/ml (f.c. 2uM or $2x10^{-6}$M).

A.2 MEDIA AND STOCKS FOR T-LYMPHOCYTES

A.2.1 Culture Media: 10% FCS RPMI-1640

Component	Volume	Product	Final concentration
[1]FCS	10ml	Globepharm	10%
L-glutamine 200mM	1ml	Sigma G7513	2mM
Sodium Pyruvate 100mM	1ml	Sigma S8636	1mM
Penicillin 10000units/ml Streptomycin 10mg/ml	1ml	Sigma P0781	100units/ml 0.01mg/ml
Non-essential amino acids (10x)	1ml	Sigma M7145	1x
[2]2-mercaptoethanol $5x10^{-2}$ M	0.1ml	Stock	$5x10^{-5}$ M
RPMI-1640	100ml	Sigma R7509	-

A.2.2 Dulbecco's Phosphate Buffered Saline (D-PBS)

Component	g/lt	MW	mM	Product
KCl	0.200	74.55	2.68	BDH 102032W
NaCl	8.000	58.44	136.89	BDH 102414J
Na_2HPO_4 $2H_2O$	1.441	177.99	8.09	BDH 103834G
KH_2PO_4	0.200	135.55	1.47	BDH 101983K
ddH2O	Up to 1lt	-	-	-

Adjust pH 7.3-7.4. Osmolarity 280-283 mOsm. Autoclave. Formula taken from Gibco 14190, but without preservatives, which are detrimental for T-lymphocytes. For Mouse Foetal Fibroblasts D-PBS was purchased from Sigma (E 6758).

[1] Foetal Calf serum was inactivated by incubating for 30min, at 56°C, in waterbath.
[2] 2-mercaptoethanol was added in most but not all experiments with T-lymphocytes (Chapter 4).

A.2.3 Phytoemagglutinin Stocks

Phytohemagglutinin, lectin from Phaseolus vulgaris (PHA), 5mg lyophilized powder to reconstitute with 2ml, 0.22uM-filtered, D-PBS (Sigma, L9132). Aliquots containing 80ug/32ul were prepared and stored at –20°C, for 12-18 months. On day of experiment, the following (2x) stocks were prepared, and filtered with 0.22uM disposable, syringe filters:

32ug/ml stock: 80ug/32ul in 2.5ml culture medium;

16ug/ml stock: 80ug/32ul in 5ml culture medium;

8ug/ml stock: 1:2 dilution of 16ug/ml stock in culture medium;

4ug/ml stock: 1.4 dilution of 8ug/ml stock in culture medium;

2ug/ml stock: 1:8 dilution of 8ug/ml stock in culture medium;

1.6ug/ml stock: 1:10 dilution of 8ug/ml stock in culture medium;

These stocks were stable for up to a week, at 4°C. The (2x) stocks were finally diluted 1.2, so that each well, of 24 well plates, would have 500ul cell suspension, in culture medium, and 500ul (2x) PHA stocks. Final PHA concentrations were: 16ug/ml, 8ug/ml; 4ug/ml; 2ug/ml; 1ug/ml; 0.8ug/ml.

A.2.4 Interleukin-2 Stock

Lyophilized mouse recombinant interleukin-2 (IL-2; Sigma I0523), was reconstituted with 1ml of 0.22 um-filtered D-PBS, pH 7.4, containing 0.1% (w/v) bovine serum albumin (BSA, Sigma A6003), to a concentration of 20ug/ml. Stored at –20°C, for several months. On day of experiments 2ul of the 20ug/ml IL-2 stock were added directly to each well, containing $2x10^6$ cells/1ml culture medium (4nM). Alternatively, when IL-2 was added together with PHA, 4ul of 20ug/ml IL-2 stock were added for each ml of PHA (2x) stock. Finally 500ul of (2x) PHA and IL-2 stock, were added to 500ul cell suspension, in culture medium, to a final concentration of 4nM (0.04ug/ml) IL-2 and 0.8ug/ml-16ug/ml, PHA.

A.2.5 Other reagents

2-mercaptoethanol $5x10^{-2}$ Stock

Prepare under chemical hood. Make a 1M solution of 2-mercaptoethanol (ME) by diluting 0.5ml 2-ME (Sigma, M7522) into 6.6ml sterile double-distilled

water. Dilute 2.5ml of the 1M stock into 47.5ml of sterile ddH_2O to give a concentration of $5x10^{-2}M$. Store at 4°C. This solution has to be made fresh each week.

[^{3}H]thymidine stock

Stock prepared by diluting 1mCi (37MBq)/ml solution (TRA 306) 1:20, in 3ml sterile D-PBS. This stock solution can be stored at 4°C for 2-3days. Add to 96 well plates, at a concentration of 1uCi/well/$0.2x10^6$ cells.

Turk's Solution

Prepared by dissolving 0.01% (w/v) gentian violet (Sigma C3886) in 3% (w/v) acetic acid (Sigma 27,931-5) in ddH_2O.

A.3 IMMUNOCYTOCHEMISTRY AND FACS REAGENTS

A.3.1 Buffers and Saline Solutions

Tris Buffer Solution (TBS)

Component	g/lt	mM	Product
NaCl	6.640	200	BDH 102414J
Tris-HCl pH 7.4	11.688	50	Sigma T4003
ddH_2O	up to 1lt	-	-

Adjust pH 7.3-7.4. Autoclave.

FACS Buffer

Component	g/500ml	(w/v)	Product
BSA	0.5	0.1%	Sigma A-6003
NaN_3	0.5	0.1%	Sigma S-2002
D-PBS	Up to 500ml	-	-

Buffer used to wash and resuspend samples processed for Fluorescence Activated Cell Sorter (FACS) analysis. Buffer was filtered and stored at 4°C for months. Stable also at room temperature.

MACS Buffer

Component	g/500ml	Final concentration	
BSA	2.5000	0.5% (w/v)	Sigma A6003
EDTA	0.2922	2mM	Sigma E6758
D-PBS	up to 500ml	-	-

Buffer used to wash and resuspend Magnetic Cell Sorting (MACS) samples. Buffer was filtered and stored at 4°C for a few months. Try and avoid bubbles as much as possible because they interfere with MACS.

"Saline GM"

Component	g/100ml	MW	mM	Product
D^+-glucose	0.1100	180.16	6.1	BDH 10117
NaCl	0.8000	58.44	137	BDH 10241
KCl	0.0400	74.55	5.4	BDH 10198
Na_2HPO_4 $7H_2O$	0.0402	268.10	1.5	Sigma S9390
KH_2PO_4	0.0122	135.55	0.9	BDH 10203
EDTA	0.0146	292.20	0.5	Sigma E6758
ddH_2O	up to 100ml	-	-	-

D-PBS/EDTA

Component	g/500ml	MW	mM	Product
EDTA	0.7305	292.20	5mM	Sigma E-6758
D-PBS	Up to 500ml	-	-	-

D-PBS was either prepared (A.2.2), for T-lymphocytes, or purchased from Sigma (E 6758) for Mouse Foetal Fibroblasts.

Buffers for DNA/microtubules staining

Component	Permeabilising	Blocking	Washing	Product
D-PBS	10ml	10ml	50ml	Sigma E-6758
BSA	30mg	30mg	30mg	Sigma A-6003
TritonX-100	50ul	10ul	50ul	Sigma T 8787
Glycine	-	75mg	-	Sigma G-7126

Adjust pH of all solutions at 7.2, filter and store at 4°C.

Buffers for DNA/microtubules/microfilaments staining

Component	*5% NGS*	**10% NGS**	Product
Goat Serum	25ml (5%)	50ml (10%)	Diagnostic Scotland S028-220
Triton X-100	0.5ml (0.1%)	0.5ml (0.1%)	Sigma T 8787
NaN_3	0.1g (0.02%)	0.1g (0.02%)	Sigma S-2002
D-PBS	Up to 500ml	Up to 500ml	Sigma E-6758

Normal Goat Serum (NGS) solutions can be stored at 4°C, for up to a month.

A.3.2 Fixatives

Paraformaldehyde 8% (w/v)

Prepared by dissolving 4g paraformaldehyde (Sigma, P-6148) in 50ml in D-PBS, and heating at 60°C, for a few hours. A few drops of NaOH 1N (Sigma S 2770), were added, to help dissolving. Filtered with 0.22uM disposable filters, to remove non-dissolved powder. Aliquots, containing 25ml or 6.25ml PF 8% (w/v), were stored at –20°C, for up to 1 month. On day of experiment, aliquots were thawed in hot water, and diluted 1.2 (PF4%) or 1:8 (PF1%) with D-PBS. Diluted PF was stable at 4°C, for 48h.

Paraformaldehyde/picric acid fixative

3.7g paraformaldehyde (Sigma P-6148) were dissolved in 60ml D-PBS (pH 7.4), by heating gradually at 60°C, stirring and adding NaOH until clear. The solution was then removed from heat, and brought at room temperature. After

adjusting pH to 7.4 with 6N HCl, 4.2ml saturated picric acid (Sigma 92540) were added and volume was brought up to 100ml.

Complex Fix

SB stock (5X)

Component	g/50ml	mM	Product
PIPES	7.55	0.1M	Sigma P 6757
$MgCl_2$	0.25	5mM	Sigma M 8266
EGTA	0.235	2.5mM	Sigma E 4378
ddH_2O	Up to 50ml	-	-

pH was adjusted to 6.1-7-5, to allow PIPES (Piperazine-N,N'-bis[2-ethanesulfonic acid]) to go into solution. Store at 4°C, for a maximum of 1 year.

Microtubule Stabilization Buffer (MTSB) stock

Component	ml/10ml	ml/ 5ml	Product
SB stock (5X)	2	1	-
DTT (1M)	0.010	0.005	Sigma D 5545
Deuterium Oxide (D_2O)	5	2.5	Aldrich 26979-4
ddH_2O	3	1.5	-

Cleland's reagent or $_{DL}$-Dithiothreitol (DTT; MW 154.2) stock was dissolved in ddH_2O, dispensed in 20ul aliquots, and stored at –20° C. D_2O was stored at room temperature. MTSB was prepared on day of use, and warmed up at 37°C, for 30min, in waterbath, to allow components to dissolve before preparing complex fix.

Complex Fix

Component	ml/10ml	ml/ 5ml	Product
MTSB	2	1	-
Triton X-100	0.010	0.005	Sigma T 8787
Formaldehyde (37%)	5	2.5	Sigma F 1268

A.3.3 Propidium Iodide (PI) staining

PI stock

Propidium Iodide (PI) powder (Sigma P4170), was diluted at a concentration of 10mg/10ml in 0.22um-filtered D-PBS supplemented with 0.1% (w/v) NaN_3. Stored at 4°C, in the dark, is stable for 2 years.

RNAse stock

Ribonuclease (RNAse) type IIA, from Bovine Pancreas (100mg, Sigma R5000), was diluted at a concentration of 1mg/ml in 0.22um-filtered D-PBS. Aliquots containing 1ml stock were prepared and stored at –20°C. Stable for 2 years.

Component	ul	ug/ml
RNAse (1mg/ml)	1000	100
PI (1mg/ml)	200	20
FACS Buffer	8800	-

This staining solution was used when samples were double stained with PI and $p27^{KIP1}$ and p130. It was 0.22um-filtered. Stored at 4°C in the dark it was stable for a few weeks.

A.3.4 PI/FITC staining solution

FITC stock

Fluorescein isothyocyanate (FITC) powder was stored at 4°C (50mg, Sigma F4274). On day of use, about 5-10mg FITC were diluted at a concentration of 1mg/ml 100% ethanol. This stock was further diluted 1:100, with 100% ethanol (10ug/ml FITC stock).

Component	ul	ug/ml
RNAse (1mg/ml)	1000	100
PI (1mg/ml)	200	20
FITC (10ug/ml)	20	0.02
FACS Buffer	8780	-

This solution was prepared on the day of experiment. Kept at 4°C. This staining solution was stable only for a short time because FITC is degraded by aqueous solutions.

A.4 ANTIBODIES

A.4.1 Primary Antibodies

All diluted antibodies were stored at 4°C, for maximal 3 days, and were centrifuged 30sec, at 13000 rpm, each time, before use.

Human anti-Human Proliferating Cell Nuclear Antigen (PCNA). Human anti-serum to human PCNA/cyclin (0.5ml; Immuno Concepts, 2037). It recognizes sheep, pig and mouse PCNA. Stored at 4°C, it is stable for 12 months. Used for immunocytochemistry, diluted 1:10 in 1% FCS-PBS. Secondary used: TXR–conjugated goat anti-human IgG (Vector Laboratories).

Mouse anti-Human cyclin D1. Mouse monoclonal antibody (5ug/100ul; clone DCS-6, subclass IgG2a; Novocastra, NCL-Cyclin D1), raised against human recombinant full-length cyclin D1 as immunogen. It also recognises mouse cyclin D1, expressed in primary mouse embryo fibroblasts (Lukas *et al.*, 1995), and can be as a blocking-antibody in immuno-knockout experiments (Baldin *et al.,* 1993; Lukas *et al.,* 1995). It recognises cyclin D1, that is positive regulator of early G1-phase, and is expressed at very low levels in G0 cells. Cyclin D1 is present in fibroblasts but not T-cells. Lyophilised antibody was reconstituted at a concentration of 5ug/ml in sterile ddH_2O. Stored at 4°C, reconstituted antibody was stable for 2 months, at 4°C, and for 12months, at-20°C. Used for immunocytochemistry, diluted 1:10 in 1% FCS-PBS. Secondary antibody used: FITC-conjugated sheep anti-mouse IgG (Diagnostic Scotland).

Mouse anti-Human cyclin D3. Mouse monoclonal antibody (5ug/100ul; clone DCS-22, subclass IgG1; Novocastra, NCL-Cyclin D3), produced using human recombinant full-length cyclin D3 as immunogen. It does not cross react with cycling D1 and D2. It recognises cyclin D3, that is a regulator of late G1 progression, and it is not expressed in G0 cells. Cyclin D3 is present in fibroblasts and T-cells. Lyophilised antibody was reconstituted at a concentration of 5ug/ml in sterile

ddH_2O. Stored at 4°C, reconstituted antibody was stable for 2 months, at 4°C, and for 12months, at-20°C. Used for immunocytochemistry, diluted 1:20 in in TBS with 0.2% TritonX-100. Secondary antibody used: FITC-conjugated sheep anti-mouse IgG (Diagnostic Scotland).

Antibodies to mouse HP1 proteins.

AFRC MAC 353 (Wregget *et al.,* 1994). Purified, rat-monoclonal antibody (IgG; 50ug/ml), raised against M31, the mouse homologue of human hHP1β. Used for immunocytochemistry at a concentration of 1ug/ml (1:50) in 10% milk powder in TBS with 0.25% Triton X-100. Secondary antibody used: FITC-rabbit anti-rat serum (a gift from Dr. Prim Singh).

MAC 385 (Horsley *et al.,* 1996). Purified, rat monoclonal antibody (IgM; 50ug/ml), raised against M32, the mouse homologue of human hHP1γ. Used for immunocytochemistry at a concentration of 5ug/ml (1:10) in 10% milk powder in TBS with 0.25% Triton X-100. Secondary antibody used: FITC-rabbit anti-rat serum (a gift from Dr. Prim Singh).

M235 (Kourmouli et *al.,* 2000). Purified, rabbit anti-serum (50ug/ml) raised against mHP1α, the mouse homologue of human hHP1α. Used for immunocytochemistry at a concentration of 1ug/ml (1:50), in 10% milk powder in TBS with 0.25% Triton X-100. Secondary used: FITC conjugated donkey anti-rabbit IgG (Diagnostic Scotland).

All the antibodies reognizing HP1 proteins were a gift from Dr. Prim Singh.

Acetylated histone H4 antibodies. Various antibodies recognizing histone H4 acetylation on different lysine residues were used for immunocytochemistry of cells and embryos:

lysines 2-4, sheep anti-serum (anti-H4.Ac2-4), diluted 1:800;

lysine 5, rabbit anti-serum (R40; anti-H4.Ac5), diluted 1:800;

lysine 8, rabbit anti-serum (R232; anti-H4.Ac8), diluted 1:1500;

lysine 12, rabbit anti-serum (R101, anti-H4.Ac12), diluted 1:400;

lysine 16, rabbit anti-serum (R251, anti-H4.Ac16), diluted 1:1500.

All antibodies recognizing acetylated histone H4 were a gift from Prof. Bryan Turner, except the anti-H4.Ac2-4 that was a gift from Dr. Prim Singh.

Antibodies anti-H4.Ac5, 8, 12, 16 had been previously characterised in detail (Turner and Fellows 1989, Turner *et al.,* 1989), and had been used to detect changes in histone acetylation in somatic cells (Thorne *et al.*, 1990; Turner and Fellows 1989, Turner *et al.,* 1989) and embryos (Adenot *et al.,* 1997; Worrad *et al.,* 1995; Ma *et al.,* 2001; Wiekowski *et al.,* 1997). All these antibodies were stable for at least 1year at –20°C.

Rabbit anti-Human p130 (Santa Cruz, Sc-317; 200ug/ml). Purified, rabbit polyclonal antibody (IgG), raised against peptide mapping carboxy terminus of human p130. Reacts with rat, human and mouse p130. Used for flow cytometry at a concentration of 2ug/10^6 cells (1:100) in 1.5% goat serum in D-PBS. Stored at 4°C. Stable for 18 months. Secondary used: FITC-conjugated goat anti-rabbit (Santa Cruz).

Mouse anti-Rat β tubulin (Sigma T-4026). Mouse monoclonal antibody raised against rat β tubulin (IgG1; clone TUB 2.1). Recognizes β tubulin in a variety of species including human, mouse, bovine, chicken. Antibody provided in solution. Stored at –20°C it is stable for at least 1 year. Secondary antibody used: FITC-conjugated anti-mouse IgG.

FITC-conjugated Mouse anti-Mouse $p27^{KIP1}$ (Neomarkers, MS256-F0; 200ug/ml). Purified, mouse monoclonal antibody (IgG1; clone DCS-72.F6) raised against mouse recombinant $p27^{KIP1}$, negative regulator of G1 progression. Reacts with human, mouse and rat $p27^{KIP1}$. Aliquotted and stored at–20°C. It is stable for 1 year. Used for flow cytometry, diluted 2ug/10^6 cells, in 1% FCS in D-PBS.

R-PE-conjugated Rat anti-Mouse CD25 (Caltag RM 6004; 50ug/0.5ml). Rat monoclonal antibody (IgG1; clone PC61 5.3) that recognizes the α chain of the IL-2 receptor (IL-2Rα) or CD25, expressed in activated B and T-cells. Stored at 4°C, for at least 1 year. Light sensitive. Used for flow cytometry and MACS separation at a final dilution of 1-2ug/10^6 cells, in FACS buffer.

FITC-Hamster anti-Mouse CD3 (Caltag HM3401; 100ug/ml). Hamster monoclonal antibody (IgG1; clone 500A2) that recognizes mouse CD3, expressed in mature T-cells. Stored at 4°C, for at least 1 year. Light sensitive. Used for flow cytometry at a final dilution of 2ug/10^6 cells, in FACS buffer.

R-PE-Rat anti Mouse Ly-6G (Gr-1; Caltag RM3004; 50ug/0.5ml). Rat monoclonal antibody (IgG2a; clone RB6-8G5) that reacts with Ly-6G, also known as GR-1, expressed on myeloid cells in the bone marrow, on monocytes, and on peripheral granulocytes. Stored at 4°C, it is stable for at least 1year. Light sensitive. Used for flow cytometry at a concentration of $1ug/10^6$ cells, in FACS buffer.

FITC-Rat anti Mouse B220 (CD45R; Caltag RM2601; 50ug/0.5ml). Rat monoclonal antibody that recognizes B220 epitope on Pan B-lymphocytes. Stored at 4°C, it is stable for at least 1year. Light sensitive. Used for flow cytometry at a concentration of $2ug/10^6$ cells, in FACS buffer.

FITC-Mouse anti-Chick α tubulin (Sigma F2168; 1.5mg/ml). Mouse monoclonal (clone DM1A) that recognizes an epitope at the carboxy-terminal of α tubulin, and is used to label microtubules. It also reacts with α tubulin from a variety of species, including human, mouse, rat, hamster, cattle and amphibia. Stored at-20°C for at least 1year. At 2-8°C, it is stable for a maximum of 1month. Used for immunocytochemistry, diluted 1:10 in 5%NGS, and, then, 1:50 in 5% NGS, to a final concentration of 3ug/ml.

Rhodamine-Phalloidin (Molecular Probes, R-415). Phalloidin is a Phallotoxin, isolated from the deadly Amanita phalloides mushroom. Phallotoxins are used to label F-actin, forming the microfilaments. Stored at–20°C, it is stable for at least 1year. Used for immunocytochemistry diluted 1:50 in absolute methanol, and, then, 1:80 in 5% NGS, to a final dilution of 1:4000. Once diluted it can be stored at 4°C for up to three weeks.

A.4.2 Secondary Antibodies

TXR–conjugated goat anti-human IgG. Initial concentration of 1.5mg/ml (VectorLaboratories, TI-3000). Used for immunocytochemistry, diluted 1:100 in 1%FCS-PBS.

FITC-conjugated anti-sheep IgG. Initial concentration unknown (a gift from Dr. Prim Singh). Used for immunocytochemistry, diluted 1:400 in 10% milk in TBS with 0.2%.

FITC-conjugated sheep anti-mouse IgG. Initial concentration 10mg/ml (Diagnostic Scotland, Z584). Used for immunocytochemistry, diluted 1.50 or 1:100 in 1%FCS-PBS or 10% milk in TBS with 0.2%.

FITC conjugated rabbit anti-rat serum (a gift from Dr. Prim Singh). Used for immunocytochemistry, diluted 1:50 in 10% milk in TBS with 0.2%. Aliquotted and stored at –20°C. Stable for 1 year.

FITC conjugated donkey anti-rabbit IgG (10mg/ml; Diagnostic Scotland, T076). Used for immunocytochemistry, diluted 1:50 or 1:100 in 10% milk in TBS with 0.2%. Aliquotted and stored at –20°C. Stable for 1 year.

FITC conjugated goat anti-rabbit IgG (400ug/ml, Santa Cruz, Sc-2012). Used for flow cytometry, diluted 1:200 in D-PBS with 1.5% goat serum. Stored at 4°C. Stable for 1year.

FITC-conjugated goat anti-mouse IgG (2-5mg/ml; Sigma F-5262). Used for immunocytochemistry, diluted 1:64 in D-PBS with 0.3% BSA. Stored at-20°C.

A.4.3 Other

Vectashield Mounting Medium, with DAPI. It contains the 1.5ug/ml 4', 6-diamidino-2-phenylindole (DAPI; VectorLaboratories, H-1200), that stain DNA in blue. Light sensitive. Stored at 4°C it is stable for 1-2 years. Used for immunocytochemistry, 5-7ul slide.

Vectashield Mounting Medium (H1000; VectorLaboratories). Used for immunocytochemistry, when Propidium Iodide was used as a DNA stain.

FITC-conjugated mouse IgG1 (100ug/ml; Caltag, MG101). Isotype control for FITC anti-$p27^{KIP1}$. Stored at 4°C for 1-2 years. Used for flow cytometry, diluted 1:30 in D-PBS with 1% FCS.

Rabbit IgG (500ug/ml; Santa Cruz, Sc-2027). Isotype control for p130 antibody. Stored at 4°C for 2 years. Used for flow cytometry at a concentration of $2ug/10^6$ cells/ml (1:250) in D-PBS with 1.5% goat serum.

Mouse IgG2a (100ug/0.5ml; Sigma M 5409). Isotype control for cyclin D1 antibody. Stored at 4°C for 2 years. Used for immunocytochemistry, diluted 1:40 in 1% FCS-PBS.

Goat anti-Rat IgG MicroBeads (Miltenyi Biotec, 48502) and **anti-R-PE MicroBeads** (Miltenyi Biotec, 48801). Colloidal super-paramagnetic Microbeads conjugated with Goat anti-Rat IgG used at a concentration of 20ul/10^7 total cells, labelled with R-PE Rat IgG, recognizing mouse CD25. Cells were separated on **MS$^+$** positive selection columns (Miltenyi, 42201), taking a maximum of 10^7 positive cells/column.

A.5 MEDIA AND STOCKS FOR NUCLEAR TRANSFER AND EMBRYO CULTURE

Hepes-CZB (Chatot *et al.*, 1989) was used to collect MII oocytes and fertilised embryos. Hepes-CZB was also used to denude oocytes, supplemented with hyaluronidase; to enucleate oocytes, supplemented with cytochalasin B; to resuspend and inject donor cells, supplemented with PVP. CZB with Ca^{2+} and Mg^{2+} (Chatot *et al.*, 1989) was used to incubate enucleated oocytes before injection and before activation. CZB without Ca^{2+} and Mg^{2+} (Chatot *et al.*, 1989), supplemented with Sr^{2+} was used to activate reconstructed embryos. M16 medium (Whittingham, 1971) was used for culture of reconstructed and fertilised embryos. M2 (Fulton and Whittingham, 1978) was used for embryo transfer. Hepes-CZB was also tested for embryo culture, but blastocyst quality obtained (embryo cell numbers) were better when M16 was used. M2 was used, for a short period of time, to collect and denude MII oocytes and fertilised embryos, but was replaced with Hepes-CZB. M2 and M16 were initially prepared as described below. More recently they have been purchased from Sigma (M2, cat. N° M7167; M16, cat. N° M7292).

A.5.1 Stocks for M2 and M16 media

Stock A (10x)	M2	M16	
Component	**g/100ml**	**g/100ml**	**Product**
NaCl	5.533	4.700	Sigma S 5886
KCl	0.356	0.356	Sigma P 5405
KH_2PO_4	0.162	0.162	Sigma P 5655
Na lactate (60% syrup)	4.349	4.349	Sigma L 7900
D^+-glucose	1.000	0.350	Sigma G 6152
Penicillin G	0.060	0.060	Sigma P 7794
Streptomycin sulfate	0.050	0.050	Sigma S 9137
EDTA	-	0.037	Sigma E 5134

Stock B (10x)			
Component	**g/100ml (M2)**	**g/100ml (M16)**	**Product**
$NaHCO_3$	0.349	2.101	Sigma S 5761
Phenol Red	0.010	0.010	Sigma P5530

Stock C (100x)			
Component	**g/10ml (M2)**	**g/10ml (M16)**	**Product**
Na pyruvate	0.036	0.040	Sigma P 4562

Stock D (100x)			
Component	**g/50ml (M2)**	**g/50ml (M16)**	**Product**
$CaCl_2\,7H_2O$	1.260	1.260	Sigma C 7902

Stock E (10x)			
Component	**g/100ml (M2)**	**g/100ml (M16)**	**Product**
Hepes (acid)	4.969	-	Sigma H 4034
Phenol Red	0.010	-	Sigma P 5530

Stock Mg (100x)			
Component	**g/25ml (M2)**	**g/25ml (M16)**	**Product**
$MgSO_4\,7H_2O$	0.7325	0.7325	Sigma M 1880

Stock Glutamine (100x)			
Component	**g/10ml (M2)**	**g/10ml (M16)**	**Product**
L-glutamine	-	0.1460	Gibco 21051016

All stocks were stored at 4°C. Stocks A, D, E and Mg were stored up to 3 months, whereas stocks C and B, had to be made up fresh every two weeks.

A.5.2 Preparation of M2 and M16 media from stocks

Stock	100ml (M2)	50ml (M16)	Product
A	10.0ml	5.0ml	-
B	1.6ml	5.0ml	-
C	1.0ml	5.0ml	-
D	1.0ml	0.5ml	-
E	8.4ml	-	-
Mg	1.0ml	0.5ml	-
BSA (Fraction V)	0.40mg	0.20mg	Sigma A 6003
L-glutamine	-	0.5ml	-
Essential Amino acids (50x)	-	1.0ml	Gibco 111-30-036
Non-essential Amino acids (100x)	-	0.5ml	Sigma M 7145

M2 medium was prepared by putting all components in a glass beaker and adding 100ml ddH_2O. After all components were dissolved, pH was adjusted to 7.4 using NaOH. Medium was filtered into sterile 30ml universals, and stored at 4°C for maximum two weeks.

M16 medium was prepared by putting all components in a glass beaker and adding 50ml ddH_2O. After all components were dissolved, osmolarity was adjusted to 260-265 mOsm. Medium was filtered into sterile 30ml universals, and stored at 4°C for maximum one week.

A.5.3 M2 medium composition

Component	g/lt	MW	mM
NaCl	5.533	58.450	94.66
KCl	0.356	74.557	4.78
KH_2PO_4	0.162	136.091	1.19
Na lactate (60% syrup)	4.349	112.100	23.28
Glucose	1.000	179.860	5.56
Penicillin G	0.060 (10^4units)	-	-
Streptomycin sulfate	0.050	-	-
$NaHCO_3$	0.349	84.020	4.15
Phenol Red	0.010	-	-
Na pyruvate	0.036	110.000	0.33
$CaCl_27H_2O$	0.252	147.200	1.71
Hepes (acid)	4.969	238.300	20.85
$MgSO_47H_2O$	0.293	246.500	1.19
BSA	4.000	-	-
ddH_2O	Up to 1lt	-	-

Water used was deionized (ddH_2O), sterile, glass distilled. Osmolarity:~280mOsm.

A.5.4 M16 medium composition

Component	g/lt	MW	mM
NaCl	4.700	58.450	80.40
KCl	0.356	74.557	4.78
KH_2PO_4	0.162	136.091	1.19
Na lactate (60% syrup)	4.349	112.100	23.28
D^+-Glucose	0.350	179.860	1.95
Penicillin G	0.060 (10^4units)	-	-
Streptomycin sulfate	0.050	-	-
EDTA	0.037	372.20	0.1
$NaHCO_3$	2.101	84.020	25.00
Phenol Red	0.010	-	-
Na pyruvate	0.040	110.000	0.36
$CaCl_27H_2O$	0.252	147.200	1.71
$MgSO_47H_2O$	0.293	246.500	1.19
BSA	2.0	-	-
L-glutamine	0.1461	146.100	1.00
Essential Amino acids	(1:50)	-	-
Non-essential Amino acids	(1:100)	-	-
ddH_2O (deionized)	Up to 1lt	-	-

Water used was deionized (ddH_2O), sterile, glass distilled. Osmolarity:~265mOsm.

A.5.5 CZB, Ca^{2+}-free CZB and Hepes-CZB media

Stocks for CZB media

Stock (1x)		
Component	**g/1000ml**	**Product**
NaCl	4.760	Sigma S 5886
KCl	0.360	Sigma P 5405
KH_2PO_4	0.160	Sigma P 5655
Na lactate (60% syrup)	5.300ml	Sigma L 7900
D^+-glucose	1.000	Sigma G 6152
EDTA 2Na	0.040	Sigma E 6635
$MgSO_4 7H_2O$	0.290	Sigma M 1880
Speciality Media Ultra Pure Water	990ml	Sigma W 1503

Hepes-CZB stock

Stock	Concentration/500ml	Product
CZB stock	500ml	-
PVA	0.05g	Sigma P 8136

Preparation of Hepes-CZB from stocks

Stock	Concentration/100ml	Product
H-CZB stock	99ml	-
Hepes (acid)	0.476g	Sigma H 4034
$NaHCO_3$	0.042g	Sigma S 5761
$CaCl_2.2H_2O$ (100x)	1ml	Stock D
Na pyruvate	0.003g	Sigma P 4562
L-glutamine	0.015g	Gibco 21051016

Preparation of CZB and Ca^{2+}-free CZB from stocks

Stock	100ml CZB	100ml Ca^{2+}-free CZB	Product
CZB stock	99ml	100ml	-
$NaHCO_3$	0.211g	0.211g	Sigma S 5761
$CaCl_2$ $2H_2O$ (100x)	1ml	-	Stock D
Na pyruvate	0.003g	0.003g	Sigma P 4562
L-glutamine	0.015g	0.015g	Gibco 21051016
BSA	0.500g	0.500g	A 6003

CZB and Ca^{2+}-free CZB media composition

	CZB	Ca^{2+}-free CZB	
Component	g/lt (mM)	g/lt (mM)	MW
NaCl	4.76 (81.43)	4.76 (81.43)	58.450
KCl	0.36 (4.76)	0.36 (4.76)	74.557
KH_2PO_4	0.16 (1.76)	0.16 (1.76)	136.091
Na lactate (60% syrup)	5.30ml	5.30ml	-
D^+-glucose	1.00 (5.56)	1.00 (5.56)	179.860
EDTA 2Na	0.04 (0.11)	0.04 (0.11)	372.200
$MgSO_47H_2O$	0.29 (1.18)	0.29 (1.18)	246.500
Hepes	-	-	-
$NaHCO_3$	2.11 (25.11)	2.11 (25.11)	84.020
$CaCl_2$ $2H_2O$ (100x)	10ml	-	147.200
Na pyruvate	0.03 (27.27)	0.03 (27.27)	110.000
L-glutamine	0.15 (1.02)	0.15 (1.02)	146.100
Speciality Media Ultra Pure Water	Up to 100ml	Up to 100ml	-

Hepes CZB media composition

Component	g/lt	MW	mM
NaCl	4.76	58.450	81.43
KCl	0.36	74.557	4.76
KH_2PO_4	0.16	136.091	1.76
Na lactate (60% syrup)	5.30ml	-	-
D^+-glucose	1.00	179.860	5.56
EDTA.2Na	0.04	372.200	0.11
$MgSO_47H_2O$	0.29	246.500	1.18
Hepes (acid)	4.76g	238.3	20.85
$NaHCO_3$	0.42g	84.020	2.38
$CaCl_2$ $2H_2O$ (100x)	10ml	147.200	-
Na pyruvate	0.03	110.000	27.27
L-glutamine	0.15	146.100	1.02
Speciality Media Ultra Pure Water	Up to 1lt	-	-

A.5.6 Hyaluronidase stock

Stock was prepared by dissolving hyaluronidase powder (Sigma H 3884) in D-PBS, at a concentration of 15000 UI/ml. Stock solution was dispensed in 20ul aliquots and stored at –20°C. Hyaluronidase was diluted in Hepes-CZB at a working dilution of 300UI/ml (1 stock aliquot/ml). At this Hyaulronidase concentration, cumulus cells removal was complete after 4-5 min, at room temperature.

A.5.7 Cytochalasin B stock

Cytochalasin B (Sigma 6762) stock was prepared in D-PBS at a dilution of 0.5mg/ml, dispensed in 10ul aliquots, and stored at –20°C. Cytochalasin B stock was diluted in Hepes-CZB at a working dilution of 5ug/ml (1 stock aliquot/ml).

A.5.8 Sr^{2+} 10mM activation medium

Sr^{2+} stock

	g/lt	Product
$SrCl_2$ $6H_2O$ (100x)	1.130	Sigma S 0390
Speciality Media Ultrapure Water	Up to 25ml	Sigma S 5761

Activation medium with Sr^{2+} 10mM

Component	Concentration	Product
CZB stock	100ml	-
Na pyruvate	0.003g	Sigma P 4562
L-glutamine	0.015g	Gibco 21051016
$NaHCO_3$	0.211g	Sigma S 5761
BSA	0.500g	A 6003
Speciality Media Ultrapure Water	Up to 100 ml	Sigma S 5761

Sr^{2+} stock can be stored at 4°C for up to three months, and activation medium for up to 1 week. It is extremely important to prepare activation medium on ice, adding components one at a time, exactly in the same order as above. Osmolarity should be 280-291mOsm.

APPENDIX B

ABNORMALITIES OBSERVED IN DEVELOPMENTALLY ARRESTED CLONED EMRBYOS

B.1 STRUCTURAL ABNORMALITIES

B.1.1 Experimental design

Reconstructed embryos from 3 out of 8 nuclear transfer experiments (Paragraph 6.4) arrested at different developmental stages were fixed and triple stained for chromatin, microtubules and microfilaments with (DAPI/FITC-anti-α tubulin/TXR-phalloidin triple staining, Methods see Paragraph 2.13). The specimens were visualised using an epifluorescent, inverted microscope with a 40x objective, and digitalized images were acquired using the AQM program (methods see Paragraph 2.14). DAPI (nuclear staining) was used to visualise the nuclei, phalloidin (microfilament staining) to visualise microfilaments and cell boundaries and tubulin (microtubule staining) to assess normal or abnormal spindle formation.

Structural abnormalities were classified as:

1) Fragmentation;
2) Abnormal nuclear segregation into daughter blastomeres;
3) Other, unknown abnormalities.

B.1.2 Results

Descriptive studies showed no significant difference in the pattern of abnormalities observed in G0 and G1-derived embryos. Both groups showed similar (cell cycle effect, p=0.6), high rates of fragmentation (40.2% vs 37.0%; p>0.5) and lower rates of abnormal segregation (18.8% vs 19.9%; p=0.83). In both G0 and G1 groups the majority of non-developing embryos had no obvious structural

abnormality ("other", 41.0%-43.1%, p=0.11). Abnormality patterns were affected by the developmental stage at which the embryos were arrested. When considering both G0 and G1- derived NT embryos (NT G0+G1) the incidence of fragmentation was maximal at the 1-cell stage and then progressively decreases reaching minimal levels at the morula stage (Table B.1). An opposite trend was observed in abnormal nuclear segregation that was minimal at the 1 and 2-cell stages and significantly higher at the 4-cell/morula stages (Table B.1). Up to the 2-cell stage fragmentation was the main structural abnormality observed, but after the 2-cell stage abnormal segregation became predominant. Fragmentation was the main structural abnormality observed in G0 and G1-NT embryos arrested at the 1-cell and the 2-cell stages. However: in the G0-group abnormal segregation was the main abnormality observed in NT embryos arrested at the 4-cell stage and morula stages; in the G1-group fragmentation was still the main abnormality observed in 4-cell arrested embryos, and abnormal segregation became predominant only at the morula stage. The percentages of arrested embryos with no obvious structural abnormalities were high in all groups.

B.1.3 Conclusions

Regardless of the cell cycle stage, nuclear fragmentation appeared to be the main feature in developmentally arrested cloned embryos, followed by abnormalities in nuclear segregation. Furthermore, high percentages of G0 and G1 arrested embryos showed no obvious structural abnormality suggesting that, in most cases, developmental arrest of NT embryos was linked to more subtle genetic or epigenetic abnormalities. High rates of developmental arrest appeared to be a feature of T-cell derived embryos, regardless of their cell cycle stage.

The results of these experiments also indicated that arrest at the 1 and 2-cell stages was mainly associated with fragmentation, while arrest at the 4-cell and morula stages was mainly associated with abnormal nuclear distribution. The spindle abnormalities and incorrect attachment of chromatids to the microtubules similar to those observed in the first hours after reconstruction (Paragraph 6.3.1), might account for the incorrect segregation of genetic material. A better understanding of these mechanisms might improve development of cloned embryos.

Table B.1 Structural abnormalities of developmentally arrested G0 and G1-NT embryos

Stage	Type	1-cell	2-cell	4-cell	M
NT (G0+G1)	abnormal	5\58 (8.6)[a]	24\156 (15.4)[a]	12\29 (41.4)[b]	10\20 (50.0)[b]
	fragmented	32\58 (55.2)[a]	59\156 (37.8)[b]	8\29 (27.6)[b,c]	2\20 (10.0)[c]
	other	21\58 (36.2)[a]	73\156 (46.8)[a]	9\29 (31.0)[a]	8\20 (40.0)[a]
NT G0	abnormal	1\24 (4.1)[a]	14\82 (17.1)[a]	6\8 (75.0)[b]	1\3 (33.3)[a]
	fragmented	13\24 (54.2)[a]	34\82 (41.5)[a]	0\8 (0.0)[b]	0\3 (0.0)[b]
	other	10\24 (41.7)[a]	34\82 (41.5)[a]	2\8 (25.0)[a]	2\3 (66.7)[a]
NT G1	abnormal	4\34 (11.8)[a]	10\74 (13.5)[a]	6\21 (28.6)[a,b]	9\17 (52.9)[b]
	fragmented	19\34 (55.9)[a]	25\74 (33.8)[b]	8\21 (38.1)[b]	2\17 (11.8)[b]
	other	11\34 (32.3)[a]	39\74 (52.7)[b]	7\21 (33.3)[a,b]	6\17 (35.3)[a,b]

Data acquired from three out of eight replicate experiments carried out to assess in vitro developmental potential of NT embryos. Non developing embryos were fixed and triple stained with anti-phalloidin/anti-tubulin/DAPI to assess nuclear and cell morphology. Embryos were classified as being fragmented or abnormal if they had an unequal nuclear/cell distribution. Embryos which did not belong tot he previous two categories were classified as "other". Values within rows with different superscripts differ significantly. Chi-square test or Fischer's exact test for 2x2 contingency (two-tailed, Mid-P-value), where expected frequencies were less than 5 (α=0.05).

The only difference in the pattern of abnormalities between G0 and G1-derived embryos was that, in the former group, abnormal segregation peaked at the 4-cell stage and fragmentation was no longer detected beyond the 2-cell stage, while in the latter group at the 4-cell stage fragmentation was still the main feature and abnormal segregation became predominant only at the later morula stage (Table B.1).

B.2 EPIGENETIC ABNORMALITIES

B.2.1 Experimental Design

G0 and G1-NT embryos, arrested at the 1 and 2-cell stages were collected in two replicate experiments on day 1 and day 2 after reconstruction (see Paragraph 6.5.2). Embryos that failed to cleave by day 1 (1-cell block embryos) or failed to reach the 4-cell stage by day 2 (2-cell block embryos), were fixed and stained for DAPI/M31/PCNA or DAPI/H4.Ac5 or H4.Ac12. Analysis focused on embryos that had no clear signs of structural abnormalities, such as fragmentation or abnormal nuclear segregation, previously classified as "other" (Paragraph B.1). Results were compared with those previously obtained for fertilised embryos (Paragraph 6.5.1).

B.2.2 Results

Out of 337 reconstructed embryos 174 (51.5%) failed to cleave (1-cell block). Of these 128/174 (74.7%) had clear structural abnormalities, such as fragmentation or abnormal nuclear segregation, while 46/174 (53.0%) had no signs of structural abnormalities and were classified as "other" (Fig.B.1). Most embryos in the "other" group were arrested at the pronuclear stage, while lower percentages of embryos arrested before pronuclear formation, retaining a condensed chromatin (condensed stage) or chromosomes (Premature Chromosome Condensation stage, PCC; Fig.B.1).

Embryos arrested at very early developmental stages ("condensed" and PCC stages) were negative for all staining. Embryos arrested at the pronuclear (PN) stage had lower percentages of $PCNA^+$ ($p<0.001$) and lower percentages of $M31^+$ embryos ($p<0.001$), although patterns of M31 staining were similar to controls (only

Figure B.1 Epigenetic abnormalities in developmentally arrested NT embryos

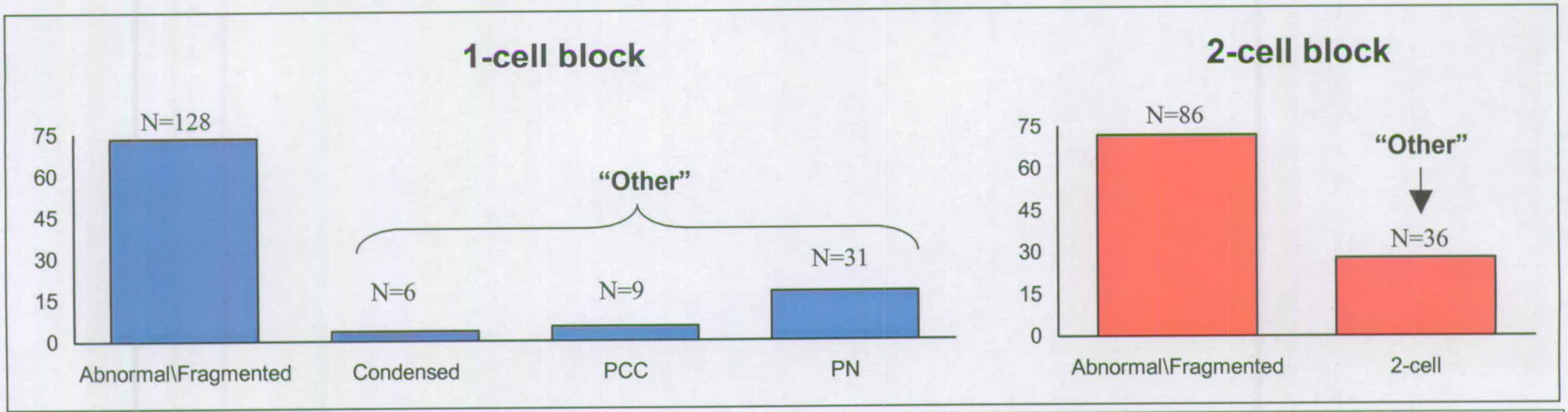

	PN (Control)	PN (NT)	2-cell (Control)	2-cell (NT)
$PCNA^+$	24\28 (85.7) [a]	6/18 (33.3) [b]	12\12 (100) [a]	14/15 (93.0) [a]
$M31^+$ (total)	24\28 (85.7) [a]	6/18 (33.3) [b]	12\12 (100) [a]	15/15 (100) [a]
$M31^+$ (condensed)	0\28 (0.0) [a]	0/18 (0.0) [a]	4\12 (33.3) [a]	0/15 (0.0) [b]
$M31^+$ (diffused)	24\28 (85.7) [a]	6/18 (33.3) [b]	8\12 (66.7) [a]	5/15 (100) [a]
$Ac5\12^+$(total)	26\48 (54.1) [a]	8/11 (72.8) [a]	30\30 (100) [a]	0/22 (0.0) [b]
$Ac5\12^+$ (peripheral)	16\48 (33.3) [a]	4/11 (36.4) [b]	28\30 (93.3) [a]	0/22 (0.0) [b]
$Ac5\12^+$ (diffused)	10\48 (20.8) [a]	4/11 (36.4) [b]	2\30 (6.7) [a]	0/22 (0.0) [b]

Developmentally arrested NT embryos with no visible structural abnormality (e.g. abnormal segregation\fragmentation), classified as "other", were stained for DAPI\PCNA\M31 or DAPI\H4.Ac5 and Ac12. Results were compared with those obtained in fertilised control embryos (Paragraph 6.5.1), at the pronuclear (PN) and 2-cell stage. Data from two nuclear transfer experiments, referred to NT embryos in "other" group, were analysed using a Pearson Chi-square or a Fisher's exact test for 2x2 contingency (two tailed test, Mid-P-value test, α=0.05), where expected frequencies were less than 5. Values within columns with different superscripts are significantly (α=0.05) different. Embryos arrested at the 1-cell stage at the "condensed" or PCC stages were not included since they were negative for all staining.

"diffused" pattern was observed). Staining for histone H4 acetylation on lysines 5 and 12 showed that embryos arrested at the PN stage had similar percentages of H4.Ac5/12$^+$ embryos (p=0.29). The peripheral acetylation pattern was predominant n control, fertilised embryos, while "peripheral" and "diffused" acetylation patterns were equally represented in cloned embryos arrested at the PN stage (Fig.B.1).

The nuclear transfer group arrested at the 2-cell stage had a similar proportion of PCNA$^+$ (p=0.556) and M31$^+$ (p=1.0) embryos compared to the control group (Fig.B.1). However the NT group had a lower proportion of M31$^+$ embryos with the "condensed" form of M31, organised in clusters, colocalised with patches of pericentromeric heterochromatin (p=0.028).

All control embryos, at the 2-cell stage, were acetylated on lysines 5 or 12 of histone H4, while all NT embryos developmentally arrested at the 2-cell stage were deacetylated on lysines 5 or 12 (p<0.0001).

B.2.3 Conclusions

Some embryos were arrested at very early stages, "condensed", maybe as a result of membrane retention, and at the PCC.

Abnormal epigenetic patterns observed at the "condensed or PCC stage included:

- Absence of acetylation staining, is in contrast with what observed in developing nuclear transfer embryos and described for fertilised embryos (Worrad *et al.,* 1995) embryos where DNA appeared to be hyperacetylated during early development;
- Absence of M31 staining, that had been observed at least in G1 derived NT embryos (no data available from fertilised embryos at this stage).

Absence of PCNA staining was normal expected at these early stages of development.

Epigenetic abnormalities observed in embryos arrested at the PN stage included:

- Lower percentages of PCNA$^+$, suggesting DNA replication problems;
- Lower percentages of M31$^+$ embryos, suggesting abnormalities in chromatin organisation;

- Lower proportions of cloned embryos with peripheral acetylation staining pattern, associated with transcriptional activation of donor cell genome.

Results of immunostaining of nuclear transfer embryos arrested at the 2-cell stage showed that they underwent normal DNA replication. However epigenetic abnormalities were observed:

- All developmentally arrested embryos failed to organise M31 in clusters while "condensed" distribution was observed in 33% of control embryos at the s2-cell stage, suggesting the presence of chromatin abnormalities;
- All NT embryos were negative for acetylation of histone H4, a state incompatible with normal transcription, while 100% of control embryos were acetylated and 93% of them were potentially transcriptionally active.

The results of these experiments showed an association between developmental arrest and epigenetic instability of cloned embryos.

REFERENCES

Adams RL and Lindsay JG (1967). Hydroxyurea: reversal of inhibition and use as a cell-synchronizing agent. *J. Biol. Chem.*, 242: 314.

Adenot PG, Szollosi MS, Geze M, Renard JP, Debey P (1991). Dynamics of paternal chromatin changes in live one-cell mouse embryo after natural fertilisation. *Mol. Reprod. Dev.*, 28: 23-34.

Adenot PG, Mercier Y, Renard JP, Thompson EM (1997). Differential H4 acetylation of paternal and maternal chromatin precedes DNA replication and differential transcriptional activity in pronuclei of 1-cell mouse embryos. *Development*, 124: 4615-4625.

Ajchenbaum F, Ando K, DeCaprio J, Griffin JD (1993). Independent regulation of human D-type cyclin gene expression during G1 phase in primary human T-lymphocytes. *J. Biol. Chem.*, 268: 4113-4119.

Alberio R, Motlik J, Stojkovic M, Wolf E, Zakhartchenko V (2000). Behavior of M-phase synchronized blastomeres after nuclear transfer in cattle. *Mol. Reprod. Dev.*, 57: 37-47.

Amano T, Tani T, Kato Y, Tsunoda Y (2001a). Mouse cloned from embryonic stem (ES) cells synchronized in metaphase with nocodazole. *J. Exp. Zool.*, 289: 139-145.

Amano T, Kato Y, Tsunoda Y (2001b). Full-term development of enucleated mouse oocytes fused with embryonic stem cells from different cell lines. *Reproduction*, 12: 729-733.

Antequera F, Macleod D, Bird AP (1989). Specific protection of methylated CpGs in mammalian nuclei. *Cell*, 58: 509-517.

Aronson I and Solter D (1987). Developmental potency of gametic and embryonic genomes revealed by nuclear transfer. In: *"Current Topics in developmental Biology"*, vol.23, NY Academic Press, pp 55-71.

Avitahl N, Winandy S, Friedrich C, Jones B, Ge Y, Georgopoulos K (1999). Ikaros sets thresholds for T cell activation and regulates chromosome propagation. *Immunity*, 10: 333-343.

Baguisi A, Behboodi E, Melican DT, Pollock JS, Destrempes MM, Cammuso C, Williams JL, Nims SD, Porter CA, Midura P, Palacios MJ, Ayres SL, Denniston RS, Hayes ML, Ziomek CA, Meade HM, Godke RA, Gavin WG, Overstrom EW, Echelard Y (2001). Production of goats by somatic cell nuclear transfer. Nat. Biotechnol.,17: 456-461.

Baldin V, Lukas J, Marcote MJ, Pagano M, Draetta G (1993). Cyclin D1 is a nuclear protein required for cell cycle progression in G1. *Gen. Dev.*, 7: 812-821.

Baqir and Smith (2000). Cell cycle arrest by means of serum starvation and confluency is associated with altered expression of imprinted genes in mouse embryonic stem cells. *Theriogenology*, 53: 402.

Barnes FL, Robl JM, First NL (1987). Nuclear transplantation in mouse embryos: assessment of nuclear function. *Biol. Reprod.*, 36: 1267-1274.

Barnes F, Endebrock M, Looney C, Powell R, Westhusin M, Bondioli K (1993). Embryo cloning in cattle: the use of *in vitro* matured oocytes. *J. Reprod. Fertil.*, 97: 317-20.

Bismuth G, Moreau JL, Sommè G, Duphot M, Dautry-Varsta A, Robb RJ, Thèze J (1985). Regulation of interleukin-2 (IL-2) receptor expression: IL-2 as an inducing signal for the expression of its own receptor on a murine T helper cell line. *Eur. J. Immunol.*, 15: 723-727.

Blow JJ, Laskey RA (1988). A role for the nuclear envelope in controlling DNA replication within the cell cycle. *Nature*, 332: 546-548.

Bordignon V, Clarke HJ, Smith LC (1999). Developmentally regulated loss and reappearance of immunoreactive somatic histone H1 on chromatin of bovine morula-stage nuclei following transplantation into oocytes. *Bio. Reprod.*, 61: 22-30.

Bordignon V, Clarke HJ, Smith LC (2001). Factors controlling the loss of immunoreactive somatic histone H1 from blastomere nuclei in oocyte cytoplasm: a potential marker of nuclear reprogramming. *Dev. Biol.*, 233: 192-203.

Boquest AC, Day BN, Prather RS (1999). Flow Cytometric analysis of cultured porcine foetal fibroblast cells. *Biol. Reprod.*, 60: 1013-1019.

Bourc'his D, Le Bourhis D, Patin D, Niveleau A, Comizzoli P, Renard JP, Viegas-Pequignot E (2001). Delayed and incomplete reprogramming of chromosome methylation patterns in bovine cloned embryos. *Curr. Biol.*, 11:1542-1546.

Bravo R, Bravo H (1987). Existence of two populations of cyclin/proliferating cell nuclear antigen during the cell cycle: associationwith DNAreplication sites. *J. Cell. Biol.*, 105: 1549-1554.

Bridger JM, Boyle S, Kill IR, Bickmore WA (2000). Re-modelling of nuclear architecture in quiescent and senescent human fibroblasts. *Curr. Biol.*, 10: 149-152.

Briggs R and King TJ (1952). Transplantation of living nuclei from blastula cells into enucleated frogs' eggs. *Proc. Nat. Acad. Sci. USA*, 39: 455-461.

Campbell KHS (1998). Look at the bright side of cloning. *Nat. Med.*, 4: 557-558.

Campbell KHS, Ritchie WA, Wilmut I (1993). Nuclear-cytoplasmic interactions during the first cell cycle of nuclear transfer reconstrycted bovine embryos: implications for deoxyribonucleic acid replication and development. *Biol. Reprod.*, 49: 933-942.

Campbell KHS, McWhir J, Ritchie W, Wilmut I (1995). Production of live lambs following nuclear transfer of cultured embryonic disc cells. *Theriogeneology*, 43: 181.

Campbell KHS, McWhir J, Ritchie WA, Wilmut I (1996a). Sheep cloned by nuclear transfer from a cultured cell line. *Nature*, 380: 64-66.

Campbell KHS, Loi P, Otaegui PJ, Wilmut I (1996b). Cell cycle co-ordination in embryo cloning by nuclear transfer. *Rev. Rep.*, 1: 40-46.

Cao X, Kozak CA, Liu YJ, Noguchi M, O'Connell E, Leonard WJ (1993). Characterisation of cDNAs encoding the murine interleukin-2 receptor (IL-2R) gamma chain: chromosomal mapping and tissue specificity of IL-2R gamma chain expression.*Proc. Nat. Acad. Sci. U.S.A.*, 90: 8464-8468.

Celis JE, Bravo R (1984). Synthesis of the nuclear protein cyclin in growing, senescent and morphologically transformed human skin fibroblasts. *FEBS Letters*, 165: 21-25.

Chatot CL, Ziomek CA, Bavister BD, Lewis JL, Torres I (1989). An improved culture medium supports development of random-bred 1-cell mouse embryos *in vitro*. *J. Reprod. Fertil.*, 86: 679-88.

Cheong HT, Takahashi Y, Kanakawa H (1993). Birth of mice after transplantation of early cell-cycle stage embryonic nuclei into enucleated oocytes. *Biol. Reprod.*, 48: 958-963.

Cheong HT, Takahashi Y, Kanakawa H (1994). Relationship between nuclear remodlling and subsequent development of mouse embryonic nuclei transferred to enucleated oocytes. *Mol. Rep. Dev.*, 37: 138-145.

Cibelli JB, Stice SL, Golueke PJ, Kane JJ, Jerry J, Blackwell C, Ponce de Leon A, Robl JM (1998). Cloned transgenic calves produced from non-quiescent foetal fibroblasts. *Science*, 280: 1256-1258.

Clarke HJ, McLay DW, Mohamed OA (1998). Linker histone transitions during mammalian oogenesis and embryogenesis. *Dev. Genet.*, 22: 17-30.

Coats S, Flanagan M, Nourse J, Roberts JM (1996). Requirement of p27KIP1 for restriction point control of the fibroblasts cell cycle. *Science*, 272: 877-880.

Coats S, Whyte P, Fero ML, Lacy S, Chung G, Randel E, Firpo E, Roberts J (1999). A new pathway for mitogen-dependent Cdk2 regulation uncovered in $p27^{KIP1}$–deficient cells. *Current Biol.*, 9: 163-173.

Collas P and Barnes FL (1994). Nuclear transplantation by microinjection of inner cell mass and granulosa cell nuclei. *Mol. Rep. Dev.*, 38: 264-267.

Collas P, Blaise JJ, Robl JM (1992a). Influence of the cell cycle stage of the donor nucleus on development of nuclear transplant rabbit embryos. *Biol. Reprod.*, 46: 492-500.

Collas P, Pinto-Correia C, Leon FD, Robl J (1992b). Effect of donor cell cycle stage on chromatin and spindle morphologyin nuclear transplant rabbit embryos. *Biol. Reprod.*, 46: 501-511.

Collas P, Robl JM (1990). Factors affecting the efficiency of nuclear transplantation in the rabbit embryo. *Biol. Reprod.*, 43: 877-884.

Collas P, Robl JM (1991). Relationship between nuclear remodelling and development in nuclear transplant of rabbit embryos. *Biol. Reprod.*, 445: 455-465.

Colman A (2000). Somatic cell Nuclear Transfer in mammals: progress and applications. *Cloning*, 1: 185-200.

Croston GE, Kadonaga JT (1993). Role of chromatin structure in the regulation of transcription by RNA polymerase II. *Curr. Op. Cell Biol.*, 5: 417-423.

Czolowska R, Modlinski JA, Tarkowski AK (1984). Behaviour of thymocyte nuclai in non activated and activated mouse embryos. *J. Cell Sci.*, 69: 19-34.

Czolowska R, Waksmundska M, Kubiak JZ, Tarkowski AK (1986). Chromosome condensation activity in ovulated metaphase II mouse oocytes assayed by fusion with interphase blastomeres. *J. Cell Sci.*, 84: 129-138.

Dauvillier S, Ott MO, Renard JP, Legouy E (2001). BRM (SNF2alpha) expression is concomitant to the onset of vasculogenesis in early mouse post-implantation development. *Mech. Dev.*, 101: 221-225.

DiBerardino MA, Orr NH, McKinnell RG (1986). Feeding tadpoles cloned from Rana erythrocyte nuclei. *Proc. Natl. Acad. Sci.USA*, 83: 8231-8234.

Dimitrov S, Almouzni G, Dasso M, Wolffe AP (1993). Chromatin transitions during early Xenopus embryogenesis: changes in histone H4 acetylation and in linker histone type. *Dev. Biol.*, 160: 214-227.

Dimitrov S, Wolffe AP (1996). Remodelling somatic nuclei in Xenopus laevis egg extracts: molecular mechanisms for the selective release of histones H1 and H1° from chromatin and the acquisition of transcriptional competence. *EMBO J.*, 15: 5897-5906.

Dimri GP, Lee X, Basile G, Acosta M, Scott G, Roskelley C, Medrano EE, Linskens M, Rubelj I, Pereira-Smith O, Peacocke M, Campisis J (1995). A biomarker that identifies senescent human cells in culture and aging skin *in vivo*. *Proc. Nat. Acad. Sci.USA*, 92: 9363-9367.

Doyle A, Griffiths JB, Newell DG (1998). Diploid strains. Culture Characteristics. In: *Cell and tissue culture laboratory procedures.* Chapter 6, Part 6A. Eds. John Wiley & Sons Ltd., Chichester, UK.

Willasden SM (1986). Nuclear transplantation in sheep embryos. *Nature,* 320: 63-65.

D'Urso D, Muller HW (1997). Ins and outs of peripheral myelin protein-22: mapping transmembrane topology and intracellular sorting. *J. Neurosci. Res.*, 49: 551-562.

Dyson N (1998). The regulation of E2F by pRb-family proteins. *Gen. Dev.*, 12: 2245-2262.

Edgar B (1995). Diversification of cell cycle controls in developing embryos. *Curr. Biol.*, 7: 815-824.

Eggan K, Akutsu H, Loring J, Jackson-Grusby L, Klemm M, Rideout WM 3rd, Yanagimachi R, Jaenisch R (2001). Hybrid vigor, foetal overgrowth, and viability of mice derived by nuclear cloning and tetraploid embryo complementation. *Proc. Natl. Acad. Sci.USA*, 98: 6209-6214.

El-Deiry WS, Tokino T, Velculescu VE, Levy DB. Parsons JM, et al. (1993). WAF1, a potential mediator of p53 tumour suppression. *Cell,* 75: 817-825.

Erard F, Corthèsy P, Smith KA, Fiers W, Conzelmann A, Nabholz M (1984). Characterisation of soluble factors that induce the cytolytic activity and the expression of T cell growth factor receptors of a T cell hybrid. *J. Exp. Med.*, 160: 584-599.

Feil R, Boyano MD, Allen ND, Kelsey G (1997). Parental chromosome-specific chromatin conformation in the imprinted U2af1-rs1 gene in the mouse. *J. Biol. Chem.*, 272: 20893-20900.

Firpo EJ, Koff A, Solomon MJ, Roberts JM (1994). Inactivation of a Cdk2 inhibitor during interleukin-2-induced proliferation of human T-lymphocytes. *Mol. Cell. Biol.*, 14: 4889-4901.

Fulton BP, Whittingham DG (1978). Activation od mammalian oocytes by intracellular injection od calcium. *Nature,* 273: 149-151.

Galat VV, Lagutina IS, Mesina MN, Chernich VJ, Prokofiev MI (1998). Developmental potential of rabbit nuclear transfer embryos derived from donor foetal fibroblasts. *Theriogenology*, 51: 203.

Galli C, Lazzari G, Flechon J, Moor RM, (1994). Embryonic stem cells in farm animals. *Zygote,* 2: 385-389.

Galli C, Duchi R, Moor RM, Lazzari G (1999). Mammalian leukocytes conatin all the genetic information necessary for the development of a new individual. *Cloning,* 1: 161-170.

Garry FB, Adams R, McCann JP, Odde KG (1996). Postnatal characteristics of calves produced by nuclear transfer cloning. *Theriogenology,* 45: 141-152.

Gelius B, Wade P, Wolffe A, Wrange O, Ostlund Farrants AK (1999). Characterisation of a chromatin remodelling activity in Xenopus oocytes. *Eur. J. Biochem.*, 262: 426-434.

Georgopoulos K (2001). Haematopoietic cell-fate decisions, chromatin regulation and ikaros. *Nat. Rev. Immunol.*, 2: 162-174.

Geppert TD, Lipsky PE (1987). Accessory cell independent proliferation of human T4 cells stimulated by immobilized monoclonal antibodies to CD3. *J. Immunol.*, 138: 1660-1666.

Gerace L, Blobel G (1980). The nuclear envelope lamina is reversibly depolymerized during mitosis. *Cell,* 19: 277-287.

Gilbert DM, Neilson A, Miyazawa H, DePamphilis ML, Burhans WC (1995). Mimosine arrests DNA synthesis at replication forks by inhibiting deoxyribonucleotide metabolism. *J. Biol. Chem.*, 270: 9597-9606.

Gregory PD and Hörtz W (1998). Chromatin and Transcription. How transcription factors battle with a repressive chromatin environment. *Eur. J. Biochem.*, 251:9-18.

Gregory RI, Randall TE, Johnson CA, Khosla S, Hatada I, O'Neill LP, Turner BM, Feil R (2001). DNA methylation is linked to deacetylation of histone H3, but not H4, on the imprinted genes Snrpn and U2af1-rs1. *Mol. Cell. Biol.*, 21: 5426-36.

Gregory RI, O'Neill LP, Randall TE, Fournier C, Khosla S, Turner BM, Feil R (2002). Inhibition of histone deacetylases alters allelic chromatin conformation at the imprinted U2af1-rs1 locus in mouse embryonic stem cells. *J. Biol. Chem.*, 277: 11728-34.

Guo Y, Sklar GN, Borkowski A, Kyprianou N (1997). Loss of the cyclin-dependent kinase inhibitor p27(Kip1) protein in human prostate cancercorrelates with tumour grade. *Clin. Cancer. Res.*, 3: 2269-2274.

Gurdon JB (1986) Nuclear Transplantation in eggs and oocytes. *J. Cell Sci. Suppl.* 4: 287-318

Gurdon JB and Uehlinger V (1966). Fertile intestine nuclei. *Nature*, 210: 1240-1241.

Gurdon JB, Laskey RA, Reeves OR (1975). The developmental capacity of nuclei transplanted from keratinized skin cells of adult frogs. *J. Emb. Exp. Morph.*, 34: 93-112.

Gurdon JB, Brennan S, Fairman S, Mohun TJ (1984). Transcription of muscle-specific actin genes in early Xenopus development: nuclear transplantation and cell dissociation. *Cell*, 38: 691-700.

Hagtin A, Karlsson C, Clute P, Jackman M, Pines J (1998). MPF localisation is controlled by nuclear export. *EMBO J.*, 17: 4127-4138.

Harlow E and Lane D (1988). Cell staining. In *Antibodies: a laboratory manual.* Cold Spring Harbor Laboratory Ed., NY, USA. Chapter 10, pp 384-390.

Heard E, Clerc P, Avner P (1997). X-chromosome inactivation in mammals. *Annu. Rev. Genet.*, 31: 571-610.

Heynman Yand Renard JP (1996). Cloning of domestic species. In: *Animal Reproduction: research and practice.* Eds. Stone GM, Evans G, Elsevier, New York, pp: 427-436.

Hill JR, Winger QA, Jones KL, Thompson JA, Burghardt RC, Westhusin ME (1998). Serum starvation of bovine foetal fibroblasts prior to nuclear transfer increases *in vitro* developmental rates. *Theriogenology,* 51: 204.

Hirji KF, Tan SJ, Elashoff RM (1991). A quasi-exact test for comparing two binomial proportions. *Statistics in Medicine,* 10: 1137-1153.

Hiyoshi H, Uno S, Yokota T, Katagiri C, Nishida H, Takai M, Agata K, Eguchi G, Abe S (1991). Isolation of cDNA for a Xenopus sperm-specific basic nuclear protein (SP4) and evidence for expression of SP4 mRNA in primary spermatocytes. *Exp. Cell Res.*, 194: 95-99.

Hochedlinger K, Jaenish R (2002). Monoclonal mice generated by nuclear transfer from mature B and T-cells. *Nature*, 718: 1-4.

Holm P, Walker SK, Seamark RF (1996). Embryo viability, duration of gestation and birth weight in sheep after transfer of *in vitro* matured and in vitro fertilised zygotes cultured in vitro or in vivo. *J. Reprod. Fertil.*, 107: 175-181.

Horsley D, Hutchings A, Butcher GW, Singh PB (1996). M32, a murine homologue of Drosophila heterochromatin protein 1 (HP1), localises to euchromatin within interphase nuclei and is largely excluded from constitutive heterochromatin. *Cytog. Cell. Genet.*, 73: 308-311.

Humpherys D, Eggan K, Akutsu H, Hochedlinger K, Rideout WM 3rd, Biniszkiewicz D, Yanagimachi R, Jaenisch R (2001). Epigenetic instability in ES cells and cloned mice. *Science*, 293: 95-97.

Hutchinson CJ, Brill D, Cox R, Gilbert J, Kill I, Ford CC (1993). DNA replication and cell cycle control in *Xenopus* egg extracts. In: *The Cell cycle.* Eds. Brooks R, Fantes P, Hunt T, Wheatley D. *J.Cell Sci., Supplement* 12:197-212.

Iatropoulos MJ, Williams GM (1996). Proliferation markers. *Exp. Toxicol. Pathol.*, 48: 175-181.

Ikeda K, Takahashi Y (2001). Effects of maturational age of porcine oocytes on the induction of activation and development in vitro following somatic cell nuclear transfer. *J. Vet. Med. Sci.*, 63:1003-1008.

Illmensee K and Hoppe PC (1981). Nuclear transplantation in Mus musculus: developmental potential of nuclei from pre-implantation embryos. *Cell*, 23: 9-18.

Inoue K, Kohda T, Lee J, Ogonuki N, Mochida K, Noguchi Y, Tanemura K, Kaneko-Ishino T, Ishino F, Ogura A (2002). Faithful expression of imprinted genes in cloned mice. *Science*, 295: 297.

James TC, Elgin SC (1986). Identification of a non-histone chromosomal protein associated with heterochromatin in *Drosophila melanogaster* and its gene, *Mol. Cell. Biol.*, 6: 3862-3872.

Jeppesen P, Turner BM (1993). The inactive X chromosome in female mammals is distinguished by a lack of histone H4 acetylation, a cytogenetic marker for gene expression. *Cell*, 74: 281-289.

Johnson RT, Rao PN (1970a). Mammalian cell fusion: studies on regulation of DNA replication and mitosis. *Nature*, 225: 159-164.

Johnson RT, Rao PN (1970b). Mammalian cell fusion: induction of premature chromosome condensation in interphase nuclei. *Nature*, 226: 717-722.

Jones DO, Cowell IG, Singh PB (2000). Mammalian chromodomain proteins: their role in genome organisation and expression. *BioEssays*, 22: 124-137.

Juan G, Darzynkiewicz Z (1998). Cell cycle analysis by flow cytometry and laser scanning cytometry. In *Cell Biology a Laboratory handbook,* Academic Press, London, pp 261-273.

Kang YK, Koo DB, Park JS, Choi YH, Chung AS, Lee KK, Han YM (2001). Aberrant methylation of donor genome in cloned bovine embryos. *Nat. Genet.*, 28: 173-177.

Kang YK, Park JS, Koo DB, Choi YH, Kim SU, Lee KK, Han YM (2002). Limited demethylation leaves mosaic-type methylation states in cloned bovine pre-implantation embryos. *EMBO J.*, 21: 1092-100.

Kanka J, Fulka JJr, Fulka J, Petr J (1991). Nuclear transplanation in bovine fine structural and autoradiographic studies. *Mol. Rep. Dev.*, 29: 110-116.

Karlsson C, Afrakhte M, Westermark B, Paulsson Y (1999). Elevated level of gas3 gene expression is correlated with G0 growth arrest in human fibroblasts. *Cell Biol. Int.*, 23: 351-358.

Kasinathan P, Knott JG, Wang Z, Jerry DJ, Robl JM (2001). Production of calves from G1 fibroblasts. *Nat. Biotech.*, 19: 1176-1178.

Kato Y, Tani T, Sotomaru Y, Kurokawa K, Kato J, Doguchi H, Yasue H, Tsunoda Y (1998). Eight calves cloned from somatic cells of a single adult. *Scence*, 282: 2095-2098.

Kato Y, Tsunoda Y (1992). Synchronous division of mouse two-cellembryoswith nocodazole *in vitro*. *J. Rep. Fert.*, 95: 39-43.

Keefer CL, Baldassarre H, Keyston R, Wang B, Bhatia B, Bilodeau AS, Zhou JF, Leduc M, Downey BR, Lazaris A, Karatzas CN (2001). Generation of Dwarf Goat (Capra hircus) Clones Following Nuclear Transfer with Transfected and Nontransfected Foetal Fibroblasts and *in vitro*-Matured Oocytes. *Biol. Reprod.*, 64: 849-856.

Keefer CL, Stice SL, Matthews DL (1994). Bovine inner cell mass cells as donor nuclei in the production of nuclear transfer embryos and calves. *Biol. Reprod.*, 50: 935-939.

Keshet I, Lieman-Hurwitz J, Cedar H (1986). DNA methylation affects the formation of active chromatin. *Cell*, 28: 535-543.

Khochbin S, Wolffe AP (1994). Developmentally regulated expression of linker-histone variants in vertebrates. *Eur. J. Biochem.*, 225: 501-510.

Kikuchi K, Naito K, Noguchi J, Shimada A, Kaneko H, Yamashita M, Aoki F, Tojo H, Toyoda Y (2000). Maturation/M-phase promoting factor: a regulator of aging in porcine oocytes. *Biol. Reprod.*, 63: 715-722.

Kikyo N, Wade PA, Guschin D, Ge H, Wolffe AP (2000). Active remodelling of somatic nuclei in egg cytoplasm by the nucleosomal ATPase ISWI. *Science*, 289: 2360-2362.

Kikyo N, Wolffe AP (2000). Reprogramming nuclei: insights from cloning, nuclear transfer and heterokaryons. *J. Cell Sci.*, 113: 11-20.

Kill IR (1991). The timing of the formation and usage of replicase clusters in S-phase nuclei of human diploid fibroblasts. *J. Cell Sci.*, 100: 869-876.

Kim YH, Proust JJ, Buchholz MJ, Chrest FJ, Nordin AA (1992). Expression of the murine homologue of the cell cycle control protein p34cdc2 in T-lymphocytes. *J. Immunol.*, 149: 17-23.

Kimura A, Ersson B (1981). Activation of T-lymphocytes by lectins and carbohydrate-oxidizing reagents viewed as an immunological recognition of cell-surface modifications seen in the context of "self" major histocompatibility complex antigens. *Eur. J. Immunol.*, 11: 475-483.

Knosp O, Talasz H, Puschendorf B (1991). Histone acetylation and histone synthesis in mouse fibroblasts during quiescence and re-stimulation into S-phase. *Mol. Cell. Biochem.*, 101: 51-58.

Koff A, Giordano A, Desai D, Yamashita K, Harper JW, Elledge S, Nishimoto T, Morgan DO, Franza BR, Roberts JM (1992). Formation and activation of a cyclin E-Cdk2 complex during the G1 phase of the human cell cycle. *Science*, 257: 1689-1694.

Koide T, Ainscough J, Wijgerde M, Surani MA (1994). Comparative anlysis of Igf-2/H19 imprinted domain: identificationof a highly conserved intergenic Dnase I hypersensitive region. *Genomics*, 24: 1-8.

Kono T (1997). Nuclear transfer an reprogramming. *Rev. Rep.*, 2: 74-80.

Kono T, Kwon OY, Nakahara T (1991). Development of enucleated mouse oocytes reconstituted with embryonic nuclei. *J. Rep. Fert.*, 93: 165-172.

Kono T, Kwon OY, Watanabe T, Nakahara T (1992). Development of mouse enucleated oocytes receiving a nucleus from different stages of the second cell cycle. *J. Rep. Fert.*, 94: 481-487.

Korfiatis N, Trounson A, Lacham-Kaplan O (2001). Cell synchronization for the purposes of nuclear transfer in the bovine. *Cloning Stem Cells*, 3: 125-138.

Kourmouli N, Theodoropoulos PA, Dialynas G, Bakou A, Politou AS, Cowell IG, Singh P, Georgatos SD (2000). Dinamic association of heterochromatin protein 1 with the nuclear envelope. *EMBO J.*, 19: 6558-6568.

Kubota C, Yamakuchi H, Todoroki J, Mizoshita K, Tabara N, Barber M, Yang X (2000). Six cloned calves produced from adult fibroblasts cells after long-term culture. *Proc. Nat. Acad. Sci. USA*, 97: 990-995.

Kurki P, Lotz M, Ogata K, Tan EM (1987). Proliferating cell nuclear antigen (PCNA)/cyclin in activated human T-lymphocytes. *J. Immunol.*, 138: 4114-4120.

Kwon OY, Kono T (1996). Production of identical sextuplet mice by transferring metaphase nuclei from 4- cell embryo. *Proc. Nat. Acad. Sci. USA*, 93: 13010-13013.

Kwon TK, Buchholtz MA, Chrest FJ, Nordin AA (1996). Staurosporine induced G1 arrest is associated with the induction and accumulation of cyclin-dependent kinase inhibitors. *Cell. Gr. Diff.*, 7: 1305.

Lai L, Tao T, Machaty Z, Kuhholzer B, Sun QY, Park KW, Day BN, Prather RS (2001). Feasibility of producing porcine nuclear transfer embryos by using G2/M-stage foetal fibroblasts as donors. *Biol. Reprod.*, 65: 1558-64.

Latham KE, Solter D, Schultz RM (1992). Acquisitio of a transcriptionally permissive state during the 1-cell stage of mouse embryogenesis. *Dev. Biol.*, 149: 457-462.

Leitch AR (2000). Higher levels of organisation in the interphase nucleus of cycling and differentiated cells. *Microbiol. Mol. Biol. Rev.*, 64: 138-152.

Leno GH, Downes CS, Laskey RA (1992). The nuclear membrane prevents replication of human G2 nuclei but not G1 nuclei in *Xenopus* egg exract. *Cell*, 69: 151-158.

Leonhardt H, Rahn HP, Weinzierl P, Sporbert A, Cremer T, Zink D, Cardoso C (2000). Dynamics of DNA replication factories in living cells. *J. Cell. Biol.*, 149: 271-279.

Liu L, Dai Y, Moor RM (1997). Nuclear transfer in sheep embryos: the effect of cell-cycle co-ordination between nucleus and cytoplasm and the use of *in vitro* matured oocytes. *Mol. Rep. Dev.*, 47: 255-264.

Loi P, Ledda S, Fulka J, Cappai P, Moor RM (1998). Development of parthenogenetic and cloned ovine embryos: effect of activation protocols. *Biol. Reprod.*, 58: 1177-1187.

Loi P, Ptak G, Barboni B, Fulka J Jr, Cappai P, Clinton M (2001). Genetic rescue of an endangered mammal by cross-species nuclear transfer using post-mortem somatic cells. *Nat. Biotechnol.*, 19: 962-964.

Lopez-Velazquez G, Marquez J, Ubaldo E, Corkidi G, Echeverria O, Vazquez Nin GH (1996). Three-dimensional analysis of the arrangement of compact chromatin in the nucleus of G0 rat lymphocytes. *Histochem. Cell Biol.*, 105:153-61.

Lukas J, Bartkova J, Rohde M, Strauss M, Bartek J (1995). Cyclin D1 is dispensable for G1 control in retinoblastoma gene-deficient cells independentely of Cdk4 activity. *Mol. Cell. Biol.*, 15: 2600-2611.

Ma J, Svoboda P, Schultz RM, Stein P (2001). Regulation of Zygotic Gene Activation in the pre-implantation mouse embryo: global activation and repression of gene expression. *Biol. Reprod.*, 64: 1713-1721.

Maison C, Bailly D, Peters AH, Quivy JP, Roche D, Taddei A, Lachner M, Jenuwein T, Almouzni G (2002). Higher-order structure in pericentric heterochromatin involves a distinct pattern of histone modification and an RNA component. *Nat. Genet.*, 30: 329-34.

Malek TR, Ashwell JD (1985). Interleukin-2 upregulates expression of its receptor on a T cell clone. J.Exp.Med., 161: 1575-1580.

Masui Y and Markert CL (1971). Cytoplasmic control of nuclear behaviour during meiotic maturation of frog oocytes. *J. Exp. Zool.*, 177: 129-145.

McCreath KJ, Howcroft J, Campbell KHS, Colman A, Schnieke AE, Kind AJ (2000). Production of gene-targeted sheep by nuclear transfer from cultured somatic cells. *Nature,* 405: 1068-1069.

McGrath J, Solter D (1984). Inability of mouse blastomere nuclei transferred to enucleated zygotes to support development *in vitro*. *Science*, 226: 1317-1319.

McGrath J, Solter D (1986). Nucleo-cytoplasmic interactions in the mouse embryo. *J. Embryol. Exp. Morphol., Suppement*, 97: 277-289.

Merrill GF (1998a) Estimating Cell Cycle Phase Durations. In: *Methods in Cell Biology.* Vol. 57, Chapter 13, Part II, pp 231-237.

Merrill GF (1998b) Measuremnets of Cell Death. In: *Methods in Cell Biology.* Vol. 57, Chapter 14, Part II, pp 253-259.

Messinger SM, Albertini DF (1991). Centrosome and microtubule dynamics during meiotic progression in the mouse oocyte. *J. Cell Sci.,* 100: 289-298.

Minami Y, Kono T, Miyazaki T, Taniguchi T (1993). The IL-2 receptor complex: its structure, function, and target genes. *Annu. Rev. Immun.*, 11: 245-268.

Mishell BB, Shiigi SM, Henry C, Chan EL, North J, Gallily R, Slomich M, Miller K, Marbrook J, Parks D, Good AH (1980). Preparation of mouse cell suspensions. Chapter 1: 1-27. In: *Selected Methods in Cellular Immunology.* Ed. WH Freeman and Company, San Francisco.

Modiano JF, Mayor J, Ball C, Chitko-McKown CG, Sakata N, Domenico-Hahn J, Lucas JJ, Gelfand EW (1999). Quantitative and qualitative signals determine T-cell cycle entry and progression. *Cell. Immunol.*, 197: 19-29.

Moreira P, Bomar J, Robl JM, Collas P (2002). Identification of A-kinase anchoring protein AKAP95 as a molecular marker of nuclear reprogramming after nuclear transfer. *Theiogenology,* 57: 436.

Morgan D (1995). Principles of CDK regulation. *Nature,* 374: 131-144.

Nagy A, Rossant J, Nagy R, Abramow-Newerly W, Roder JC (1993). Derivation of completely cell culture-derived mice from early passage embryonic cells. *Proc. Nat. Acad. Sci. USA*, 90: 8424-8428.

Nakazumi H, Sasano H, Iino K, Ohashi Y, Orikasa S (1998). Expression of cell cycle inhibitor p27 and Ki-67 in human adrenocortical neoplasms. *Mod. Pathol.,* 11: 1165-1170.

Nash ML, Hungerford LL, Nash TG, Zinn GM (1996). Risk factors for perinetal and postnatal mortality in lambs. *Vet .Rec.,* 139: 64-67.

Newell-Price J, Clark AJ, King P (2000). DNA methylation and silencing of gene expression. *Trends Endocrinol.*, 11: 142-8.

Nobori T, Miura K, Wu DJ, Lois A, Takabayashi K, Carson DA (1994). Deletions of the cyclin-dependent kinase-4 inhibitor gene in multiple human cancers. *Nature*, 368: 753-756.

Noda AY, Ning S, Venable S, Pereira Smith O, Smith J (1994). Cloning of senescent cell-derived inhibitors of DNA synthesys using an expression screen. *Exp. Cell. Res.*, 211: 90-98.

Nourse J, Firpo E, Flanagan M, Coats S, Polyak K, Lee MH, Massague J, Crabtree GR, Roberts JM (1994). Interleukin-2-mediated elimination ofthe p27KIP1 cyclin-dependent kinase inhibitor prevented by rapamycin. *Nature*, 372: 570-573.

Nurse P (1990). Universal control mechanism regulating the onset of M-phase, *Nature,* 344: 503-507.

Ogura A, Inoue K, Ogonuki N, Noguchi A, Takano K, Nagano R, Suzuki O, Lee J, Ishino F, Matsuda J (2000). Production of male cloned mice from fresh, cultured, and cryopreserved immature Sertoli Cells. *Biol. Reprod.*, 62: 1579-1584.

Ohgane J, Wakayama T, Kogo Y, Senda S, Hattori N, Tanaka S, Yanagimachi R, Shiota K (2001). DNA methylation variation in cloned mice. *Genesis,* 30: 45-50.

Ohtsubo M, Theodoras AM, Schumacher J, Roberts JM, Pagano M (1995). Human cyclin E, a nuclear protein essential for the G1-to-S phase transition. *Mol. Cell. Biol.,* 15: 2612-2624.

Onishi A, Iwamoto M, Akita T, Mikawa S, Takeda K, Awata T, Hanada H, Perry AC (2000). Pig cloning by microinjection of foetal fibroblast nuclei. *Science*, 289:1188-90.

Ono Y, Shimozawa N, Ito M, Kono T (2001a). Cloned mice from foetal fibroblast cells arrested at metaphase by a serial nuclear transfer. *Biol. Reprod*, 64: 44-50.

Ono Y, Shimozawa N, Muguruma K, Kimoto S, Hioki K, Tachibana M, Shinkai Y, Ito M, Kono T (2001b). Production of cloned mice from embryonic stem cells arrested at metaphase. *Reproduction*, 122: 731-6

Orr NH, DiBerardino MA, McKinnell RG (1986). The genome of frog erythrocytes displays centuplicate replications. *Proc. Natl. Acad. Sci. USA*, 83: 1369-73.

Otaegui PJ, O'Neill GT, Campbell KH, Wilmut I (1994). Transfer of nuclei from 8-cell stage mouse embryos following use of nocodazole to control the cell cycle. *Mol. Reprod. Dev.*, 39: 147-52.

Pagano M (1996). *Cell cycle-Material and Methods.* Ed. Springer-Verlag, NY.

Pagano M (1997). Cell cycle regulation by the ubiquitin pathway. *FASEB J.,* 11: 1067-1075.

Patskan GJ, Baxter CS (1985). Specific Stimulation of histone H2B and H4 phosphorylation in mouse lymphocytes by 12-O-Tetradecanoylphorbol 13-Acetate. *J.Biol.Chem.*, 260: 12899-12903.

Perreault SD (1992). Chromatin remodelling in mammalian zygotes. *Mutat. Res.*, 296: 43-55.

Peura TT, Trounson AO (1998). Recycling bovine embryos for nuclear transfer. *Reprod. Fertil. Dev.*, 10: 627-632.

Pieper RO, Lester KA, Fanton CP (1999). Confluence-induced alterations in CpG island methylation in cultured normal human fibroblasts. *Nucleic. Acids Res.*, 27: 3229-3235.

Pines J, Hunter T (1991). Cyclin-dependent kinases: a new cell cycle motif? *Trends Cell. Biol.*, 1: 117-121.

Pogo BG, Allfrey VG, Mirsky AE (1966). RNA synthesis and histone acetylation during the course of gene activation in lymphocytes. *Proc. Natl. Acad.Sci. USA*, 55: 805-12.

Polejaeva IA, Chen SH, Vaught TD, Page RL, Mullins J, Ball S, Dai Y, Boone J, Walker S, Ayares DL, Colman A, Campbell KH. (2000). Cloned pigs produced by nuclear transfer from adult somatic cells. *Nature*, 407: 86-90.

Polyak K, Kato J, Solomon M, Sherr C, Massague J, Roberts J, Koff A (1994a). P27KIP1, a cyclin-CDK inhibitor links transforming growth factor B and contact inhibition to cell cycle arrest. *Gen. Dev.*, 8: 9-22.

Polyak K, Lee MH, Erdjument-Bromage H, Koff A, Roberts J, Massague J (1994b). Cloning of p27kip1, a cyclin dependent kinase inhibitor and a potential mediator of extracellular antimitogenic signals. *Cell*, 78: 59-66.

Pompidou A, Rousset S, Mace B, Michel P, Esnous D, Renard N (1984). Chromatin structure and nucleic acid synthesis in human lymphocyte activation by phytohemagglutinin. *Exp. Cell Res.*, 150: 213-225.

Prather RS, First NL (1990). Nuclear transfer in mammalian embryos. *Int. Rev. Cytol.* 120:169-190.

Prather RS, Barnes FL, Sims MM, Robl JM, Eyestone WH, First NL (1987). Nuclear transplantation in bovine embryo: assessment of donor nuclei and recipient oocyte. *Biol. Reprod.*, 37: 859-866.

Prather RS, Sims MM, Maul GG, First NL, Schatten G (1989). Nuclear lamin antigens are developmentally regulated during porcine and bovine embryogenesis. *Biol. Reprod.*, 41: 123-32.

Prather RS, Sims MM, First NL (1990). Nuclear transplantation in the pig embryo: nuclear swelling. *J. Exp. Zool.*, 225: 355-358.

Prochazka R, Fiser PS (1995). Behaviour of blastomere nuclei fused to mouse oocytes is affected by oocyte enucleation and age. *Reprod. Nutr. Dev.*, 35: 695-701.

Proust JJ, Shaper NL, Buchholz MA, Nordin A (1991). T cell activation in the absence of interleukin-2 (IL-2) results in the induction of high affinity IL-2receptor unable to transmit a proliferative signal. *Eur. J. Immunol.*, 21: 335-341.

Ram PT, Schultz RM (1993). Reporter gene expression in G2 of the 1-cell mouse embryo. *Dev. Biol.*, 156: 552-556.

Renard JP (1998). Chromatin remodelling and nuclear reprogramming at the onset of embryonic development in mammals. *Reprod. Fertil. Dev.*,10: 573-580.

Renard JP, Chastant S, Chesné P, Richard C, Marchal J, Cordonnier N, Chavatte P, Vignon X (1999). Lymphoid hypoplasia and somatic cloning. *The Lancet*, 353: 1489-1491.

Resnitzky D and Reed S (1995). Different roles for cyclins D1 and E in regulation of the G1-to-S transition. *Mol. Cell. Biol.*, 15: 3463-3469.

Rhodes N, Hicks R, Kasenally AB, Innes CL, Paules RS, Propst F (1994). V-mos transformed cells fail to enter quiescence but growth arrest in G1 following serum withdrawal. *Exp. Cell. Res.*, 213: 210-217.

Rideout WM, Wakayama T, Wutz A, Eggan K, Jackson-Grusby L, Dausman J, Yanagimachi R, Jaenish R (2000). Generation of mice from wild type and targeted ES cells by nuclear cloning. *Nat. Gen.*, 24: 109-110.

Rivard N, L'Allemain G, Bartek J, Pouyssegur J (1996). Abrogation of p27KIP1 by cDNA antisense DNA Suppressess quiescence (G0 state) in fibroblasts. *J. Biol. Chem.*, 271: 18337-18341.

Robb RJ, Munck A, Smith KA (1981). T cell growth factor receptors. Quantitation, specificity, and biological relevance. *J. Exp. Med.*, 154: 1455-1474.

Roberts JM, Koff A, Polyak K, Firpo E, Collins S, Ohtsubo M, Massague J (1994). Cyclins, Cdks, and cyclin kinase inhibitors. *Cold Spring Harb. Symp. Quant. Biol.*, 59: 31-38.

Robl JM, Gilligam B, Critser ES, First NL (1986). Nuclear transplantation in mouse embryos: assessment of recipient cell stage. *Biol. Reprod.*, 34: 733-739.

Ryan J, Llinas AJ, White DA, Turner BM, Sommerville J (1999). Maternal histone deacetylase is accumulated in the nuclei of Xenopus oocytes as protein complexes with potential enzyme activity. *J. Cell Sci.*, 112: 2441-2452.

Schneider C, King RM, Philipson L (1988). Genes specifically expressed at growth arrest of mammalian cells. *Cell*, 54: 787-793.

Schnieke AE, Kind AJ, Ritchie WA, Mycock K, Scott AR, Ritchie M, Wilmut I, Colman A, Campbell KHS (1997). Human factor iX transgenic sheep produced by transfer of nuclei from transfected foetal fibroblasts. *Science,* 278: 2130-2133.

Schultz RM (1993). Regulation of zygotic gene activation in the mouse. *BioEssays* 15; 531-538.

Schultz RM, Worrad DM (1995). Role of chromatin structure in zygotic gene activation in the mammalian embryo. *Semin. Cell. Biol.*, 6: 201-8.

Schwartz A, Cook PR, Harris H (1971). Correction of a genetic defect in a mammalian cell. *Nature,* 230: 5-8.

Setterfield G, Hall R, Bladon T, Little J, Kaplan JG (1983) Changes in structure and composition of lymphocyte nuclei during mitogenic stimulation. *J. Ultrastruct. Res.*, 82: 264-282.

Sheaff RJ, Groudine M, Gordon M, Roberts JM, Clurman BE (1997). Cyclin E-Cdk2 is a regulator of p27KIP1. *Gen. Dev.*, 11: 1464-1478.

Sherr C and Roberts J (1995). Inhibitors of mammalian G1 cyclin-dependent kinases. *Gen. Dev.*, 9: 1149-1163.

Sherr CJ (1993). Mammalian G1 cyclins. *Cell,* 73: 1059-1065.

Sherr CJ (1996). Cancer cell cycle. *Science,* 274: 1672-1677.

Shiels PG, Kind AJ, Campbell KH, Waddington D, Wilmut I, Colman A, Schnieke AE. (1999). Analysis of telomere lengths in cloned sheep. *Nature*, 399: 316-317.

Shiga K, Fujita T, Hirose K, Sasae Y, Nagai T (1999). Production of calves by transfer of nuclei from cultured somatic cells obtained from Japanese black bulls. *Theriogenology,* 52: 527-535.

Sims M and First NL (1994). Production of calves by transfer of nuclei from cultured inner cell mass cells. *Proc. Natl. Acad. Sci USA.*, 91: 6143-6147.

Singh PB, Miller JR, Pearce JJ, Burton RD, Paro R, James TC, Gaunt SJ (1991). A sequence motif found in *Drosophila* heterochromatin protein is conserved in animals and plants. *Nucl. Acid. Res.*, 19:789-793.

Smith EJ, Leone G, DeGregori J, Jakoi L, Nevins JR (1996). The accumulation of an E2F-p130 transcriptional repressor distinguishes a G0 cell state from a G1 cell state. *Mol. Cell. Biol.*, 16: 6965-6976.

Smith LC, Wilmut I (1989). Influence of nuclear and cytoplasmic activity on the development *in vivo* of sheep embryos after nuclear transplantation. *Biol. Reprod.*, 40: 1027-1035.

Smith RK, Johnson MH (1986). Analysis of the third and fourth cell cycles of mouse early development. *J. Reprod. Fertil.* 76: 393-9.

Soldaini E, Pla M, Beerman F, Espel E, Corthésy P, Barangè S, Waanders GA, MacDonald HR, Nabholz M (1995). Mouse Interleukin-2 Receptor α Gene Expression. *J. Biol. Chem.*, 270: 10733-10742.

St. Croix B, Sheehan C, Rak JW, Florenes VA, Slingerland JM, Kerbel RS (1998). E-cadherin-dependent growth suppression is mediated by the cyclin-dependent kinase inhibitor p27KIP1. *J. Cel. Biol.*, 142: 557-571.

Stein P, Worrad DM, Belyaev ND, Turner BM, Schultz RM (1997). Stage-dependent redistributions of acetylated histones in nuclei of the early pre-implantation mouse embryo. *Mol. Rep. Dev.*, 47: 421-429.

Stice S, Robl JM (1988). Nuclear reprogramming in nuclear transplant rabbit embryos (1988). *Biol. Reprod.*, 39: 657-664.

Stice SL, Strelchenko NS, Keefer CL, Matthews L (1996). Pluripotent bovine embryonic cell lines direct embryonic development following nuclear transfer. *Biol. Reprod.*, 54: 100-10.

Strelchenko N, Mitalipova M, Stice S (1995). Further characterisation of bovine pluripotent stem cells. *Theriogenology,* 43: 327.

Strouboulis J, Damjanovski S, Vermaak D, Meric F, Wolffe AP (1999). Transcriptional repression by XPc1, a new Polycomb homolog in Xenopus laevis embryos, is independent of histone deacetylase. *Mol. Cell. Biol.*, 19: 3958-68.

Sun FZ and Moor R (1995). Nuclear transplantation in mammalian eggs and embryos. In: *Current Topics in Developmental Biology.* Academic Press, New York.

Szöllösi D, Czolowska R, Soltynska MS, Tarkowski AK (1986a). Ultrastructure of cell fusion and premature chromosome condensation of thymocyte nuclei in metaphse II mouse oocytes. *Biol. Cell.*, 56: 239-149.

Szöllösi D, Czolowska R, Soltinska MS, Tarkowski AK (1986b). Remodelling of mouse thymocyte nuclei in activated mouse oocytes: an ultrastructural study. *Eur.J.Cell Biol.*, 42: 140-151.

Szöllösi D, Czolowska R, Szöllösi MS, Tarkowski AK (1988). Remodelling of mouse thymocyte nuclei depends on the time of their transfer into activated, homologous oocytes. *J. Cell. Sci.*, 91: 603-613.

Szöllösi D, Czolowska R, Borsuk E, Szöllösi MS, Debey P (1998). Nuclear envelope removal/maintenance determines the structural and functional remodelling of embryonic red blood cell nuclei in activated mouse oocytes. *Zygote*, 6: 65-73.

Tanaka T, Tsudo M, Karasuyama H, Kitamura H, Kono T, Hatakayama M, Taniguchi T, Miyasaka M (1991). A novel monoclonal antibody against murine IL-2 receptor beta-chain. Characterisation of receptor expression in normal lymphoid cells and EL-4 cells. *J .Immunol.*, 147: 2222-2228.

Telford NA, Watson AJ, Schultz GA (1990). Transition from maternal to embryonic control in early mammalian development: a comparison of several species. *Mol. Rep. Dev.*, 26: 90-100.

Thompson JG, Gardner DK, Pugh PA, McMillan WH, Tervit HR (1995). Lamb birth weight is affected by culture system utilized during in vitro pre-elongation development of ovine embryos. *Biol. Reprod.*, 53: 1385-1391.

Thorne AW, Kmiciek D, Mitchelson K, Sautiere P, Crane-Robinson C (1990). Patterns of histone acetylation. *Eur. J. Biochem.*, 193: 701-713.

Tian XC, Lonergan P, Jeong BS, Evans AC, Yang X (2002). Association of MPF, MAPK, and nuclear progression dynamics during activation of young and aged bovine oocytes. *Mol. Reprod. Dev.*, 62: 132-138.

Todaro GJ, Green H (1963). Quantitative studies of the growth of mouse embryo cells in culture and their development into established lines. *J. Cell. Biol.*, 17: 299-313.

Truneth A, Albert F, Goldstein P, Shmitt Verhulst AM (1985). Early steps of lymphocyte activation bypassed by synergy between calcium ionophores and phorbol ester. *Nature*, 313: 318-320.

Tsunoda Y, Kato Y (1997). Full term development after transfer of nuclei from 4-cell and compacted morula stage embryos to enucleated oocyte in the mouse. *J. Exp. Zool.*, 278: 250-254.

Tsunoda Y, Yasui T, Shioda Y, Nakamura K, Uchida T, Sugie T (1987). Full-term development of mouse blastomere nuclei transplanted into enucleated two-cell embryos. *J. Exp. Zool.*, 242: 147-151.

Tsunoda Y, Tokunaga T, Imai H, Uchida T (1989). Nuclear transplantation of male primordial germ cells in mouse. *Dev.*, 107: 407-412.

Turner BM, Fellows G (1989). Specific antibodies reveal ordered and cell-cycle related use of histone-H4 acetylation sites in mammalian cells. *Eur. J. Biochem.*, 193: 701-713.

Turner BM, O'Neill LP, Allan IM (1989). Histone H4 acetylation in human cells. Frequency of acetylation at different sites defined by immunolabelling with site-specific antibodies. *FEBS Lett.*, 253: 141-145.

Verma PJ, Du ZT, Grupen CG (1998). Effect of cell cycle synchronization on porcine nuclear transfer. *Theriogenology*, 51: 215.

Vignon X, Chesne P, LeBourhis D, Heyman Y and Renard JP (1998). Developmental potential of bovine embryos reconstructed with somatic nuclei cultured skin and muscle foetal cells. *Theriogenology*, 49: 392.

Voncken JW, Schweizer D, Aagaard L, Sattler L, Jantsch MF, van Lohuizen M (1999). Chromatin-association of the Polycomb group protein BMI1 is cell cycle-regulated and correlates with its phosphorylation status. *J. Cell Sci.*, 112: 4627-4639.

Wabl MR, Brun RB, Du Pasquier L (1975). Lymphocytes of the toad Xenopus laevis have the gene set for promoting tadpole development. *Science*, 190: 1310-1312.

Wade PA, Jones PL, Vermaak D, Veenstra GJ, Imhof A, Sera T, Tse C, Ge H, Shi YB, Hansen JC, Wolffe AP (1998). Histone deacetylase directs the dominant silencing of transcription in chromatin: association with MeCP2 and the Mi-2 chromodomain SWI/SNF ATPase. *Cold Spring Harb. Symp. Quant. Biol.*, 63: 435-445.

Wakayama T and Yanagimachi R (1999). Cloning of male mice from adult tip cells. *Nature Genetics*, 22: 127-128.

Wakayama T and Yanagimachi R (2001). Mouse cloning with nucleus donor cells of different age and type. *Mol. Rep. Dev.*, 58: 376-383.

Wakayama T, Perry ACF, Zuccotti M, Johnson KR, Yanagimachi R. (1998). Full-term development of mice from enucleated oocytes injected with cumulus cell nuclei. *Nature*, 394: 369-374.

Wakayama T, Rodriguez I, Perry ACF, Yanagimachi R, Mombaerts P (1999). Mice cloned from embryonic stem cells. *Proc. Nat. Acad. Sci. USA*, 96: 14984-14989.

Wakayama T, Shinkai Y, Tamashiro KL, Niida H, Blanchard DC, Blanchard RJ, Ogura A, Tanemura K, Tachibana M, Perry AC, Colgan, DF, Mombaerts P, Yanagimachi R (2000a). Cloning of mice to six generations. *Nature,* 407: 318-9.

Wakayama T, Tateno H, Mombaerts P, Yanagimachi R (2000b) Nuclear transfer into mouse zygotes. *Nat. Genet.*, 24: 108-9.

Waldmann TA (1989). The multi-subunit interleukin-2 receptor. *Annu. Rev. Biochem.*, 58: 875-911.

Walker SK, Heard TM, Seamark MF (1992). *In vitro* culture of sheep embryos without co-culture: success and perspectives. *Theriogenology*, 37: 111-126.

Walker SK, Hartwich KM, Seamark RF (1996). The production of unusually large offspring following embryo manipulation: concepts and challenges. *Theriogenology,* 45: 111-120.

Weimer R, Haaf T, Krüger J, Poot M, Schmid M (1992). Characterisation of centromere arrangements and test for random distribution in G0, G1, S, G2, G1 and early S-phase in human lymphocytes. *Hum. Gen.,* 88: 673-682.

Wells DN (2002). Cloning in livestock agriculture. *Reproduction*, Supplement 61. In Press.

Wells DN, Misica PM, Day AM, Tervit HR (1997). Production of cloned lambs from established embryonic cell line: a comparison between *in vivo* and *in vitro* cytoplasts. *Biol. Reprod.*, 57: 385-393.

Wells DN, Misica PM, Tervit HR, Vivanco WH (1998a). Adult somatic nuclear transfer is used to preserve the last surviving cow of the Enderby Island cattle breed. *Rep. Fertil. Dev.,* 10: 369-378.

Wells DN, Misica PM, Day AM, Peterson AJ, Tervit HR (1998b). Cloning sheep from cultured embryonic cells. *Rep. Fert. Dev.,* 10: 615-626.

Wells DN, Misica PM, Tervit HR (1999). Production of cloned calves following nuclear transfer with cultured adult mural granulosa cells. *Biol Reprod.*, 60: 996-1005.

Whitfield JF, Boynton AL, Rixon, L, Youndale T (1985). The control of cell proliferation by calcium, Ca2+-calmodulin and cyclic AMP. In: *Control of animal cell proliferation,* vol. 1, pp 331-365. Eds. Boynton AL and Leffert HL, Academic Press, London.

Whittingham DG (1971). Culture of mouse ova. *J. Reprod. Fert., Supplememnt,* 14: 7-21.

Wiekowski M, Miranda M, Nothias JY, DePamphilis (1997). Changes in histone synthesis and modification at the beginning of mouse development correlate with the establishment of chromatin mediated repression of transcription. *J. Cell Biol.,* 110: 1147-1158.

Willadsen SM (1986). Nuclear transplantation in sheep embryos. *Nature*, 320: 63-65.

Wilmut I, Schnieke AE, McWhir J, Kind AJ, Campbell KHS (1997). Viable offspring derived from foetal and adult mammalian cells. *Nature,* 385: 810-813.

Worrad DM, Ram PT, Schultz RM (1994). Regulation of gene expression in the mouse oocyte and early preimplatation embryo: developmental changes in Sp1 and TATA box-binding protein, TBP. *Development*, 120: 2347-2357.

Worrad DM, Turner BM, Schultz RM (1995). Temporally restricted spatial localisation of acetylated isoforms of histone H4 and RNA polymerase II in the 2-cell mouse embryo. *Development*, 12: 2949-59.

Wreggett KA, Hill F, James PS, Hutchings A, Butcher GW, Singh PB (1994). A mammalian homologue of *Drosophila* heterochromatin protein 1 (HP1) is a component of constitutive heterochromatin. *Cytog. Cell Genet.*, 66: 99-103.

Wrenzycki C, Wells D, Herrmann D, Miller A, Oliver J, Tervit R, Niemann H (2001). Nuclear transfer protocol affects messenger RNA expression patterns in cloned bovine blastocysts. *Biol. Reprod.*, 65: 309-17.

Young LE, Sinclair KD and Wilmut I (1998). Large offspring syndrome in cattle and sheep. *Rev. Rep.*, 3: 155-163.

Zakhartchenko V, Durcova-Hills G, Stojkovic M, Schernthaner W, Prelle K, Steinborn R, Muller M, Brem G, Wolf E (1999a). Effect of serum starvation and re-cloning on the efficiency of nuclear transfer using bovine foetal fibroblaststst. *J. Rep. Fert.*, 115: 325-331.

Zakhartchenko V, Alberio R, Stojkovic M, Prelle K, Schernthaner W, Stojkovic P, Wenigerkind H, Wanke R *et al.*. (1999b). Adult cloning in cattle: potential of nuclei from a permanent cell line and from primary cultures. *Mol. Rep. Dev.*, 54: 264-272.

Zhou Q, Jouneau A, Brochard V, Adenot P, Renard JP (2001). Developmental potential of mouse embryos reconstructed from metaphase embryonic stem cell nuclei. *Biol. Reprod.*, 65: 412-9.